GENETIC ANALYSIS OF DEVELOPMENTAL TRAITS ASSOCIATED WITH ENHANCED WINTER SURVIVAL IN AUTUMN-SEEDED RYE (*Secale cereale* L.)

A Thesis Submitted to the College of

Graduate and Postdoctoral Studies

In Partial Fulfillment of the Requirements

For the Degree of Doctor of Philosophy

In the Department of Plant Sciences

University of Saskatchewan

Saskatoon, Saskatchewan

By

Hirbod Bahrani

PERMISSION TO USE

In presenting this thesis in partial fulfillment of the requirement of a postgraduate degree from the University of Saskatchewan, I agree that the Libraries of this University may make it freely available for inspection. I further agree that permission for copying of this thesis in any manner, in whole or in part, for scholarly purpose may be granted by the professor or professors who supervised this thesis work or, in the absence, by the Head of the Department or the Dean of the College in which this thesis was done. It is understood that any copying or publication or use of this thesis or part thereof for financial gain shall not be allowed without my written permission. It is also understood that due recognition shall be given to me and to the University of Saskatchewan in any scholarly use which may be made of any material in my thesis.

Requests for permission to copy or to make other use of material in this thesis in whole or part should be addressed to:

Head of the Department of Plant Sciences,
51 Campus Drive,
University of Saskatchewan,
Saskatoon,
Saskatchewan,
S7N 5A8
Canada

or

Dean
College of Graduate and Postdoctoral Studies
University of Saskatchewan
116 Thorvaldson Building, 110 Science Place
Saskatoon, Saskatchewan
S7N 5C9
Canada

ABSTRACT

Autumn seeded winter cereals are ecologically friendly and usually yield higher than spring seeded cereals. However, the low and unpredictable winter field survival (WFS) is a major factor limiting the widespread adoption of winter cereals on the Canadian prairies. In the autumn, winter cereals seedlings exposed to gradual low temperatures along with changes in day length and light quality, initiate cold acclimation and accumulate low temperature tolerance (LTT) to overcome the extreme low temperatures in the winter. Simultaneously, the plants undergo vernalization and initiate developmental changes at the shoot apical meristem to adjust to the low temperatures. The research in this thesis is based on the hypothesis that the complex WFS trait is largely affected by the LTT accumulated during cold acclimation and low-temperature induced plant developmental traits. Autumn seeded rye (*Secale cereale* ssp. *cereale* L.) is the most cold-hardy winter cereal among cultivars adapted to the Northern latitudes. A panel of 96 rye genotypes from diverse geographic regions and growth habits was assessed for WFS by five years of field trials (Saskatoon, SK, Canada). The plants were also assessed for LTT by whole plant freeze tests in a climate chamber, and six developmental traits during growth under controlled conditions in a growth room or greenhouse. From the Best Linear Unbiased Estimates (BLUEs) for five years of field tests, five WFS classes were defined for the rye panel (i) very high (64.5 - 92.5%; 19 genotypes), (ii) high (56.7 - 64.3%; 20 genotypes), (iii) moderate (46.2 - 56.6%; 19 genotypes), (iv) low (30.5 - 43.7%; 19 genotypes), and (v) very low (0.0 - 25.2%; 19 genotypes). The WFS BLUE values correlated strongly with LTT ($r = 0.90$, $p < 0.001$); inferring that cold acclimation efficiency was the major contributor to WFS. Among the six plant developmental traits, WFS showed strongest correlations ($p < 0.001$) with final leaf number (FLN, $r = 0.80$), prostrate growth habit (PGH, $r = 0.61$), and plant height (PHT. $r = 0.34$). The same panel of rye genotypes was also analyzed for anthocyanin (ANT) production in leaves and crown tissues during cold acclimation. With the use of a high-performance liquid chromatography system combined with quadrupole time-of-flight mass spectrometry (HPLC-QTOF MS/MS), a total of 18 different anthocyanidins (cyanidins, delphinidins, and pelargonidins) in glycosylated forms were identified. Among anthocyanins, seven compounds correlated with WFS, and Cya-3-Glc had the strongest correlation ($r = 0.35$, $p < 0.001$).

In this study, association genetic studies allowed identification of genes associated with WFS in rye, due to the outcrossing nature of rye that provided a low linkage disequilibrium (LD) and the availability of a near complete genome sequence in 2021. The 96 rye genotypes were genotyped by sequencing (GBS), resulting in a total of 357.1 million reads with an average read length of 108 bp. Alignment of the processed sequences to the scaffolds of rye inbred line Lo7 (version 2) produced 252,158 single nucleotide polymorphism (SNP) markers, which after data filtering yielded 10,244 SNP markers with no missing data. Genome wide association studies (GWAS) revealed 679 marker-trait-associations (MTAs; p <0.01). The ten most significant SNPs (p <1.49e-04) associated with WFS, corresponded to nine different genes. Seven candidate genes were also associated with LTT, and developmental traits (FLN, PGH), suggesting a close linkage between acquisition of LTT and plant development. Allelic variations for genes encoding Inducer of CBF Expression 1 (ICE1), Cold-regulated 413-Plasma Membrane Protein 1 (COR413-PM1), Ice Recrystallization Inhibition Protein 1 (IRIP1), Jasmonate-resistant 1 (JAR1*)*, BIPP2C1-like protein phosphatase, and Chloroplast Unusual Positioning Protein-1 (CHUP1) were among the most significant candidate genes for WFS. Among the anthocyanins, the four most significant SNP markers associated with WFS (p < 2.76e-04), corresponded to phenylpropanoid pathway genes including, Chalcone Synthase 2 (CHS2), Anthocyanidin 3-O-Glucosyltransferase (3GT), and Phenylalanine Ammonia-Lyase 8 (PAL8). The winter-hardy rye genotypes generally carried additional allele variants for candidate genes, which suggested allele diversity was a major contributor to cold acclimation efficiency and consistent high WFS under varying field conditions.

The present study identified candidate genes associated with WFS, LTT and developmental traits in rye. The results confirmed the complex nature of WFS and a close association with plant developmental traits affected by changes in shoot apical meristem during cold acclimation. Since rye chromosomes are syntenous with wheat and barley, the knowledge can be used to increase WFS in the ecologically friendly temperate winter cereals of interest in the Northern hemisphere.

ACKNOWLEDGEMENTS

I sincerely thank my supervisors Dr. Ravindra N. Chibbar and Dr. Monica Båga for their guidance, encouragement and trust throughout the entire research project. Also, my sincere thanks to my advisory committee members, namely, Dr. Jamie Larsen, Dr. Karen Tanino, Dr. Christopher Eskiw and Dr. Tom Warkentin for their advice and constructive suggestions. I am grateful to Dr. R. Sammynaiken and Mr. Ken Thoms, Saskatchewan Structural Sciences Centre, University of Saskatchewan, for their help in anthocyanins characterization studies.

Financial support during my studies from Department of Plant Sciences, Saskatchewan Winter Cereals Development Commission, Canada Research Chairs program, Western Grains Research Foundation, Winter Cereals Manitoba, Alberta Wheat Commission and NSERC Collaborative Research is gratefully acknowledged. I want to thank all technicians and students in Molecular Crop Quality group for their help during my studies. I would like to thank my family for their support and encouragement.

PERMISSION TO USE

Permission to use information published in the following publications is being sought.

Bahrani, H., Thoms, K., Båga, M., Larsen, J., Graf, R., Laroche, A., Sammynaiken, R., and Chibbar, R.N. (2019) Preferential accumulation of glycosylated cyanidins in winter-hardy rye (S*ecale cereale* L.) genotypes during cold acclimation. Environmental and Experimental Botany 164: 203 – 212.

Bahrani, H., Båga, M., Larsen, J., Graf, R.J., Laroche, A., and Chibbar, R.N. (2021) The relationship between plant developmental traits and winter field survival in rye (*Secale cereale* L.) Plants 10: 2455

Båga, M., Bahrani, H., Larsen, J., Hackauf, B., Graf, R.J., Laroche, A., and Chibbar, R.N. (2022). Association mapping of autumn-seeded rye (*Secale cereale* L.) reveals genetic linkages between genes controlling winter hardiness and plant development. Scientific Reports, 12: 5793.

RESEARCH PUBLICATIONS FROM THESIS

Bahrani, H., Thoms, K., Båga, M., Larsen, J., Graf, R., Laroche, A., Sammynaiken, R., and Chibbar, R.N. (2019) Preferential accumulation of glycosylated cyanidins in winter-hardy rye (S*ecale cereale* L.) genotypes during cold acclimation. Environmental and Experimental Botany 164: 203 – 212.

Author contributions: Ravindra Chibbar, Monica Båga, Robert Graf, Andre Laroche and Jamie Larsen developed and conceptualized the project. Jamie Larsen collected the germplasm, Robert Graf and Jamie Larsen conducted field tests in Lethbridge, Monica Båga, Hirbod Bahrani conducted Saskatoon field tests and analyzed field survival data, Hirbod Bahrani collected tissue samples, extracted anthocyanins, Ramaswami Sammynaiken and Ken Thoms helped with HPLC-QTOF MS-MS analysis. Hirbod Bahrani and Monica Båga prepared the first drafts of the manuscript. Ravindra Chibbar edited the manuscript that was edited and approved for submission by all the authors.

Bahrani, H., Båga, M., Larsen, J., Graf, R.J., Laroche, A., and Chibbar, R.N. (2021) The relationship between plant developmental traits and winter field survival in rye (*Secale cereale* L.) Plants 10: 2455

Author Contributions: HB**:** Investigation, formal analysis, writing original draft. MB**:** Conceptualization, funding acquisition, methodology, resources, writing - review & editing: JL**:** Conceptualization, resources, funding acquisition, review. RJF**:** Conceptualization, funding acquisition, review. AL**:** Conceptualization, funding acquisition, review. RNC**:** Conceptualization, funding acquisition, supervision, project administration, writing - review & editing. All authors have read agreed to the published version of the manuscript

Båga, M., Bahrani, H., Larsen, J., Hackauf, B., Graf, R.J., Laroche, A., and Chibbar, R.N. (2022). Association mapping of autumn-seeded rye (*Secale cereale* L.) reveals genetic linkages between genes controlling winter hardiness and plant development. Scientific Reports 12: 5793.

Author contributions: MB: Conceptualization, funding acquisition, experimental, data analysis, manuscript first draft preparation and editing; HB: Experimental, data analysis, manuscript writing; JL: Conceptualization, funding acquisition, resources, manuscript review; BH: Data analysis, manuscript review and editing; RJG: Conceptualization, resources, manuscript review and editing; AL: Conceptualization, funding acquisition, data analysis, manuscript review and editing; RNC: Conceptualization, funding acquisition, project management, data analysis, manuscript review and editing.

TABLE OF CONTENTS

PERMISSION TO USE i

ABSTRACT ii

ACKNOWLEDGEMENTS iv

PERMISSION TO USE v

RESEARCH PUBLICATIONS FROM THESIS vi

TABLE OF CONTENTS vii

LIST OF TABLES xiv

LIST OF FIGURES xv

LIST OF APPENDICES xviii

LIST OF ABBREVIATIONS xx

CHAPTER 1 1

INTRODUCTION 1

1.1 Winter rye – a cold-hardy winter cereal 1

1.2 Cold acclimation increases winter-survival potential in winter cereals 1

1.3 Genetics of cold tolerance 2

1.4 A genome wide association study (GWAS) to identify trait-marker relationships 3

1.5 Hypothesis 4

1.6 Objectives 4

CHAPTER 2 5

LITERATURE REVIEW 5

2.1 The rye genome 5

2.1.1 Origin and domestication or rye 5

2.1.2 Rye production and utilization 7

2.2 Growth habits among temperate cereals 7
2.2.1 Spring type growth habit 8
2.3.2 Winter type growth habit 8
2.3.3 Facultative type growth habit 12
2.4 Factors determining winter survival potential among winter cereals 12
2.5 VRN and CBF regulon have major roles for WFS in winter cereals 15
2.6 The influence of light on vernalization response and cold acclimation 17
2.6.1 Photoperiod sensitivity in cereals 17
2.6.2 Registration of light properties by photoreceptors 19
2.6.3 Integration of light and cold signals to regulate development 20
2.7 Vernalization requirement in plants 21
2.7.1. Genetic control of vernalization in Triticeae species 21
2.7.2 Additional factors controlling phase switches in plants 24
2.8 Development of freezing tolerance in plants 25
2.8.1 Perception of cold and cold signaling in plants 25
2.8.2 Cold acclimation in winter cereals 28
2.8.3 Role of the ICE-CBF-COR regulon during cold acclimation 28
2.8.4. Regulation of CBF expression 29
2.9 Plant responses to low temperature 31
2.9.1 Adjustment of photosynthesis during cold acclimation 32
2.9.2 Changes in carbohydrate metabolism during cold acclimation 35
2.9.3 Response to oxidative stress during cold exposure 36
2.10 Role of plant growth regulators during cold acclimation 37
2.10.1 Gibberellic acid 38
2.10.2 Abscisic acid 38

2.10.3 Jasmonic acid 40
2.10.4 Ethylene 40
2.10.5 Brassinosteroids 41
2.11 Accumulation of cold stress-related proteins and compounds 41
2.11.1 Dehydrin proteins 41
2.11.2 Anti-freeze proteins (AFP) and ice recrystallization inhibitor proteins (IRIPs) 42
2.11.3 Flavonoid and anthocyanin compounds 42
2.12 Genetic maps – QTL Mapping 44
2.13 Genome-Wide Association Study (GWAS) 45
2.14 SNP markers 46
2.15 Genotyping-by-sequencing (GBS) 46
2.16 Phenotypic variation 47
2.17 Winter field survival in autumn seeded cereals – a complex trait 48
2.18 Rye is a good model for the study of complex trait WFS 49
CHAPTER 3 50
MATERIALS AND METHODS 50
3.1 Plant material and seed production 50
3.2 Field tests for determination of WFS 50
3.3 Freeze tests for determination of LTT 55
3.4 Collection of phenotypic data for developmental traits 56
3.5 Statistical analyses for phenotypic traits 61
3.6 Anthocyanin analysis 61
3.6.1 Preparation of plant extracts 61
3.6.2 HPLC-QTOF MS/MS analysis of anthocyanins 62
3.7 Genotyping by Sequencing (GBS) 63

3.7.1 DNA extraction 63
3.7.2 DNA sequencing 66
3.8 SNP calling 66
3.9 Analysis of population structure 67
3.10 Marker-trait association (MTA) analysis 67
3.11 Prediction of candidate genes 68
CHAPTER 4 69
RESULTS 69
4.1 A multi-trait approach to study WFS 69
4.2 Rye genotypes showed a range of WFS[1] 69
4.3 Freezing test determined LTT corresponded to WFS in rye genotypes 75
4.4 Analysis of developmental traits 76
4.4.1 Final Leaf Number (FLN) 76
4.4.2. Prostrate growth habit (PGH) 80
4.4.3 Plant height (PHT) and top internode length (TIL) 80
4.4.4 Days to anthesis (DTA) 81
4.4.5 Flag leaf area (FLA) 81
4.4.6 Correlation among developmental traits 81
4.5. Bi-plot analysis supports WFS is primarily determined by developments at SAM during cold acclimation. 83
4.6 Determination of heritability 83
4.7 Anthocyanins 87
4.7.1 Higher flavonoid accumulation in leaves of cold-hardy versus cold-sensitive rye genotypes 87
4.7.2 Anthocyanin characterization 89
4.7.3 Low amounts and diversity for anthocyanins identified in crown tissues 94

4.7.4 The cyanidin group of anthocyanin compounds were preferentially accumulated during cold acclimation 94
4.7.5 The accumulation of glycosylated delphinidins and pelargonidins were unrelated to high winter-hardiness 99
4.7.6 Correlation of anthocyanins with WFS 99
4.8 Structure analysis of GBS data generated for rye population 101
4.9 Identification of SNP markers associated with developmental and cold tolerance traits 105
4.10 Ten most significant marker-trait associations (MTAs) 108
4.10.1 BIPP2C1-like protein phosphatase 108
4.10.2 Ice Recrystallization Inhibition Protein 1 (IRIP1) 108
4.10.3 COR413-PM1-like 114
4.10.4 Inducer of CBF Expression 1 (ICE1) 116
4.10.5 Jasmonate-resistant 1 (JAR1) 119
4.10.6 FRIGIDA4-like (FRL4-like) 119
4.10.7 Chloroplast Unusual Positioning Protein-1 (CHUP1) 122
4.11 MTAs in group 2 124
4.11.1 Expansin-like 1 (EXLA1) 124
4.11.2 Gibberellin 2-beta-dioxygenase-A11 (GA2ox-D11) 124
4.11.3 ATP-binding cassette transporter C-like family member 8 (ABCC8) 127
4.11.4 Alpha-glucosidase 130
4.11.5 Zinc finger CCCH-30 130
4.11.6 Peroxisomal (S)-2-hydroxy-acid oxidase 3 (GLO3) 130
4.11.7 Alpha-1,3-arabinosyltransferase-like 3 (XAT3) 130
4.11.8 Tyrosine kinase (HCK) 133
4.11.9 Lecithin-cholesterol acyltransferase-like1 (LCAT1) 133
4.11.10 Zinc finger protein1-like (ZPR1-like) 136

4.11.12 Chemocyanin 136
4.11.13 MTAs located within intron or in untranslated regions 136
4.11.14 MTAs not matched with Lo7 rye annotated genes 138
4.12 Variation for CBF genes showed low significance for WFS in group 3 139
4.13 Bi-plot analysis supports WFS and associated traits are controlled by several common genes. 142
4.14 Identification of SNP markers associated with anthocyanins and WFS 142
4.15 Most significant MTA related to anthocyanins, WFS and developmental traits 155
4.15.1 Enzymes of the phenylpropanoid pathway 155
4.15.2 Markers associated with WFS and anthocyanins 159
4.15.3 Markers associated with only anthocyanins 165
4.15.4 MTAs not matched with Lo7 rye annotated genes 168
4.15.5 Markers associated with anthocyanins and developmental traits 169
4.16 Markers associated with WFS and anthocyanins in group 2 169
4.17 Markers associated with anthocyanins and developmental traits in group 2 170
4.18 Bi-plot analysis supports WFS and associated cyanidins are controlled by several common genes. 170
CHAPTER 5 173
DISCUSSION 173
5.1 Background 173
5.2 Rye population provided a wide variation of WFS 174
5.3 Efficiency of cold acclimation process was a major factor for WFS 174
5.4 A multi-trait approach to study WFS 175
5.4.1 WFS strongly correlated to LTT, FLN, PGH and PHT 175
5.4.2 Rye – a good source of winter hardiness genes 177
5.5 Membrane integrity 178

5.6 Photosynthesis adjustment during cold acclimation 180
5.7 ICE-CBF-COR regulon 181
5.8 Jasmonic acid influence on cold acclimation 182
5.9 Alterations at shoot apical meristem (SAM) during cold acclimation process 183
5.10 Accumulation of anthocyanin compounds upon LT exposure 184
5.11 Cyanidins group of anthocyanins are associated with enhanced winter hardiness 185
5.12 MTAs with possible role in phenylpropanoid pathway 186
5.13 Higher heterozygosity of stress related alleles in winter-hardy rye 187
5.14 Conclusions 188
5.15 Future studies 191
REFERENCES 193

LIST OF TABLES

Table 2. 1 Cold acclimated wheat and rye cultivars low temperature tolerance (LT_{50}) values 14
Table 3. 1 Rye genotypes used in the study 51
Table 3. 2 Local climatological data during consecutive growing seasons 2014 to 2019. 53
Table 4. 1 Classification of rye genotypes based on winter field survival score. 70
Table 4. 2 Correlations between LTT and WFS 72
Table 4. 3 Correlations between WFS, LTT, and developmental traits 82
Table 4. 4 Analysis of variance and heritability of WFS and developmental traits. 86
Table 4. 5 Winter field survival and anthocyanin color score in 96 rye genotypes 88
Table 4. 6 Anthocyanins identified in cold-acclimated tissues of rye 92
Table 4. 7 Quantification of three anthocyanins in leaf and crown tissues of cold-acclimated rye. 95
Table 4. 8 Number of anthocyanin compounds identified in 96 cold-acclimated rye genotypes. 96
Table 4. 9 Correlations between WFS, LTT, and anthocyanins. 100
Table 4. 10 Total number and shared SNP markers between traits... 106
Table 4. 11 Most significant MTAs of developmental traits in the study 107
Table 4.12 Most significant MTAs of developmental traits in group 2 125
Table 4.13 Markers associated with CBF genes in group 3. 140
Table 4. 14 Number of shared SNP markers between WFS and anthocyanins 154
Table 4. 15 Markers associated with phenylpropanoid pathway enzymes and WFS identified in the study. 156
Table 4. 16 Most significant markers associated with anthocyanins and WFS identified in the study. 160
Table 4. 17 Most significant markers associated with only anthocyanins identified in the study 167
Table 5. 1 **S**ignificant MTA affecting Winter Field Survival 189

LIST OF FIGURES

Figure 2. 1 Phylogeny and evolution of genome size in the grasses. 6
Figure 2. 2 Spring and winter rye growth habits. 9
Figure 2. 3 schematic sketch of cold acclimation and vernalization period in winter rye cultivars. 10
Figure 2. 4 Transition from vegetative to reproductive growth at the shoot apical meristem. 11
Figure 2. 5 Genomic regions associated with LTT in winter wheat. 16
Figure 2. 6 Interaction between light signaling and temperature. 18
Figure 2. 7 Hypothetical model proposed for interaction between vernalization and cold induced genes. 22
Figure 2. 8 Ca^{2+} signaling and the ICE-CBF-COR network. 26
Figure 2. 9 Chloroplast response under low temperature stress 34
Figure 2. 10 Plant growth regulators mediated regulation of CBF regulon during cold acclimation. 39
Figure 3. 1 Plant recovery scales from 0 to 5 used in LTT test to calculate LT_{50} values. 57
Figure 3. 2 LTT test scoring analysis. 59
Figure 3. 3 Rye genotypes used in this study separated into three groups based on their prostrate growth habit: (i) erect, (ii) intermediate, and (iii) prostrate growth habit. 60
Figure 3. 4 DNA extracted from rye genotypes used in the study. 65
Figure 4. 1 Distribution of frost hardiness determined for rye population of 96 accessions. 73
Figure 4. 2 Distribution of frost hardiness determined for rye population of 96 accessions in winter and non-wintergenotypes 74
Figure 4. 3 Distribution of developmental traits values for rye population of 96 accessions 77
Figure 4. 4 Distribution of developmental traits values for rye population of 96 accessions in winter and non-winter genotypes. 79
Figure 4. 5 PCA bi-plot of rye genotypes based on PC1 and PC2 components and vectors of traits analyzed in the study. 84
Figure 4. 6 PCA bi-plot of rye genotypes based on PC1 and PC2 components and vectors of traits analyzed in the study. Genotypes with winter (W), spring (S), facultative (F), and perennial (P) growth habit are indicated. 85

Figure 4. 7 HPLC-vis chromatogram of anthocyanins in tissue extracts of rye genotypes 91
Figure 4. 8 Anthocyanin peaks identified by HPLC-vis analysis of leaf extracts 93
Figure 4. 9 Principal component analysis (PCA) score plot. 102
Figure 4. 10 STRUCTURE plot for rye population. 103
Figure 4. 11 Neighbor-joining phylogenetic tree for rye population 104
Figure 4. 12 Location of significant markers for traits identified on rye physical map. 112
Figure 4. 13 Box-whisker plots showing the allele effects for the SNP marker (Xuos526258) (*p* <1.49e-04). 113
Figure 4. 14 Box-whisker plots showing the allele effects for the SNP marker (Xuos530120) (*p* <1.49e-04). 115
Figure 4. 15 Box-whisker plots showing the allele effects for the SNP marker (Xuos613978) (*p* <1.49e-04). 117
Figure 4. 16 Box-whisker plots showing the allele effects for the SNP marker (Xuos615052) (*p* <1.49e-04). 118
Figure 4. 17 Box-whisker plots showing the allele effects for the SNP marker (Xuos75199) (*p* <1.49e-04). 120
Figure 4. 18 Box-whisker plots showing the allele effects for the SNP markers (Xuos372616 and Xuos2264) (*p* <1.49e-04). 121
Figure 4. 19 Box-whisker plots showing the allele effects for the SNP markers (Xuos519455, Xuos76228a and Xuos76228b) (*p* <1.49e-04) 123
Figure 4. 20 Box-whisker plots showing the allele effects for the SNP marker (Xuos615123) (*p* <0.001). 126
Figure 4. 21 Box-whisker plots showing the allele effects for the SNP markers (Xuos527421 and Xuos614178a) (*p* <0.001) 129
Figure 4. 22 Box-whisker plots showing the allele effects for the SNP marker (Xuos79812) (*p* <0.001) 131
Figure 4. 23 Box-whisker plots showing the allele effects for the SNP markers (Xuos76179 and Xuos643564) (*p* <0.001) 132
Figure 4. 24 Box-whisker plots showing the allele effects for the SNP markers (Xuos448335 and Xuos173426) (*p* <0.001) 134

Figure 4. 25 Box-whisker plots showing the allele effects for the SNP markers (Xuos176122 and Xuos172463) (p <0.001).. 135
Figure 4. 26 Box-whisker plots showing the allele effects for the SNP marker (Xuos628254) (p <0.001) 137
Figure 4. 27 Box-whisker plots showing the allele effects for the SNP markers (Xuos369733, Xuos390086, Xuos370362, Xuos76905 and Xuos328096) (p <0.01).. 141
Figure 4. 28 PCA bi-plot visualizing SNP effects on WFS analyzed for rye population of 96 genotypes. 143
Figure 4. 29 PCA bi-plot visualizing SNP effects on LTT analyzed for rye population of 96 genotypes 144
Figure 4. 30 PCA bi-plot visualizing SNP effects on FLN analyzed for rye population of 96 genotypes 145
Figure 4. 31 PCA bi-plot visualizing SNP effects on PGH analyzed for rye population of 96 genotypes 146
Figure 4. 32 PCA bi-plot visualizing SNP effects on PHT analyzed for rye population of 96 genotypes 147
Figure 4. 33 PCA bi-plot visualizing SNP effects on TIL analyzed for rye population of 96 genotypes 148
Figure 4. 34 Location of significant markers for anthocyanins identified on rye physical map. 153
Figure 4. 35 Box-whisker plots showing the allele effects for the SNP markers (Xuos519455, Xuos76228a, Xuos76228b, and Xuos271947) (p < 2.76e-04) 158
Figure 4. 36 Box-whisker plots showing the allele effects for the SNP markers (Xuos612807, Xuos76837, Xuos617869, and Xuos370689) (p < 2.76e-04) 161
Figure 4. 37 Box-whisker plots showing the allele effects for the SNP markers (Xuos2344, Xuos643564, Xuos276365, and Xuos80120) (p < 2.76e-04) 164
Figure 4. 38 Box-whisker plots showing the allele effects for the SNP markers (Xuos651130, Xuos524368, Xuos373302, and Xuos172463) (p < 2.76e-04) 166
Figure 4. 39 PCA bi-plot visualizing SNP effects on WFS analyzed for rye population of 96 genotypes 171
Figure 4. 40 PCA bi-plot visualizing SNP effects on cyanidins analyzed for rye population of 96 genotypes 172

LIST OF APPENDICES

(Supplied as a flash drive to be attached to the thesis)

Appendix 1. Frequency distribution for WFS data obtained for rye population in five field trials……A1

Appendix 2. Frequency distribution and correlation analysis for FLN data obtained for rye population in four studies……A2

Appendix 3. Frequency distribution and correlation analysis for PGH data obtained for rye population in four studies ……A3

Appendix 4. Frequency distribution and correlation analysis for DTA data obtained for rye population in four studies ……A4

Appendix 5. Frequency distribution and correlation analysis for PHT data obtained for rye population in four studies ……A5

Appendix 6. Frequency distribution and correlation analysis for TIL data obtained for rye population in four studies ……A6

Appendix 7. Frequency distribution and correlation analysis for FLA data obtained for rye population in four studies……A7

Appendix 8. Development trait data for different growth habit classes of rye A8

Appendix 9. Anthocyanins identified in leaf tissues of cold-acclimated rye genotypes E1

Appendix 10. Anthocyanins identified in crown tissues of cold-acclimated rye genotypes.. .....E2

Appendix 11. Chemical structure of peleargonidin glucosides identified in cold-acclimated rye tissues..... A11

Appendix 12. Chemical structure of cyanidin glucosides identified in cold-acclimated rye tissues.. ..... A12

Appendix 13. Chemical structure of delphinidin glucosides identified in cold-acclimated rye tissues..... A13

Appendix 14. All significant MTA with developmental traits, WFS and LTT identified by GWAS of rye population E3

Appendix 15. Allele distribution for SNP markers of groups 1 and 2 strongly associated with WFSand group 3 associated with CBFs in rye population of 96 genotypes……E4

Appendix 16. All significant MTAs with anthocyanins and WFS identified by GWAS of rye population E5

Appendix 17. Biosynthesis of anthocyanins in plants. A14
Appendix 18. Allele distribution for 16 SNP markers strongly associated with WFS and anthocyanins in rye population of 96 genotypes ……..E6

LIST OF ABBREVIATIONS

3GT	:	Anthocyanidin 3-O-glucosyl- transferase
AARS	:	Aminoacyl-tRNA synthetase
ABA	:	Abscisic acid
ABC	:	ATP-binding cassette
ABRE	:	ABA responsive element
AFP	:	Antifreeze protein
ALDH	:	Aldehyde dehydrogenase
AM	:	Association mapping
ANS	:	Anthocyanidin synthase
AP2	:	APETALA2
bHLH	:	Basic helix-loop-helix
BIPP2C1	:	Benzothiadiazole-induced protein phosphatase 2C1
BLUE	:	Best linear unbiased estimates
BR	:	Brassinosteroid
BZ	:	Bronze
BZR	:	Brassinazole resistant
CAMTA	:	Calmodulin-binding transcriptional activator
CBF	:	C – repeat binding factor
CBL	:	Calcineurin B-like protein
CBP	:	Calcium binding protein
CDPK	:	Calcium-dependent protein kinase
CHS	:	Chalcone synthase
CHUP	:	Chloroplast unusual positioning protein
cM	:	Centimorgan
CML	:	Calmodulin like protein
COR	:	Cold – regulated
COR413-PM	:	Cold-regulated plasma membrane 413 protein
CPK	:	Calcium-dependent protein kinase
CRT	:	C – repeat
CS	:	Cysteine synthase
CTAB	:	Hexadecetyltrimethylammonium bromide
CTL	:	Choline transporter-related
Cya-3,5-diGlc	:	Cyanidin 3,5-O-diglucoside
Cya-3-AcGlc-5-Glc	:	Cyanidin 3-O-acetylglucoside-5-O-glucoside
Cya-3-Glc	:	Cyanidin 3-O-glucoside
Cya-3-*pC*ou-Sam	:	Cyanidin 3-*p*-coumaryl-sambubioside
Cya-3-Rut	:	Cyanidin 3-O-rutinoside
Cya-3-Sam	:	Cyanidin 3-sambubioside

Cya-3-Sam-5-Glc	:	Cyanidin 3-sambubioside-5-glucoside
Cya-3-Xyl-Glc	:	Cyanidin 3-xyloglucoside
Cya-*p*-Cou-diGlc	:	Cyanidin *p*-coumaryl-diglucoside
Del-3-Caf-Glc	:	Delphinidin 3-O-caffeoyl-glucoside
Del-3-*p*Cou-diGlc	:	Delphinidin *p*-coumaryl-diglucoside
Del-3-*p*Cou-Glc	:	Delphinidin 3-O-*p*-coumaryl-monoglucoside
DFR	:	Dihydroflavonol 4-reductase
DHN	:	Dehydrin
DRE	:	Dehydration responsive
DREB	:	Dehydration responsive binding element
DTA	:	Days to anthesis
EBF	:	EIN-binding F-box
EDC	:	Enhancer of mRNA-decapping protein
EIN	:	Ethylene insensitive
ERF	:	Ethylene – Responsive Element
ET	:	Ethylene
EXLA	:	Expansin-like A
F3H	:	Flavanone 3-hydroxylase
FAO	:	Food and Agriculture Organization
FDR	:	False discovery rate
FLA	:	Flag leaf area
FLC	:	Flowering locus C
FLN	:	Final leaf number
Fr-2	:	Frost resistance-2
FRI	:	FRIGIDA
FT	:	Flowering locus T
G×E	:	Genotype by Environment Interaction
GA	:	Gibberellic acid
GA2OX	:	Gibberellin 2-beta-dioxygenase
Gb	:	Giga base
GBS	:	Genotyping by sequencing
GLO3	:	Peroxisomal (S)-2-hydroxy-acid oxidase 3
GNC	:	GATA nitrate-inducible carbon-metabolism involved
GNL	:	GNC-Like
GWAS	:	Genome-wide association studies
h^2	:	Broad sense heritability
HCK	:	Tyrosine kinase
HHP	:	Heptahelical protein
HPLC-QTOF MS	:	High-pressure liquid chromatography-quadrupole time of flight mass spectrometry
IBP	:	Ice-binding protein

ICE	:	Inducer of CBF expression
IRIP	:	Ice recrystallization inhibition protein
JA	:	Jasmonic acid
JAC	:	J-domain protein required for chloroplast accumulation response
JAR1	:	Jasmonate-resistant 1
JAZ	:	JASMONATE-ZIM DOMAIN
LCAT1	:	Lecithin-cholesterol acyltransferase
LD	:	Linkage Disequilibrium
LEA	:	Late Embryogenesis Abundant
LRR	:	Leucine-rich repeat
LT	:	Low temperature
LTT	:	Low temperature tolerance
MAF	:	Minimum allele frequency
Mal-3-*pC*ou-Glc	:	Malvidin 3-O-*p*-coumaryl-monoglucoside
Mb	:	Mega base
MeJA	:	Methyl jasmonate
MLM	:	Mixed linear model
MTERF	:	Mitochondrial transcription termination factor
MYB	:	MYB proto-oncogene, transcription factor
NCBI	:	National Cancer for Biotechnology Information
NGS	:	Next generation sequencing
OPR	:	Oxophytodienoate reductase
OST1	:	Open Stomata1
PAL	:	Phenylalanine ammonia-lyase
PCA	:	Principal component analysis
Pel-3-6-Mal-βGlc	:	Pelargonidin 3-O-(6-O-malonyl-beta-D-glucoside)
Pel-3-Glc	:	Pelargonidin 3-O-glucoside
Pel-3-Sam	:	Pelargonidin 3-sambubioside
Peo-3-Rut	:	Peonidin 3-O-rutinoside
Pet-3-*p*Cou-Glc	:	Petunidin 3-O-*p*-coumaryl-monoglucoside
PGH	:	Prostrate growth habit
PHT	:	Plant height
PIF	:	Phytochrome interacting factor
PPD	:	Photoperiod
QTL	:	Quantitative trait locus
R / FR	:	Red / Far – red
RFLP	:	Restriction fragment length polymorphism
RIL	:	Recombinant inbred line
ROS	:	Reactive oxygen species
SAM	:	Shoot apical meristem

SAM tools	:	Sequence Alignment/Map tools
SNP	:	Single nucleotide polymorphisms
SOC	:	SUPPRESSOR OF OVEREXPRESSION OF CONSTANS 1
SSR	:	Simple sequence repeats
TIL	:	Top internode length
UGT	:	UDP glucose-flavonoid 3-O-glucosyltransferase
UV	:	Ultra – violet
VCF	:	Variant call format
VRN	:	Vernalization locus
WEB	:	Weak chloroplast movement under blue light
WFS	:	Winter field survival
XAT3	:	Alpha-1,3-arabinosyltransferase-like
XRN	:	Exoribonuclease
XYXT1	:	Beta-1,2-xylosyltransferase1
ZPR1	:	Zinc finger protein1

CHAPTER 1

INTRODUCTION

1.1 Winter rye – a cold-hardy winter cereal

Rye (*Secale cereal* L.*)* is a grass belonging to the Triticeae tribe of the Pooideae subfamily, which also includes wheat (*Triticum aestivum* L.), barley (*Hordeum vulgare* L.), oats (*Avena sativa*), and several forage grasses. The production volume of grain from cultivated rye (*Secale cereale* ssp. *Cereale* L.) is ranked tenth among the Triticeae species. Worldwide, rye is a relatively small crop (11.3 million tons in 2018; http://www.fao.org/faostat) and mainly grown for its grain that is destined for food or feed purposes. In comparison to most cereal crops, rye has high biotic stress resistance and high tolerance to abiotic stresses such as frost (Geiger and Miedaner, 2009; Schlegel, 2014). These properties enable rye to survive well during winter at Northern latitudes and rye varieties adapted to the Canadian Prairies exhibit the highest freezing tolerance among all cultivated winter cereals (Fowler *et al.*, 2014). The inherent high freezing tolerance makes rye an ideal plant system to study physiological and molecular mechanisms underlying winter field survival (WFS) in cereals grown in temperate climates. These studies are important for the development of more resilient cereals to counteract the effects of climate change.

Genome sequencing data and phylogenetic studies show the rye diploid genome (2n = 2x = 14; RR) is highly syntenous with the A, B, and D genomes of hexaploid wheat, and the H genome of diploid barley. Rye has a high haplotype diversity as it is an open-pollinated species, (Li *et al.*, 2011*b*), whereas the self-pollinating wheat and barley cultivars have lost a large amount of their initial genetic diversity due to extensive breeding.

1.2 Cold acclimation increases winter-survival potential in winter cereals

Most of the temperate grasses exhibit low freezing tolerance at the very young seedling stage but develop low-temperature tolerance (LTT) through an extended acclimation to low but non-freezing temperatures (Thomashow, 1999). Cold acclimation occurs prior to the winter season for autumn-seeded cereals and starts when plants respond to environmental signals received from a gradual reduction of daily temperature, photoperiod, light intensity, and red/far-red ratio in

incoming light (Franklin and Whitelam, 2007; Lee and Thomashow, 2012; Legris *et al.*, 2016). Two major physiological processes occur in plants during the four to eight-week long cold acclimation period: (a) an accumulation of LTT; and (b) a shift from vegetative to reproductive, growth at the shoot apical meristem, a process termed as vernalization. An early response to inducing environmental signals result in an early start, longer acclimation period, and higher amount of accumulated LTT tolerance (Fowler, 2008). Upon vernalization saturation (floral transition), further development of floral organs is paused until spring, when inductive photoperiod and warm temperature stimulate new growth from the crown tissue (Law and Worland, 1997).

During cold acclimation, winter-hardy plants undergo a multitude of developmental adjustments to build up LTT (Thomashow, 1999). Growth is repressed and energy is channeled towards production of various stress-protection compounds like cryo-protectants (Shinozaki and Yamaguchi-Shinozaki, 1996; Cook *et al.*, 2004), antifreeze proteins (Griffith and Yaish, 2004), cold shock proteins (Sasaki and Imai, 2012), and antioxidants (Cook *et al.*, 2004). Carbon pools in crowns are also stockpiled to be utilized during deacclimation periods during winter and regrowth in the spring (Hüner *et al.*, 2012; Zuther *et al.*, 2015). The cold-induced morphological changes in cereals generally include increased compact and dwarf growth (Scott *et al.*, 2004) and switch to prostrate growth habit (Roberts, 1990; Gray *et al.*, 1997; Limin and Fowler, 2000). Many of the physiological responses to low temperature are mediated by epigenetic modifications at the histone and DNA levels (Pavangadkar *et al.*, 2010; Baulcombe and Dean, 2014) and extensive crosstalk between signaling pathways involving Ca^{2+}, reactive oxygen species (ROS), and phytohormones (Smékalová *et al.*, 2014; Eremina *et al.*, 2016; Hu *et al.*, 2017). The genetic mechanisms of cold acclimation are very complex as revealed by transcriptome, metabolome, proteomic, and transgenic studies primarily done in Arabidopsis (Fowler and Thomashow, 2002; Stitt and Hurry, 2002; Cook *et al.*, 2004; Hannah *et al.*, 2005; Kaplan *et al.*, 2007).

1.3 Genetics of cold tolerance

The vernalization 1 (*VRN1*) and Frost Resistance (*FR*) loci on homoeologous group 5 chromosomes are the major determinants for LTT within the Triticeae tribe (Law and Jenkins, 1970; Sutka and Snape, 1989). Winter cereals seeded in the autumn carry recessive *VRN1* alleles encoding the vernalization requirement and development of high freezing tolerance upon cold acclimation (Brule-Babel and Fowler, 1988). In addition to *VRN1*, the *FR-2* locus explains about

30–67% of the LTT variance in wheat, barley, and rye bi-parental populations (Francia *et al.*, 2004; Båga *et al.*, 2007; Erath *et al.*, 2017). Cold-tolerance provided by the *FR-2* loci is mediated by *C-repeat Binding Factors* (*CBFs*) transcription factors, which regulate expression of cold-regulated (*COR*) genes (Stockinger *et al.*, 1997; Thomashow *et al.*, 2001). The importance of *CBF* genes during cold acclimation is demonstrated by up-regulation of *CBF* genes in transgenic Arabidopsis resulting in enhanced cold tolerance at both low and normal temperatures (Gilmour *et al.*, 2000, 2004). In addition to *CBF* regulon, there are additional *CBF*-independent pathways responding to cold stress (Xin and Browse, 1998; Seki *et al.*, 2001; Fowler and Thomashow, 2002; Kreps *et al.*, 2002; Vlachonasios *et al.*, 2003; Vogel *et al.*, 2005; Park *et al.*, 2018).

1.4 A genome wide association study (GWAS) to identify trait-marker relationships

Association or linkage disequilibrium (LD) mapping utilizes GWAS to identify causative alleles / loci for traits showing variation in a population of unrelated genotypes (Alqudah *et al.*, 2020). Genotyping of the population is generally done by genotyping by sequencing (GBS) techniques, which produce a large number of single nucleotide polymorphism (SNP) markers and greatly enhances the power of LD mapping (Voss-Fels and Snowdon, 2016; Nguyen *et al.*, 2019). Through GBS of large populations, the limitations of linkage mapping can be overcome and polygenic traits such as LTT and WFS in plants can be studied. The low disequilibrium linkage (LD) of about 520 bp in rye (Li *et al*., 2011*a*) is of advantage for association mapping. With a large number of SNP markers obtained by GBS, availability of a near complete assembly of the rye genome (Rabanus-Wallace *et al.*, 2021), and phenotypic data obtained from repeated trials, the basic requirement for association mapping are met to understand the molecular basis of WFS in rye.

In this study, a panel of 96 rye genotypes from diverse geographic regions was assessed for WFS, LTT (LT_{50} values), and seven developmental traits [final leaf number (FLN), prostrate growth habit (PGH), plant height (PHT), days to anthesis (DTA), flag leaf area (FLA), top internode length (TIL), and anthocyanin (ANT) production]. The population was genotyped by GBS and SNP alleles associated with the various traits were identified by association mapping. In total, 679 marker-trait associations (MTA; $p<0.01$) were obtained and several of the traits were shown to be genetically interconnected through shared MTAs. The ten most significant SNPs were all associated with WFS and corresponded to nine strong candidate genes with associations to cold

hardiness in other plant species. Analyses of leaf and crown tissues using a high-performance liquid chromatography system combined with quadrupole time-of-flight mass spectrometry (HPLC-QTOF MS/MS) led to the identification of 18 anthocyanin compounds that accumulated during cold acclimations. Production of eleven different glycosylated anthocyanins associated with increased WFS and 15 candidate genes for ANT were identified in the study.

1.5 Hypothesis

(i) Trait variation for WFS in rye is to a large extent determined by genotype, which allows candidate genes for the trait to be revealed by LD mapping.

(ii) WFS in fall-seeded cereals depends on interactions between genes determining LTT and plant development.

(iii) Accumulation of anthocyanin compounds during cold acclimation increases WFS potential in rye.

1.6 Objectives

(i) Determine WFS by field tests and LTT by freezing tests for rye panel of 96 genotypes.

(ii) Analyze six developmental traits and anthocyanin concentration and type for rye panel grown in the greenhouse or field.

(iii) Genotype rye panel by GBS method.

(iv) Identify SNPs/genes associated with WFS, LTT, and developmental traits by association mapping.

CHAPTER 2

LITERATURE REVIEW

2.1 The rye genome

Cultivated rye (*Secale cereale* ssp. *cereale* L.) is an annual crop belonging to the Triticeae tribe of the Pooideae subfamily within the Poaceae family (Fig 2.1). Rye is adapted to temperate climates in the Northern hemisphere like several other Pooideae crops such as wheat (*Triticum aestivum* L.), barley (*Hordeum vulgare* L.), and oats (*Avena sativa* L.). DNA sequence comparisons show the rye R genome is closely related to the wheat individual genomes (A, B, and D) and barley H genome, but is about 1.5-fold larger, (2C=15.95 pg; 1C=7.9 Gb) and contains a high amount (84.4%) repetitive DNA (Doležel *et al.*, 2018; Rabanus-Wallace *et al.*, 2021). The high synteny among the Triticeae genomes supports they are all derived from a common progenitor genome (Moore *et al.*, 1995; Martis *et al.*, 2013). Overtime, numerous translocations have occurred within the rye genome as initially revealed by genetic mapping (Devos *et al.*, 1993) and later confirmed by transcript mapping and genome sequence assemblies (Martis *et al.*, 2013; Rabanus-Wallace *et al.*, 2021). In contrast to wheat and barley, rye maintains a high haplotype diversity as propagation occurs by cross-pollination due to the presence of an effective gametophytic self-incompatibility system (Lundqvist, 1956). However, some erosion of genetic diversity is observed in improved rye germplasm, whereas landraces and wild rye species exhibit very high genotypic diversity that is available for mining (Schlegel, 2014; Targońska *et al.*, 2015).

2.1.1 Origin and domestication or rye

Rye is believed to originate from two separate regions in Southwestern Asia: (i) a primary region stretching from Tabriz (Iran) to the Black Sea and (ii) a secondary region east of Iran and towards Afghanistan (Schlegel, 2014). During the 3,000–4,000 BC time period, rye cultivation started around the Caspian Sea, from where it spread to Eastern Europe around 500 BC. The migration northward likely occurred through Turkey and across the Balkan Peninsula followed by dissemination into Russia, Scandinavia, Poland and Germany (Schlegel, 2014). Over time, a strong rye belt developed from Germany to Eastern Siberia and was maintained until the 1960s. In

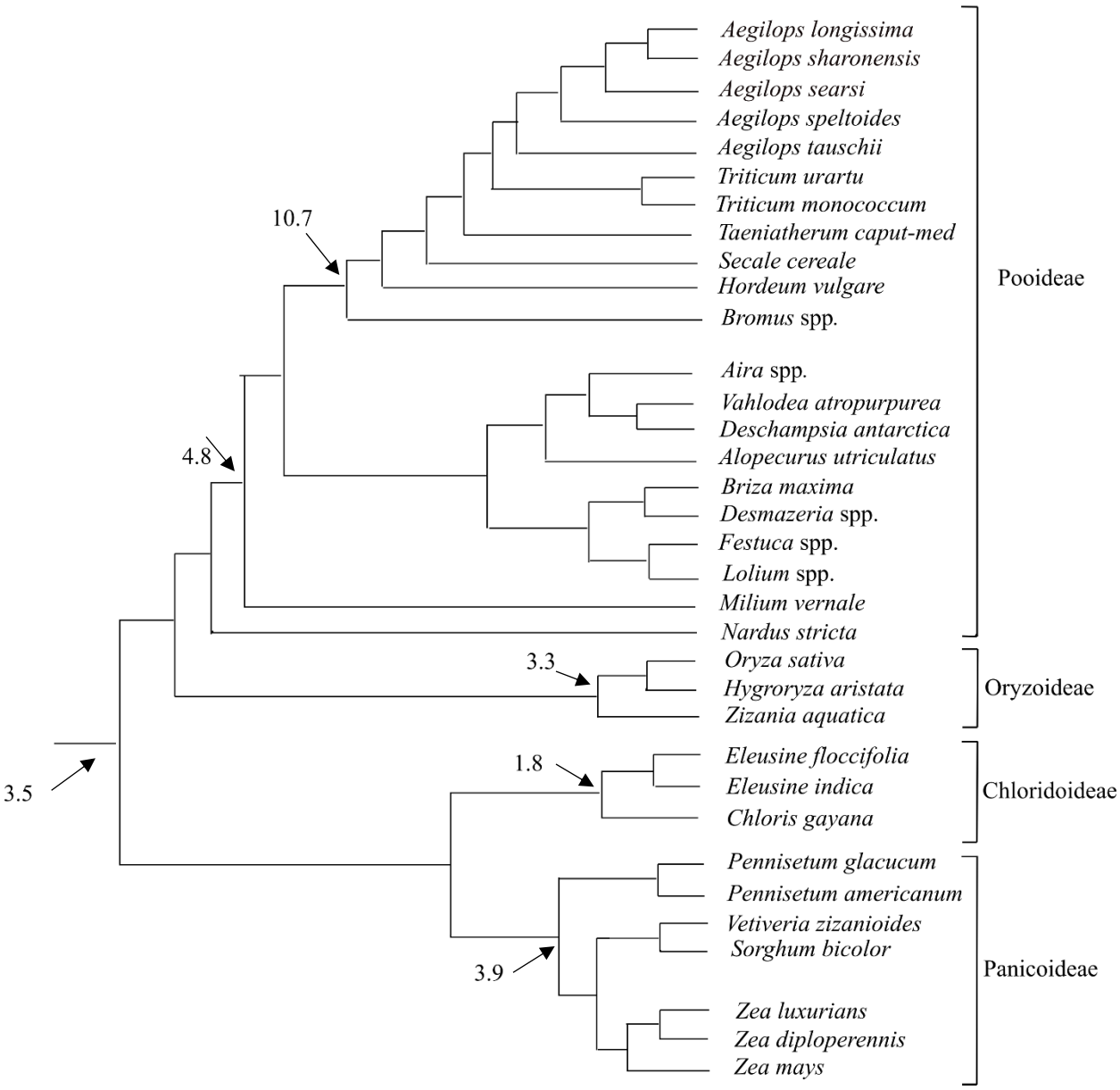

Fig. 2.1. Phylogeny and evolution of genome size among the grasses. The illustration shows the increase of genome size from the ancestral grasses (3.5 pg of DNA per 2C nucleus) to large genomes of the Triticeae ancestor (10.7 pg DNA per 2C nucleus). The relationships among the subfamilies are based on data from Kellogg, 1998.

Scandinavia, winter-hardy rye was introduced to areas north of the 60th parallel, where winter wheat does not overwinter and summers are too short for spring wheat cultivation. In the sixteenth and seventeenth century, European settlers brought rye to North America and western South America (Schlegel, 2014). The earliest Chinese rye came from southwestern Asia and later spread to Japan (Schlegel, 2014). All present-day rye cultivars are derived from *Secale cereale*, which shows highest genetic identity to *S. vavilovii* (Jones and Flavell, 1982). It is postulated crossbreeding *Secale vavilovii* with the perennial *S. anatolicum* and *S. montanum* led to the development of *S. cereale* (Schlegel, 2014).

2.1.2 Rye production and utilization

In comparison to most cereal crops, rye has a relatively high pathogen resistance and a high tolerance to abiotic stresses such as cold, drought, and salinity (Geiger and Miedaner, 2009; Schlegel, 2014). This allows rye to be cultivated on nutrient-poor soil that is not suitable for most other crops. During 2019, the harvested area and worldwide production of rye grain was 4.2 million hectares and 12.8 million tonnes, respectively (http://www.fao.org/faostat). Russia and Poland in Eastern and Germany in Western Europe are the largest rye producers in the world. Rye production in Canada was 333,400 tonnes in 2019 (http://www.fao.org/faostat). In Saskatchewan, 43,000 tonnes winter rye was harvested in 2018: thus, much lower than winter wheat at 156,000 tonnes (www.agriculture.gov.sk.ca). Most of the currently cultivated rye are open-pollinated varieties, but hybrid lines are increasing in popularity due to 10-20 % higher yields (Geiger and Miedaner, 2009). Rye grain is mainly used for production of animal feed, bread, and alcoholic beverages like beer, whiskey, and vodka. A small amount of rye is also grown as fodder, green manure, or raw material for the biofuel industry (Newell and Butler, 2013; Galán *et al.*, 2020).

2.2 Growth habits among temperate cereals

Plant development is defined as progression of the plant life cycle in distinct phases broadly consisting of seed germination, vegetative phase, reproductive phase, and senescence. These stages are influenced by environmental conditions such as temperature and light conditions, which control growth, development, distribution, and seasonal behavior of plants (Andrés and Coupland, 2012). Flowering time is a critical factor for seasonal and geographical adaptation of plants and determines the reproductive success of species. Due to adaptation to a wide range of agroclimatic regions, both annual and perennial types exist among the Triticeae crops including rye (Schlegel,

2014). The annual rye flowers once during its life cycle, whereas perennial rye rotates multiple times between vegetative and reproductive growth and can survive for several years. Three growth habits are broadly recognized among the annual Triticeae crops: spring, facultative (intermediate), and winter types. Based on their day-length requirements, the Triticeae crops are further classified as short-day, long-day, or day-neutral (Garner and Allard, 1920). Short-day plants flower when the night length is longer than a critical minimum, whereas long-day plants flower when the day becomes longer, and day-neutral plants flower regardless of day-length.

2.2.1 Spring type growth habit

In cereal crops, spring types are long-day plants that do not need a cold period to induce flowering (vernalization). Upon being sown and established in the spring, the spring types transition quickly from the vegetative to reproductive phase in the early summer, thus allowing grains to mature and be harvested in the autumn (Fig 2.2A). In contrast to spring wheat, designated spring rye varieties have a very weak vernalization requirement that is fulfilled within 10-12 days of cold exposure in the early spring (Schlegel, 2014). Nowadays, few cultivated rye varieties are spring types and most rye grown is of winter type with long-day photoperiod requirement (Schlegel, 2014). This preference for winter types may be due to the early recognition that spring cereals are less freezing tolerant than winter and facultative types (Hayes and Aamodt, 1927).

2.3.2 Winter type growth habit

Winter types are biennial (winter-annual) plants that are seeded in the autumn, overwinter as seedlings, and flower the following summer (Fig 2.2B). Those with a long-day photoperiod requirement require four to eight weeks of exposure to non-freezing temperature (typically 4-10 °C) prior to winter to become vernalized (Chouard, 1960; Thomashow, 1999), which leads to transition of the vegetative shoot apical meristem to an early reproductive phase prior to winter. Simultaneously with cold acclimation, the plants accumulate LTT during a cold acclimation process (Fig 2.3), which is described below. During vernalization/cold acclimation, new leaf primordia are continuously being laid down on the flanks of the shoot apical meristem (Fig 2.4). Due to the additional leaf initials, mature winter cereals plants produce a high final leaf number (FLN), typically 12 to 22 leaves depending on the genotype and time to vernalization saturation. Spring types, with no vernalization requirement, produce only seven to eight leaves. Thus, there

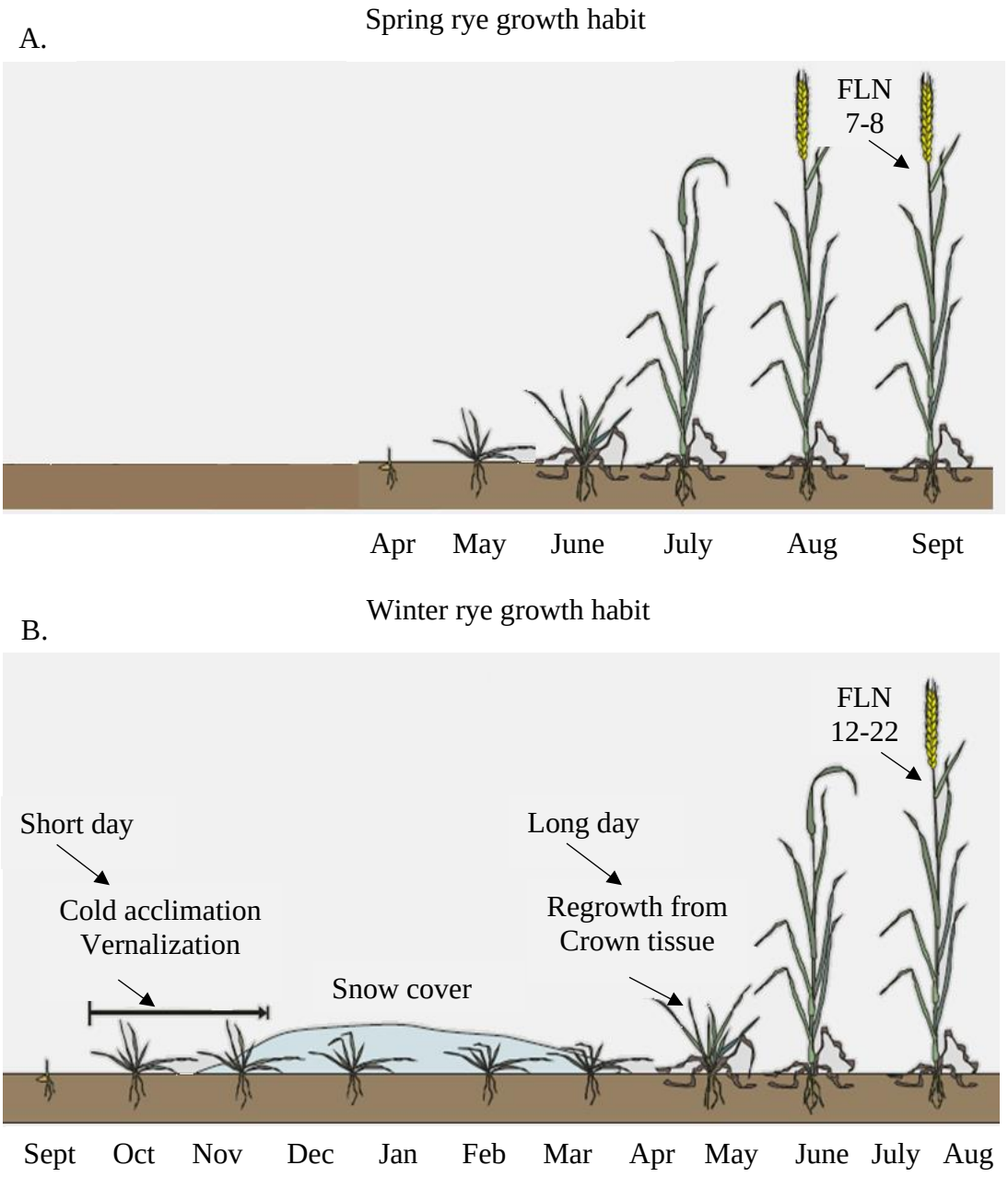

Fig. 2.2. Spring and winter rye growth habits. (A) The spring rye cultivars seeded in mid-spring quickly undergo the transition from the vegetative to the reproduction phase. (B) The autumn seeded winter rye cultivars have an obligatory requirement for cold acclimation and vernalization period before long days in the spring for floral initiation and harvested at the end of summer.

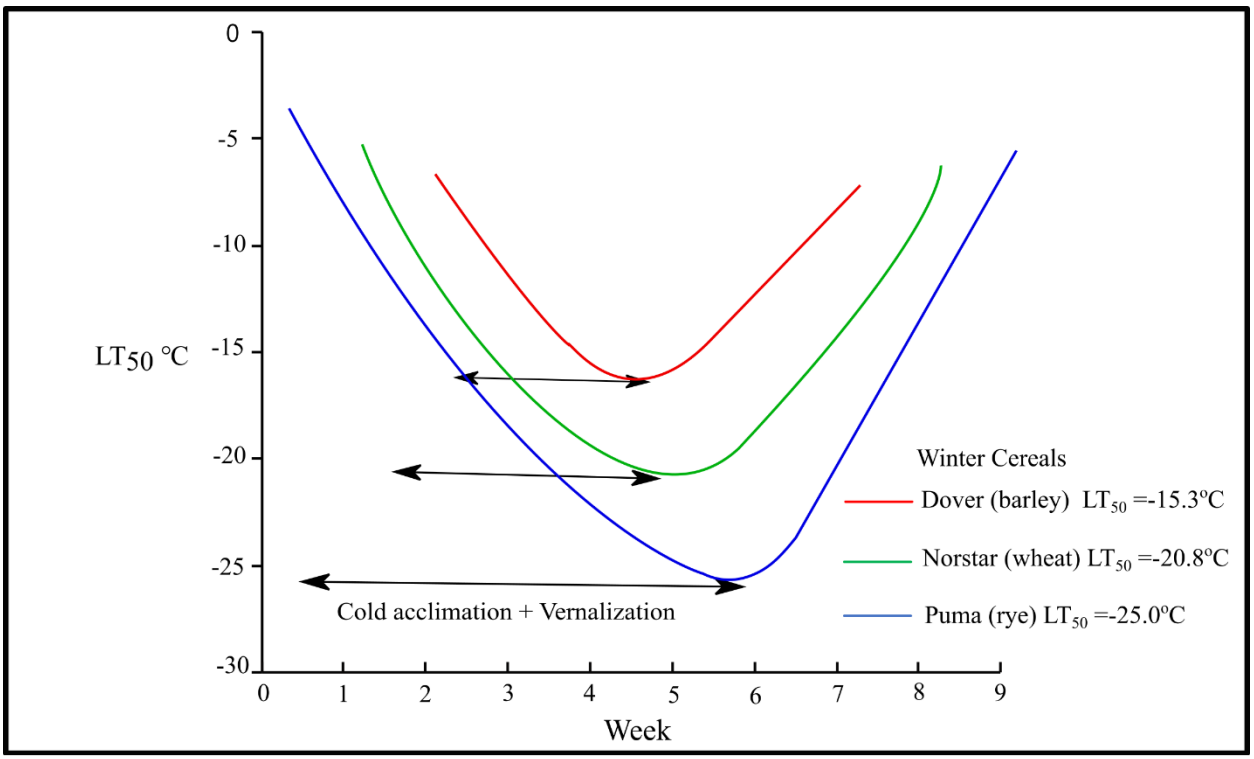

Fig. 2.3. schematic sketch of cold acclimation and vernalization period in winter cereals. Cold acclimation and vernalization period are longer in rye compared to wheat and barley. Winter rye has more time to accumulate LTT and hence can tolerate lower temperatures in extremely cold winters on the Canadian prairies (LT_{50} values from Fowler *et al*., 1996*b*).

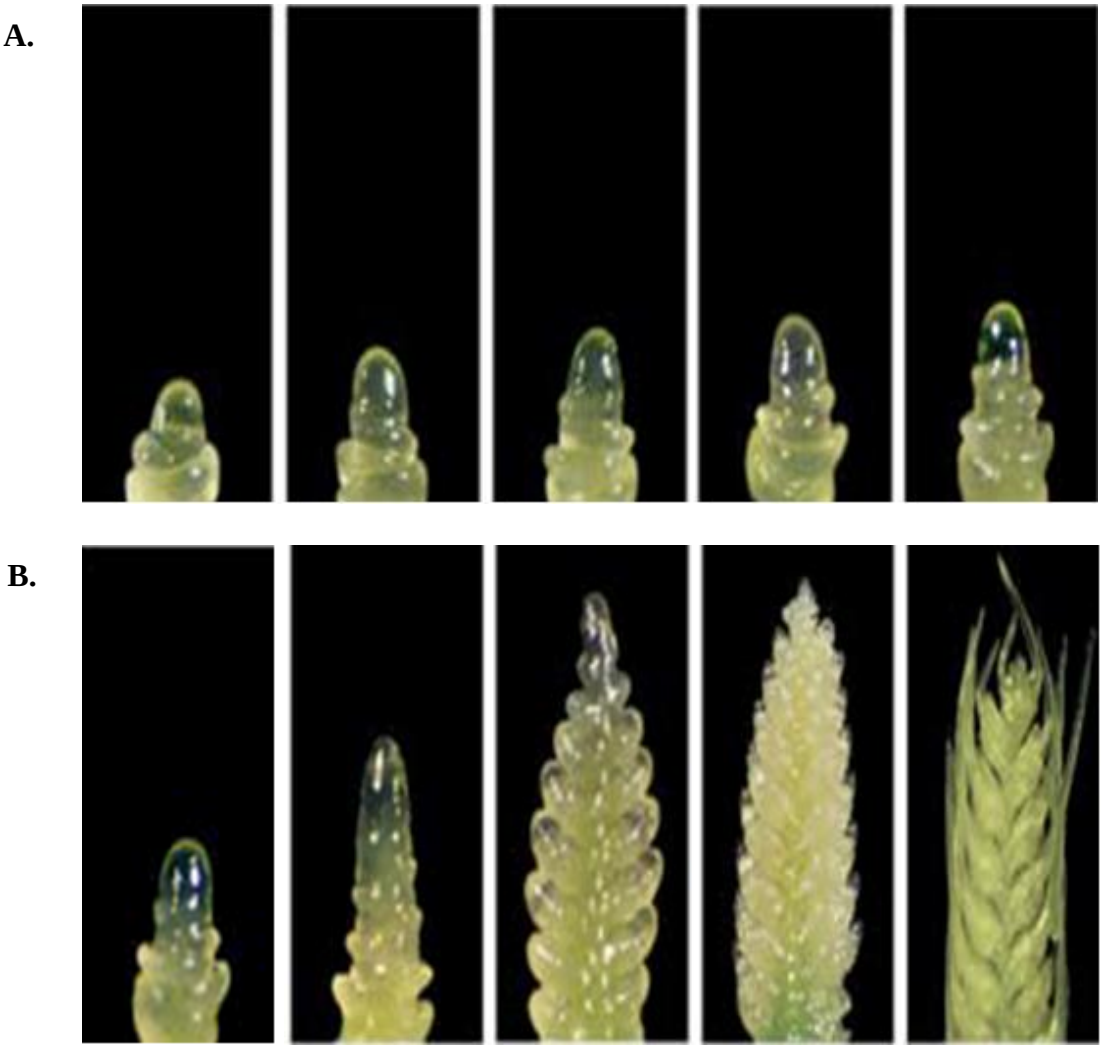

Fig. 2.4. Transition from vegetative to reproductive growth at the shoot apical meristem. Winter-habit plants in the temperate regions need prolonged exposure to low but non-freezing temperatures to induce flowering under inductive photoperiods (long day). This process is defined as vernalization. (A) During vernalization, the vegetative apical meristem transitions to the reproductive phase in autumn (short day), but further progress (B) can occur only under the inductive photoperiod conditions (long day) in the spring, leading to flowering (Picture from http://www.fao.org/docrep).

Is a positive correlation between LTT (LT_{50} values), WFS and FLN in winter cereals (Fowler *et al.*, 1996*b*).

At the completion of the vegetative phase, formation of new leaf primordia ceases and the shoot apical meristem dome becomes enlarged (Waddington *et al.*, 1983). Thereafter, the meristem starts to elongate, and floret primordia are formed above each leaf primordia, which is observed as microscopically visible double-ridges on the shoot apical meristem; this stage marks the vernalization saturation when an early reproductive shoot apical meristem has been formed (Waddington *et al.*, 1983). Due to the short-day conditions in autumn, further developments of the early inflorescence and stem elongation are paused until spring (Trevaskis *et al.*, 2007). This developmental arrest in long-day winter types is an adaptive response to prevent production of cold-sensitive floral organs in the late autumn (Fowler *et al.*, 1996*b*). In the spring, regrowth initiates from the crown tissue and the long day conditions allows early inflorescences to resume development of spikes to yield mature seeds in the late summer. In summary, cold acclimation, vernalization, and timing of floral transition in winter types are important for the accumulation of LTT, timing of floral transition, delay of floral morphogenesis until spring, and winter survival. The plants response to temperature and light signals are the main environmental determinants for the winter growth habit (Trevaskis *et al.*, 2007).

2.3.3 Facultative type growth habit

The facultative types have much reduced or no vernalization requirement, but often possess strong photosensitivity (von Zitzewitz *et al.*, 2005; Kosová *et al.*, 2008). These types can cold acclimate when exposed to low temperature in the autumn. Thus, facultative types are either seeded in the early spring or in the late autumn in areas with mild winters. As compared to winter types, over-wintering facultative types resume growth earlier in the spring and flower earlier in the summer (Kosová *et al.*, 2008).

2.4 Factors determining winter survival potential among winter cereals

Temperate crops like wheat and rye are relatively resistant to chilling stress (0–15 °C) and can tolerate temperatures a few degrees below zero without prior experience of cold. However, much higher levels of freezing tolerance are obtained after cold acclimation in the autumn (Thomashow, 1999; Chinnusamy *et al.*, 2007; Ding *et al.*, 2019). The cold hardening process

typically allows winter wheat and rye varieties adapted to Northern latitudes to tolerate -19 to -22 °C temperatures at crown level (e.g. LT_{50} values) prior to winter (Fowler *et al.*, 1996*b*) (Table 2.1). Certain rye genotypes develop exceptionally high freezing tolerance with LT_{50} values around -25 °C. This level of LTT provides reliable WFS for rye on the Canadian Prairies and would be desired for all winter wheat and barley cultivars grown at these latitudes. The LT_{50} values obtained upon cold acclimation and WFS averaged over several years of field trials on the Prairies are highly correlated (r = -0.95) for winter wheat (Limin and Fowler, 2000). This supports freezing tolerance level prior to winter is the main factor for WFS in this region.

During winter, freezing of plant tissues starts in the vascular system of the bottom and oldest leaves and then migrates to sequentially younger leaves (Livingston *et al.*, 2018). Freezing leads to severe dehydration stress when ice crystals form in the apoplast or, more severely, in the cytoplasm. Due to frost damage, much of the leaf and root tissues will not survive winter, but crown located below soil surface needs to stay alive throughout winter to assure regrowth in the spring. Thus, WFS at any time during winter is determined by the remaining LTT in the crown tissue. A gradual depletion of accumulated LTT in crowns occurs throughout the winter months to reach very low levels in the spring. Thus, differences in deacclimation rates is expected to explain some of the WFS variation among genotypes (Rapacz *et al.*, 2017); however, deacclimation rates do not necessarily relate to genotypes cold acclimation rates or length of acclimation (Zuther *et al.*, 2015; Rapacz *et al.*, 2017).

WFS is affected by many environmental factors such as temperature minima during winter, length of winter, snow cover depth, and the number of freeze-thaw incidents (Gusta and Wisniewski, 2013). For example, can delayed seedling emergence in autumn and/or early onset of winter cause early termination of cold acclimation and thereby increase the risk of winter kill due to low accumulated LTT? An extended period of low soil temperature (< -10°C), sometimes due to lack of snow cover, often leads to extensive winter kill for the most winter-hardy wheat and barley genotypes. Deacclimation rates may also increase dramatically during repeated freeze-thaw cycles occurring in the winter. These types of weather incidents are expected to increase with climate change (Pagter and Arora, 2013), which urges the need of higher frost tolerance in overwintering crops.

When the soil temperature fluctuates around 0 °C, small ice crystals formed in the extra-cellular space of plant tissues grow larger and aggravate the dehydration stress. Cell lysis may

Table 2.1 Low temperature tolerance (LT_{50}) values determined for cold acclimated spring and winter cultivars of wheat and rye.

Cultivar	***LT_{50} (ºC)**	**Wheat/Rye growth habit**
		Spring habit
Glenlea	-5.7	wheat
Manitou	-6.0	wheat
Oslo	-6.7	wheat
Gazelle	-6.9	rye
Chinese spring	-8.5	wheat
		Winter habit
Cappelle	-12.0	wheat
Dover	-15.3	barley
Fredrick	-16.2	wheat
Augusta	-16.4	wheat
Pioneer 2548	-16.8	wheat
Bezostaja	-16.9	wheat
Cheyenne	-19.0	wheat
Winalta	-19.4	wheat
Hume	-20.2	wheat
Norstar	-20.8	wheat
Puma	-25.0	rye

*LT_{50} values from Fowler *et al.*, 1996*b.*

follow due to expansion-induced lysis (Uemura *et al.*, 2006) or ice crystals puncturing the plasma membrane (Pearce, 2001). Some protection against ice formation and recrystallization is provided by anti-freeze proteins, ice recrystallization inhibition proteins (IRIPs), and chitinases accumulating to high levels in the apoplast during cold acclimation of winter-hardy genotypes (Bredow and Walker, 2017). Resealing of membranes punctured by ice crystals is proposed to occur in Arabidopsis, where an endosome recycling protein, synaptotagmin SYT1, has a role in the healing process (Yamazaki *et al.*, 2008).

Temperatures hovering around 0°C under snow cover stimulate growth of psychrophilic pathogens such as snow molds, which can infect and kill overwintering cereals (Gaudet *et al.*, 1999). Thus, snow mold resistance in regions with long-lasting snow cover is important for winter survival of cereals. Fructan is proposed to give some protection against snow mold infections based on resistant wheat genotypes accumulate higher amounts of sugars as compared to susceptible genotypes and low fructan depletion during winter (Yoshida *et al.*, 1998; Meguro-Maoka and Yoshida, 2016). Other snow mold resistant wheat lines accumulate multi-domain cystatins to high levels in crowns (Christova *et al.*, 2006), whereas high amounts of catalase, superoxide dismutase, and peroxidase antioxidant activities are noted in crowns of snow mold resistant rye (Pociecha *et al.*, 2013).

Regrowth in the spring depends on survival of the crown tissue, from which new shoots and roots develop. The regrowth from surviving crowns may be reduced or not occur when a period of warm temperatures is followed by frost nights, as the crown has lost all of its frost tolerance at this stage. The initiation of roots from the lower apical region is especially sensitive to freezing as compared to regrowth of shoots from the upper region (Chen *et al.*, 1983); thus, overwintering plants may die in the early spring due to inability to form roots. This difference in shoot and root regrowth may relate to accumulation of higher freezing tolerance in the apical region of the crown as compared to the lower crown region during cold acclimation (Tanino and McKersie, 1985; Livingston *et al.*, 2006; Willick *et al.*, 2018).

2.5 VRN and CBF regulon have major roles for WFS in winter cereals

Genetic mapping studies of bi-parental populations show *Frost resistance* (*FR-2*) and *Vernalization 1* (*VRN-1*) regions located on homoeologous group 5 chromosomes account for 30 – 40% of the variance for LTT in wheat (Båga *et al.*, 2007) and barley (Francia *et al.*, 2004) (Fig

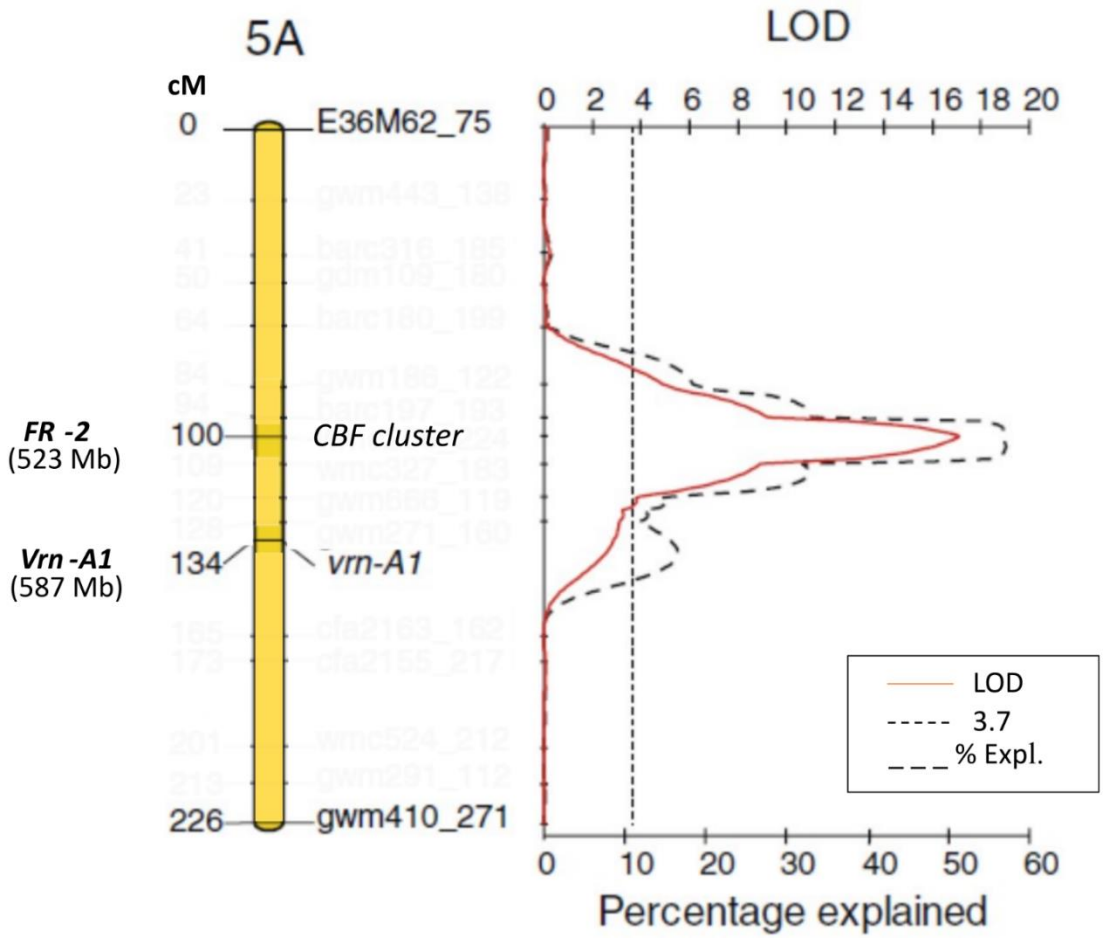

Fig. 2.5. Genomic regions associated with LTT in winter wheat. The 5A QTL included the *FR-2* and *Vrn-A1* loci that explained about 40% of the variance for LTT in winter wheat (Båga *et al*., 2007).

2.5). Association mapping of rye confirms *Fr-R2* is the main locus for LTT and explains up to 67% of the variance in freezing tolerance (Li *et al.*, 2011*a*; Erath *et al.*, 2017). All the *FR-2* loci in Triticeae species carry clusters of *CBF* genes (Skinner *et al.*, 2005; Miller *et al.*, 2006; Båga *et al.*, 2007; Campoli *et al.*, 2009), for which variations in *CBF* copy numbers and haplotypes are associated with LTT tolerance levels in wheat (Båga *et al.*, 2007; Knox *et al.*, 2010; Sieber *et al.*, 2016; Würschum *et al.*, 2017), barley (Francia *et al.*, 2007; Pearce *et al.*, 2013) and rye (Li *et al.*, 2011*a*; Erath *et al.*, 2017; Jung and Seo, 2019). However, a large-scale association mapping study of a panel of 1,739 European rye genotypes did not find a strong association between SNP variation for individual *CBF* genes and freezing tolerance (Zhao *et al*., 2013).

Although *VRN1* and *FR-2* appear to be the main loci determining cold hardiness in cereals, the two loci interact negatively with each other (Stockinger *et al.*, 2007; Dhillon *et al.*, 2010). A low *CBF* expression is observed in genotypes with active *VRN1*, such as spring types and cold acclimated winter types. Thus, *VRN1* down-regulates *CBF* expression after cold acclimation (Stockinger *et al.*, 2007).

2.6 The influence of light on vernalization response and cold acclimation

The cold signalling pathway leading to vernalization fulfilment and cold acclimation in winter cereals is optimized by the light and temperature conditions that occur in the autumn (Fig 2.6). An important environmental factor is day length, where short-days in the autumn promote higher accumulation of freezing tolerance in plants as compared to long-days (Crosatti *et al.*, 1999; Kim *et al.*, 2002; Lee and Thomashow, 2012). Light quality also has a role as demonstrated by COR14b protein accumulation in etiolated barley plants exposed to pulses of red and blue light, but not by far-red or green light pulses (Crosatti *et al.*, 1999). A decrease in the red to far-red ratio (R:FR) in incoming light that naturally occurs in the autumn increases the accumulation of cold tolerance in Arabidopsis (Franklin and Whitelam, 2007).

2.6.1 Photoperiod sensitivity in cereals

The photoperiod sensitivity in winter cereals promotes (i) expression of LT tolerance related genes during autumn when days are short, (ii) delay of flowering until spring, (iii) induction of flowering in spring as day-lengths are becoming longer (Fowler *et al.*, 2001). The *PHOTOPERIOD1* (*Ppd1*) gene is the main determinant for day-length sensitivity in Triticeae

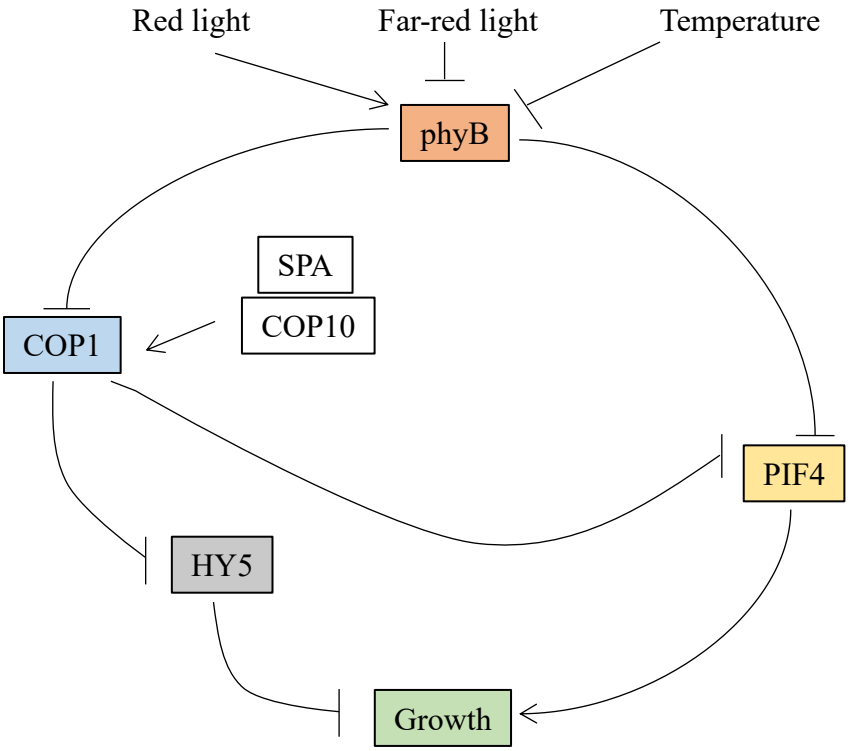

Fig. 2. 6. Interaction between light signaling and temperature. The first convergence point is the PhyB, which detects light and temperature. The signaling center, which is downstream of PhyB, contains two branches, one containing PIF4 and one with COP1 and HY5. Each of the main signaling components depends upon light and temperature conditions for their aggregation and/or localization dynamics. PhyB, phytochrome B; SPA, Suppressor of phyA; COP1, Constitutive photomorphogenic 1; HY5, Elongated hypocotyl 5; PIF4, Phytochrome interacting factor 4 (Redrawn from Legris *et al*., 2017).

species and exists as three homoeologous copies on the group 2 chromosomes in wheat (Law and Worland, 1997). *Ppd1* encodes a PSEUDO-RESPONSE REGULATOR (PRR) protein that is orthologous to Arabidopsis *PRR7*, a component of the circadian clock (Nakamichi *et al.*, 2007). Flowering is induced by Ppd1 in long-day plants, but different degrees of photoperiod-insensitivity is provided by various mutations in the *Ppd-B1* and *Ppd-D1* genes (Beales *et al.*, 2007; Díaz *et al.*, 2012; Shaw *et al.*, 2012).

2.6.2 Registration of light properties by photoreceptors

Light provides energy to drive CO_2 fixation in the photosynthesis reaction, which provides energy and metabolites to the plant's overall metabolism. In addition, light can through it's wavelength, intensity, duration and direction provide plants with environmental information that plants use to adjust their growth and development (Hayes, 2020). Incoming light signals are registered by at least five different classes of plant photoreceptors: UV-B receptor UVR8, red/far-red light phytochromes PHYA to E, blue/UV-A phototropins PHOT1 to 2, cryptochromes CRY1 to 3, UV-B and blue/UV-A Zeitlupe-type proteins (Paik and Huq, 2019). Phytochromes phyA and phyB switch between a red-light absorbing conformation (Pr) and a far-red light absorbing form (Pfr), of which activated Pfr translocate from the cytosol to the nucleus for interaction with various nuclear proteins (Kircher *et al.*, 2002; Rockwell *et al.*, 2006). For example, the E3-ligase CONSTITUTIVE PHOTOMORPHOGENIC 1 – SUPRESSOR OF PHYA-105 (COP1-SPA) complex, and bHLH transcription factors PHYTOCHROME INTERACTING FACTORS (PIFs) and basic zippers (bZIP) ELONGATED HYPOCOTYL5 (HY5) and its orthologue HY5 HOMOLOG (HYH) controlling photomorphogenesis are regulated by Pfr photoreceptors (Duek and Fankhauser, 2005; Monte *et al.*, 2007; Zhang *et al.*, 2011; Kahle *et al.*, 2020). The interaction between Pfr and PIFs results in degradation of both proteins (Paik and Huq, 2019).

Multiple photoreceptors register variations in day-length and entrain the light signals into the circadian clock, which keeps a roughly 24 h rhythm across a range of temperatures (Thomas, 2006) and can be considered a gatekeeper of environmental responses (Guadagno *et al.*, 2018). Through the distinct ratios between active Pfr to inactive Pr, plants can detect changes in light quality, quantity, and periodicity, which provide information about diurnal and seasonal time. Thus, the outputs from the circadian system in the form of 24-h gene expression profiles guides plants to adjust their physiological and developmental processes accordingly to the day or season

(Harmer, 2009; Shim *et al.*, 2017). A key output from the circadian clock is the oscillatory pattern of the CONSTANS (CO) transcript, for which the encoded CO activates *FT* transcription during long-days to promote flowering (Putterill *et al.*, 1995).

2.6.3 Integration of light and cold signals to regulate development

It was concluded from the early studies of cold acclimation that maximal cold acclimation in winter rye is dependent on interactions between light and temperature signals (Gray *et al.*, 1997). Subsequent studies show plants register the information from the fluctuating light and temperature signals and integrate these cues into converging signaling pathways (Legris *et al.*, 2017; Casal and Qüesta, 2018; Hayes, 2020). Thus, a characterization of the mechanisms underlying the plant recognition of environmental signals and translation of this information into metabolism and growth adjustments will further our understanding of the cold acclimation process in winter cereals.

Phytochrome PhyB and phototropins PHOT1 and PHOT2 can sense temperature in addition to light (Jung *et al.*, 2016; Legris *et al.*, 2016; Fujii *et al.*, 2017). The membrane-bound phototropins are blue light receptors regulating phototropism and leaf flattening (Legris *et al.*, 2021), but are also involved in in temperature-dependent positioning of chloroplasts (Fujii *et al.*, 2017; Krzeszowiec *et al.*, 2020). Studies in liverwort show cool temperatures (5 °C) promote chloroplast movement to the cell periphery in a process denoted ‘cold-avoidance’, which also occurs in Arabidopsis cells (Fujii *et al*., 2017). Similar to chloroplast-avoidance response triggered by high light (Wada *et al*. 2003), the cold-avoidance movement is suggested position the chloroplasts for optimal photosynthesis (Fujii *et al.*, 2017). The chloroplast movement may also fine-tune incoming light signals and regulate signalling pathways (Wilson and Ruban, 2020).

Photoreceptor PhyB has special properties as it can relay both light and temperature signals to the circadian clock (Jung *et al.*, 2016; Legris *et al.*, 2016; Casal and Qüesta, 2018). The active Pfr conformation of PhyB is thermally unstable and can spontaneously revert back to the inactive Pr conformation in a light-independent two-step process called dark or thermal reversion (Rockwell *et al.*, 2006). Thus, PhyB act as a thermosensor and provides temperature information to the circadian clock that generates the outputs for adjustment of thermomorphogenesis at temperatures above 10 °C (Casal and Qüesta, 2018). During cold acclimation in Arabidopsis, induced CBF associate with PIF3 resulting in increased stability of phyB and increased freezing

tolerance (Jiang *et al.*, 2020). Whether a similar CBF-PIF3-phyB module regulates freezing tolerance in winter cereals has so far not been studied.

2.7 Vernalization requirement in plants

The vernalization process was first described in the temperate cereals, wheat, barley, and rye (Chouard, 1960), and is required for overwintering cereals to transition to early reproductive phase prior to winter. Simultaneously, the plants adapt to cold and prepare for upcoming freezing temperatures. The main gene controlling vernalization in Arabidopsis is a MADS-box gene denoted *FLOWERING LOCUS C* (*FLC*) encoding a repressor of flowering (Michaels and Amasino, 1999; Alexandre and Hennig, 2008). During cold acclimation, *FLC* expression is down-regulated by a complex interplay between sense and anti-sense *FLC* transcripts, mRNA processing steps, and temperature-sensitive chromatin remodelling (Deng *et al.*, 2011; Hawkes *et al.*, 2016; Liu *et al.*, 2021). An *APETALA1* (*AP1*)-like MADS-box gene (*VRN1*) is the main regulator of vernalization in monocot species. *VRN1* is not orthologous to *FLC*, but to the meristem identity genes *AP1*, *CAULIFLOWER* (*CAL*) and *FRUITFULL* in Arabidopsis (Yan *et al.*, 2003). In contrast to *FLC*, *VRN1* is induced during vernalization and functions as a promoter of flowering (Yan *et al.*, 2003). Thus, the vernalization mechanism in monocots and dicot plants involves different factors (Trevaskis *et al.*, 2007).

2.7.1. Genetic control of vernalization in Triticeae species

Through genetic and molecular studies primarily done in wheat and barley, vernalization in winter cereals is primarily determined by the *VERNALIZATION1* (*VRN1*), *VRN2*, and *VRN3* loci (Trevaskis *et al.*, 2007; Kennedy and Geuten, 2020) (Fig 2.7). A fourth vernalization locus (*VRN4*) on chromosome 5D is similar to *VRN1* sequence and function, but only carried by South Asian spring types (Kippes *et al.*, 2015). Spring cereals carry at least one dominant *VRN1* allele, which encodes a MADS box transcription factor that is constitutively expressed (Yan *et al.*, 2003); thus, spring types do not respond to vernalization. Winter types carry recessive and cold-inducible *VRN1* alleles (Danyluk *et al.*, 2003; Yan *et al.*, 2003; Trevaskis *et al.*, 2003), which before vernalization are repressed by a GLYCINE-RICH RNA-BINDING PROTEIN 2 (TaGRP2), binding to the *VRN1* pre-mRNA (Xiao *et al.*, 2014). TaGRP2 is an orthologue to AtGRP7 promoting floral transition in Arabidopsis (Steffen *et al.*, 2019). During vernalization, TaGRP2

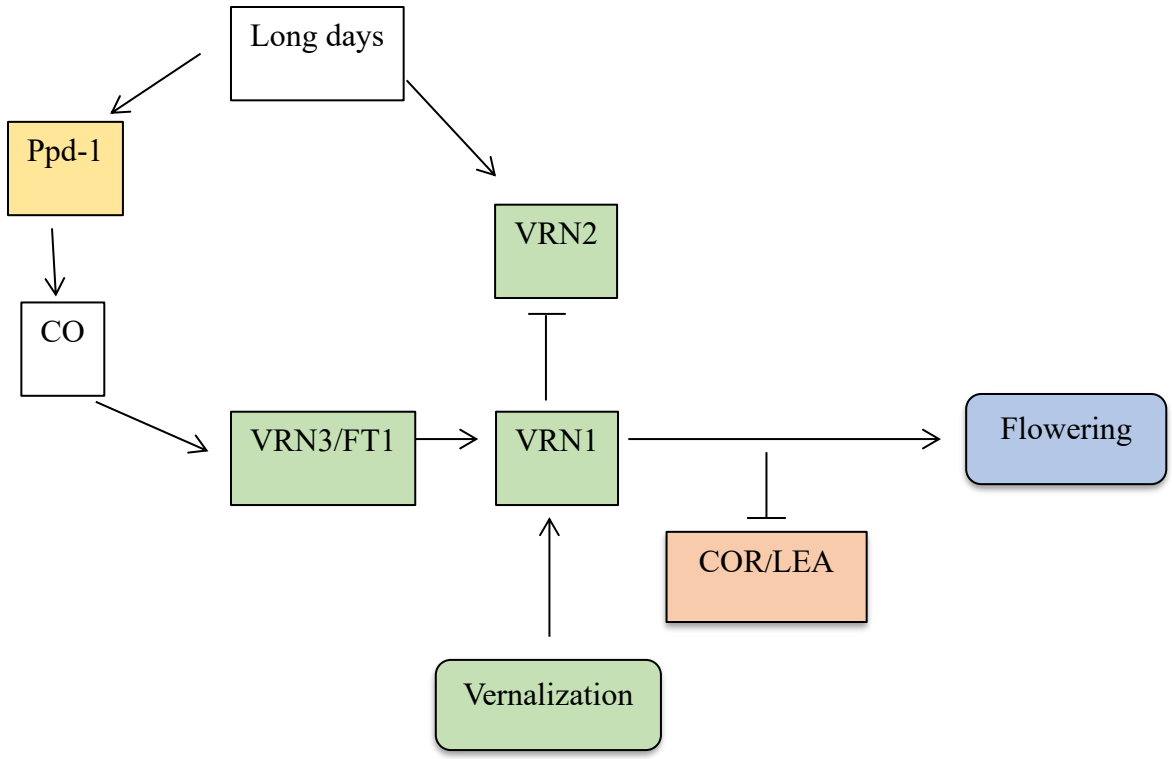

Fig. 2.7. Hypothetical model proposed for interaction between vernalization and cold induced genes. The vernalization process is largely controlled by the VERNALIZATION 1 (VRN1) and VRN2 genes that are part of the VRN1-VRN2-VRN3 regulatory Cold exposure leads to vernalization saturation characterized by induction of VRN1 expression at shoot apical meristem (SAM) and leaves, whereas VRN2, the main repressor of flowering, becomes down-regulated. VRN: vernalization; Ppd-1: photoperiod-1; CO: constants; FT1: Flowering locus T1; COR: Cold responsive genes; LEA: Late embryogenesis abundant (Redrawn from Galiba *et al*., 2009).

becomes O-GlcNAcylated, which favors TaGRP2 binding to jacalin-like lectin *VER2* and leaving *VRN1* de-repressed (Xiao *et al.*, 2014). The gradual activation of *VRN1* during the vernalization process down-regulates the floral repressor gene *VRN2* at the shoot apical meristem (Yan *et al.*, 2004). This allows the meristem to shift to early reproductive phase. Studies in barley demonstrated *VRN1* expression during vernalization is regulated by histone modifications at *VRN1* locus, where the epigenetic control is suggested to mediate a "memory of vernalisation" upon vernalization saturation (Oliver *et al.*, 2009).

In the spring, repressed *VRN2* and active *VRN1* promote *VRN3* expression in leaves, where VRN3 forms a feed-back regulatory loop with *VRN1* (Li and Dubcovsky, 2008). *VRN3* is dependent on long-days for expression and encoded protein is highly similar to Arabidopsis FLOWERING LOCUS T (FT) (Kobayashi *et al.*, 1999; Yan *et al.*, 2006). In Arabidopsis, FT constitutes a flowering-inducing signal produced in leaves, from where it mobilizes via the phloem to the shoot meristem to induce flower development (Corbesier and Coupland, 2006); thus, FT has florigen properties (Chailakhyan, 1936). FT expression is induced by the light/circadian rhythm-regulated transcriptional factor CONSTANS produced in leaves during long days (Kobayashi *et al.*, 1999; Samach *et al.*, 2000). Through FT interaction with bZIP type transcription factor FLOWERING LOCUS D (FD) at the shoot apical meristem, floral meristem-identity genes are induced and flower development is initiated (Abe *et al.*, 2005).

VRN1 has a central role during vernalization in the Triticeae species and its expression level affects the duration of the process, and thereby the amount of LTT accumulated and WFS potential for the species (Fowler *et al.*, 1996*a*). Several different *VRN1* allele variants are known to affect the time to vernalization saturation in wheat (Eagles *et al.*, 2011; Díaz *et al.*, 2012; Li *et al.*, 2013; Muterko and Salina, 2018). The mechanism for vernalization process in Arabidopsis and grasses was initially believed to have evolved independently, as the main vernalization gene *FLC* in dicots appeared to be missing in monocot species (Trevaskis *et al.*, 2007; Alexandre and Hennig, 2008). However, *FLC*-like genes in cereals with possible roles during vernalization have been identified (Greenup *et al.*, 2010; Ruelens *et al.*, 2013; Sharma *et al.*, 2017). The two *FLC*-like genes in wheat, *ODDSOC1* and *ODDSOC2*, are up-regulated and down-regulated, respectively during vernalization (Winfield *et al.*, 2009; Sharma *et al.*, 2017). Current studies suggest ODDSOC2 has a role in repressing reproductive transition under warm temperatures until full saturation of vernalization requirement has been accomplished (Dixon *et al.*, 2019).

Transition to the early reproductive phase in some rye, wheat, barley, oat genotypes is stimulated by short-day conditions in a process called short-day vernalization (Purvis and Gregory, 1937; Heide, 1994). A repressed *VRN2* causes the short-day vernalization phenotype in these plants (Dubcovsky *et al.*, 2006). The process leads to competence to flower (early reproductive phase), but inductive long-day conditions are needed to induce *VRN1* expression and production of flower organs.

2.7.2 Additional factors controlling phase switches in plants

In addition to *FLC* in Arabidopsis and *VRN* genes in winter cereals, the vegetative to early reproductive phase change is affected by many factors. For example, gibberellic acid (GA) is proposed to have a role as exogenously added GA promotes transition to adult phase in Arabidopsis, maize, and rice (Evans and Poethig, 1995; Tanaka *et al.*, 2011). The GA levels are low in maize during the juvenile phase, but high GA levels are required to establish the adult phase (Evans and Poethig, 1995). In contrast, Jasmonic acid (JA) with antagonistic effect towards GA, shows high levels during the juvenile phase, but relatively low levels in the adult phase (Osadchuk *et al.*, 2019). The relative abundance of microRNA 156 (miR156) expressed during juvenile phase and miR172 accumulating during adult phase are also implicated in the timing of juvenile to adult vegetative phase change (Wu *et al.*, 2009). A high sugar concentration in leaves promotes the vegetative phase at the shoot apical meristem (Yang *et al.*, 2013; Xu *et al.*, 2021). Recently, cytosolic invertase CINV1/2, catalyzing conversion of sucrose to glucose and fructose, is identified as the key factor controlling juvenile-to-adult transition in Arabidopsis (Meng *et al.*, 2021).

FT, *TWIN SYSTER OF FT* (*TSF*), SUPPRESSOR OF OVEREXPRESSION OF CONSTANS1/(SOC1), and LEAFY (LFY) strongly promote flowering in Arabidopsis (see review by Andrés and Coupland, 2012). Gibberellic acid (GA) activates expression of *SOC1*, which is an activator of *LFY* (Moon *et al.*, 2003). In addition, anti-florigen factors influence flowering time (Matsoukas *et al.*, 2012; Gaarslev *et al.*, 2021). For example, *TERMINAL FLOWER 1* (*TFL1*) coding for a member of the phosphatidylethanol-amine-binding protein (PEBP) family, acts as an anti-florigen suppressing flowering in Arabidopsis (Bradley *et al.*, 1997). The vegetative to reproductive phase switch in plants is also regulated by a conserved "aging pathway", that involves miR156 and its target, the SQUAMOSA-PROMOTER BINDING PROTEIN-LIKE (SPL)

transcription factor family (see review by Wu and Poethig, 2006). Constitutive expression of miR156 delays flowering, whereas overexpression of *SPL* target results in abandonment of the juvenile phase and early flowering (Wu and Poethig, 2006). An analysis of the barley SPL/miRNA system suggests the cereal miR156-SPL-miR172 module has similar roles regulating phase switches as observed in Arabidopsis (Tripathi *et al.*, 2018).

2.8 Development of freezing tolerance in plants

2.8.1 Perception of cold and cold signaling in plants

It is generally viewed that thermo-sensing in plants occurs at the plasma membrane as it undergoes thermodynamic and compositional alterations in response to temperature changes (Murata and Los, 1997; Los and Murata, 2004; Uemura *et al.*, 2006; Vaultier *et al.*, 2006) (Fig 2.8). Furthermore, it is believed changes in membrane rigidity is recognized by various membrane proteins acting as primary sensors or regulators (Los and Murata, 2004; Solanke and Sharma, 2008). Some of the putative cold sensors at the membrane are Ca^{2+} channels, histidine kinases, receptor kinases, phospholipases, and the photosynthetic apparatus (Solanke and Sharma, 2008). Many studies demonstrate cold-induced changes in membranes result in an immediate transient reorganization of the cytoskeleton and a rapid influx of Ca^{2+} into the cytosol (Monroy and Dhindsa, 1995; Knight *et al.*, 1996; Örvar *et al.*, 2000; Sangwan *et al.*, 2001). The cold-induced $[Ca^{2+}]_{cyt}$ surge is registered as a "Ca^{2+} signature" with specific amplitude, frequency and duration (Knight *et al.*, 1996; McAinsh and Pittman, 2009). The involvement of cytoskeleton in the cold response is supported by chemicals inducing reorganization of actin microfilament can stimulate similar cytosolic Ca^{2+} influx and cold-induced gene expression as cold treatment (Örvar *et al.*, 2000). The level of microtubule de-polymerization induced by cold in rye root tips relates to the plants ability to accumulate freezing tolerance by cold acclimation (Kerr and Carter, 1990*a*,*b*). Thus, it appears that a transient and partial disassembly of microtubules is required to initiate cold acclimation (Abdrakhamanova *et al.*, 2003). A wheat actin-depolymerizing factor, *TaADF*, and two alpha tubulin genes accumulating to higher levels in cold tolerant as compared to tender genotypes may have roles in the cold response in wheat (Danyluk *et al.*, 1996; Ouellet *et al.*, 2001; Christov *et al.*, 2008).

Two calcium-permeable mechanosensitive channels, MCA1 and MCA2 are involved incold-induced Ca^{2+} influxes in Arabidopsis (Mori *et al*., 2018). A different factor, G-protein

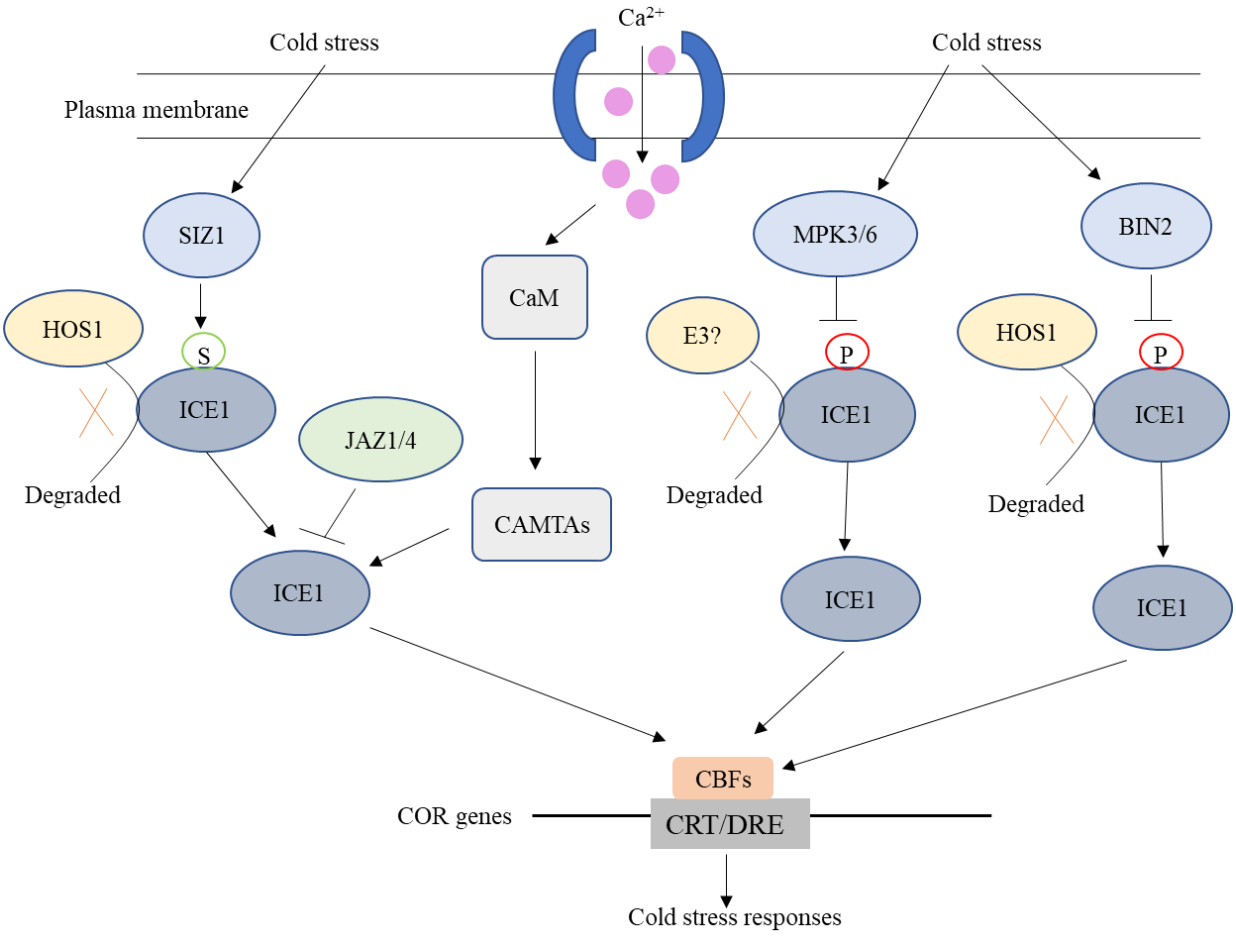

Fig. 2.8. Ca^{2+} signaling and the ICE-CBF-COR network. Ca^{2+} is involved in ICE-CBF-COR network that can be transduced by CAMTAs. Phosphorylation and sumoylation of ICE1 inhabit degradation by the E3 ubiquitin ligase HOS1 and stabilize ICE1 under cold stress. MPK, Mitogen-activated protein kinase; BIN2, BRASSINOSTEROID-INSENSITIVE2; JAZ, JASMONATE ZIM-DOMAIN PROTEIN; CaM, calmodulin; CAMTA, CALMODULIN-BINDING TRANSCRIPTION ACTIVATOR; P, phosphorylation; S, SUMO (small ubiquitin-related modifier); SIZ1, SUMO E3 ligase; U, ubiquitin; HOS1, high expression of osmotically responsive genes1 (Redrawn from Ding *et al*., 2020).

regulator CHILLING TOLERANCE DIVERGENCE 1 (COLD1) present on the plasma membrane and endoplasmic reticulum membrane is involved in cold stress signalling in chilling-tolerant rice (Ma *et al*., 2015). The COLD1 sensing in rice involves an interaction with RICE G-PROTEIN a SUBUNIT 1 (RGA1) and results in activation of a Ca^{2+} channel, G-protein GTPase activity, and development of higher chilling tolerance. A similar light-regulated trans-membrane protein in wheat, TaCOLD1, regulates plant height, but is not associated with freezing tolerance (Dong *et al*., 2019). Thus, chilling (e.g. rice) and frost tolerant (e.g. Arabidopsis, winter cereals) plant species may have evolved different mechanisms for cold stress recognition and signaling (Wei *et al.*, 2021).

As a secondary messenger, Ca^{2+} is involved in many signaling transduction networks, which generally involve Ca^{2+} binding proteins such as calcineurin B-like proteins (CBLs), calcium-dependent protein kinases (CDPKs), calmodulin (CaM), and CaM-like proteins (CMLs) (DeFalco *et al.*, 2010; Guo *et al.*, 2018). Upon Ca^{2+} binding, the proteins often undergo conformational changes that facilitates interactions with downstream effectors (Clapham, 2007). One effector in the cold-response cascade is CBL-INTERACTING PROTEIN KINASE 7 (OsCIPK7) contributing to chilling tolerance in rice (Zhang *et al.*, 2019). Other components of the Ca^{2+} relay include protein phoshatases (PP2A, PP2B) and mitogen-activated protein kinases (MAPKs), which relay the signals to activate down-stream transcriptional cascades (Solanke and Sharma, 2008). An extensive crosstalk between different signaling cascades makes the overall signaling very complex (Smékalová *et al.*, 2014).

Down-stream of the initial cold recognition and relay, the responses are mediated by large number of transcription factors affecting gene expression (Fowler and Thomashow, 2002). The best described cold-inducible regulon is the CBF-COR regulon (Thomashow, 1999), which induces *CBF* transcription within 15 min and *CBF* target *COR* genes within 2h of plant exposure to cold (Gilmour *et al.*, 1998). Studies in Arabidopsis support a local cold exposure induces a rapid systemic response resulting in CBF expression in all tissues (Gorsuch *et al.*, 2010). Thus, the quick action from a cold-sensing and acclimation mechanisms ensures plant survival due to sudden environmental changes and provides plants with an overall high fitness (Kollist *et al.*, 2019). However, the nature of the postulated mobile and systemic “cold signal” not been identified.

2.8.2 Cold acclimation in winter cereals

Cold acclimation in autumn-seeded winter cereals initiates when the emerging seedlings sense and integrate signals from a shorter day-length, lower light intensity, increased amount of far-red wavelengths in incoming light, and a decrease in the average daily temperature (Franklin and Whitelam, 2007; Lee and Thomashow, 2012). The temperature at which cold acclimation starts varies among winter cereal genotypes. The very winter-hardy rye variety Puma has a high threshold temperature around 17 °C, whereas the most winter-hardy wheat and barley cultivars start their acclimation when the temperature is lowered to about 15°C and 11°C, respectively (Fowler, 2008). Due to an early start and late floral transition time, the hardiest rye varieties cold-acclimate for seven to eight weeks; which provides a high amount LTT and high winter survival potential (Fowler *et al.*, 1996*a*; Mahfoozi *et al.*, 2000). Cold acclimation for four to six weeks in hardy winter wheat and barley genotypes results in lower LTT and WFS than rye. Upon completion of cold acclimation, winter cereals have acquired tolerance to freezing temperatures ranging from -12 °C down to -25 °C in very winter-hardy rye Puma (Fowler *et al.*, 1996*b*). After cold acclimation, winter-hardy cereals including rye undergo a 'second phase hardening' or 'sub-zero hardening' when the temperature decreases to a few degrees below 0^{o}C (Olien, 1984; Livingston, 1996). Transcriptional analyses reveal differential gene induction during the above-zero and sub-zero cold acclimation processes (Herman *et al.*, 2006; Le *et al.*, 2015*b*). Particularly genes involved in cell wall biosynthesis, hormone metabolism and RNA regulation are expressed at higher levels during the sub-zero hardening than during cold acclimation (Le *et al.*, 2015*a*).

During cold acclimation in the field, plants experience frequent variations in light intensity and temperature, which prime plants to increase their cold acclimation and winter survival potential (Mayer *et al.*, 2020). Such triggering events may include a short cold spell prior to a longer period of cold or exposure to slightly sub-zero temperatures initiating a second hardening step (Skinner and Bellinger, 2011; Leuendorf *et al.*, 2020).

2.8.3 Role of the ICE-CBF-COR regulon during cold acclimation

CBF proteins carry a highly conserved AP2 DNA binding domain (Stockinger *et al.*, 1997) flanked by two signature motifs: the upstream CMIII-3 (PKK/RPAGRxKFxETRHP) and the downstream CMIII-1 (DSAWR) (Jaglo *et al.*, 2001). Cold-induced *CBFs* regulate COR genes by binding to C-repeat (CRT)/dehydration-responsive (DRE) elements (CCGAC) present in the

promoters of the target COR genes (Stockinger *et al.*, 1997; Gilmour *et al.*, 1998; Sakuma *et al.*, 2002) (Fig 2.8). CBFs belong to the "first wave" of transcription factors, which are rapidly induced in wheat leaves within the first two hours of cold exposure (Kume *et al.*, 2005). This induction is followed by increases in CBF target gene expressions in both leaves and crowns within the first two days, to thereafter gradually decline to a steady-state level after weeks of cold acclimation (Ganeshan *et al.*, 2008). At least 17 additional "first wave" transcription factors (ZF, CZF1, RAV1, CZF2, MYB73, ZAT12, DOF1.10, ZAT10, HSFC1, DEAR1, MYB44, ERF5, CRF2, WRKY33, ERF6, CRF3 and RVE2) are co-expressed with CBFs in Arabidopsis to form a "low-temperature regulatory network" (Park *et al.*, 2015). Among the 2,637 identified COR genes in Arabidopsis, it is estimated 11% are up-regulated and 3% down-regulated by one or several CBFs (Park *et al.*, 2015). Thus, the remaining COR genes are regulated by CBF-independent factors. An analysis of the Arabidopsis *cbf123* mutant support "first wave" transcription factors HSFC1, ZAT12, and CZF1 (Vogel *et al.*, 2005; Park *et al.*, 2015) are members of *CBF*-independent cold responsive pathways (Zhao *et al.*, 2016).

The important role of CBFs is demonstrated by higher freezing tolerance in various transgenic plants over-expressing *CBFs* at both low and warm temperatures (Jaglo-Ottosen *et al.*, 1998; Liu *et al.*, 1998; Gilmour *et al.*, 2004). At warm temperatures, the transgenic plants show similar phenotypes as cold acclimated wild-type plants demonstrating stunted growth, delayed flowering, and higher concentration of accumulated proline, glucose, fructose, and raffinose (Gilmour *et al.*, 2004; Achard *et al.*, 2008).

2.8.4. Regulation of CBF expression

Cold, circadian and light signaling are integrated into the CBF signaling cascade to regulate plant responses to cold stress in Arabidopsis (Fowler *et al.*, 2005; Franklin and Whitelam, 2007; Lee and Thomashow, 2012) and winter cereals (Stockinger *et al.*, 2007; Badawi *et al.*, 2007). In autumn-seeded plantlets, the low red to far-red (R/FR) light ratio activates the circadian-gated *CBF* transcription resulting in increased *COR* expression even at relatively warm temperatures (Franklin and Whitelam, 2007). The photoperiod effect on *CBF* expression in the autumn results in higher induction during cold mornings than equally cold temperature at the end of the day (Dong *et al.*, 2011; Lee and Thomashow, 2012). Further on, an enhancement of freezing tolerance accumulation in the autumn is obtained by stabilization of the phyB thermosensor by CBFs interaction with PIF3

(Jiang *et al.*, 2020). Thus, the CBFs-PIF3-phyB interactions demonstrated in Arabidopsis represents a separate module responding to light and temperature signals and regulating development of freezing tolerance (Jiang *et al.*, 2020; Xu and Deng, 2020). Under long-day conditions and warm temperatures in the spring, *CBF* expression is repressed by PhyB and its interacting partners PIF4 and PIF7 (Lee and Thomashow, 2012).

The basic helix–loop–helix (bHLH) proteins Inducer of CBF expression (ICE) 1 and 2 are among the best characterized regulators of *CBF* expression (Lissarre *et al.*, 2010). Stimulation of *CBF* expression occurs via ICE1/ICE2 interactions with E-box cis-elements (CANNTG) present in the *CBF* promoters. In Arabidopsis, *ICE1* induces primarily *CBF3* expression (Chinnusamy *et al.*, 2003). *ICE2* activates *CBF1, CBF3,* and a 9-cis-epoxycarotenoid dioxygenase (*NCED3*) gene stimulating ABA biosynthesis during cold acclimation (Fursova *et al.*, 2009; Kurbidaeva *et al.*, 2014; Kim *et al.*, 2015). As many COR genes carry E-boxes in their promoters, *ICE* factors may also regulate *COR* genes directly (Tang *et al.*, 2020). Overexpression of *ICE1* in Arabidopsis provides transgenic plants with enhanced freezing tolerance, whereas an *ice1* mutant does not induce CBF3 upon cold exposure and shows reduced expression of CBF-target genes resulting in low chilling and freezing tolerance (Chinnusamy *et al.*, 2003). The cereal ICE factors are expected to have a similar role to those in Arabidopsis, as supported by increased LTT in transgenic Arabidopsis overexpressing wheat *TaICE41* and *TaICE87* (Badawi *et al.*, 2008). In addition to increasing cold tolerance, ICE factors influence plant development as demonstrated by delayed floral transition in Arabidopsis plants overexpressing *ICE2* (Kurbidaeva *et al.*, 2014). In addition, *ICE1* and *ICE2*, also denoted SCREAM1 (*SCRM1*) and *SCRM2*, have roles in the differentiation of guard cells and stomata patterning in leaves (Kanaoka *et al.*, 2008). About 40% of the COR genes are affected by the *ice1* mutation, and account for more than the estimated 7 to 15% COR genes regulated by *CBFs* (Park *et al.*, 2015; Jia *et al.*, 2016). Therefore, ICE factors are considered master regulators controlling CBF regulon, but also other cold-induced regulons. Like the *CBFs*, *ICE1* and *ICE2* are regulated by many factors as summarized in Figure 2.8. Many of the upstream factors regulating the ICE-CBF regulon are transcription factors regulated by phytohormone levels that are affected by cold; thus, the ICE-CBF regulon and phytohormone signaling pathways are tightly interconnected. (Eremina *et al.*, 2016).

Several links between cold-induced Ca^{2+} influx to cytosol and the ICE-CBF regulon are known from studies in Arabidopsis. For example, the CALMODULIN BINDING

TRANSCRIPTION ACTIVATORs CAMTA1, CAMTA2 and CAMTA3 activate *ICE2* (Doherty *et al.*, 2009) and similarly MAPKs and CBL-CIPK interact with ICE1 to trigger cold defense responses (Zhao *et al.*, 2009; Zhang *et al.*, 2017). A negative effect on freezing tolerance is demonstrated by cold-activated receptor-like cytoplasmic kinase COLD-RESPONSIVE PROTEIN KINASE 1 (CRPK1), which destabilizes CBFs (Liu *et al.*, 2017).

2.9 Plant responses to low temperature

The precise molecular mechanisms underlying cold acclimation are very complex as revealed by studies in winter cereals and other plants showing an extensive reprogramming of transcriptome, metabolome, and proteome during the process (Thomashow, 1999; Cook *et al.*, 2004; Winfield *et al.*, 2010; Xu *et al.*, 2013, 2019; Kosová *et al.*, 2013). Generally, cold adaptation is attained in different stages to adjust the plants cellular state to a new optimal acclimated steady state (Herrmann *et al.*, 2019). The first cold response (alarm phase) constitutes an unregulated thermodynamic response (e.g. membrane modification) that occurs within seconds to minutes. Studies in wheat support the early stress response involves suppression of growth (Kosová *et al.*, 2012). This shock response is followed by regulated short term changes lasting for minutes to hours, during which protein activities obtain a new adjusted cellular state (acclimation phase). During this stage plants reallocate energy towards production of stress protective compounds. Finally, gene expression changes cause proteome alteration that result in an acclimated cellular steady state known as metabolic homeostasis or resistance phase (Herrmann *et al.*, 2019). Thus, it is postulated that the vegetative phase of acclimating plants represents a “a stressed state” that is relieved upon phase switch to reproductive phase (Beydler *et al.*, 2016).

The initial chilling stress quickly induces changes to membrane structures, reduces the kinetics of enzymatic reactions, and induces thermodynamic changes to RNA and protein molecular structures with effects on molecular interactions and stability of protein complexes (Ruelland *et al.*, 2009). In winter rye, a transcriptome study of the early stage of cold acclimation (24 to 72h) reveals genes related to photosynthesis, plasma membrane stability, glucose and energy metabolism, cold-response transcription factors (particularly MYB and bHLH genes), and genes synthesizing extracellular components such as cutins, suberins and waxes are induced (Kong *et al.*, 2020). At the metabolome level, a variety of solutes including proline, sugars, glycine betaine accumulate in rye during cold acclimation (Koster and Lynch, 1992). The late-response COR

genes in plants generally encode osmolytes to combat the cold-induced drought stress, fatty acid desaturases to maintain membrane fluidity, anti-freeze/ice-recrystallization inhibitor proteins to reduce damage by ice crystals, antioxidants for detoxification of ROS, and chaperones to stabilize proteins/protein complexes (Thomashow, 1999; Ruelland *et al.*, 2009). However, from monitoring gross changes of transcripts levels during stress, it is generally observed that gene expression levels do not correspond well with protein concentrations or activity (Bogeat-Triboulot *et al.*, 2007). This is likely due to COR proteins often undergo extensive post-translational modifications such as phosphorylation, ubiquitination, glycosylation and SUMOylation that alter protein structure, function, stability, and/or subcellular localization (Barrero-Gil and Salinas, 2013).

Cold acclimation confers changes to plant growth and morphology, which in cold-hardy cereals generally includes an increased compact, dwarf growth (Scott *et al.*, 2004) and a switch to prostrate growth habit (Roberts, 1990; Gray *et al.*, 1997; Limin and Fowler, 2000). The growth repression results from re-direction of photosynthate resources from growth to processes that increase cold defense, whereas an increased negative gravitropism is proposed to underlie prostrate growth habit (Wyatt *et al.*, 2002). Plants also become sturdier by producing thick leaves (Hüner *et al.*, 1981) and stronger cell walls (Takahashi *et al.*, 2019), which is accomplished by various changes to cell wall biosynthesis (Seifert and Blaukopf, 2010; Le *et al.*, 2015*a*). Rigid cell walls may be an important factor for resistance to freeze-induced dehydration of cells (Rajashekar and Lafta, 1996). Changes to cell wall properties are also noted in wheat crowns, where methyl-esterified cross-linking of glucuronoarabinoxylans in the freezing-sensitive vascular transition zone occurs in freezing-tolerant genotypes (Willick *et al.*, 2018). In addition, the initial cold-induced thermodynamic changes to membrane structure and fluidity (Steponkus and Lynch, 1989; Uemura *et al.*, 1995) are followed by alterations of lipid composition and production of signaling molecules such as Ca^{2+}, phosphatidic acid and inositol-trisphosphate (InsP3) acting as secondary metabolites (Li *et al.*, 2004, 2015; Vergnolle *et al.*, 2005; Ruelland *et al.*, 2009). In addition to some of the above-mentioned phenotypes, most cold-hardy rye varieties develop narrow and short rosette leaves, short mesocotyl, and a deep tillering node (Schlegel, 2014).

2.9.1 Adjustment of photosynthesis during cold acclimation

The development of freezing tolerance in plants by cold acclimation in the autumn requires an active photosynthesis (Svensson *et al.*, 2006), which places the chloroplast at the center of the

cold hardening process. The chloroplast is also the cell compartment that is most affected by unfavorable light and temperature conditions (Fig 2.9). The energy needed for the cold acclimation process is provided by an overall up-regulation of catabolic processes and simultaneous down-regulation of anabolic processes (Hüner *et al.*, 2012). Upon the first encounter of cold in the autumn, the plants enzymatic reactions, including those of the photosynthetic pathway, become thermodynamically down-regulated (Stitt and Hurry, 2002). Since electron flow in the photosynthesis and electron chains occurs independent of temperature, cold causes an excess of incoming electrons versus electrons consumed by metabolism in photosynthetic cells (Ensminger *et al.*, 2006; Hüner *et al.*, 2012). This energy imbalance is registered through alteration in the excitation pressure of photosystem II, which through redox signals and retrograde signals down-regulate chloroplast and nuclear photosynthetic gene expression (Fey *et al.*, 2005; Ensminger *et al.*, 2006). Plants respond to this oxidative stress in a species-specific way, which in cereals involves remodeling of the photosynthesis mechanism to regain photostasis and readjustment of carbohydrate metabolism that allows for metabolic homeostasis to be established [see review by (Hüner *et al.*, 2012) and references therein for details]. Briefly described, winter cereals shift to dwarf growth during cold acclimation without changing the overall plant biomass. The light absorption efficiency is maintained at a relatively high level and sucrose biosynthesis in the chloroplast is increased and efficiently transported to cytosol. In the cytosol, sucrose is metabolized to other sugars that are transported to other cell compartments/tissues or exported from leaves to sink tissues. This metabolic readjustment reduces the feedback inhibition of photosynthesis, suppresses photorespiration and lowers the risk of ROS generation in chloroplasts (Xu *et al.*, 2013). Ultimately, the photosynthesis becomes more efficient per leaf area basis resulting in higher biomass production (Dahal *et al.*, 2012) and cell metabolism redirected towards carbohydrate production and other attuned solutes for stress protection (Savitch *et al.*, 2002; Kurepin *et al.*, 2013).

Recent studies in Arabidopsis support proper chloroplast positioning within the cell is an important factor for adjustment of photosynthesis and metabolism when plants are adapting to cold (Kitashova *et al.*, 2021). Through these migrations, chloroplasts are proposed to optimize photosynthesis under high light, low light, dark, or low temperature conditions (Wada and Kong, 2018; Fujii *et al.*, 2020). The blue light receptor PHOT2 has an important role during the cold-avoidance response reported in Arabidopsis (Fujii *et al.*, 2017). In addition, chloroplast make

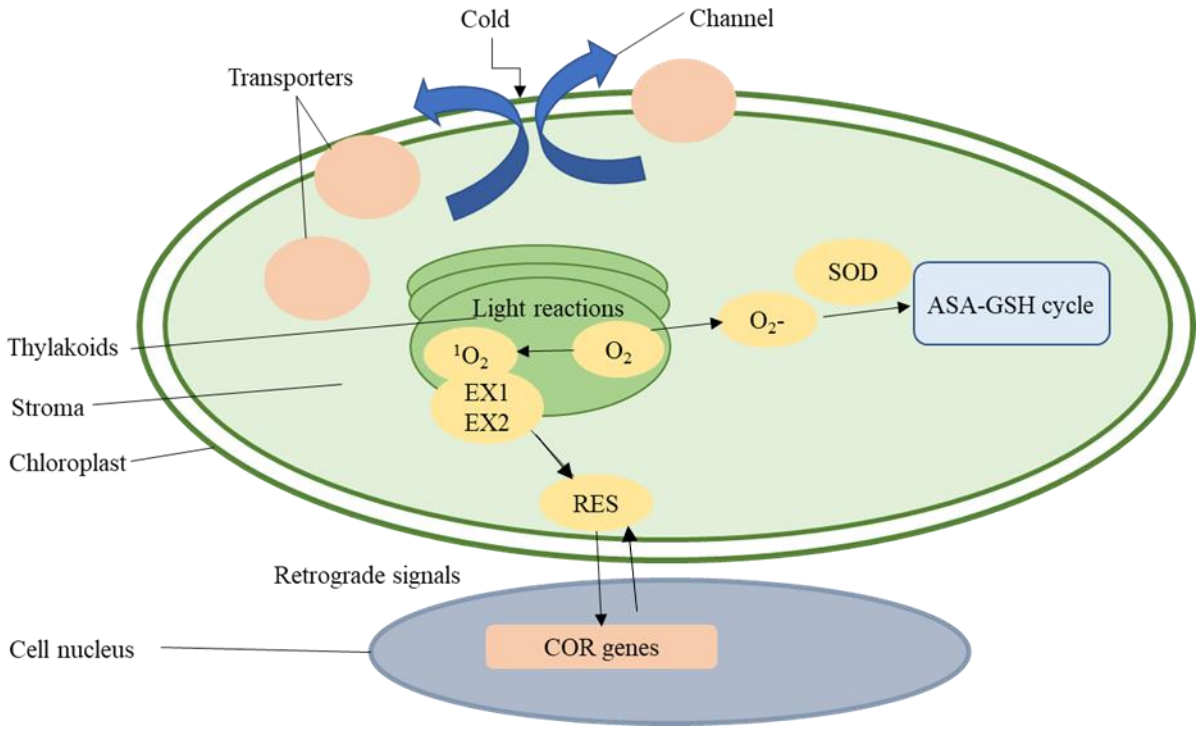

Fig. 2.9. Chloroplast response under low temperature stress. Cold stress signals are sensed via channel proteins or transporter proteins. Low-temperature stress is also characterized by a greater risk of oxidative damage. Augmented generation of ROS such as O^{2-} induces increases formation of ROS scavenging species, which activate the antioxidant systems of SOD and ascorbate-glutathione cycle. $^1O_2$ (singlet oxygen) bound to EXECUTER (EX1) and EX2 (calcium-sensitive receptor proteins on the thylakoid membrane) mediate retrograde signals to the nucleus to activate COR genes. ASA, ascorbic acid; GSH, glutathione; RES, Reactive electrophile species; SOD, superoxide dismutase (Redrawn from Gan *et al*., 2019).

physical contacts with nuclei and both organelles migrate together within the cell (Jung and Chory, 2010). The co-migration of organelles may facilitate retrograde signaling in cells, which is expected to have an important role during adaptation to cold acclimation (Hüner *et al.*, 2012). The proposed retrograde signaling mediates redox imbalances in chloroplasts and mitochondria to the nucleus for remodeling of gene expression. Whether chloroplast migration has a role in the re-establishment of photostasis and energy balance in winter cereals needs to be confirmed in future studies.

2.9.2 Changes in carbohydrate metabolism during cold acclimation

Carbohydrates are the primary products of photosynthesis and the major participants in energy metabolism, plant development, and stress signalling. During cold acclimation in the autumn, there are large restructurings of the sugar metabolism and transport in photosynthetic tissues to allow for plant adaptation to the lower temperature (Nägele and Heyer, 2013; Tarkowski and Van den Ende, 2015) as briefly described above. The increased biosynthesis of sucrose in chloroplasts (Nägele *et al.*, 2012) is coordinated with efficient sucrose transport to the cytosol by plastidic sugar transporter pSuT; this sucrose translocation is required for timely transition to early inflorescence phase and development of high freezing tolerance in Arabidopsis (Patzke *et al.*, 2019). Some of cytosolic sucrose in cold-hardy cereals is converted to fructans or raffinose family oligosaccharides (RFOs) or through by cytosolic invertase (cINV) activities converted to glucose and fructose. Fructans are compartmentalized to vacuoles or apoplasts of crown tissues, leaf and stem mesophyll cells during cold acclimation (Livingston *et al.*, 2009), whereas synthesized RFOs are imported into chloroplasts (Schneider and Keller, 2009). In winter-hardy cereals, cytosolic sucrose in leaves is at a low concentration due to efficient sucrose translocation to sink tissues (Hüner *et al.*, 2012).

Sugars, for example sucrose, glucose and trehalose, protect membranes by interacting with phosphate groups of lipids (Strauss *et al.*, 1986), prevent dehydration-induced increase in the temperature at which membranes undergo the gel–fluid phase transition (Lenné *et al.*, 2007), and they can lower the freezing point and reduce ice migration in cells (Gusta *et al.*, 2004). Both fructans and RFOs increase membrane stability (Hincha *et al.*, 2000; Livingston *et al.*, 2009) possibly by inserting between polar head-groups of phospholipidic mono- and bilayers (Vereyken *et al.*, 2001). RFOs provide protection of thylakoid membranes, and thus preserve photosystem II

integrity and photosynthesis during cold acclimation (Nishizawa *et al.*, 2008; Schneider and Keller, 2009; Knaupp *et al.*, 2011). Fructans provide energy during regrowth in the spring (Tamura *et al.*, 2014), produce stress signals in the phloem (Van Den Ende *et al.*, 2004), increase snow-mold resistance (Meguro-Maoka and Yoshida, 2016), or act as damage-associated molecular patterns (DAMPs) in the apoplast (Versluys *et al.*, 2017). During deacclimation in the winter, the raffinose, glucose, fructose, and sucrose concentrations are reduced in over-wintering plants (Zuther *et al.*, 2015).

Starch, the end-product of photosynthesis and the predominant storage carbohydrate, is tightly regulated under abiotic stress and a major determinant of plant fitness (Thalmann and Santelia, 2017). In Arabidopsis, cold stress activates certain beta amylase and starch degradation is increased (Guy *et al.*, 2008; Sicher, 2011). The dynamics in starch metabolism can relieve the feed-back inhibition of the Calvin Cycle enzymes and allow the release of inorganic phosphate under cold stress (Fürtauer *et al.*, 2019). In summary, starch is proposed to act as a protectant against abiotic stress by its ability to affect whole plant carbon allocation through interconversion with sugars (Dong and Beckles, 2019). The availability of sugars in response to abiotic stress may be a key convergence point in plant stress response (Dong and Beckles, 2019).

In addition to providing energy and structural components of cells, plant sugars are also signaling molecules (Li and Sheen, 2016). For example, sucrose regulates many genes encoding enzymes in the phenylpropanoid biosynthetic pathway (Teng *et al.*, 2005) and regulate invertase genes controlling compartment-specific sucrose/hexose ratios in cells (Meng *et al.*, 2021). Sugar signaling is suggested to be a basic mechanism mediating multi-stress tolerance in plants (Puniran-Hartley *et al.*, 2014).

2.9.3 Response to oxidative stress during cold exposure

Plants exposed to abiotic (e.g., cold and drought) or biotic stress are at risk of oxidative stress and impaired redox homeostasis due to increased levels of reactive oxygen species (ROS) being produced when ROS scavenging activities are low (Hasanuzzaman *et al.*, 2020*a*). The ROS produced in plants include (i) free radicals like hydroxyl radical (OH) and superoxide anion ($O_2^{\bullet}$) and (ii) non-radical entities such as singlet oxygen (O_2) and hydrogen peroxide (H_2O_2). These molecules are generally generated at high levels in chloroplasts due to stress-induced inefficiencies in electron transport reactions associated with photosynthesis or respiration (Mignolet-Spruyt *et*

al., 2016). During bright days in the autumn, the high-light condition combined with low temperature are highly conducive for high ROS-production in chloroplasts. Other sites of ROS production in cells include mitochondria, peroxisomes, apoplast, and the plasma membrane (Suzuki and Mittler, 2006; Heyno *et al.*, 2011). ROS production at low levels regulates plant metabolism through the use of ROS as signaling molecules and negative effects on plant metabolism and growth are not observed (Baxter *et al.*, 2014; Mignolet-Spruyt *et al.*, 2016; Noctor and Foyer, 2016). When ROS accumulates to high levels due to stress, cytotoxic damage to cellular components might occur. This damage includes protein oxidation and enzyme inhibition, ion leakage and lipid peroxidation in membranes, nucleic acid damage, damage to photosystem II reaction centre, activation of programmed cell death pathways, and ultimately cell death (Ruelland *et al.*, 2009; Hasanuzzaman *et al.*, 2020*b*). The stress also induces strong retrograde signaling where ROS and metabolites like β-cyclocitral, MecPP (2-C-methyl-d-erythritol 2,4-cyclodiphosphate), PAP (3′-phosphoadenosine 5′-phosphate), and intermediates of the tetrapyrrole biosynthesis pathway mediate signaling from plastids to the nucleus (Kleine *et al.*, 2013). ROS-scavenging enzymes such as superoxide dismutase (SOD), ascorbate peroxidase (APX), catalase (CAT), glutathione peroxidase (GPX), and antioxidants such as ascorbic acid and glutathione peroxiredoxin (PrxR) are essential for ROS scavenging and reducing ROS damage (Mittler *et al.*, 2004). Thus, a balance between ROS production and ROS scavenging is needed to protect the photosynthetic machinery and maintain the integrity of membranes, nucleic acids, and proteins in cells (Suzuki and Mittler, 2006).

Cold-tolerant plants can more efficiently manage ROS excess than cold-sensitive genotypes as deduced from proteomic studies (Xu *et al.*, 2013; Kosová *et al.*, 2013). Expression of genes encoding ROS-scavenging enzymes is regulated by a MEKK1-AtMKK2-AtMPK4/AtMPK6 signaling cascade in Arabidopsis (Teige *et al.*, 2004). Under longer stress, the contents of antioxidants gradually increase as a result of acclimation and most plants accumulate both non-enzymatic antioxidants and anti-oxidative enzymes during cold acclimation.

2.10 Role of plant growth regulators during cold acclimation

Plant growth regulators play an important role during cold acclimation by influencing plant development and accumulation of LTT (Shi *et al.*, 2015; Eremina *et al.*, 2016). Most of the known plant growth regulators affecting LTT are connected to the *CBF* regulon and influence the

phenological development of plants (Eremina *et al.*, 2016). Thus, *CBF* regulon constitutes a central node for hormone crosstalk, where CBF expression is controlled by GA, JA, ABA, ethylene, and BRs as schematically illustrated (Fig 2.10). Other plant growth regulators such as salicylic acid (SA), auxins, and cytokinin are also associated with LTT, but their roles are less direct.

2.10.1 Gibberellic acid

Plants exposed to low temperature develop higher levels of GA2 oxidase activity, which inactivates GA and alters GA signalling (Achard *et al.*, 2008; Richter *et al.*, 2013). GA restrain the action of DELLA proteins, which have growth-repressing functions in cells; thus, the cold-induced reduction of GA causes a reduction in plant growth (Hsieh *et al.*, 2002; Achard *et al.*, 2008). Both GA-insensitive and GA-deficient Arabidopsis mutants are unable to develop full LTT during cold acclimation (Achard *et al.*, 2008; Richter *et al.*, 2013). In contrast, impaired GA production in *gal1* mutants increase *CBF1, CBF2* and *COR15A* expressions and provide higher freezing tolerance as compared to wild type plants (Richter *et al.*, 2013). Studies of the GA impaired mutants show cold tolerance in Arabidopsis is regulated by two GATA transcription factors, GATA, NITRATE-INDUCIBLE, CARBON-METABOLISM INVOLVED (GNC) and GNC-like (GNL) which show cross-repressive actions with *SOC1* transcription to regulate both flowering and cold tolerance (Richter *et al.*, 2013). The role of DELLA proteins in mediating cold acclimation involves interaction with other plant growth regulators and sugar signaling mechanisms (Fig. 2.10), and thus DELLA can be considered a hub modulating the balance between growth and stress responses in plant (De Bruyne *et al.*, 2014).

2.10.2 Abscisic acid

Cold stress in plants induces ABA production (Lång *et al.*, 1994), which leads to induction of *CBF* expression (Knight *et al.*, 2004). Arabidopsis mutants deficient in ABA biosynthesis, *aba deficient 1* (*aba1*) and *aba3*, are unable to cold acclimate, supporting ABA has an important role in the development of cold tolerance (Gilmour and Thomashow, 1991; Nordin *et al.*, 1993; Xiong *et al.*, 2001). Wheat exposed to cold shows immediate and rapid transient increase of ABA levels, with higher response in winter types compared to spring types (Kosová *et al.*, 2012). The induction of CBF expression by ABA involves a MYB96 transcription factor, three heptahelical proteins HHP1, HHP2, HHP3), and OPEN STOMATA 1 (OST1) kinase, which regulate *CBF* upstream

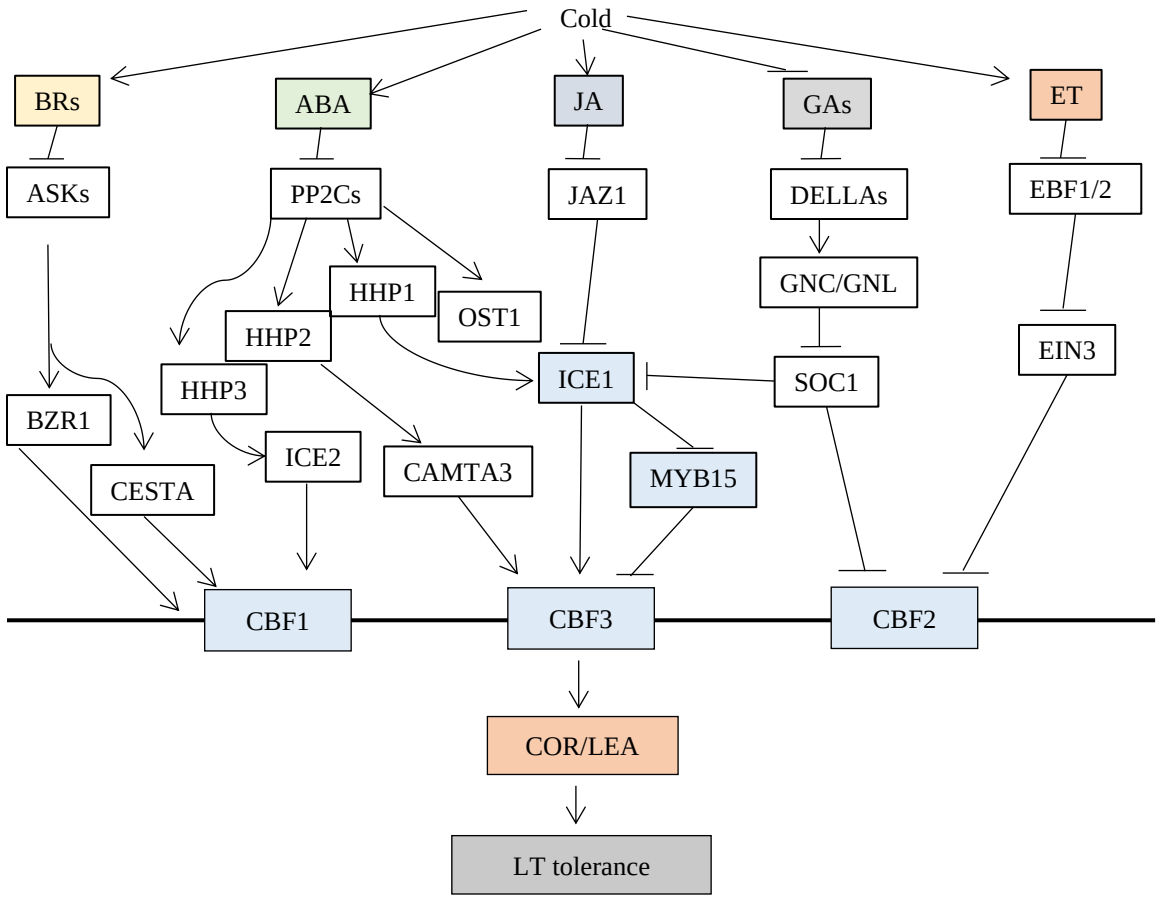

Fig. 2. 10. Plant growth regulators mediated regulation of CBF regulon during cold acclimation. BRs, Brassinosteroids; ABA, Abscisic acid; JA, jasmonic acid; GA, Gibberellic acid; ET, ethylene; PP2Cs, protein phosphatases type 2C; JAZ1, Jasmonate Zim-Domain1; EIN3, ethylene insensitive 3; EBF1, EIN3-binding F-box 1; HHP, Heptahelical proteins; OST1, Open Stomata1; GNC, GATA nitrate-inducible carbon-metabolism involved; GNL; GNC-Like; ICE, Inducer of CFB expression; SOC1, SUPPRESSOR OF OVEREXPRESSION OF CONSTANS1; BZR1, Brassinazole resistant1; CESTA, basic helix-loop-helix transcription factor; CAMTA3, Calmodulin-binding transcriptional activators; MYB15, Myeloblastosis15; CBF, C-repeat binding factor; COR: Cold responsive genes; LEA: Late embryogenesis abundant (Redrawn from Barrero-Gil and Salinas, 2018).

factors *CAMTA3*, *ICE1*, and *ICE2* activities (Ding *et al.*, 2015; Lee and Seo, 2015). In response to cold, OST1 phosphorylates and stabilizes ICE1, promoting the expression of CBF and downstream cold-tolerance genes (Ding *et al.*, 2015).

2.10.3 Jasmonic acid

Jasmonic acid (JA) is an oxylipin, which increases in concentration during cold acclimation in wheat (Kosová *et al.*, 2012). Through exogenous applications of JA, it has been shown that JA has a positive influence on *CBF* and *CBF*-regulated *COR* expression, and promotes LTT in Arabidopsis (Hu *et al.*, 2013). On the contrary, Arabidopsis plants with compromised JA biosynthesis are hyper-sensitive to cold stress (Hu *et al.*, 2013). JA stimulates CBF expression by binding to Skp1-Cullin1-F-box-type (SCF) protein ubiquitin ligase, which forms complexes with Jasmonate Zim Domain-1 (JAZ) factors. JA promotes degradation of complex-bound JAZ proteins including those repressing *ICE1*; thereby repression of *CBF* expression is relieved (Sheard *et al.*, 2011). Analyses of mutants deficient in JA signalling (*coil-1*) suggests JA may also influence cold acclimation through a CBF-independent pathway (Hu *et al.*, 2013). The participation of JA in cold acclimation in cereals is demonstrated in bread wheat, by over-expressing a gene in the JA biosynthetic pathway, *12-OXOPHYTODIENOATE REDUCTASE 3* (*AtOPR3*), resulting in improved LTT and delayed flowering time (Pigolev *et al.*, 2018).

2.10.4 Ethylene

Cold treatment of many plants including wheat results in increased ethylene production (Kosová *et al.*, 2013), but this response is not observed in all species (Eremina *et al.*, 2016). A rapid increase of the ethylene precursor aminocyclopropane carboxylic acid upon cold exposure may underlie the early cold-induced ethylene production in wheat (Kosová *et al.*, 2012). In the cold and ethylene-responding Arabidopsis, components of the ethylene signaling pathway have a negative effect on *CBF* expression, as demonstrated by increased freezing tolerance by ethylene signaling mutants (Shi *et al.*, 2012). It is determined that transcription factor *ETHYLENE-INSENSITIVE 3* (*EIN3*) acts as a negative regulator of cold responses in Arabidopsis (Shi *et al.*, 2012).

2.10.5 Brassinosteroids

BRs are polyhydroxylated steroids that regulate many aspects of plant growth and development (Clouse, 2011). The compounds are synthesized from campesterol via the action of several cytochrome P450 enzymes (Clouse, 2011). A role for BR during cold stress is shown by exogenous application of BR causing increased *CBF1* expression during cold treatment of *Brassica napus* (Kagale *et al.*, 2007). An enhanced *COR15A* expression and higher freezing tolerance is obtained in Arabidopsis by overexpression of a gene encoding a BR biosynthetic enzyme, DWARF4 (DWF4) (Divi and Krishna, 2009). Subsequent studies show that three transcription factors in the brassinosteroid (BR) signaling pathway: BZR1 (BRASSINAZOLE-RESISTANT 1), BES1 (BRI1-EMS-SUPPRESSOR 1) and CESTA are involved in the activation of *CBF* expression (Eremina *et al.*, 2016; Li *et al.*, 2017*a*). BR signaling in Arabidopsis is connected to light signaling through PhyB interaction with BES1 (Wu *et al.*, 2019*a*).

2.11 Accumulation of cold stress-related proteins and compounds

2.11.1 Dehydrin proteins

Dehydrins are heat-stable, highly hydrophilic proteins with disorganized structure that belong to the group II late embryogenesis abundant (LEA) protein family (Hundertmark and Hincha, 2008). This class of proteins are produced in vegetative tissues upon exposure to dehydrating conditions such as cold, drought, heat, or salinity (Hanin *et al.*, 2011). Wheat dehydrins are associated with freezing tolerance (Danyluk *et al.*, 1994; Limin *et al.*, 1995) and an active involvement of dehydrins in freezing tolerance is demonstrated by transgenic Arabidopsis co-expressing multiple dehydrin genes (Puhakainen *et al.*, 2004). Several of the cold-inducible dehydrin genes in wheat are expressed at higher levels in crowns of cold-hardy wheat as compared to crowns of cold-sensitive genotypes (Ganeshan *et al.*, 2008). An exceptionally strong correlation exists between freezing tolerance and accumulation of *wcs120* mRNA and protein in wheat (Limin *et al.*, 1995) and therefore, the peripheral membrane protein WCS120 is often used as biomarker for WFS in winter cereals (Vítámvás *et al.*, 2019). Experiments done *in vitro* show dehydrins provide protection from cell dehydration through interactions with dehydrated proteins (Danyluk *et al.*, 1998; Hanin *et al.*, 2011). Other *in vitro* studies show dehydrins interacting with phospholipid and lipid vesicles by electrostatic forces (Kovacs *et al.*, 2008) and exhibit radical-scavenging and ion-binding functions (Hanin *et al.*, 2011). Interestingly, a *Medicago truncatula*

dehydrin (MtCAS31) interacts with ICE1, which reduces stomatal density in Arabidopsis plants (Xie *et al.*, 2012).

2.11.2 Anti-freeze proteins (AFP) and ice recrystallization inhibitor proteins (IRIPs)

Ice crystals start to form in the intracellular spaces (apoplast) of plant tissues when the temperature falls to subzero levels. This causes a cellular osmotic imbalance that is counteracted by water migrating out of the cells, which leads to cellular dehydration. If ice propagation occurs unrestricted, membrane damages including expansion-induced lysis, lamellar-to-hexagonal-II phase transitions or fracture jump lesion may occur and cause cell death (Uemura *et al.*, 1995). Though cells might survive cellular dehydration or mechanical damage caused by ice, the condition can be quite damaging for cellular metabolism due to increased apoplastic ROS production or proteins being denatured or inactivated.

To prevent severe ice crystal formation in plant tissues, many freezing tolerant plants accumulate apoplastic anti-freeze proteins (AFPs), which often show sequence similarities to glucanases, chitinases, or thaumatin-like proteins (Yu and Griffith, 2001). AFPs adhere to ice and prevent further ice growth through thermal hysteresis and thereby reduce dehydration stress when the temperatures approach the freezing point. However, during freeze-thaw conditions, a thermodynamically driven process denoted ice recrystallization may occur wherein certain small ice crystals rapidly grow large at the expense of smaller ones. This process can cause cell death due to quick cell dehydration or crystals penetrating membranes. To prevent ice recrystallization, the Pooideae subfamily of cereals produce ice recrystallization inhibitor proteins (IRIPs) in addition to AFPs during cold acclimation (Tremblay *et al.*, 2005; Sandve *et al.*, 2008). Transgenic Arabidopsis plants expressing *IRIP* genes of *Lolium perenne* show an increased level of freezing tolerance (Bredow *et al.*, 2017).

2.11.3 Flavonoid and anthocyanin compounds

Flavonoids is a large group of polyphenolic molecules classified as secondary metabolites in plants. The compounds originate from the malonyl-CoA and p-coumaroyl-CoA primary metabolites derived from the acetate/malonate and phenylpropanoid pathways, respectively (Winkel-Shirley, 2001). Flavonoids are produced in response to environmental conditions generating changes to cellular redox homeostasis and are important modulators of stress responses

(Taylor and Grotewold, 2005; Pourcel *et al.*, 2013). As part of the cellular antioxidant machinery, flavonoids reduce free radical formation and scavenge stress-induced ROS to prevent destructive protein oxidation, lipid peroxidation, and nucleic acid breakage in stressed cells (Pietta, 2000; Gill and Tuteja, 2010). Flavonoids also have photon scavenging ability and protect plants against photo inhibition and chlorophyll photo bleaching caused by excess light (Havaux and Kloppstech, 2001; Steyn *et al.*, 2002; Agati and Tattini, 2010). In addition, flavonoids can chelate redox-active metal ions (Fedenko *et al.*, 2017), modulate auxin signaling and transport (Murphy *et al.*, 2000; Brown *et al.*, 2001; Brunetti *et al.*, 2018), and protect against UV-B irradiation (Emiliani *et al.*, 2013).

The flavonoids influence on phytohormone signaling (primarily auxin and ABA) is suggested to strongly control the plant physiology and morphology (Buer *et al.*, 2010; Brunetti *et al.*, 2018). Several studies in Arabidopsis show flavonoid biosynthesis is up-regulated during cold acclimation and the amounts of flavonoids accumulated correlates relatively well with the degree of freezing tolerance acquired by the plants (Hannah *et al.*, 2006; Korn *et al.*, 2008; Schulz *et al.*, 2016; Tohge *et al.*, 2018).

Anthocyanins are glycosides of polyhydroxy and polymethoxy derivatives of 2-phenylbenzopyrylium and are the most versatile compounds among the flavonoids. These pigmented compounds are generally produced in leaves and stems of overwintering cereals during the cold acclimation process in the autumn. The antioxidant activity is mediated through the structure and substituents of the flavonoid B and C rings, where the presence of a positively charged oxygen atom on the C ring makes anthocyanins the most efficient antioxidants among flavonoids (Bors *et al.*, 1990; Pietta, 2000). Current studies show anthocyanin biosynthesis is regulated by an extensive crosstalk between several signaling pathways that are triggered by light quality, plant growth regulators (cytokinin, ethylene, JA, GA, ABA, and BR) and sucrose (Das *et al.*, 2012; Petridis *et al.*, 2016). The various signaling pathways converge on a MYB-bHLH-WD40 (MBW) transcription complex that serves as a hub for regulation of genes conferring anthocyanin accumulation in plants (Ramsay and Glover, 2005). The accumulation of anthocyanins in plants under cold stress conditions enables plants to maintain ROS-homeostasis and osmotic adjustments to stabilize proteins and membranes.

2.12 Genetic maps – QTL Mapping

Genetic recombination and segregation in the progeny of bi-parental cross affect the genetic mapping resolution, allele diversity and identification of quantitative trait locus (QTL) affecting a phenotype. Apart from identifying genomic regions governing target traits, QTL mapping is an effective tool to define loci in a population that co-segregate with the target phenotype (Alqudah *et al*., 2020). A wide range of genetic populations such as double-haploid (DH) populations, backcrosses, or recombinant inbred lines (RILs) families, have been studied using diverse genetic marker technologies including restriction fragment length polymorphism (RFLP), amplified fragment length polymorphism (AFLP), microsatellite or simple sequence repeat (SSR), diversity array technology (DArT) (Backes *et al*., 1995; Ganeshan *et al*., 2011: Båga *et al*., 2009), and SNP markers. SNP chip genotyping have been used to detect QTLs for developmental, agronomic and yield traits (Romero *et al*., 2018).

QTL mapping in Triticeae species has identified that *Vernalization 1* (*VRN1*) and *Frost resistance-2* (*FR-2*) loci, major determinants for freezing tolerance located on homoeologous group 5 chromosomes (Cattivelli *et al.*, 2002). The QTL (*FR loci*) located at the group 5 chromosome contains tandemly arranged *AP2/ERF* transcription factor genes denoted *C-repeat Binding Factors* (*CBFs*), and variations in *CBF* expression levels, copy numbers, and haplotypes affect freezing tolerance and WFS levels in hexaploid wheat (Pearce *et al*., 2013; Würschum *et al*., 2017), barley (Francia *et al*., 2007) and rye (Erath *et al*., 2017; Li *et al*., 2011*a*). However, haplotype variation in the *cbf* partially (30 – 40%) explain the LTT accumulation and / or WFS. Fowler and Limin (2004) suggested that the plant developmental traits also influence cold acclimation and vernalization process during the autumn, which subsequently affect the WFS. Båga *et al*, (2009) used a winter wheat bi-parental mapping population to show the interaction between the genomic regions associated with developmental traits and the low temperature loci. The results to-date suggest that the genetic mechanism for WFS is complex and controlled by several factors, such as rate and length of the cold acclimation process and the developmental program of the plant controlled by individual genes alone or in concert with other genes (Båga *et al*., 2009; Dhillon *et al*., 2010). For example, genotypes with high vernalization requirement exhibit a long cold acclimation process, develop a prostrate growth habit (PGH), initiate a high number of leaf primordia at the SAM, leading to a high final leaf number (FLN) at maturity (Båga *et al*., 2009; Limin and Fowler, 2000; Mahfoozi *et al*., 2001). The PGH displayed prior to winter

is an adaptive response proposed to suppress weed growth, reduce water evaporation from soil, increase photosynthetic efficiency, and allow plants to benefit from warmer temperature and reduced wind exposure at ground level (Tan *et al.*, 2008; Körner, 2016). In the spring, the most-hardy winter hardy genotypes tend to flower late, grow tall and produce small and narrow leaves (Limin and Fowler, 2000). In summary, it is imperative to identify the genomic regions and / or genes associated with plant developmental traits influencing LTT accumulation and WFS.

2.13 Genome-Wide Association Study (GWAS)

The GWAS is a population-based strategy that uses historical recombination events in natural populations to identify small haplotype blocks associated with phenotypes of interest across species scale diversity (Bazakos *et al*., 2017). It is based on the correlation between each marker and a phenotype scored in a diverse set of unrelated, distantly related and/or heterogeneous individuals (Huang and Han, 2014), to identify causative loci/genes and genome-phenotype associations. The historical recombination events (Rafalski, 2010) available in large populations, combined with substantial number of markers obtained by high-throughput sequencing technology contribute to the robustness and high resolution of GWAS (Alqudah *et al.,* 2020). The mapping method has been successfully used to dissect complex traits in crops like wheat, barley, and rye (Garcia *et al*., 2019; Reinert *et al*., 2016; Gaikpa *et al*., 2020). The ability of GWAS to identify true association is dependent on five major factors. Three factors are related to the population and include, the degree of phenotypic variation, number of individuals in the population (size) and the relatedness of the individuals in the population (structure). The markers are used to detect subgroups within the experimental population and considered as fixed effects and used as co-factors in the analysis. This method uses a set of random markers to infer the population structure and ancestry of the experimental panel. The population structure can be determined using the computer software STRUCTURE (Pritchard *et al.*, 2000) or a simple computational method, principal component analysis (PCA) (Price *et al*., 2006). The other two factors include the allele frequency (markers) and the linkage disequilibrium (LD) that defines the interval of the highly associated markers, that can affect the characterization of the most significant loci. A significant correlation between the covariance of a marker polymorphism and trait of interest is defined as an association and forms the basis of a QTL (Sotocerda and Cloutier, 2012). Physical linkage is not associated with LD, as many allelic variants that are very close to each other may have low LD

either due to recombination or the variants are not at equal frequencies. SNPs in LD can also be located on different chromosomes. The mapping resolution is high if the LD decays within a short distance, on the contrary LD extends over a long distance the mapping resolution is low (Rafalski, 2002). High resolution mapping requires a high number of markers, while a small number of markers are needed for low resolution mapping. Closely linked adjacent SNP (5-15 markers) are used to characterize a genomic region (QTL, multi-allelic) under selection by breeders (Buntjer *et al*., 2005; Famoso *et al*., 2011). Haplotypes based on single SNP are biallelic and can be used to identify candidate genes underlying traits of interest (Yonemaru *et al*., 2014).

2.14 SNP markers

Molecular (DNA-based) markers are the predominant marker system for genetic investigation and crop enhancement (Liu *et al*., 1998). The major factors contributing to their use are 1) abundance; 2) unaffected by the environment or growing conditions; and 3) more objective than the phenotype markers. The single-nucleotide polymorphisms (SNP) markers are biallelic, co-dominant markers that are abundant in the genome (Syvanen, 2001). Insertion-deletion markers are also prevalent and can provide polymorphism to be used as markers. The mutation rate in SNPs is relatively low, they can be used to investigate complex physiological processes and the evolution of genomes (Batley *et al*., 2003). Initially, implementation cost was a major challenge for the use of SNP markers in crop improvement. Recently the commercial high throughput SNP genotyping platforms have reduced the cost and made SNP markers efficient for use in crop improvement. SNPs have been used to develop high-density genetic maps for several crops (Verdeprado *et al*., 2018) and it has become a standard method gene and QTL discovery for several crops (Wang *et al*., 2010; Raflaski, 2010; Younis *et al.*, 2020; Ibrahim *et al*., 2020).

2.15 Genotyping-by-sequencing (GBS)

The technical advances in DNA sequencing technology from Sanger sequencing to nanopore sequencing has made it more efficient and cost effective to be used in a vast array of biological processes (Delseny *et al.,* 2010). Modern biology has been transformed by the next generation sequencing (NGS) that is high throughput and low cost (Schuster, 2008; Shendure *et al.,* 2017). The NGS includes three basic steps: (i) library construction with fragmented genomic DNA; (ii) PCR mediated DNA amplification in the library; and (iii) sequencing the amplified DNA

(Mardis, 2008). GBS is the incorporation of reduced-representation sequencing (RRS) with NGS to make it cost efficient (Elshire *et al.,* 2011), while allowing adequate genome coverage to sample the whole genome. This allows the analyses of large segregating populations and / or diversity panels to identify marker trait associations using LD and even genomic selection (Baxter *et al*., 2016; Poland *et al.,* 2012*b*; Wang *et al.,* 2019). To efficiently use GBS in plants with large and complex genomes, the highly repetitive sections of the genome must be avoided and that each individual is sampled at homologous regions (Peterson *et al*., 2012). This is achieved using specific restriction endonucleases that exclude highly repetitive regions of genomes and target low-copy regions with high efficiency (Mascher *et al*., 2013). GBS libraries are limited because they cannot cover essential genomic regions when the restriction sites are unavailable around those areas. A set of restriction enzyme combinations, such as frequent – rare, rare – rare, frequent – frequent or methylation sensitive enzymes are used to alleviate these limitations. Another feature to achieve a higher read coverage per locus is to increase the degree of multiplexing during GBS (Davey *et al*., 2011). Initially GBS strategies largely used sequencing with the Illumina GAII and HiSeq platforms (Poland *et al*., 2012*a*); however, the utilization of semiconductor devices for non-optical genome sequencing (Rothberg *et al*., 2011), have been used for routine sequencing with the Ion Torrent PGM and Proton sequencing which adds a dNTP to the DNA polymer and it releases a H^+ causing a pH change that is monitored. The innovations in DNA sequencing combined with refined bioinformatics algorithms have been used to understand the domestication of cereal crops such as barley (Mascher *et al.,* 2016; Pankin *et al.,* 2018), rice (Meyer *et al.,* 2016) and maize (Ramos-Madrigal *et al.,* 2013).

2.16 Phenotypic variation

The main objective of GWAS is to characterize the relation between an allele or genotype frequency to a trait status. Therefore, a basic consideration in GWAS is to identify a method to score the trait in an appropriately sized population showing adequate trait variance. The population size contributes to both phenotypic and genotypic variation, thus it is a major factor contributing to the success of a GWAS study. A higher population size improves the phenotypic and genotypic variation, identify meaningful associations with large effect and reduce the effect of rare variants. However, due to pragmatic considerations, a population size between 100 to 500 is needed for acceptable GWAS (Kumar *et al*., 2012). The individuals are selected for their expected phenotypic

and genotypic variation based on their geographic origin, growth habit, trait response and any factor influencing the phenotypic characterization. The raw phenotypic data needs to be carefully examined to filter outliers before conducting the analysis. Outliers refer to noisy data points, that can interfere with the normal distribution and affect the association analysis. However, care should be taken to note that avoiding outliers in the analyses does not influence the outcome of the experiment. Presenting the phenotypic data by boxplots is used to identify the outliers. Trait heritability strongly indicates the contribution made by genetic variance in phenotype and the degree to which phenotype is connected with the genotype (Alqudah *et al*., 2020). Therefore, traits with medium to high heritability are amenable to GWAS. Low heritability is a major factor limiting the use of GWAS to determine trait marker relationship. In field experiments, such as determination of winter field survival, genotypes for phenotypic evaluation are often repeated over number of years and / or locations. The genotype by environment interaction has the potential to reduce trait heritability. Statistical data analyses, such as the best linear unbiased predictor (BLUP) or best linear unbiased estimator (BLUE), is used to adjust the phenotypic data obtained from several years and / or locations to normalize the estimates of phenotypic variation taking into consideration the genotype x environment interaction (Alqudah *et al*., 2020). The association between a SNP and phenotypic trait is determined by the estimation of variance, which in GWAS is also called SNP-based heritability. This is used to genetically dissect variation and help to understand complex traits such as winter field survival in the present study. The added benefit of the GWAS analyses is that the most significant SNP associated with a trait can be directly used in a crop improvement program to identify and / or develop genotypes with improved trait of interest.

2.17 Winter field survival in autumn seeded cereals – a complex trait

Autumn seeded winter cereals such as wheat and rye provide several environmental benefits such as spring growth at a time of optimal moisture from snow melt (Entz and Fowler, 1991), making them more competitive against weeds (Beres *et al.*, 2010), reducing soil erosion in the fall (Delgado *et al.,* 1999) and an agronomy package built around no-till production system (reviewed in Larsen *et al.*, 2018). The major challenge in the incorporation of winter cereals in the Canadian prairies is the unpredictable winter field survival. Molecular biological strategies have been used to understand the genetic and molecular techniques to study low temperature tolerance in model plants (Arabidopsis) and winter cereals such as wheat, barley, oats and pulse

crops such as winter pea and beans. Most of the studies have focused on the characterization and genetic dissection of cold acclimation and vernalization which are adaptive strategies for plant survival in the field. However, winter field survival is a complex and it includes the interaction between the accumulation of low temperature tolerance during the cold acclimation process and changes in plant developmental traits established during cold acclimation and vernalization processes (Baga *et al.*, 2009; Dhillon *et al*., 2010; Bahrani *et al*., 2021). To improve WFS, a holistic strategy is needed to understand the genetics underlying the accumulation of LTT during cold acclimation, vernalization induced changes in the SAM contributing to plant development traits.

2.18 Rye is a good model for the study of complex trait WFS

Autumn seeded rye is one of the most-cold hardy winter cereals (Fowler and Carles, 1979), can grow under abiotic stress conditions on nutrient-poor soils (Schlegel, 2014). Rye belongs to the Triticeae, which likely has common progenitor genome which explains the high sequence synteny between the seven rye chromosomes of the diploid rye genome (2n=2x=14), diploid H genome of barley and the three genomes (A, B and D) of hexaploid wheat (Martis *et al*., 2013). The open-pollination nature of rye has increased nucleotide diversity and speedy LD (Li *et al*., 2011*b*; Auringer *et al*., 2016) as compared to wheat and barley which are self-pollinated and subject to extensive breeding efforts over the last several decades (Chao *et al*., 2010; Zhou *et al*., 2012). Low level of LD (520 bp; Li *et al*., 2011*b*) in rye can be used to increase resolution with the lowest possibility of false association to characterize the genetic architecture for complex traits. However, low LD requires large numbers of markers and necessitates the use of high-density genotyping platforms (Voss-Fels and Snowdon, 2016). The availability of next generation sequencing technology combined with the recently reported near full-length annotated rye genomes (85%; Rabanus-Wallace *et al*., 2021; 98.5%, Li *et al*., 2021) can be used to identify and characterize genes associated with WFS, LTT and developmental traits.

CHAPTER 3

MATERIALS AND METHODS

3.1 Plant material and seed production

A panel of 96 genotypes of rye (*Secale cereale* L.) originating from Canada and different regions of the world (Table 3.1) were used in the study. The genotypes included 72 winter, eight spring, eight facultative, and eight perennial types. To produce seeds, genotypes were seeded in 38-well trays (PL-38-STAR-DP; T.O. Plastics, Clearwater, MN, USA) containing LG3 Propagation Mix (Sungro Horticulture, Agawam, MA, USA) supplemented with 577 g slow-release Type 100 NPK 14-14-14 (Arysta Lifescience America Inc., Burton, OH, USA) and 79 g Micromax micronutrients (ICL Specialty Fertilizers, Dublin, OH, USA) per bag of soil (79 L). Plants were initially grown in a growth chamber with 16/8 h day/night cycle, 20 °C/18 °C day/night temperature, 50% humidity, and 250 μE m^{-2} s^{-1} light irradiance. Thereafter, the conditions for two-week-old plants were changed to 4 °C, 8/16 h day/night cycle, 120 μE m^{-2} s^{-1} light intensity and 50% humidity to allow for seven weeks of cold-acclimation. Cold-acclimated plants were transferred to six-inch pots containing soil and slow-release fertilizers as described above and grown to maturity in a greenhouse set at 17/7 h light/dark regime, 1500 μE m^{-2} s^{-1} light irradiance, 23 °C/18 °C day/night, and 50% relative humidity. During growth, nutrients were supplemented with 0.36 g/L NPK 20-20-20 once a week during watering. To assure self-pollination, five plants per genotype were grown together within 1.2 m^3 pollination bags made from polyester screening mesh (Vogel *et al*., 2014). Seeds were collected at maturity and stored at room temperature until use.

3.2 Field tests for determination of WFS

All field trials were conducted at the University of Saskatchewan Experimental Farm, Saskatoon, Saskatchewan, Canada (52° 10’ N, 106° 30’ W, 457 m altitude). Fifty of the 96 genotypes were tested for winter survival in the field during five consecutive growing seasons with

Table 3.1. Rye genotypes used in the study.

A. Fifty rye genotypes assessed in five years (2014/2015, 2015/2016, 2016/2017, 2017/2018, and 2018/2019).

Genotype	Growth habit	Origin	Genotype	Growth habit	Origin
AC Remington	Winter	Canada	Kustro	Winter	Canada
AC Rifle	Winter	Canada	Motto	Winter	Poland
Amilo	Winter	Poland	Musketeer	Winter	Canada
Animo	Winter	Netherlands	Othello	Winter	Sweden
Anna	Winter	Finland	Pearl	Winter	Denmark
Antelope	Winter	Canada	Petkus	Winter	Germany
Caribou	Winter	Canada	Ponsi	Winter	Sweden
Carolkurz	Winter	Germany	Prima	Winter	Canada
Carsten	Winter	Germany	Protector	Winter	Germany
Cougar	Winter	Canada	Puma	Winter	Canada
Dakold	Winter	USA	R003-4	Winter	Canada
Dakota	Winter	Canada	Saratovskaja 4	Winter	Russia
Dankowskie Nowe	Winter	Poland	Sellino	Winter	Germany
Dankowskie Selekcyjne	Winter	Poland	SM 4R	Winter	Canada
Dankowskie Srebrne	Winter	Poland	Stoir	Winter	Ukraine
Dominant	Winter	Netherlands	Toivo	Winter	Finland
Esprit	Winter	Germany	Visa	Winter	Finland
Frontier	Winter	Canada	Vitallo	Winter	Germany
GC-100	Winter	Russia	Voima	Winter	Finland
Halo	Winter	Germany	Balbo	Facultative	Italy
Hazlet	Winter	Canada	Gator	Facultative	USA
Horton	Winter	Canada	Maton	Facultative	USA
Kharkivska 95	Winter	Ukraine	Oklon	Facultative	USA
Kharkivska 98	Winter	Ukraine	Wren Abruzzi	Facultative	USA
Kodiak	Winter	Canada	Florida 401	Spring	USA

B. Forty-six rye genotypes assessed in three years (2016/2017, 2017/2018, and 2018/2019).

Genotype	Growth habit	Origin	Genotype	Growth habit	Origin
Adams	Winter	USA	SM 38R	Winter	Canada
Baltia	Winter	Russia	Somro	Winter	Germany
Clse 35	Winter	USA	Syn 20-L	Winter	Germany
Culpan	Winter	Russia	Vaschod	Winter	Belarus
Danae	Winter	Germany	Wheeler	Winter	USA
Danko	Winter	Poland	Elbon	Facultative	USA
Emerald	Winter	USA	Explorer	Facultative	USA
Enzi	Winter	Finland	Wintergrazer 70	Facultative	USA
Galma	Winter	Belgium	Extra Early Rye1	Spring	Mexico
Gauthier	Winter	Canada	Fl-Synt	Spring	USA

Gulzow Kunz CT1	Winter	Germany	Gazelle	Spring	Canada
Hardy white spring Rye	Winter	Austria	Harach	Spring	Canada
L-145-N	Winter	Germany	Prolfic Spring	Spring	Canada
L-145-P	Winter	Germany	Rogo	Spring	Germany
L-18-R	Winter	Germany	SR4A-S5	Spring	Canada
L-286-R	Winter	Germany	ACE-1	Perennial	Canada
Leth Coulee Rye	Winter	Canada	R1210	Perennial	South Africa
M.Karlic CT2	Winter	Russia	R538	Perennial	UK
Ottawa Select	Winter	Canada	R550	Perennial	Czech
Petkus Kurzstroh	Winter	Germany	R797	Perennial	Poland
Rymin	Winter	USA	R903	Perennial	Unknown
Sangaste	Winter	Estonia	R904	Perennial	Unknown
Sc-73	Winter	Canada	Reimann Philipp	Perennial	Germany

Table 3.2. Local climatological data during consecutive growing seasons 2014 to 2019.

	Sep	Oct	Nov	Dec	Jan	Feb	Mar	Apr	May	Jun	Jul	Aug
2014/2015												
Maximum temperature* (°C)	30	24	8	7	6	1	16	27	28	32	33	32
Minimum temperature (°C)	-2	-4	-29	-32	-34	-30	-30	-9	-4	4	5	2
Average maximum temperature (°C)	19	13	-6	-6	-7	-11	2	12	18	24	25	24
Average minimum temperature (°C)	6	1	-13	-13	-16	-22	-6	-1	2	11	13	11
Maximum soil temperature (°C)	16	11	3	-1	-1	-8	3	9	17	21	23	20
Minimum soil temperature (°C)	8	2	-10	-13	-19	-15	-12	0	6	12	17	12
Average soil temperature (°C)	12	8	-3	-4	-7	-10	0	5	11	18	20	17
Precipitation (mm)	13.0	15.2	14.2	0.0	1.0	0.3	1.0	19.6	8.9	33.5	37.1	68.6
2015/2016												
Maximum temperature (°C)	27	26	10	6	4	5	11	25	33	30	29	29
Minimum temperature (°C)	-5	-5	-24	-27	-31	-24	-17	-7	-2	5	8	3
Average maximum temperature (°C)	18	13	1	-5	-8	-3	2	12	22	24	24	23
Average minimum temperature (°C)	6	1	-6	-13	-12	-12	-6	-1	6	11	12	11
Maximum soil temperature (°C)	16	11	7	3	-2	-2	2	8	16	22	22	20
Minimum soil temperature (°C)	6	3	-2	-6	-7	-7	-6	0	5	15	17	15
Average soil temperature (°C)	11	6	2	-3	-4	-4	0	4	12	18	19	18
Precipitation (mm)	45.5	32.0	11.7	0.3	1.0	2.0	2.3	2.0	39.4	50.0	55.4	51.6
2016/2017												
Maximum temperature (°C)	29	17	20	2	6	8	12	21	30	33	30	27
Minimum temperature (°C)	-2	-3	-10	-30	-35	-31	-26	-9	-3	4	6	6
Average maximum temperature (°C)	19	6	7	-9	-7	-5	-1	10	19	22	26	25
Average minimum temperature (°C)	5	-1	-2	-18	-17	-13	-10	-2	5	10	12	10
Maximum soil temperature (°C)	18	12	6	-1	-3	-1	3	6	18	22	23	20
Minimum soil temperature (°C)	9	2	-1	-12	-7	-6	-6	0	6	11	18	15
Average soil temperature (°C)	12	2	1	-7	-5	-3	-2	2	10	15	21	18
Precipitation (mm)	26.4	30.7	8.6	0.0	1.8	0.0	1.0	15.7	55.9	45.7	24.6	14.7

Table 3.2. (*Continued*)

	Sep	Oct	Nov	Dec	Jan	Feb	Mar	Apr	May	Jun	Jul	Aug
2017/2018												
Maximum temperature (°C)	30	23	6	6	6	2	3	26	31	30	33	33
Minimum temperature (°C)	-1	-9	-23	-35	-30	-32	-26	-22	-1	5	6	4
Average maximum temperature (°C)	20	11	-4	-7	-8	-11	-3	5	22	24	25	24
Average minimum temperature (°C)	6	-1	-14	-16	-17	-23	-13	-7	7	10	12	10
Maximum soil temperature (°C)	19	12	1	-1	-4	-7	-3	7	18	21	22	22
Minimum soil temperature (°C)	8	3	-2	-11	-12	-13	-7	-5	7	11	17	13
Average soil temperature (°C)	14	6	-1	-2	-6	-9	-4	0	11	18	20	17
Precipitation (mm)	32.8	14.5	0.3	0.0	0.0	0.0	0.3	5.1	23.1	6.6	31.8	25.1
2018/2019												
Maximum temperature (°C)	23	21	4	5	4	-11	14	22	31	34	29	34
Minimum temperature (°C)	-9	-10	-23	-30	-31	-39	-34	-10	-10	4	6	3
Average maximum temperature (°C)	12	9	-4	-5	-8	-22	7	12	17	22	24	24
Average minimum temperature (°C)	3	-4	-10	-14	-19	-31	-17	-3	1	9	12	10
Maximum soil temperature (°C)	15	5	3	-2	-3	_	_	10	18	19	22	_
Minimum soil temperature (°C)	3	1	-2	-6	-9	_	_	0	4	12	15	_
Average soil temperature (°C)	9	4	-1	-3	-7	_	_	4	11	15	18	_
Precipitation (mm)	31.0	6.4	4.8	0.3	2.3	0.0	4.6	2.3	7.6	63.2	67.8	3.8

*(www.weatherlink.com)

harsh temperature variation in the cold season (Table 3.2): (i) 2014/2015, (ii) 2015/2016, (iii) 2016/2017, (iv) 2017/2018, and (v) 2018/2019. The remaining 46 genotypes were tested during the 2016/2017, 2017/2018, and 2018/2019 trials (Table 3.1). Seeding was done in early September, and every genotype was seeded in triplicate in a randomized complete block design (RCBD). Each genotype was seeded in three randomly placed 3.6 m rows with 100 seeds/row. Row spacing was 30 cm and field was fertilized with NPK 12-52-0 (50 kg/ha) at seeding and ammonium nitrate NPK 34-0-0 (50 kg/ha) in the early spring. The number of germinated seeds per row was determined six weeks upon seeding and percentage surviving plants per row was determined the following spring. Based on the best linear unbiased estimates (BLUEs) scores for the population, the winter hardiness for the genotypes was divided into five groups: very high (64.5–92.5%; 19 genotypes), high (56.7–64.3%; 20 genotypes), moderate (46.2–56.6%; 19 genotypes), low (30.5–43.7%; 19 genotypes) and very low (0–25.2%; 19 genotypes) winter field survival (Table 4.1)

3.3 Freeze tests to determine LTT

To determine the LTT (negative LT_{50} values), freeze tests were performed on 96 rye genotypes using cold-hardy winter wheat (*Triticum aestivum* L.) cv. Norstar as internal control. In this assay, plants were grown to the four-leaf stage in a growth chamber as described in section 3.1. The plants were cold acclimated for five weeks at 4ºC, day/night cycle of 8/16 h, light intensity of 120 μE m^{-2} s^{-1}, and 50% humidity. A total of 60 cold-acclimated plants per genotype were transplanted into five six-inch pots with 12 plants per pot. Plants were then acclimatized in the dark to -3°C for 12 h in an EPZ-4H test chamber (ESPEC North America Inc., Hudsonville, MI, USA). Thereafter, the chamber temperature was lowered at a rate of 2.0ºC per h. When the first test temperature was reached, one pot per genotype was removed from the freezing chamber and transferred to a 4°C growth chamber for thawing. The remaining pots in the freezing chamber were removed one after the other upon every 1.5°C additional decrease in temperature. For genotypes with highest LTT, the five freezing test temperatures ranged from –24 to –30ºC, whereas test temperatures ranged from –13.5 to –19.5ºC for genotypes with the lowest freezing tolerance. The selected test temperatures were pre-determined based on WFS data (Table 4.1) and small-scale freezing tests.

Cold-exposed plants were maintained at 4°C, 8/16 h day/night cycle, 120 μE m^{-2} s^{-1} light intensity, and 50% humidity for 20 hours before being trimmed to one-inch height and transferred

to a growth room set at 20°C/18°C day/night temperature, 16/8 h day/night cycle 50% humidity, and 250 μEm^{-2} s^{-1} light irradiance. The plants were fertilized once per week with NPK 20-20-20 (35 g/L) during watering. After two weeks of regrowth, plant recovery was rated for each of the 60 plants per genotype using a scale from 0 to 5: (i) "0" indicated that the plant is completely dead or is presumed to die if regrowth were to continue; (ii) "1" indicated that the plants showed almost no regrowth but are presumed to survive if given more time for regrowth; (iii) "2" indicated that that the plant regrew, but regrowth was < 1 inch in length from the trim point; (iv) "3" indicated that the plant regrew >1 inch in length, but one or more tillers failed to grow back; (v) "4" indicated that that the plant and all of its tillers regrew, but the plant height was not the same as it was before the LTT test; and (vi) "5" indicated that the plant regrew fully with all of its tillers and at least one stem matched or was nearly the same height that it was before the LTT test (Fig. 3.1). Average survival scores obtained at each test temperature were plotted against freezing test temperature to generate a kill curve (Fig 3.2). The freezing temperature at which 50% of the plants survived was determined as the LT_{50} value. The freezing tests were repeated twice to determine an average LT_{50} value for each genotype.

3.4 Collection of phenotypic data for developmental traits

To analyze the plant developmental traits, 96 rye cultivars were assessed over four years. Fifty of the 96 genotypes were tested in the years 2015/2016, 2016/2017, 2017/2018, and 2018/2019, and the remaining 46 genotypes were tested during the 2016/2017, 2017/2018, and 2018/2019 seasons (Table 3.1). Five of the six developmental traits [final leaf number (FLN), prostrate growth habit (PGH), plant height (PHT), days to anthesis (DTA), and top internode length (TIL)] were assessed on plants cold acclimated in a growth room and grown to maturity in a greenhouse. Flag leaf area (FLA) was determined on plants grown in the field. Each trait was examined in four separate trials with five plants per genotype in each test. To determine FLN, the leaves were labelled numerically as they developed from the primary stem and the number for the flag leaf was recorded as the FLN. When the rye plants were fully cold acclimated in the growth room, PGH for the individual plants was rated based on three different growth habits: (1) erect, (2) intermediate, or (3) prostrate (Fig 3.3). The number of days from the end of cold acclimation and first anther extrusion was recorded as DTA. The three longest stems of mature plants were measured from the soil surface to the top of the head with awn length excluded to record the PHT.

A - 0 B - 1 C - 2 D- 3 E - 4 F - 5

Fig. 3.1. Visual rating of plant regrowth two weeks after freezing tests. Plant recovery scale from 0 to 5 used in LTT test to calculate LT_{50} values. A. indicated – 0; B. indicated – 1; C. indicated – 2; D. indicated – 3; E. indicated – 4; F. indicated – 5.

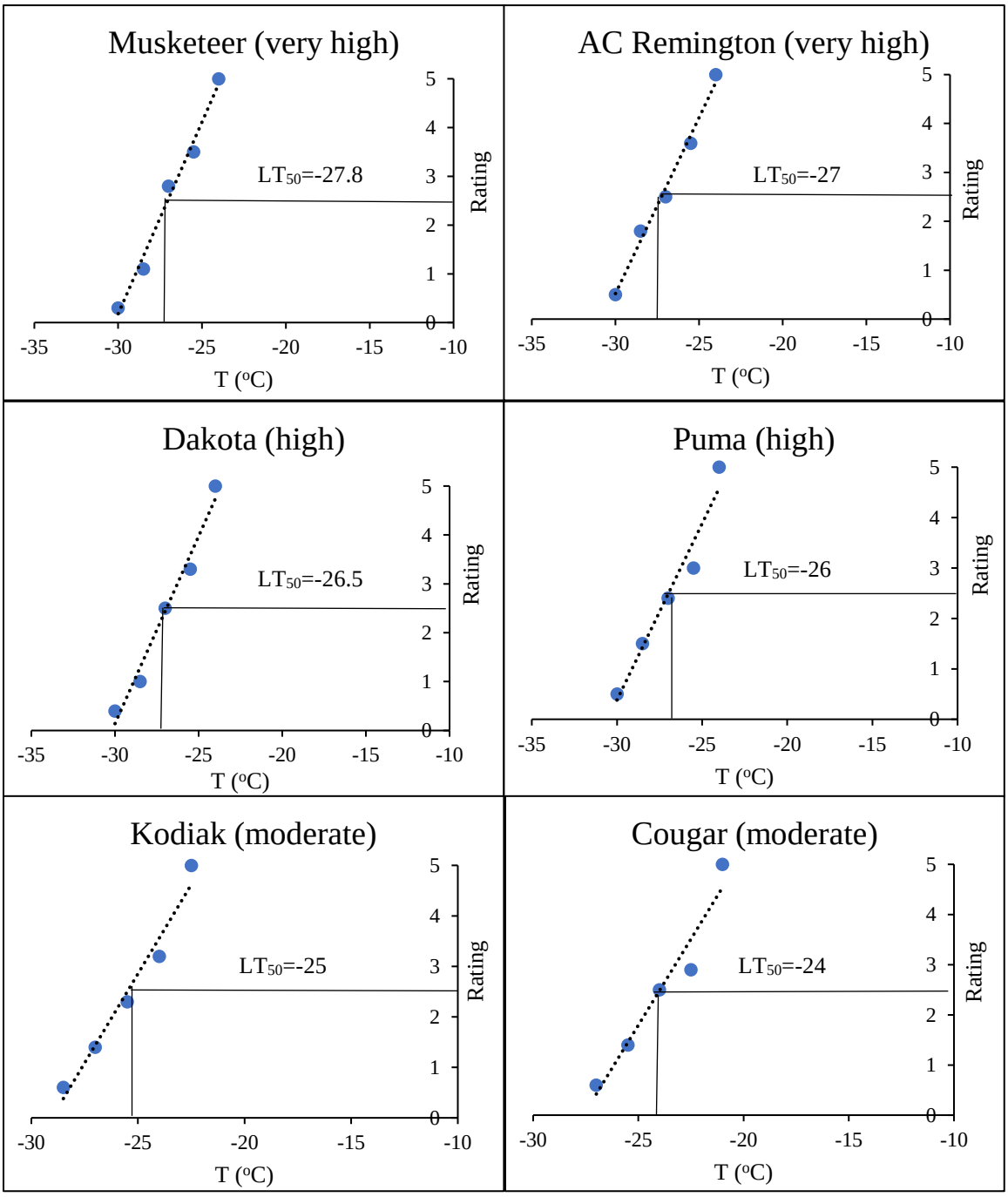
Musketeer (very high)
LT50=-27.8
AC Remington (very high)
LT50=-27
Dakota (high)
LT50=-26.5
Puma (high)
LT50=-26
Kodiak (moderate)
LT50=-25
Cougar (moderate)
LT50=-24
Rating
T (ºC)

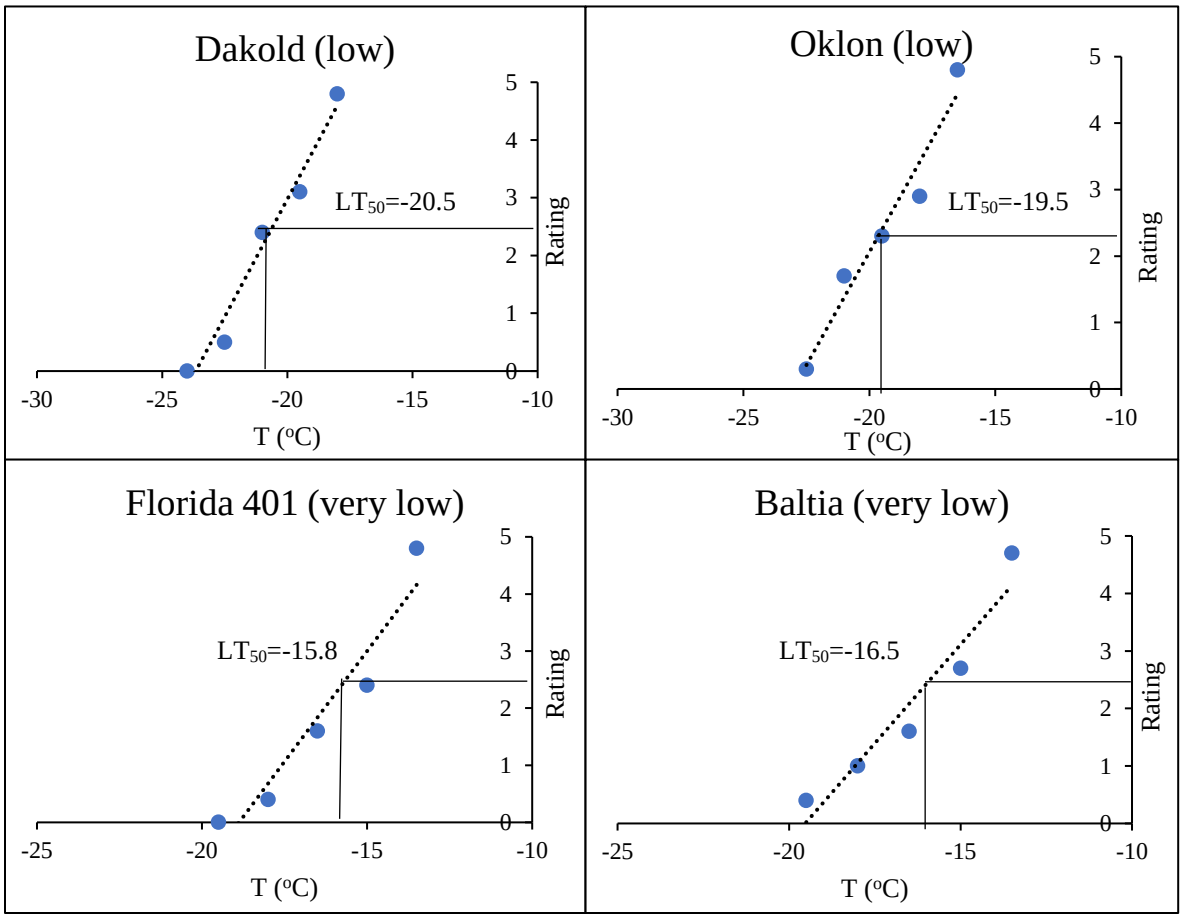

Fig. 3.2. Determination of LT_{50} value from kill curves. The average plant recovery score (0 to 5; 12 plants) for 12 plants per freezing temperature is shown on the y-axis and corresponding freezing temperatures on the x-axis. LT_{50} value was determined by the freezing temperature at which 50% of the plants survived.

(i) Erect (ii) Intermediate (iii) Prostrate

Fig. 3. 3. Rye genotypes used in this study separated into three groups based on their growth: (i) Erect, (ii) Intermediate, and (iii) Prostrate growth habit

The top internode length for the three culms were noted as TIL. FLA was determined on field-grown plants upon full extension of inflorescence and done on three plants per genotype with five flag leaves sampled per plant. The FLA measurements were done using a Portable Area Meter (LI-3000A) connected to a Transparent Belt Conveyor (LI-3050A) instrument (LI-COR Inc., Lincoln, Nebraska, USA).

3.5 Statistical analyses for phenotypic traits

The phenotypic data collected was assessed for normality using the Minitab 19 Statistical Software (Minitab, LLC, State College, PA, USA). Analysis of variance (ANOVA) was done by the general linear model using the GEA-R software (Genotype x Environment Analysis with R for Windows) version 4.1 (CIMMYT Research Data & Software Repository Network, Mexico). Mean sum of squares from ANOVA were applied to calculate heritability (h^2) for each trait (Singh *et al*., 1993). To determine the overall trait score for each genotype, the Best Linear Unbiased Estimates (BLUEs) was calculated for all the phenotype data collected (Piepho *et al*., 2008). The calculation was conducted using the statistical analysis software META-R (Multi Environment Trial Analysis with R) version 6.04 (CIMMYT Research Data & Software Repository Network, Mexico). Correlation analyses and principal component analysis (PCA) were conducted using RStudio package version 3.5.1 software (Chavent *et al*., 2012). The first two components were used to create biplot illustrating the relationships between genotypes and measured traits.

3.6 Anthocyanin analysis

Anthocyanins were analyzed in the leaves and crown tissue of the 96 rye genotypes that had been cold acclimated as described in section 3.1. To serve as controls, 15 non-cold acclimated control genotypes (Musketeer, AC Rifle, Prima, Kodiak, Danko, Hazlet, Puma, Cougar, Antelope, Carsten, Dakold, Gator, Petkus, Wren Abruzzi and Florida 401) were grown for seven weeks in the growth room under normal conditions (16/8 h day/night cycle, 20 °C/18 °C day/night temperature, 50% humidity, and 250 μE m^{-2} s^{-1} light irradiance).

3.6.1 Preparation of plant extracts

Tissue samples were collected from three-week-old plants of each genotype. A pool of 12 crowns per genotype were excised from all 96 genotypes upon cold acclimation in a growth room.

Three leaf samples per genotype and crown tissues (12 crowns per genotype) were also collected from 15 non-cold acclimated control genotypes listed above. Another set of leaf tissues (three samples/genotype) were collected for all 96 rye genotypes upon six weeks cold acclimation in the field during the fall of 2017. All sampled tissues were quick-frozen in liquid nitrogen and stored at −80 °C until being used for preparation of extracts. A modified method was used to prepare flavonoid extracts (Abdel-Aal and Hucl, 2003). Briefly, frozen leaf (100 mg) or crown tissue (250 mg) tissues were ground to a fine powder in liquid nitrogen using a mortar and pestle and suspended in 1.0 mL methanol, 1 M HCl (85:15 v/v). The samples were shaken (150 r/min) for four hours in a 32 °C water bath to extract soluble compounds. Insoluble material was removed by two centrifugations at 20,000 × g, 20 min and the resulting supernatant was stored at 4 °C. Immediately prior to HPLC-QTOF MS/MS analysis, the extracts were cleared by another centrifugation (20,000 × g, 20 min, +4 °C) and filtered through a 0.45 µm regenerated cellulose filter (Waters Corp., Milford, MA, USA).

3.6.2 HPLC-QTOF MS/MS analysis of anthocyanins

The flavonoid extracts were analysed by high-pressure liquid chromatography (HPLC) followed by peak identification by quadrupole-time of flight mass spectrometry (QTOF-MS) analysis using a MDS Sciex QSTAR XL LC/MS/MS TOF instrument (Applied Biosystems, Foster City, CA, USA). The QTOF-MS system was operated with positive electrospray ionization mode and calibrated with the Sex Pheromone Inhibitor iPD1 (BACHEM California Inc., Torrance, CA, USA) and cesium iodide (Sigma-Aldrich Chemistry, Milwaukee, WI, USA). Sample injection volume was set to 10 µL, flow rate to 0.5 mL/min and the 250 mm × 4.6 mm, 2.6 µm C18 Aeris column (Phenomenex, Torrance, CA, USA) was equilibrated to 40 °C. Elution of samples was done with mobile phases A (1% formic acid) and B [22.5% (v/v) methanol, 22.5% (v/v) acetonitrile]. The elution gradient was set to 9% B for 0–12 min, followed by 35% B for 12–25 min, and 50% B for 25–40 min and 9% B for 40–55 min. Elution peaks were detected at 520 nm using a DAD 1100 detector (Agilent, Santa Clara, CA, USA). HPLC grade methanol, hydrogen chloride, acetonitrile and formic acid were purchased from Thermo Fisher Scientific (Waltham, MA, USA). HPLC water (18.2 µmhos/cm) was prepared from distilled water using a Barnstead Nanopure system (Fisher Scientific, Waltham, MA, USA). The cyanidin-3-O-glucoside (Cya-3-Glc), cyanidin-3-O-rutinoside (Cya-3-Rut) and pelargonidin 3-O-glucoside (Pel-3-Glc)

compounds diluted to 0–40 ng, μL^{-1} concentration in methanol, 1 M HCl solution (85:15 v/v) were used as external standards. The r^2 coefficients for the standard curves ranged from 0.9981 to 0.9989. The concentrations of Cya-3-Glc, Cya-3-Rut and Pel-3-Glc determined for samples were expressed as μg, g^{-1} fresh weight tissue and the concentration of the remaining anthocyanins were quantified as relative peak areas. Standard solutions were obtained from Sigma-Aldrich (St. Louis, MO, USA). The HPLC-QTOF MS/MS data was analyzed using the Analyst QS 1.1 software (Applied Biosystems, Foster City, CA, USA). Confidence of the anthocyanin identification was based on ±5 ppm difference between the theoretical and the experimental mass determinations.

3.7 Genotyping by Sequencing (GBS)

3.7.1 DNA extraction

Leaf tissue (about 130 mg) was collected from five two-week-old plants of each genotype and ground to a fine powder in liquid nitrogen using a mortar and pestle. DNA was extracted from the homogenized leaf material according to a modified hexadecetyltrimethylammonium bromide (CTAB) method (Healey *et al*., 2014). Briefly, flash frozen fresh young leaves (130 mg) from five plants of each genotype and ground in liquid nitrogen using a mortar and pestle. Approximately half of the ground leaf material was transferred to a tube containing 2 mL of pre-warmed (65ºC) CTAB extraction buffer [2.5% CTAB, 100 mM Tris-HCl pH 8.0, 1.5 M NaCl, 20 mM EDTA pH 8.0, 1% PVP (Mw 10,000, Sigma Aldrich, St Louis, MO, USA) with 0.5% β-mercaptoethanol] and mixed immediately by rapidly inverting the tube. The samples were incubated at 65°C for 1 h, and the tubes were inverted every 5 min to keep the samples well mixed. After incubation for 1h, 2 mL of chloroform/isoamyl alcohol (24:1) was added and the tubes inverted > 50 times to make a water/chloroform emulsion. The emulsion was centrifuged in a microfuge (Eppendorf 5804R centrifuge, F-34-6-38 rotor, Eppendorf, AG-22331, Hamburg, Germany) at 10,000×g for 10 min at room temperature. Approximately 1.7 mL of the upper phase was slowly removed and transferred to a new 5.0 mL tube; taking care that nothing from the interphase layer was transferred. The tubes were centrifuged at 10,000×g for 2 min to force any chloroform to the bottom of the tube (samples must not mix after centrifugation). RNAase A [1.5 μL, 20 mg, mL^{-1} RNAase A (Bovine RNAase in glycerol, DNAase-free; Sigma R6513)] was added to the solution. The samples were incubated for 15 min in a 50°C water bath and then mixed and centrifuged at 10,000×g for 1 min in a microfuge (Eppendorf 55415R centrifuge, F-45-24-11 rotor, Eppendorf,

AG-22331, Hamburg, Germany). An additional 1.5 µL RNAase was added to the solution without mixing. The solution was incubated for 15 min at 50°C. Then, 1.2 mL isopropanol was added and mixed by inversion until the DNA precipitated (samples rested on the bench for 10 min). Using a 1000-µL pipette at its lowest possible setting, the DNA was carefully transferred into new, labeled, empty tubes, and 2 mL ethanol (70% v/v) was added. The tubes were inverted a few times to rinse. The tubes were incubated at room temperature for 10 min on a gel shaker (repeated twice). The DNA precipitate was carefully transferred to fresh, empty, labeled tubes using a 1000 µL pipette. An attempt was made to transfer over as little 70% ethanol as possible. Using a 10-µL pipette, liquid (as much as possible) was carefully removed from the precipitate. TE buffer (500 µL, 10 mM Tris-HCl pH 8.0, 1.0 mM EDTA) was added and the solution re-suspended by flicking the tubes, which were then incubated for 10 min at 37°C in a water bath. Chloroform/isoamyl alcohol (500 µL, 24:1) was added to the tubes and inverted > 50 times, followed by centrifugation at 10000×g for 10 min at room temperature. Then, 400 µL of supernatant was transferred to new 2.0 mL tubes containing 50 µL 3 M sodium acetate and 1.25 mL of ethanol (100%). The solution was mixed by inverting the tubes > 10 times and allowing them to sit on the bench for 10 min. The tubes were centrifuged at 10000×g for 10 min. The supernatant was pipetted off without disturbing the DNA pellet. Ethanol (1 mL, 70% v/v) was added, and the tubes inverted to rinse (all tubes must have their pellets). The tubes were placed on the bench for 5 min and then centrifuged at 10000×g for 5 min. The supernatant was removed, and the ethanol (70% v/v) wash was repeated. The samples were centrifuged at 10000×g for a few seconds to collect the remaining liquid in the bottom of the tube. Then, all liquid was pipetted from the pellet. The samples were air-dried for about 10 min at 37°C to evaporate the ethanol. The pellets were dissolved in 100 µL TE buffer (low EDTA, 10 mM Tris-HCl pH 8.0, 0.1 mM EDTA). The tubes were flicked (not vortexed) to loosen the pellets and were incubated at 37°C for 10 min incubated on ice for 10 min to completely dissolve the DNA. The integrity of the DNA was assessed by gel electrophoresis. DNA (100 ng) from each sample was run on agarose (0.8% w/v) gel electrophoresis and visualized by ethidium bromide staining to determine whether the RNAase treatment was complete (Fig 3.4). The 260/280 and 230/260 absorbance ratios of the DNA were measured using a DU 730 spectrophotometer (Beckman Coulter, CA, USA). The DNA samples having absorbance ratios (260/280) greater than 1.8 and 230/260 ratios around 2.0–2.2 were considered of adequate quality for sequencing.

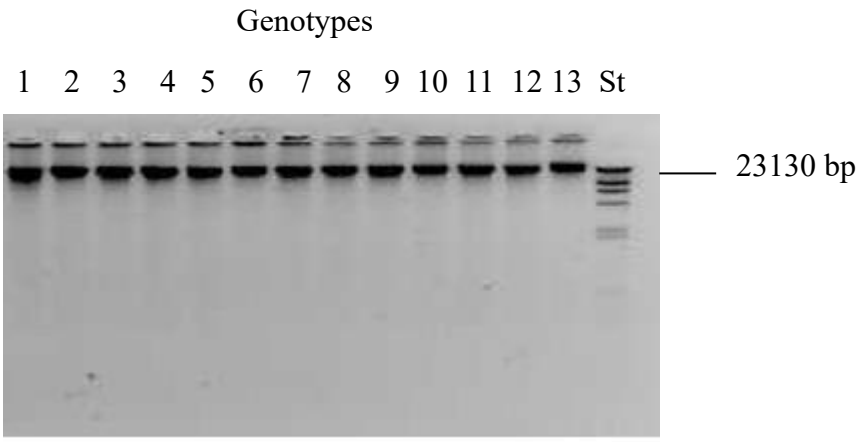

Fig. 3. 4. Agarose gel analysis of DNA extracted from rye genotypes used in the study. Ethidium bromide-stained agarose gel (0.8%) showing DNA separated by electrophoresis to show the high molecular weight (a marker for DNA integrity) and effectiveness of RNAse treatment. DNA samples (10 µL containing 0.1 µg) were loaded in each well. Lack of fast migrating nucleic acids and high molecular weight fragments migrating slower than the largest Hind III fragment (lambda DNA) were used as a criterion for good quality DNA. DNA samples from the rye genotypes were analyzed. 1: AC Remington; 2: AC Rifle; 3: Musketeer; 4: Prima; 5: Puma; 6: Kodiak; 7: Leth Coulee Rye; 8: Gauthier; 9: Saratovskaja 4; 10: Rymin; 11: Petkus; 12: Carsten; 13: Wren Abruzzi.

The concentration of DNA was determined using a DNA binding assay (Quant-iT™ PicoGreen® dsDNA Assay Kit, Invitrogen, Molecular Probes, Eugene, OR, USA). Standard solutions consisted of Lambda DNA (100 ng/µL) 200× diluted to 1.0 µg, mL^{-1} in 1× TE buffer (10 mM Tris-HCl pH 8.0, 1.0 mM EDTA). Standard solutions with concentrations of 0 (blank), 0.005, 0.025, 0.0675, 0.125, 0.250, 0.375, 0.500, 0.750, and 1.000 µg, mL^{-1} were used to make a linear standard curve. Samples were warmed at 37°C for 15 min, and the tubes were flicked to ensure that all DNA was dissolved and homogeneous. Diluted (100×) DNA samples in 1× TE buffer were made and 99 µL of 1× TE buffer was added to the wells of 96-well microtiter plate, and then 1 µL of 100× diluted DNA samples was added to each well. One-hundred microliters of diluted PicoGreen solution (200× in 1× TE buffer) were added and mixed gently by pipetting, and the well plate was wrapped in aluminum foil to protect the fluorescent dye from light. The plate was incubated for 5 min at room temperature and a SpectraMAX Gemini XS Fluorescence reader (Molecular Devices, USA) was used [excitation wavelength (Ex) at λ490; emission wavelength (Em) at λ525; emission cut-off filter at λ515] to determine the DNA fluorescence generated from each sample. The concentration was calculated from a previously prepared standard curve using known DNA concentrations.

3.7.2 DNA sequencing

Normalized DNA preparations at 10 ng, μL^{-1} (20 µL in total) were used for library preparations for DNA sequencing. Reduced-representation libraries were prepared from *PstI* and *MspI* double-digested DNA (Poland *et al*., 2012*a*) were used for chip (P1 V3 chips) preparations (Mascher *et al*., 2013) using an Ion CHEF System, Hi-Q reagents (ThermoFisher Scientific, Life Technologies Inc., ON, Canada). The DNA sequencing (six deep) was done by Ion Proton Sequencer (ThermoFisher Scientific, Life Technologies Inc., Waltham, MA, USA) by a service provider Plateforme d'analyses Génomiques of the Institut de Biologie Intégrative et des Systèmes (IBIS, Université Laval, Québec, Canada.

3.8 SNP calling

Raw FASTQ files obtained from GBS analyses of the 96 rye genotypes were processed by Trimmomatic version 0.36 (Bolger *et al*., 2014) with a four-base window setting and a minimum average quality score of 16. Barcodes, adaptors, and reads less than 36 bp were eliminated. The

output sequences were aligned to scaffolds of rye inbred line Lo7– version 2 (Bauer *et al*., 2017) using Bowtie 2.0 version 2.2.6 (Langmead and Salzberg, 2012). Duplicates were removed using the rmdp function (Li, 2011) and SNPs including insertions/deletions (InDels) were detected by Sequence Alignment/Map tools (SAM tools) version 0.1.19 (Li, 2011). The markers were filtered using the Variant Call Format (VCF) tool version 0.1.14 (Danecek *et al*., 2011) using a minimum allele frequency (MAF) ≤ 5% and a minimum reading depth of 6.0.

3.9 Analysis of population structure

The genetic relationship among the 96 rye genotypes was analyzed using a model-based clustering method implemented by the STRUCTURE version 2.3.4 software (Pritchard *et al*., 2000). Based on an admixed model and allele frequencies correlated, the number of subpopulations (K) ranging from 1 to 9 were tested with burn-in time set to 50,000 and Markov Chain Monte Carlo replication number to 100,000. A total of 20 runs were performed for each data set to compute the log likelihood for each simulated K value. The STRUCTURE HARVESTER version 0.6.94 software (Earl and von Holdt, 2012) was used to establish the optimal number of subpopulations according to the ΔK method (Evanno *et al*., 2005).

To visualize the relative genetic distances between the rye genotypes, the SNP data was subjected to a principal component analysis (PCA) conducted using RStudio package version 3.5.1 software (Chavent *et al*., 2012). The evolutionary relationships among the rye genotypes was calculated using TASSEL version 5.2.77 based on method described by Nei (Nei, 1972). The result from the analysis was displayed as a neighbor-joining dendrogram tree (NJTree).

3.10 Marker-trait association (MTA) analysis

The population structure obtained from STRUCTURE version 2.3.4, kinship data generated with TASSEL version 5.2.77 along with genetic and phenotypic data, was analyzed to identify MTAs using the mixed linear model (MLM) available in TASSEL version 5.2.20 (Bradbury *et al*., 2007). BLUE scores were used for WFS, FLN, PGH, DTA, PHT, TIL, and FLA trait data. Significant SNPs were initially tested based on a false discovery rate (FDR)-adjusted *p*-value of 0.05 following a step-wise procedure (Benjamini and Hochberg, 1995), and lowest adjusted *p*-values (threshold $p < 1.49e-04$) were identified after Bonferroni correction (Robertson *et al*., 2019).

To analyze the anthocyanins-associated SNPs the MLM used BLUE score analyses from three replicates of anthocyanins extracted from leaf and crown tissue. Significant SNPs were initially tested based on a false discovery rate (FDR)-adjusted *p*-value of 0.05 following a stepwise procedure (Benjamini and Hochberg, 1995), and lowest adjusted *p*-values (threshold $p < 2.76e-04$) were identified after Bonferroni correction (Robertson *et al*., 2019).

3.11 Prediction of candidate genes

The marker sequences carrying SNP of interest underwent BLASTN searches against the *Secale cereale* Lo7_v1 pseudomolecules hosted by Graingenes (Mar 2021; (https://wheat.pw.usda.gov/blast/)) and the IPK Rye Blast Server (ipk-gatersleben.de) to identify matches to the latest assembled Lo7 rye genome, chromosomal location for scaffolds, SNP position and its annotated genes (Rabanus-Wallace *et al*., 2021). BLAST searches against the National Cancer for Biotechnology Information (NCBI) nucleotide, transcript, and protein databases (https://blast.ncbi.nlm.nih.gov) were done to identify possible expressed gene sequences. The DNASTAR software package version 15.3.0 (DNASTAR. Madison, WI, USA) was used to analyze gene sequences in detail. The MapChart software version 2.3 (Voorrips, 2002) was used to construct a genetic map.

CHAPTER 4

RESULTS

4.1 A multi-trait approach to study WFS

Winter field survival (WFS) in autumn-seeded winter cereals is a complex trait contributed by LTT, and also associated with several plant developmental traits such as FLN, PGH, DTA, PHT, and ANT production. The traits TIL and FLA with no obvious association with WFS were also analyzed. In addition, low temperature stress induces red/purple colored pigmentation attributed to anthocyanins in plant tissues. Therefore, the concentrations of selected anthocyanins in leaf and crown tissue were also analyzed to study their association with WFS.

4.2 Rye genotypes showed a range of WFS[1]

Five field trials were conducted during the years 2014 to 2019 to determine WFS for 96 rye genotypes listed in Tables 3.1 and 4.1. The winter conditions in Saskatoon, Canada, during the trials varied (Table 3.2) and the highest survival was seen during the 2015/2016 growing season (92.5 % average WFS; Appendix 1), which provided adequate snow cover and relatively mild winter. In contrast, survival in the 2017/2018 winter season was much lower (6.8 % average WFS) due to deeper and longer cold spells and incidents of poor snow cover. The 2014/15, 2016/17, and 2018/19 trials generated wide distributions of WFS values within the population (Appendix 1), which was valuable for the association mapping studies. The 2016/2017 and 2018/2019 trials showed the strongest correlation ($r = 0.67$, $p < 0.001$), whereas the 2015/2016 and 2017/2018 trials did not significantly correlate with each other ($r = 0.17$, $p > 0.05$) (Table 4.2). Best linear unbiased estimates (BLUEs) calculated from all five trials produced WFS scores ranging from 0.0 to 92.5% (Table 4.1) and a distribution skewed towards higher values (Fig. 4.1A). WFS scores for winter genotypes (n = 72) ranged from 0.0 to 92.5%, however, WFS scores for non-winter genotypes (n = 24) ranged from 7.1 to 59.6% (Fig 4.2A). The correlation between BLUEs and the WFS values

---

[1] Bahrani, H., Båga, M., Larsen, J., Graf, R.J., Laroche, A., and Chibbar, R.N. (2021) The relationship between plant developmental traits and winter field survival in rye (*Secale cereale* L.) Plants 10: 2455.

Table 4.1. Classification of rye genotypes based on winter field survival score.

Winter survival class: genotype	WFS BLUE score*	LT_{50} value	PCA cluster	Evolutionary relationship (NJTree)
Very High:				
1-Leth Coulee Rye	92.5	-26.8	II	Iia
2-Gauthier	90.1	-26.2	II	Iia
3-AC Remington	86.2	-27.0	II	Iib
4-AC Rifle	85.9	-27.0	I	I
5-Musketeer	83.0	-27.8	II	Iia
6-SM 38R	77.5	-24.0	II	Iia
7-Prima	77.0	-27.5	II	Iib
8-Saratovskaja 4	71.8	-26.8	II	Iia
9-SM 4R	71.0	-26.8	I	I
10-Pearl	69.5	-26.6	II	Iia
11-Kustro	68.8	-25.8	II	Iia
12-Kharkivska 95	67.9	-24.8	II	Iia
13-Kharkivska 98	66.9	-24.0	II	Iia
14-Esprit	66.3	-22.8	II	Iia
15-Ponsi	66.0	-24.8	I	I
16-Hazlet	65.5	-23.6	I	I
17-Antelope	65.3	-26.2	II	Iia
18-Emerald	65.2	-22.0	II	Iia
19-Anna	64.5	-22.0	II	Iib
High:				
20-R003-4	64.3	-24.0	II	Iia
21-Voima	64.2	-23.8	I	I
22-Dakota	64.1	-26.7	II	Iib
23-Sc-73	64.0	-22.4	II	Iia
24-Animo	63.6	-25.2	II	Iia
25-Caribou	63.6	-23.8	I	I
26-Puma	62.4	-26.0	I	Iia
27-Othello	62.2	-22.0	II	Iia
28-Rymin	61.9	-23.4	II	Iia
29-Adams	61.5	-22.8	I	I
30-Sangaste	60.3	-23.0	II	Iib
31-Visa	59.9	-24.2	II	Iib
32-Vitallo	59.6	-23.5	II	Iia
33-Halo	59.5	-26.2	I	I
34-Balbo	59.4	-26.0	II	Iib
35-Frontier	58.6	-24.4	II	Iib
36-Enzi	58.4	-22.0	II	Iib
37-Explorer	58.4	-23.4	II	Iib
38-Motto	58.0	-23.6	II	Iia
39-Dankowskie Selekcyjne	56.7	-23.8	I	I
Moderate:				
40-Galma	56.6	-22.6	I	I
41-Cougar	56.1	-24.0	I	Iia
42-Dominant	55.8	-23.6	I	I
43-Dankowskie Nowe	54.9	-24.6	II	Iia
44-Danko	54.2	-24.8	I	I
45-ACE-1	54.0	-19.4	I	I
46-Dankowskie Srebrne	53.9	-24.2	I	1
47-Carolkurz	53.2	-23.8	II	Iia
48-Horton	53.1	-24.0	II	Iib
49-Kodiak	51.8	-25.0	II	Iib

Table 4.1. (*continued*)

Winter survival class: genotype	WFS score-BLUE*	LT_{50} value	PCA cluster	Evolutionary relationship (NJTree)
50-GC-100	51.6	-23.0	II	IIb
51-Amilo	49.2	-20.8	II	IIa
52-Sellino	48.5	-21.8	I	I
53-R538	48.1	-21.6	II	IIb
54-Protector	47.8	-22.4	II	IIa
55-Toivo	47.5	-23.8	II	IIb
56-Culpan	47.0	-22.6	II	IIb
57-Hardy white spring Rye	46.9	-21.6	II	IIa
58-Maton	46.2	-19.5	III	IIb
Low:				
59-Stoir	43.7	-22.2	II	IIa
60-Vaschod	43.7	-21.2	II	IIa
61-R550	43.6	-21.4	I	I
62-Reimann Philipp	42.4	-21.0	II	IIa
63-Oklon	40.9	-19.6	II	IIb
64-Carsten	39.5	-18.0	II	IIa
65-R903	38.9	-22.0	III	IIb
66-Harach	38.8	-21.4	II	IIa
67-Danae	37.1	-21.2	I	I
68-Clse 35	36.8	-20.2	II	IIb
69-Gator	36.0	-23.2	II	IIb
70-Elbon	35.9	-17.0	I	I
71-L-286-R	35.7	-16.4	I	I
72-R904	35.4	-19.8	III	IIb
73-Syn 20-L	35.3	-21.8	II	IIa
74-SR4A-S5	33.2	-17.6	II	IIa
75-Dakold	31.1	-20.5	II	IIb
76-Wheeler	31.0	-20.8	II	IIb
77-M.Karlic CT2	30.5	-19.5	I	I
Very low:				
78-Wintergrazer 70	25.2	-20.2	II	IIb
79-Petkus Kurzstroh	24.1	-19.0	II	IIa
80-Gazelle	23.6	-19.0	I	IIa
81-Petkus	22.9	-21.2	II	IIb
82-Prolfic Spring	22.1	-19.2	II	IIb
83-Wren Abruzzi	20.0	-18.0	I	I
84-Extra Early Rye1	19.7	-16.4	II	IIb
85-Somro	16.0	-18.8	II	IIb
86-R1210	15.7	-16.0	III	IIb
87-Baltia	15.6	-16.8	II	IIb
88-R797	13.2	-16.0	III	IIb
89-Fl-Synt	12.9	-16.4	II	IIb
90-Ottawa Select	12.9	-16.8	I	I
91-Gulzow Kunz CT1	12.4	-16.2	II	IIa
92-Rogo	12.4	-16.2	II	IIa
93-Florida 401	7.1	-15.8	II	IIb
94-L-145-N	0.0	-17.0	I	I
95-L-145-P	0.0	-16.5	I	I
96-L-18-R	0.0	-16.5	I	I

* Winter survival class based on BLUE scores calculated as described (Piepho *et al*., 2008).

Table 4.2. Correlations between LTT and WFS.

Trait	WFS 2014/15	WFS 2015/16	WFS 2016/17	WFS 2017/18	WFS 2018/19	WFS-BLUE
Low-temperature tolerance (LTT)[1]	0.70***	0.62***	0.82***	0.54***	0.81***	0.90***
Winter field survival 2014/15		0.44**	0.54***	0.37**	0.63***	0.66***
Winter field survival 2015/16			0.66***	0.17	0.49***	0.76***
Winter field survival 2016/17				0.36**	0.67***	0.91***
Winter field survival 2017/18					0.58***	0.59***
Winter field survival 2018/19						0.88***
Winter field survival BLUE score[2]						

[1/] LTT is defined as negative LT_{50} value. [2/] BLUE score determined from five WFS trials. **significance of Pearson correlation coefficient $p < 0.01$; ***$p < 0.001$

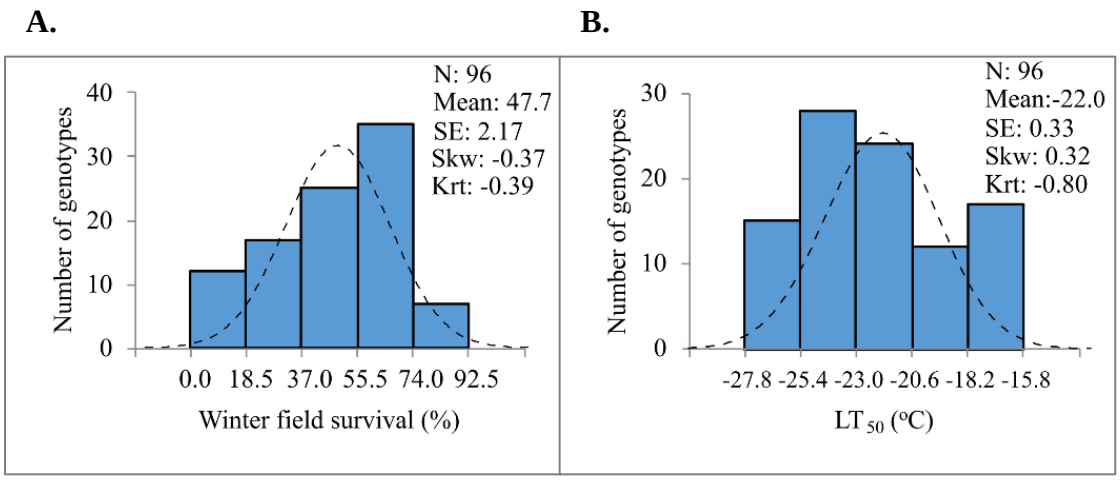

Fig. 4.1. Distribution of cold hardiness determined for rye population of 96 accessions. (A) WFS (BLUE scores) determined from five years of field trials. (B) Average LT_{50} values determined from controlled freezing tests.

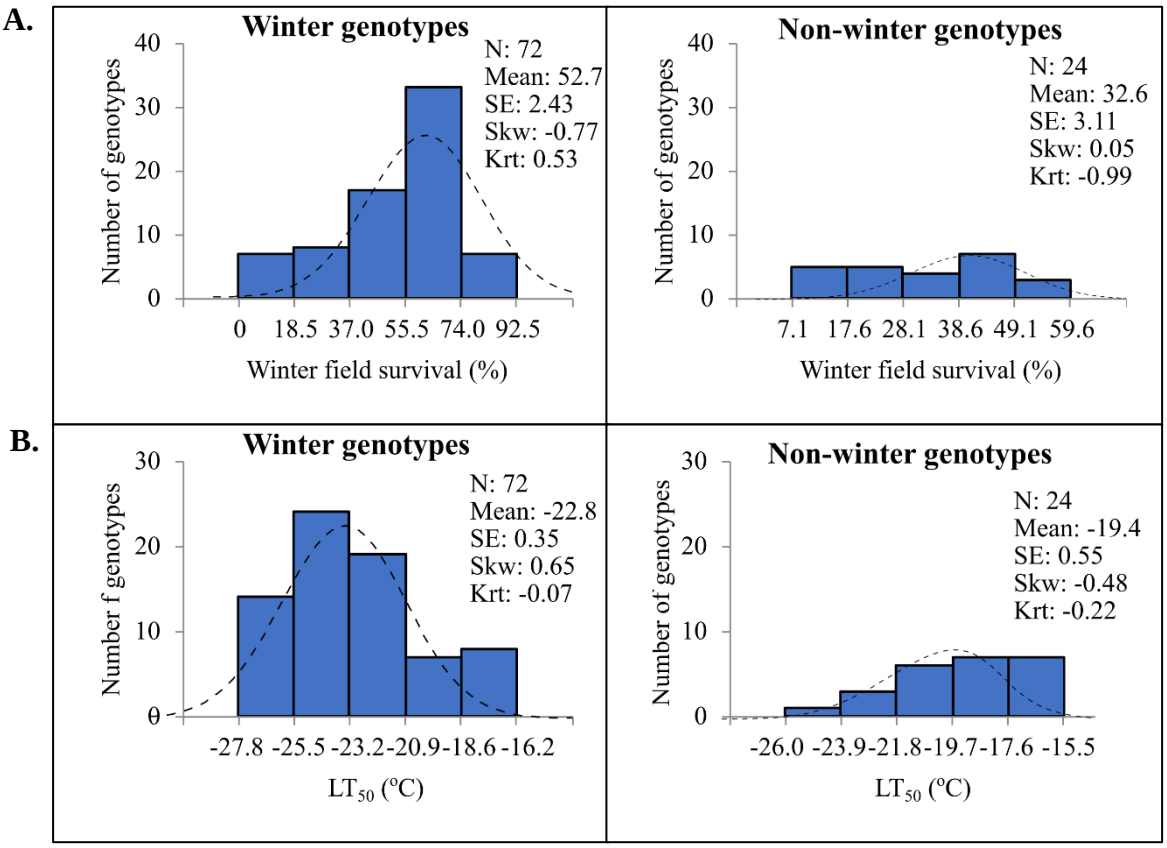

Fig. 4.2. Distribution of cold hardiness determined for rye population of 96 accessions. (A) WFS (BLUE scores) determined from five years of field trials in winter and non-winter genotypes (facultative, perennial and spring growth habits). (B) Average LT_{50} values determined from controlled freezing tests in winter and non-winter growth habits.

for the individual trials were significant ($p < 0.001$) and ranged from 0.59 to 0.91 and were overall higher than seen between the individual trials (Table 4.2).

Winter types showed as expected the highest BLUEs (0.0-92.5%; mean = 52.8), followed by facultative types (20.0-59.4%; mean = 40.3), perennial types (13.2-54.0%; mean = 36.4), and spring types (7.1-38.8%; mean = 1.2). From the WFS_BLUEs, five WFS classes were defined for the rye panel: (i) very high (64.5-92.5%; 19 genotypes), (ii) high (56.7-64.3%; 20 genotypes), (iii) moderate (46.2-56.6%; 19 genotypes), (iv) low (30.5-43.7%; 19 genotypes), and (v) very low (0.0-25.2%; 19 genotypes) (Table 4.1). Ten of the 19 genotypes within the very high WFS class were cultivars adapted to the cold Canadian winters (Leth Coulee Rye, Gauthier, AC Remington, AC Rifle, Musketeer, SM 38R, Prima, SM 4R, Hazlet, and Antilope). Carsten and Petkus, which have frequently been used for breeding in Europe (Schlegel, 2014), were placed in the low and very low WFS classes, respectively (Table 4.1).

4.3 Freezing test determined LTT corresponded to WFS in rye genotypes

One component of WFS is LTT, built up during cold acclimation prior to winter and this trait was estimated by controlled freezing tests. Cold-hardy wheat cultivar Norstar used as control showed an average LT_{50} value of -21.4 °C, whereas higher LTT (lower LT_{50} values) was noted for 59 of the 96 (61%) rye genotypes tested (Table 4.1). A range of LT_{50} values from -27.8 °C for the most frost resistant cultivar (Musketeer) to -15.8 °C for the spring type Florida 401 was determined (Table 4.1). A range of LT_{50} values from -27.8 °C to -16.2 °C for winter genotypes (n = 72) was determined (Fig 4.2 B). Genotypes of very high WFS class showed the highest LTT values (LT_{50} average of -25.4°C) and a gradual increase in average LTT was seen for the following WFS classes: high WFS (LT_{50_AVR} = -24.0°C), moderate WFS (LT_{50_AVR} = -22.8°C), low WFS 4 (LT_{50_AVR} = -20.3°C) and very low 5 (LT_{50_AVR} = -17.5°C) (Table 4.1). Canadian winter cultivars Musketeer (LT_{50} = -27.8°C), Prima (LT_{50} = -27.5°C), AC Remington (LT_{50} = -27.0°C), and AC Rifle (LT_{50} = -27.0°C) had the highest LTT (Table 4.1). An analysis of the WFS data from the individual field tests and determined LTT values for the rye genotypes showed negative correlation factors ranging from -0.54 to -0.82 ($p < 0.001$) for the five field trials (Table 4.2). However, a stronger correlation (r = -0.90, $p < 0.001$) was noted between WFS-BLUEs and LTT values. Like WFS, the skewness and kurtosis absolute values for LT_{50} values were < 1.0, indicating continuous trait variation within the population (Fig. 4.1A, 4.1B).

The LTT and WFS studies confirmed highest frost hardiness in winter types, but a few winter genotypes such as Baltia, Ottawa Select, Gulzow Kunz CT1, and three highly inbred lines (94-L-145-N, 95-L-145-P, and 96-L-18-R) survived poorly in the field (WFS_BLUE < 15.6%) and exhibited low LTT (LT_{50} > -17°C) (Table 4.1). A range of LT_{50} values from -26.0°C to -15.5°C for the non-winter genotypes (n = 24) was determined (Fig 4.2B). The rye facultative genotypes in the study showed overall low WFS except for genotypes Balbo (WFS_BLUE = 59.4%; LT_{50} = -26°C) and Explorer (WFS_BLUE = 58.4%; LT_{50} = -23.4°C), which were included in the high WFS class (Table 4.1). Among the perennial genotypes, the Canadian ACE-1 developed for pasture and silage production (Acharya *et al*., 2004) performed best, but did not accumulate sufficient winter hardiness prior to winter to survive well on the Canadian Prairies (WFS_BLUE = 54.0%; LT_{50} = -19.4°C; Table 4.1). The lowest WFS and LTT (WFS_BLUE ≤ 38.8%; LT_{50} ≥ -19.4°C; Table 4.1) were recorded for spring genotypes, for which seven out of eight genotypes showed no survival in the 2017/18 trial (data not shown). Spring types lack vernalization requirement and are not able to induce *COR* genes to high levels when exposed to cold *(*Fowler *et al*., 1996*a*; Ganeshan *et al*., 2008).

4.4 Analysis of developmental traits

Phenotypic data for FLN, PGH, DTA, PHT, TIL, and FLA collected from four independent experiments (Appendices 2-7) were used to determine BLUEs for each trait and genotype. Average trait scores for the different classes of rye are shown in Appendix 8. The distribution for most developmental traits did not follow a normal distribution (Fig. 4.3). PGH, PHT, and TIL were skewed towards higher values, whereas FLN values were slightly skewed towards lower values. FLA_BLUEs and DTA_BLUEs for rye population showed normal distribution.

4.4.1 Final Leaf Number (FLN)

The BLUEs for FLN varied from 7.7 to 12.4 leaves per plant, with an average of 9.6 leaves (Fig. 4.3). High FLN (11 to 13 leaves) was found in 11 out of 19 (58%) genotypes belonging to the very high WFS class, whereas all 19 genotypes of the very low WFS class had low FLN values, less than nine leaves (Appendix 8). Perennial, facultative and spring genotypes had overall lower FLN than winter types (Fig 4.4 and Appendix 8). Rye genotypes Musketeer, AC Rifle, AC Remington with the highest FLN (≥ 12.0 leaves; Appendix 8) were among the most winter-hardy

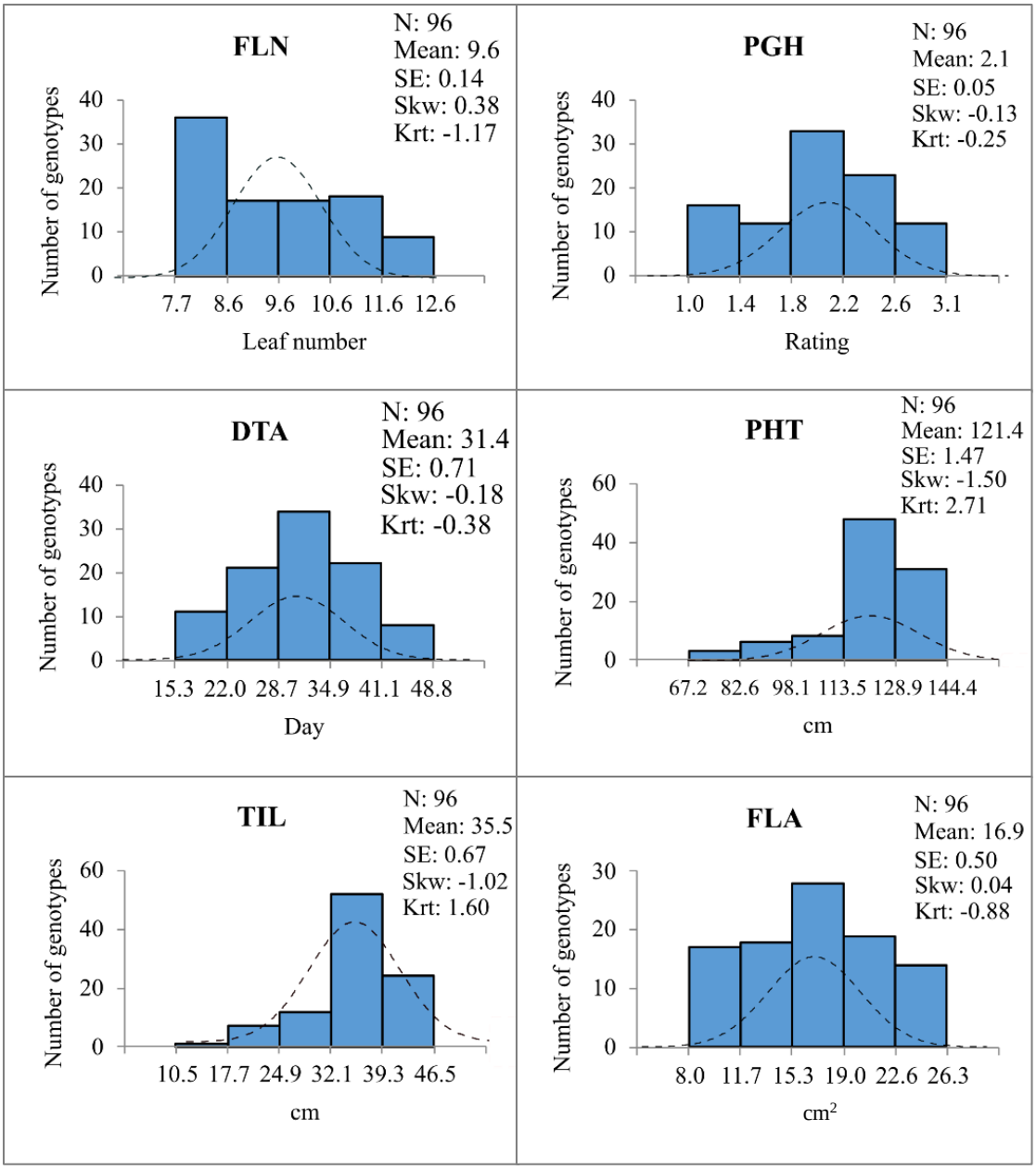

Fig. 4.3. Distribution of developmental traits values for rye population of 96 accessions. Histograms show BLUE scores calculated for final leaf number (FLN), prostrate growth habit (PGH), days to anthesis (DTA), plant height (PHT), top internode length (TIL), and flag leaf area (FLA) determined from four independent trials.

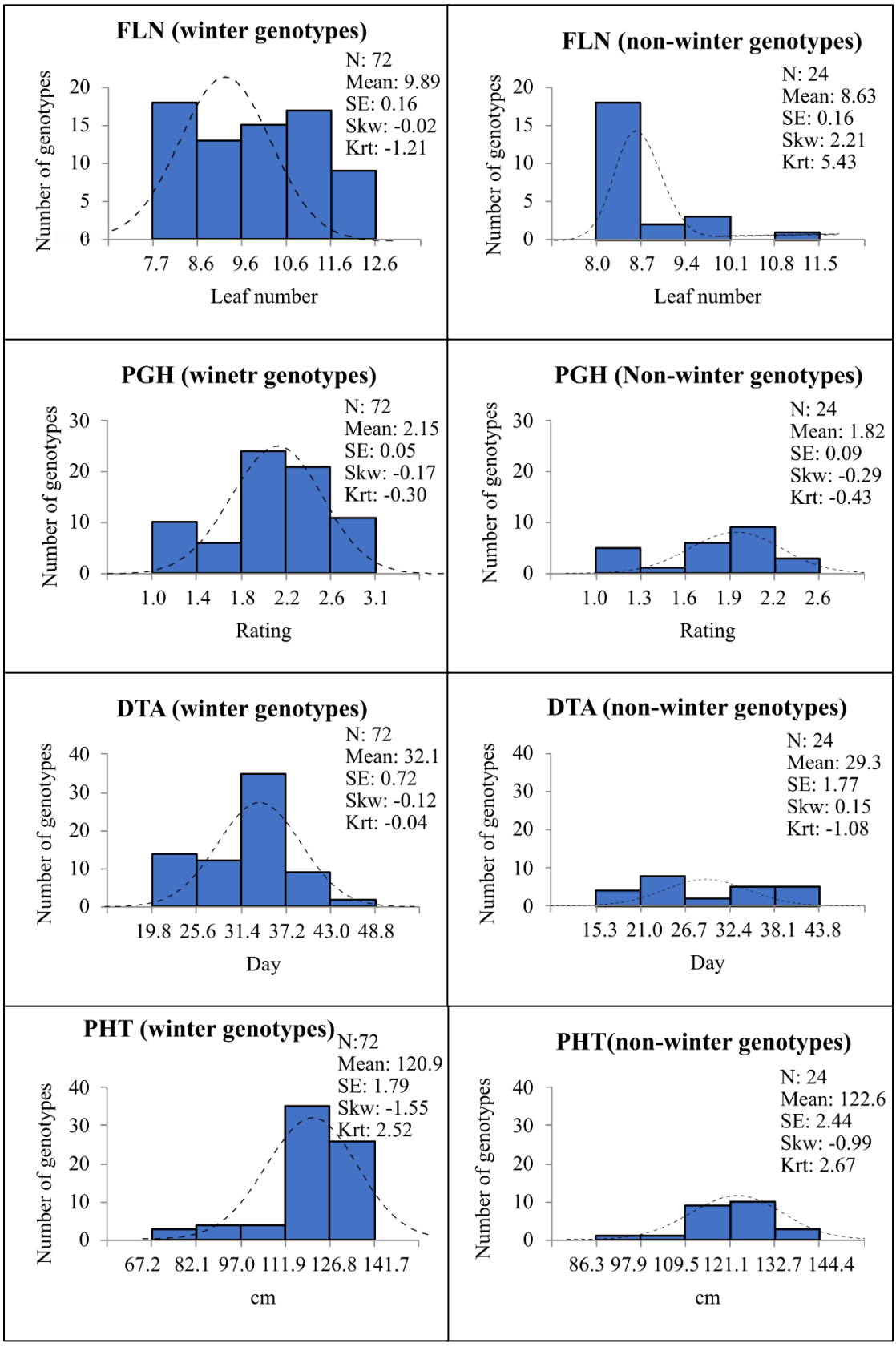
FLN (winter genotypes)
N: 72
Mean: 9.89
SE: 0.16
Skw: -0.02
Krt: -1.21
Number of genotypes
0 5 10 15 20
7.7 8.6 9.6 10.6 11.6 12.6
Leaf number
FLN (non-winter genotypes)
N: 24
Mean: 8.63
SE: 0.16
Skw: 2.21
Krt: 5.43
Number of genotypes
0 5 10 15 20
8.0 8.7 9.4 10.1 10.8 11.5
Leaf number
PGH (winetr genotypes)
N: 72
Mean: 2.15
SE: 0.05
Skw: -0.17
Krt: -0.30
Number of genotypes
0 10 20 30
1.0 1.4 1.8 2.2 2.6 3.1
Rating
PGH (Non-winter genotypes)
N: 24
Mean: 1.82
SE: 0.09
Skw: -0.29
Krt: -0.43
Number of genotypes
0 10 20 30
1.0 1.3 1.6 1.9 2.2 2.6
Rating
DTA (winter genotypes)
N: 72
Mean: 32.1
SE: 0.72
Skw: -0.12
Krt: -0.04
Number of genotypes
0 10 20 30 40
19.8 25.6 31.4 37.2 43.0 48.8
Day
DTA (non-winter genotypes)
N: 24
Mean: 29.3
SE: 1.77
Skw: 0.15
Krt: -1.08
Number of genotypes
0 10 20 30 40
15.3 21.0 26.7 32.4 38.1 43.8
Day
PHT (winter genotypes)
N:72
Mean: 120.9
SE: 1.79
Skw: -1.55
Krt: 2.52
Number of genotypes
0 10 20 30 40
67.2 82.1 97.0 111.9 126.8 141.7
cm
PHT(non-winter genotypes)
N: 24
Mean: 122.6
SE: 2.44
Skw: -0.99
Krt: 2.67
Number of genotypes
0 10 20 30 40
86.3 97.9 109.5 121.1 132.7 144.4
cm

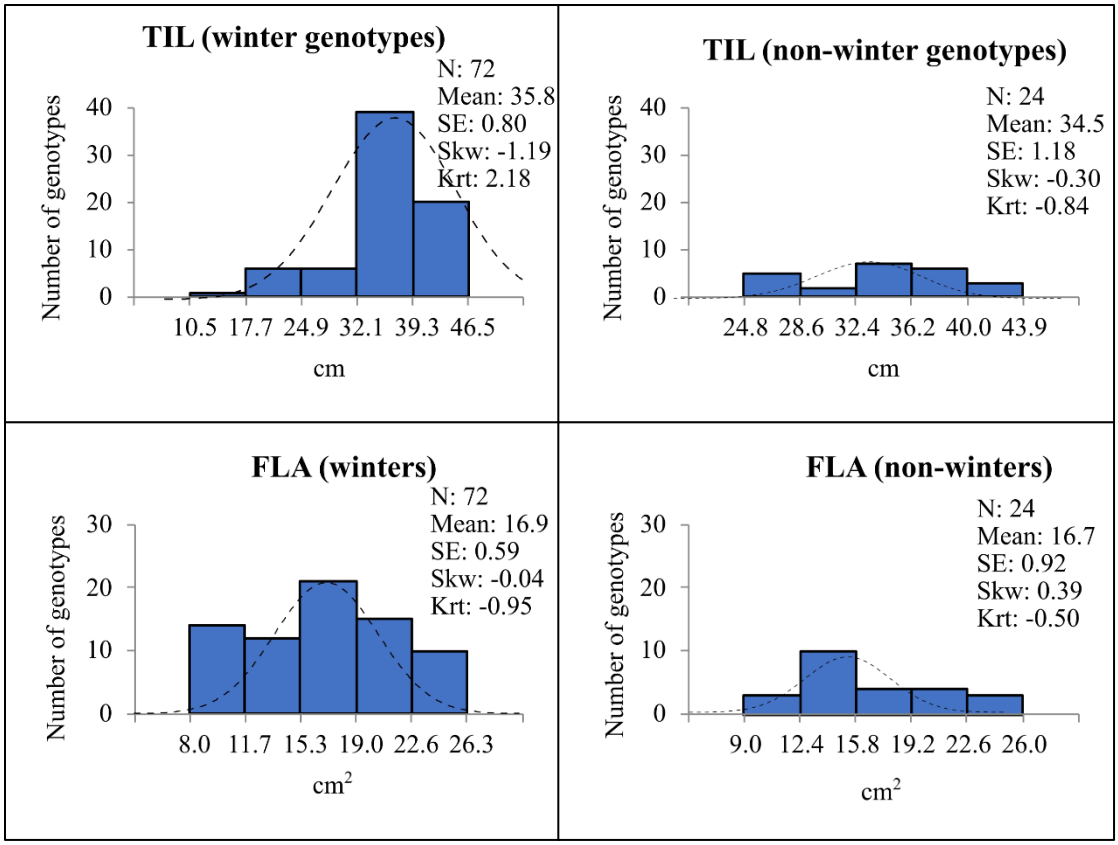

Fig. 4.4. Distribution of developmental traits values for rye population of 96 accessions in winter and non-winter genotypes (facultative, perennial and spring growth habits). Histograms show BLUE scores calculated for final leaf number (FLN), prostrate growth habit (PGH), days to anthesis (DTA), plant height (PHT), top internode length (TIL), and flag leaf area (FLA) determined from four independent trials.

(WFS ≥83%) and developed highest LTT during cold acclimation (LT_{50} < -27.0 °C) (Table 4.1). In contrast, breeding lines Petkus and Carsten had relatively low FLN (8.0 and 8.6, respectively; Appendix 8) combined with low winter-hardiness and relatively high LT_{50} values (Table 4.1). The FLN values determined for the rye population were strongly associated (p <0.001) with WFS (r = 0.80) and LTT (r = 0.71) values, respectively (Table 4.3).

4.4.2. Prostrate growth habit (PGH)

The PGH_BLUEs determined from visual scoring ranged from 1.0 to 3.1 with an average of 2.1 for the rye population, low scores for erect plants and high scores for prostrate plants (Fig. 4.3). The winter and perennial genotypes with vernalization requirements showed overall higher PGH scores (mean 2.1) than the facultative and spring types (mean ~1.6) that flower timely without vernalization (Fig 4.4 and Appendix 8). About 67% of the cold-treated genotypes displayed consistent PGH (score ≥2) in all trials, where the phenotypes were seen as a curvature of the shoot at the base of the crown (Appendix 3). However, the cold-induced tiller angle was not permanent as the rye plants revert to erect growth habit when they return to normal temperature and long-day conditions. Winter and perennial genotypes showed overall the highest PGH scores (Appendix 8). PGH showed strong correlations (p < 0.001) with both WFS (r = 0.61) and LTT (r = 0.59) (Table 4.3).

4.4.3 Plant height (PHT) and top internode length (TIL)

The length of the longest stem and the top internode showed that PHT_BLUEs for the rye population ranged from 62.7 to 144.4 cm, with an average height of 121.4 cm (Fig. 4.3). TIL_BLUEs varied from 10.5 to 46.5 cm with a mean of 35.5 cm (Fig. 4.3) and constituted 15.6 to 38.3 % of the total height for the rye genotypes. Genotypes with short stature (PHT < 100 cm) was only identified among spring and winter types (Fig 4.4 and Appendix 8). The strong correlation data between PHT and TIL (r = 0.72, p < 0.001; Table 4.3) agreed with previous studies in cereals showing PHT was largely determined by the peduncle length (McKim, 2019). Both PHT and TIL showed similar associations with WFS (r = 0.34, p < 0.001 versus 0.30, p <0.01) and LTT (r = 0.39 versus 0.36, p < 0.001) (Table 4.3). The relatively strong correlation also noted between LTT and PHT (r = 0.39, p < 0.001) and TIL (r = 0.36, p < 0.001), respectively, suggest that the final plant height is affected by events at the shoot apical meristem during cold acclimation.

4.4.4 Days to anthesis (DTA)

DTA was determined for plants vernalized under controlled conditions by counting days from the end of cold acclimation to the start of anthesis. DTA_BLUE variation ranging from 15.3 to 48.8 days with a mean of 31.4 days was observed in the rye population (Fig. 4.3). Except for genotype SR4A-S5, the spring lines showed early flowering (DTA < 26 days), and to reach longest delay of flowering was noted for the perennial genotypes, which all needed at least 34 days to reach anthesis (Fig 4.4 and Appendix 8). DTA showed relatively weak association with WFS (r = 0.25, $p < 0.05$), but no significant association with LTT (Table 4.3).

4.4.5 Flag leaf area (FLA)

Field grown plants from four trials revealed FLA_BLUEs varied from 8.0 to 26.3 cm^2 with a mean of 16.9 cm^2 and showed normal distribution (Fig 4.3). FLA showed no significant ($p < 0.05$) association with any of the other traits studied (Table 4.3), and thus did not seem to be affected by factors controlling cold acclimation.

4.4.6 Correlation among developmental traits

A statistical analysis of LT_{50} values and BLUEs determined for the various traits (Table 4.3) revealed WFS was very strongly correlated ($p < 0.001$) with LTT (r = -0.90) and FLN (r = 0.80), PGH (r = 0.61), and PHT (r = 0.34). Weaker correlations were noted between WFS and TIL (r = 0.30, $p < 0.01$) and DTA (0.25, $p < 0.05$), respectively (Table 4.3). In contrast to the other developmental traits, FLA was not significantly ($p < 0.05$) correlated to WFS, LTT or any of the other developmental trait studied and thus did not seem to be affected by factors acting during cold acclimation. Like WFS, LTT scores showed similar correlation with FLN (r = -0.71, $p < 0.001$), PGH (r = -0.59, $p < 0.001$; Table 4.3). Among the developmental traits, FLN showed highest correlation with PGH (r = 0.43, $p < 0.001$) followed by PHT (r = 0.28, $p < 0.01$) and TIL (r = 0.26, $p < 0.05$; Table 4.3). However, PGH and PHT were not significantly ($p < 0.05$) associated with each other (Table 4.3).

Table 4.3. Correlations between WFS, LTT, developmental traits and anthocyanins.

	LTT	**FLN**	**PGH**	**DTA**	**PHT**	**TIL**	**FLA**	**ANT**
Winter field survival (WFS)[1]	0.90***	0.80***	0.61***	0.25*	0.34***	0.30**	0.13	0.38***
Low-temperature tolerance (LTT)[2]		0.71***	0.59***	0.17	0.39***	0.36***	0.14	0.44***
Final leaf number (FLN)[1]			0.43***	0.14	0.28**	0.26*	0.11	0.25*
Prostrate growth habit (PGH)[1]				0.43***	0.03	0.06	0.11	0.33***
Days to anthesis (DTA)[1]					-0.29**	-0.25*	0.13	0.16
Plant height (PHT)[1]						0.72***	0.05	0.19
Top internode length (TIL)[1]							0.05	0.12
Flag leaf area (FLA)[1]								-0.02
Anthocyanins (ANT)								

[1/] BLUE scores. [2/] Negative LT_{50} values. Pearson correlation coefficient were determined at * $p<0.05$; ** $p<0.01$; *** $p < 0.001$

4.5. Bi-plot analysis supports WFS is primarily determined by developments at SAM during cold acclimation.

In a PCA bi-plot analysis, the first two PCs determined 67.5% of the total variations for the developmental traits studied in the rye population (Fig. 4.5). PC1 accounted for 48.1% of the total variation and was mainly associated with WFS, LTT, FLN, PGH, and DTA. PC2 with 19.4% share of total variation was mainly associated with DTA. The PHT and TIL vectors indicated associations with both PC1 and PC2. WFS, LTT, FLN, PGH, and DTA vectors were closely spaced and directed in the same orientation on the biplot (Fig. 4.5), which suggested high association as confirmed by the correlation analysis (Table 4.3). A near right angle between DTA and PHT/TIL vectors suggested a negative association that was also supported by the correlation data (Table 4.3). However, the correlation analysis did not support a negative association between FLA and TIL as indicated by the biplot.

Winter genotypes were positioned in all four quadrants (Fig. 4.6), with all of the very high WFS class positioned in the second and third quadrants (Fig. 4.5). Genotypes with low or very low WFS class including most spring lines were positioned within the first and fourth quadrants. Perennial genotypes were clustered in the middle, and most facultative genotypes were positioned on the lower half of the plot (Fig. 4.6). The developmental traits FLN, PGH, and DTA were primarily associated with the winter-hardy genotypes in second quadrant, whereas PHT and TIL vectors were mainly directed towards a sub-group of the winter-hardy genotypes positioned in the third quadrant. This sub-group included genotypes from Northern Europe such as Anna, Pearl, and Ponsi, which are relatively tall (> 133cm; Appendix 8). In contrast, most of the winter-hardy Canadian genotypes primarily positioned in the second quadrant appeared to rely more on PGH and FLN traits for their high WFS (Fig. 4.5).

4.6 Determination of heritability

All traits studied showed significant ($p < 0.001$) effects of genotype (G) alone and genotype x environment (G x E) interactions as revealed by the ANOVA analysis (Table 4.4). The environmental factor was largest for WFS, due to large variations in winter conditions during the trials (Appendix 1). Estimations of broad-sense heritability (h^2) generated values ranged from 0.45 (PGH) to 0.84 (DTA) for the different traits (Table 4.4). Heritability values above 0.6 are generally considered high (Ayele, 2011) and were estimated for FLN (0.81), DTA (0.84), PHT (0.74), TIL

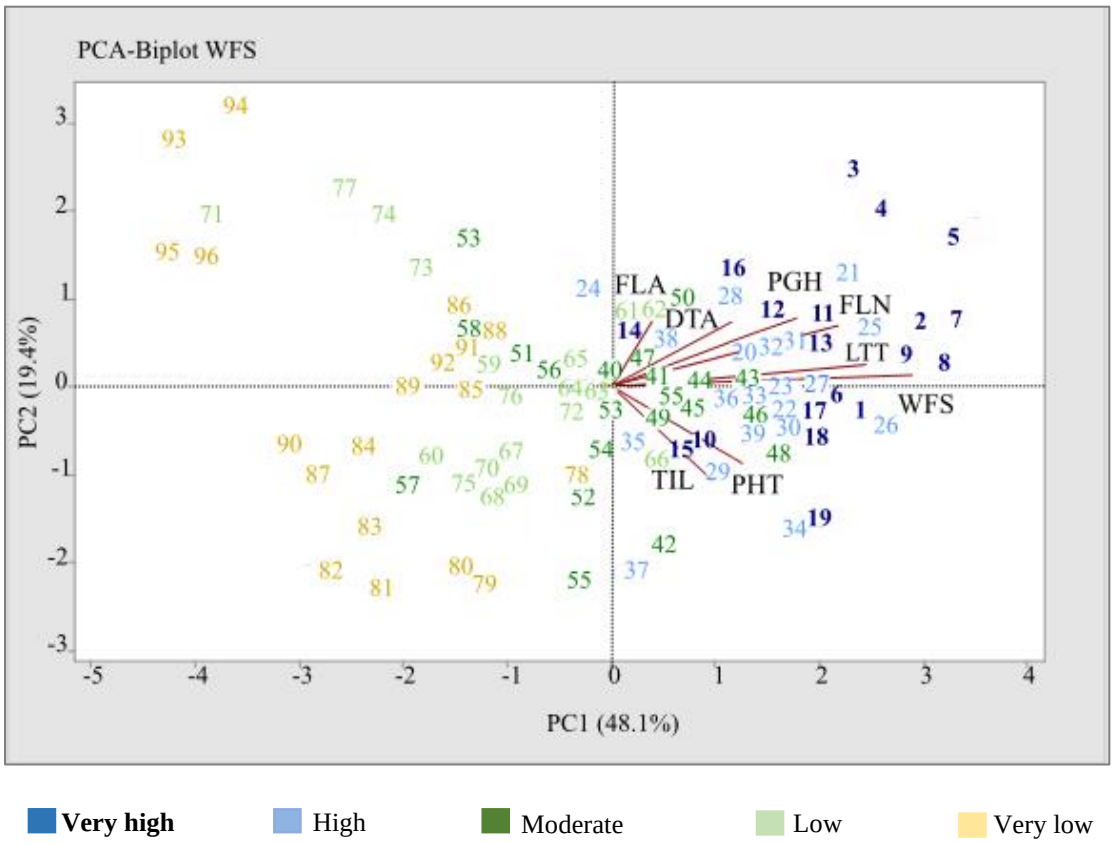

Fig. 4.5. PCA biplot of rye genotypes based on PC1 and PC2 components and vectors of traits analyzed in the study. WFS classes for genotypes are indicated by color-scheme shown below plot. Genotype numbers refer to Table 4.1.

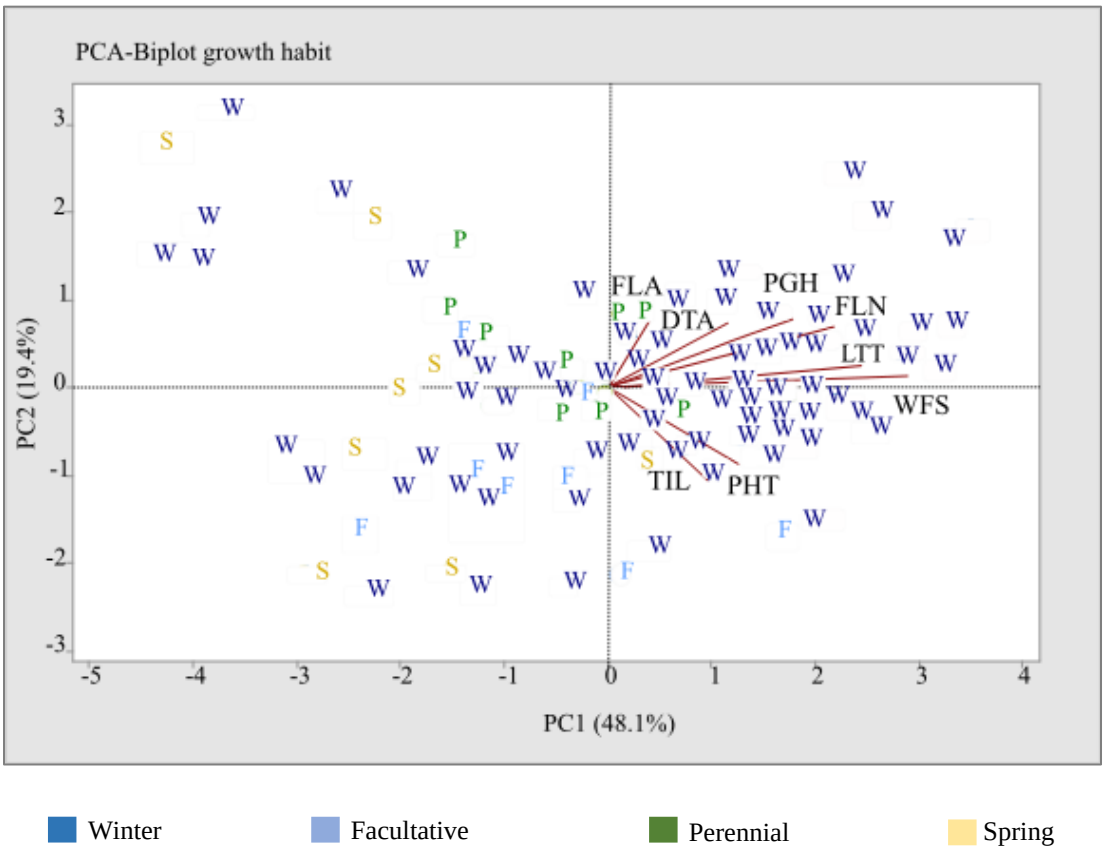

Fig. 4.6. PCA biplot of rye genotypes based on PCA1 and PCA2 components and vectors of traits analyzed in the study. Genotypes with winter (W), spring (S), facultative (F), and perennial (P) growth habit are indicated.

Table 4.4 Analysis of variance and heritability of WFS and developmental traits.

Trait[1]	Mean sum of squares			
	Genotype (G)	Environment (E)	G × E	Heritability (h^2)
Winter field survival (WFS)	65990.78***	3303871.00***	13242.97***	0.48
Final leaf number (FLN)	177.85***	196.48***	9.30***	0.81
Prostrate growth habit (PGH)	28.02***	15.57***	6.38***	0.45
Days to anthesis (DTA)	6546.93***	2173.40***	285.18***	0.84
Plant height (PHT)	23717.40***	15098.94***	1815.25***	0.74
Top internode length (TIL)	4077.32***	871.38***	314.83***	0.74
Flag leaf area (FLA)	2547.20***	1901.13***	184.37***	0.76

[1/] BLUE scores. Pearson correlation coefficient determined at *** $p < 0.001$.

(0.74), and FLA (0.76). A medium range heritability (0.30-0.60) was estimated for WFS (0.48) and PGH (0.45). Moderate to high heritability displayed by WFS, LTT, FLN, PGH, and PHT suggest that genetics has a large influence; thus, these traits can be considered for GWAS studies in population with good segregation for phenotype data (Alqudah *et al*., 2020).

4.7 Anthocyanins[2]

4.7.1 Higher flavonoid accumulation in leaves of cold-hardy versus cold-sensitive rye genotypes

To study anthocyanin accumulation in rye upon cold acclimation, the 96 rye genotypes were grown in the field and in a growth chamber, respectively, to allow for seven weeks of LT exposure. During cold acclimation in the field, 71 genotypes developed a reddish-purple color on their lower leaves and stems, which was a clear indication of anthocyanin accumulation (Chalker-Scott, 1999). Except for the GC-100 and Galma genotypes, anthocyanin accumulation was observed in all 58 genotypes with very high, high or moderate winter hardiness (Table 4.5). Among the remaining 38 genotypes with very low or low WFS, the red/purple pigmentation was weak (score = 1) for 16 genotypes and absent (score = 0) for 22 genotypes (Table 4.5). Although there appeared to be a correlation between red/purple color intensity in vegetative tissues and winter hardiness, the data had to be taken with caution as the amount of red light reflected from plants does not always correlate with anthocyanin content in tissues (Neill and Gould, 1999).

---

[2] Bahrani, H., Thoms, K., Båga, M., Larsen, J., Graf, R., Laroche, A., Sammynaiken, R., and Chibbar, R.N. (2019) Preferential accumulation of glycosylated cyanidins in winter-hardy rye (S*ecale cereale* L.) genotypes during cold acclimation. Environmental and Experimental Botany 164: 203 – 212.

Table 4. 5 Winter field survival and anthocyanin color score in 96 rye genotypes

WFS class/genotype	Color score*	WFS class/genotype	Color score*
Very high:		Kodiak	2
Leth Coulee Rye	2	GC-100	0
Gauthier	2	Amilo	1
AC Remington	2	Sellino	2
AC Rifle	2	R538	1
Musketeer	3	Protector	2
SM 38R	1	Toivo	1
Prima	3	Culpan	1
Saratovskaja 4	2	Hardy white spring Rye	1
SM 4R	1	Maton	1
Pearl	2	**Low:**	
Kustro	2	Stoir	1
Kharkivska 95	2	Vaschod	1
Kharkivska 98	1	R550	1
Esprit	1	Reimann Philipp	1
Ponsi	2	Oklon	1
Hazlet	3	Carsten	1
Antelope	2	R903	0
Emerald	1	Harach	1
Anna	1	Danae	1
High:		Clse 35	1
R003-4	1	Gator	0
Voima	2	Elbon	1
Dakota	3	L-286-R	0
Sc-73	1	R904	0
Animo	3	Syn 20-L	0
Caribou	1	SR4A-S5	0
Puma	1	Dakold	1
Othello	1	Wheeler	1
Rymin	1	M.Karlic CT2	0
Adams	2	**Very low:**	
Sangaste	1	Wintergrazer 70	0
Visa	1	Petkus Kurzstroh	0
Vitallo	1	Gazelle	1
Halo	2	Petkus	0
Balbo	1	Prolfic Spring	0
Frontier	1	Wren Abruzzi	0
Enzi	1	Extra Early Rye1	1
Explorer	1	Somro	0
Motto	1	R1210	0
Dankowskie Selekcyjne	1	Baltia	1
Moderate:		R797	0
Galma	0	Fl-Synt	0
Cougar	1	Ottawa Select	0
Dominant	3	Gulzow Kunz CT1	1
Dankowskie Nowe	1	Rogo	0
Danko	2	Florida 401	0
ACE-1	1	L-145-N	0
Dankowskie Srebrne	1	L-145-P	0
Carolkurz	1	L-18-R	0
Horton	2		

* Rating of reddish/purple pigment accumulation in leaves and stems of cold-acclimated plants in the field. A score of 3 indicates strongest coloration and 0 indicates no visible accumulation of anthocyanins.

4.7.2 Anthocyanin characterization

Alcohol-soluble leaf and crown extracts of cold-acclimated genotypes grown in the field and growth room, respectively, were produced and analyzed by HPLC-QTOF MS/MS to identify the accumulated anthocyanin species. The control HPLC chromatograms of leaf and crown extracts prepared from 15 genotypes (Musketeer, AC Rifle, Prima, Kodiak, Danko, Hazlet, Puma, Cougar, Antelope, Carsten, Dakold, Gator, Petkus, Wren Abruzzi and Florida 401) grown at normal temperature (18–20 °C) did not reveal any major (mAu > 5) absorbance peaks at 520 nm, which was supported by QTOF MS/MS data (representative chromatograms for five control genotypes with different winter hardiness levels are shown in Fig 4.7). In contrast, chromatograms of 74 leaf extracts and 51 crown extracts prepared from cold-acclimated genotypes grown in the field revealed between one to ten peaks (Appendices 9 and 10; chromatograms for five representative samples are shown in Fig 4.7).

Based on the retention times for three external standards used in the analysis, peaks 6, 14, and 15 corresponded to cyanidin-3-O-glucoside (Cya-3-Glc), pelargonidin 3-O-glucoside (Pel-3 Glc), and cyanidin-3-O-rutinoside (Cya-3-Rut), respectively (Table 4.6). The identities of these peaks were confirmed by comparing the mass-to-charge-ratios (m/z) values for the components with MS/MS spectral data available in literature and allowing a ± 5 ppm difference between theoretical and experimental masses (Table 4.6). For the remaining chromatography peaks, 15 of these (1–5, 7–13 and 16–18 in Fig 4.8) were identified as glycosylated forms of the three most common anthocyanidin aglycone structures: pelargonidin, cyanidin, and delphinidin (Appendices 11-13). Upon complete analysis of all extracts, a total of 18 compounds were identified from leaf extracts and seven of these were also present in crown tissue extracts (Table 4.6). No identification could be made for ten peaks in the chromatograms (Appendices 9 and 10).

One or two of the following glycosylations were present on the identified anthocyanins: a glycoside or a di-saccharide (rutinoside, xyloglucoside, sambubioside), acetyl-glucoside, and/or glycosylated phenylacetyl groups (coumaryl-glucoside, caffeoyl-glucoside, malonyl-glucoside) (Table 4.6; Appendices 11-13). Ten of the identified anthocyanins belonged to the cyanidin group of anthocyanins and included Cya-3-Glc, Cya-3,5-diGlc, Cya-pCou-diGlc, Cya-3-AcGlc-5-Glc, Cya-3-Xyl-Glc, Cya-3-Rut, Cya-3-Sam, Cya-3-Sam-5-Glc, Cya-3-pCou-Sam and Peo-3-Rut. The delphinidin group of anthocyanins consisted of five phenylacetylated-glycosylated compounds: Del-3-Caf-Glc, Del-3-pCou-diGlc, Del-3-pCou-Glc, and Del-3-pCou-Glc, Mal-3-pCou-Glc, and

Musketeer (very high winter hardiness)

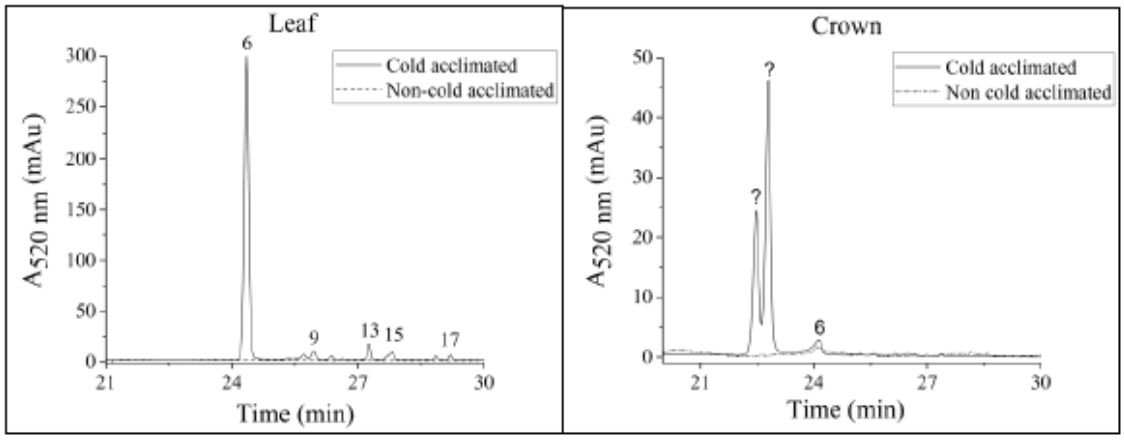

Kodiak (moderate winter hardiness)

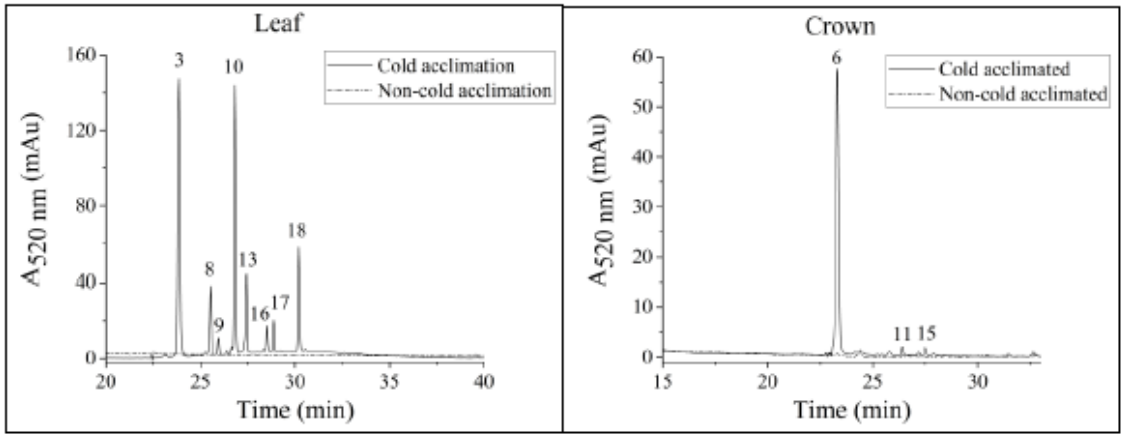

Cougar (moderate winter hardiness)

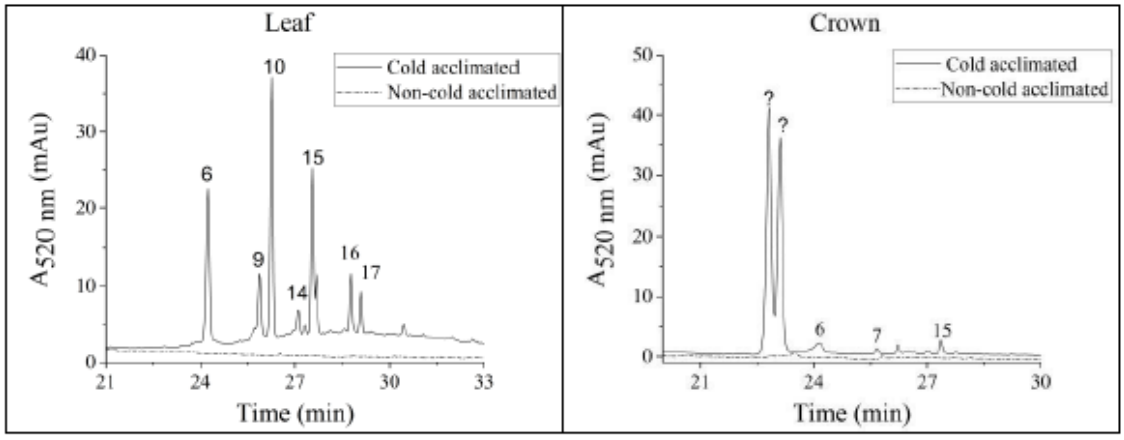

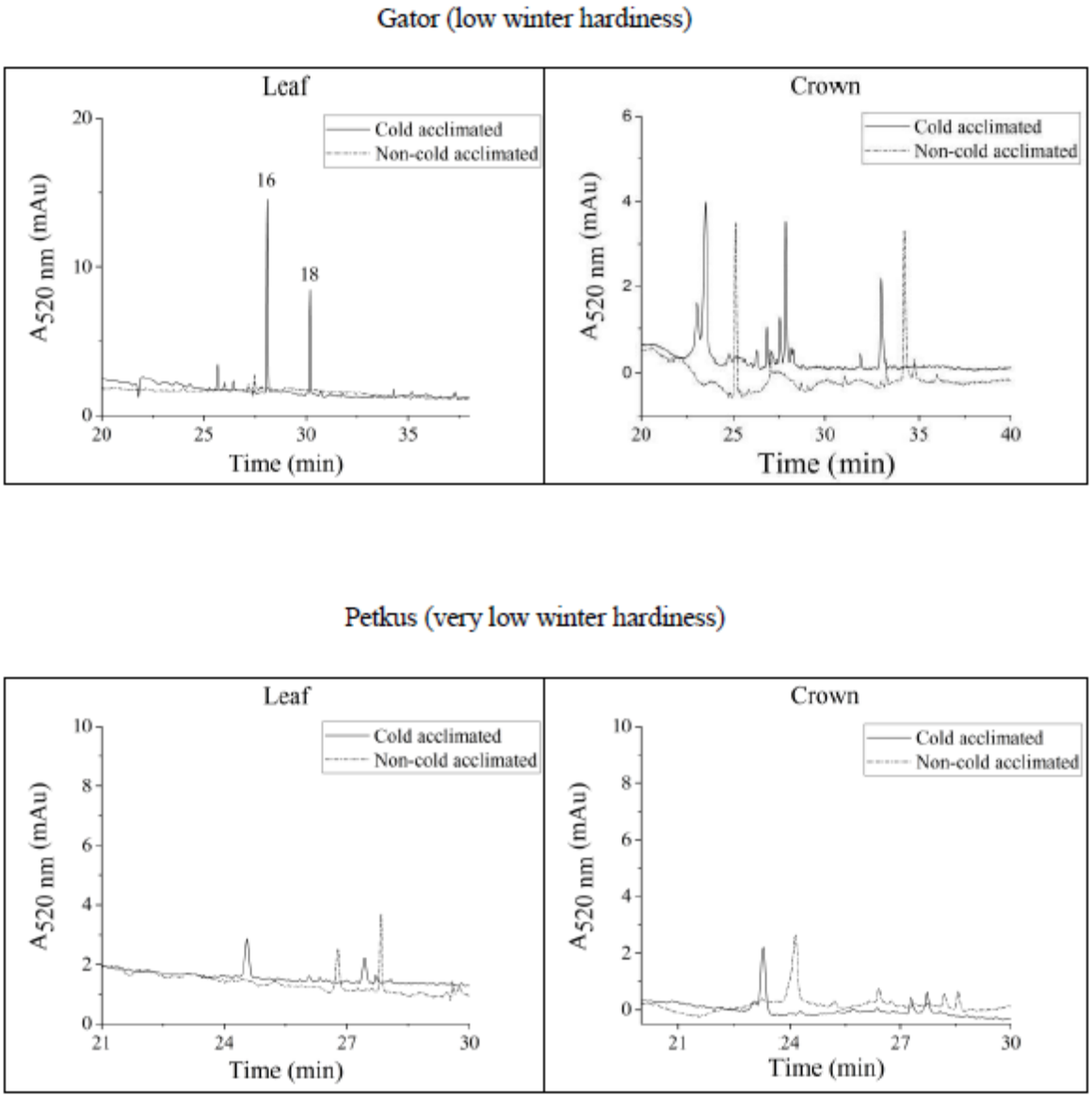

Fig. 4. 7. HPLC-vis chromatogram of anthocyanins in tissue extracts of rye genotypes. The graphs show analysis of acidic methanol extracts prepared from non-acclimated and cold-acclimated leaf and crown tissues of five rye genotypes with different winter hardiness levels. Peaks with mAu < 5.0 and lacking MS/MS data were not considered.

Table 4. 6 Anthocyanins identified in cold-acclimated tissues of rye

Anthocyanin	Abbreviation	Formula	m/z^+ experimental	m/z^+ calculated	Error ppm	RT (min)	Peak no*	Tissue	
								Leaf	Crown
Cyanidin glucosides:									
Cyanidin 3-O-glucoside	Cya-3-Glc	$C_{21}H_{21}O_{11}$	449.1059	449.1078	4.2	24.41	6	+	+
Cyanidin 3,5-O-diglucoside	Cya-3,5-diGlc	$C_{27}H_{31}O_{16}$	611.1622	611.1607	-2.5	25.47	7	+	+
Cyanidin *p*-coumaryl-diglucoside	Cya-*p*-Cou-diGlc	$C_{36}H_{37}O_{18}$	757.1988	757.1974	-1.8	23.95	2	+	-
Cyanidin 3-O-rutinoside	Cya-3-Rut	$C_{27}H_{31}O_{15}$	595.1652	595.1657	0.8	27.88	15	+	+
Cyanidin 3-sambubioside	Cya-3-Sam	$C_{26}H_{29}O_{15}$	581.1525	581.1501	-4.1	25.93	9	+	-
Cyanidin 3-sambubioside-5-glucoside	Cya-3-Sam-5-Glc	$C_{32}H_{39}O_{20}$	743.2028	743.2029	0.1	23.12	1	+	-
Cyanidin 3-*p*-coumaryl-sambubioside	Cya-3-*pC*ou-Sam	$C_{35}H_{34}O_{17}$	726.1772	726.1791	2.6	23.97	3	+	-
Cyanidin 3-xyloglucoside	Cya-3-Xyl-Glc	$C_{26}H_{27}O_{15}$	579.1360	579.1344	-2.8	28.86	17	+	-
Cyanidin 3-O-acetylglucoside-5-O-glucoside	Cya-3-AcGlc-5-Glc	$C_{29}H_{33}O_{17}$	653.1738	653.1712	-4.0	30.23	18	+	-
Peonidin 3-O-rutinoside	Peo-3-Rut	$C_{28}H_{33}O_{15}$	609.1831	609.1814	-2.8	28.46	16	+	+
Delphinidin glucosides:									
Delphinidin 3-O-*p*-coumaryl-monoglucoside	Del-3-*p*Cou-Glc	$C_{30}H_{27}O_{14}$	611.1408	611.1398	-1.6	25.62	8	+	+
Delphinidin *p*-coumaryl-diglucoside	Del-3-*p*Cou-diGlc	$C_{36}H_{37}O_{19}$	773.1943	773.1924	-2.5	23.99	4	+	-
Delphinidin 3-O-caffeoyl-glucoside	Del-3-Caf-Glc	$C_{30}H_{27}O_{15}$	627.1349	627.1344	-0.8	24.23	5	+	-
Malvidin 3-O-*p*-coumaryl-monoglucoside	Mal-3-*pC*ou-Glc	$C_{32}H_{31}O_{14}$	639.1724	639.1708	-2.5	26.44	10	+	+
Petunidin 3-O-*p*-coumaryl-monoglucoside	Pet-3-*p*Cou-Glc	$C_{31}H_{29}O_{14}$	625.1572	625.1552	-3.2	27.28	12	+	-
Pelargonidin glucosides:									
Pelargonidin 3-O-glucoside	Pel-3-Glc	$C_{21}H_{21}O_{10}$	433.1112	433.1129	3.9	27.52	14	+	-
Pelargonidin 3-sambubioside	Pel-3-Sam	$C_{26}H_{29}O_{14}$	565.1561	565.1552	-1.6	27.36	13	+	-
Pelargonidin 3-O-(6-O-malonyl-beta-D-glucoside)	Pel-3-6-Mal-βGlc	$C_{24}H_{23}O_{13}$	519.1146	519.1133	-2.5	26.88	11	+	+

*See Fig. 4.8.

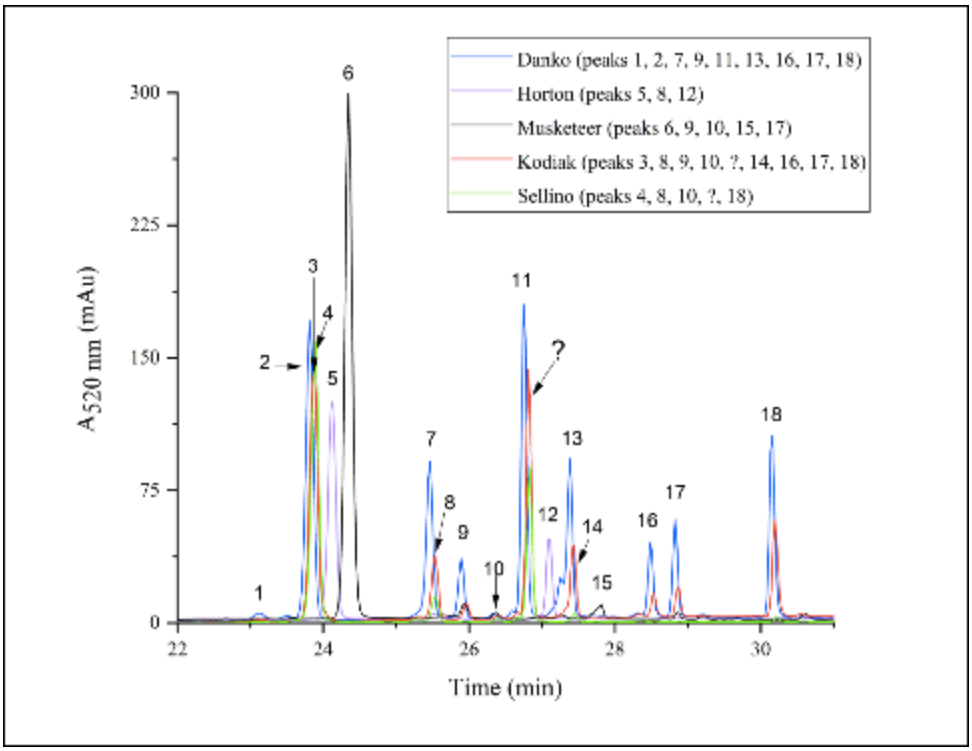

Fig. 4. 8. Anthocyanin peaks identified by HPLC-vis analysis of leaf extracts. The graphs for five rye genotypes collectively showing all 18 anthocyanins identified and one unknown compound (?). See Table 4.6 for the identification of peaks 1-18.

Pet-3-pCou-Glc. However, only three compounds belonged to the pelargonidin group: Pel-3-Glc, Pel-3-6-Mal-βGlc and Pel-3-Sam.

4.7.3 Low amounts and diversity for anthocyanins identified in crown tissues

The concentration determined for the Cya-3-Glc compounds in cold-acclimated leaf extracts ranged from 3.8 to 232.5 μg, g^{-1} fresh weight and was overall much higher than the concentrations in corresponding crown tissues (0.9 to 16.8 μg, g^{-1} fresh weight; Table 4.7). When compared to Cya-3-Glc, the Cya-3-Rut and Pel-3-Glc compounds were less abundant in leaves (2.1 to 27.6 and 3.4 to 22.8 μg, g^{-1} fresh weight, respectively; Table 4.7). A low amount of Cya-3-Rut was detected in crown tissues (2.3 to 7.7 μg, g^{-1} fresh weight; Table 4.7), but Pel-3-Glc could not be identified in this tissue. Four glycosylated cyanidins (Cya-3-Glc, Cya-3-Rut, Cya-3,5- diGlc and Peo-3-Rut), two delphinidin compounds (Del-3-pCou-Glc and Mal-3-pCou-Glc) and only one pelargonidin compound (Pel-3-6-Mal-Glc) was found in rye crown tissues (Appendix 10). Overall, the profiles of the anthocyanin species in crown tissues were similar to anthocyanin composition identified in corresponding leaf tissue, but the amounts of each compound were much lower in the crown tissues.

4.7.4 The cyanidin group of anthocyanin compounds were preferentially accumulated during cold acclimation

The HPLC-QTOF MS/MS analysis showed on average 4.5 compounds per genotype in leaf extracts prepared from the 39 genotypes classified as having very high and high WFS (Table 4.8 and Appendix 9). For the 38 genotypes with low and very low winter hardiness, the average number of anthocyanins was only 1.8 per genotype. The accumulation of the cyanidin group of anthocyanin compounds was most frequent among the 39 highest cold-hardy genotypes, of which 35 genotypes (89.7%) accumulated one up to six different glycosylated cyanidins in their leaves (Table 4.8 and Appendix 9). For genotypes with low or very low winter hardiness, five out of 38 genotypes (13.1%) accumulated glycosylated cyanidins in leaves, but detectable levels of these compounds could not be found in corresponding crown tissues. Cya-3-Glc, which is the first product of the cyanidin branch of the anthocyanin pathway (Appendix 12), showed the highest accumulation in leaves of Canadian cold-hardy cultivars Musketeer (232.5 μg, g^{-1} fresh weight) and Prima (174.3 μg, g^{-1} fresh weight; Table 4.7). Both Musketeer and Prima are the highly

Table 4. 7 Quantification of three anthocyanins in leaf and crown tissues of cold-acclimated rye.

Genotype	WFS	Cya-3-Glc (µg g^{-1} fresh weight)		Cya-3-Rut (µg g^{-1} fresh weight)		Pel-3-Glc (µg g^{-1} fresh weight)
		Leaf	Crown	Leaf	Crown	Leaf
Musketeer	Very high	232.5	5.3	7.5		
Prima	Very high	174.3				
Hazlet	Very high	74.3	3.3	25.5	4	17.5
Kharkivska 95	Very high	62.6	7.9	8	3.8	
Kustro	Very high	40				20.6
Saratovskaja 4	Very high	33.2		27.6	3.1	16.8
Pearl	Very high	29.7	5.1	4.6		22.8
AC Rifle	Very high	25.5		2.6	5.1	
Leth Coulee Rye	Very high	23.3	5.6	13.2	6.9	
Kharkivska 98	Very high	8.3	6.5	3.2	3.3	15
Gauthier	Very high		4.9		6.1	
SM 4R	Very high		6.7	2.1		
SM 38R	Very high		8.6	2.4		3.4
Antelope	Very high		3		3.8	7
Animo	High	115.9				
Halo	High	35.2	6.4		3.5	
Dakota	High	25.3	4.5	2.9	5.6	
Adams	High	21.5	5.7			
Sc-73	High	21.5			3.2	
Dominant	High	20.9		9.7		
Visa	High	11.6	4.1		4.8	10.6
Caribou	High	5.2				
Explorer	High	4.5		2.7	2.8	
Voima	High	3.8		3.1		
Othello	High					9.6
Dankowskie Selekcyjne	High			53.6	4	
R003-4	High		3.3		3.1	
Balbo	High		7.9		7.7	
Motto	High					7.8
Vitallo	High		3.3			
Kodiak	Moderate	32.8				
Cougar	Moderate	30.7	7.8	9.2		
Carolkurz	Moderate	13.7	2.9	3.7	3.1	12.3
Dankowskie Nowe	Moderate	11.2		4.8	2.3	
Culpan	Moderate		16.8		2.5	4.6
Toivo	Moderate					6.9
Horton	Moderate		0.9			
Maton	Moderate					4.4
Vaschod	Low	6.8				3.9
Carsten	Low					5.7
Dakold	Low					5.3
Danae	Low					13.5
Harach	Low					7.6
Wheeler	Low					6.8
Extra Early Rye1	Very low					4.4
Gazelle	Very low					10.9
Baltia	Very low					5.3

Table 4. 8 Number of anthocyanin compounds identified in 96 cold-acclimated rye genotypes

Winter survival class: Genotype	Number of anthocyanin compounds							
	Cya		Del		Pel		Total	
	Leaf	Crown	Leaf	Crown	Leaf	Crown	Leaf	Crown
Very high:								
Leth Coulee Rye	4	2	-	-	2	-	6	2
Gauthier	2	2	-	-	1	-	3	2
AC Remington	1	1	-	-	1	1	2	2
AC Rifle	4	1	-	-	-	-	4	1
Musketeer	4	1	1	-	-	-	6	1
SM 38R	2	2	2	-	1	-	5	2
Prima	1	-	-	1	-	-	1	1
Saratovskaja 4	6	1	1	-	3	-	10	1
SM 4R	1	2	2	1	1	-	4	3
Pearl	2	1	2	-	1	-	5	1
Kustro	5	1	2	-	3	-	10	1
Kharkivska 95	6	2	1	-	2	-	9	2
Kharkivska 98	3	2	2	-	1	-	6	2
Esprit	-	-	1	-	1	-	2	-
Ponsi	2	1	-	-	1	-	3	1
Hazlet	6	2	1	-	3	-	10	2
Antelope	5	2	1	-	3	-	9	2
Emerald	1	-	-	-	1	-	2	-
Anna	2	1	-	-	1	-	3	1
High:								
R003-4	1	1	1	-	-	-	2	1
Voima	6	-	-	-	3	-	9	-
Dakota	6	1	-	-	2	-	8	1
Sc-73	2	2	1	-	1	-	4	2
Animo	4	-	2	-	3	-	9	-
Caribou	1	-	-	-	-	-	1	-
Puma	-	1	2	-	1	1	3	2
Othello	1	1	1	-	2	-	4	1
Rymin	1	-	1	-	-	-	2	-
Adams	2	2	-	-	1	-	3	2
Sangaste	1	-	-	-	-	-	1	-
Visa	1	2	-	-	-	-	1	2
Vitallo	2	1	1	-	1	-	4	1
Halo	2	2	-	2	1	-	3	4
Balbo	4	1	-	-	-	-	4	1
Frontier	-	-	-	-	1	-	1	-
Enzi	-	-	1	1	-	-	1	1
Explorer	4	-	2	-	-	-	6	-
Motto	3	2	4	1	2	-	9	3
Dankowskie Selekcyjne	1	1	-	-	-	-	1	1
Moderate:								
Galma	-	-	-	-	-	-	-	-
Cougar	5	3	1	-	1	-	7	3
Dominant	2	1	-	1	1	-	3	2
Dankowskie Nowe	3	2	1	-	1	-	5	2
Danko	7	-	-	-	2	-	9	-
ACE-1	-	-	1	-	1	-	2	-
Dankowskie Srebrne	1	1	1	-	2	-	4	1

Table 4.8 (*Continued*)

Winter survival class: Genotype	Number of anthocyanin compounds							
	Cya		Del		Pel		Total	
	Leaf	Crown	Leaf	Crown	Leaf	Crown	Leaf	Crown
Carolkurz	1	-	1	-	-	1	2	1
Horton	-	2	3	-	-	-	3	2
Kodiak	5	2	2	-	1	1	8	3
GC-100	-	-	-	-	-	-	-	-
Amilo	-	-	1	-	-	-	1	-
Sellino	-	-	3	-	1	-	4	-
R538	2	-	3	1	-	-	5	1
Protector	-	-	3	-	2	-	5	-
Toivo	1	1	-	-	1	-	2	1
Culpan	3	1	1	1	-	-	4	2
Hardy White Spring Rye	-	-	2	-	-	-	2	-
Maton	1	-	3	-	2	-	6	-
Low:								
Stoir	-	-	3	-	1	-	4	-
Vaschod	-	-	1	-	2	-	3	-
R550	-	-	2	-	2	-	4	-
Reimann Philipp	-	-	2	1	-	-	2	1
Oklon	-	-	3	-	1	-	4	-
Carsten	1	-	2	-	3	-	6	-
R903	-	-	-	1	-	-	-	1
Harach	1	-	1	-	2	-	4	-
Danae	-	-	1	-	1	-	2	-
Clse 35	-	-	2	1	1	-	3	1
Gator	2	-	-	-	-	-	2	-
Elbon	-	-	1	-	1	-	2	-
L-286-R	-	-	-	2	-	-	-	2
R904	-	-	-	1	-	-	-	1
Syn 20-L	-	-	-	-	-	-	-	-
SR4A-S5	-	-	-	-	-	-	-	-
Dakold	2	-	5	-	3	-	10	-
Wheeler	1	-	2	-	1	-	4	-
M.Karlic CT2	-	-	-	1	-	-	-	1
Very low:								
Wintergrazer 70	-	-	-	-	-	-	-	-
Petkus Kurzstroh	-	-	-	-	-	-	-	-
Gazelle	-	-	2	-	2	-	4	-
Extra Early Rye1	-	-	4	-	1	-	5	-
Petkus	-	-	-	-	-	-	-	-
Prolfic Spring	-	-	-	-	-	-	-	-
Wren Abruzzi	-	-	1	-	-	-	1	-
Somro	-	-	-	-	-	-	-	-
R1210	-	-	1	1	-	-	1	1
Baltia	-	-	2	-	2	-	4	-
R797	-	-	-	-	-	-	-	-
Fl-Synt	-	-	-	1	-	-	-	1
Ottowa Select	-	-	-	-	-	-	-	-
Gulzow Kunz CT1	-	-	1	-	1	-	2	-
Rogo	-	-	-	-	-	-	-	-

Table 4.8 (*Continued*)

Winter survival class: Genotype	Number of anthocyanin compounds							
	Cya		Del		Pel		Total	
	Leaf	Crown	Leaf	Crown	Leaf	Crown	Leaf	Crown
Florida 401	-	-	-	1	-	-	-	1
L-145-N	-	-	-	1	-	-	-	1
L-145-P	-	-	-	1	-	-	-	1
L-18-R	-	-	-	-	-	-	-	-

productive Canadian winter rye cultivar with extremely high winter hardiness (McLeod *et al*., 1985, 1981).

4.7.5 The accumulation of glycosylated delphinidins and pelargonidins were unrelated to high winter-hardiness

Of the five delphinidin compounds identified, Pet-3-pCou-Glc was most abundant and accumulated in 27 genotypes with winter hardiness ranking from very low to very high (Table 4.8; Appendices 9 and 10). Also, the three pelargonidin compounds (Pel-3-Glc, Pel-3-6Mal-Glc, and Pel-3-Sam) were distributed among genotypes with different winter hardiness levels (Table 4.8; Appendices 9 and 10). In contrast to the cyanidin group of anthocyanins, the delphinidin and pelargonidin group of anthocyanidins could not be associated with WFS levels for the 96 rye genotypes.

4.7.6 Correlation of anthocyanins with WFS

A statistical analysis of WFS values and various anthocyanins (Table 4.9) revealed that only seven cyanidins had significant correlations with WFS (Table 4.9). The strongest correlation ($r = 0.35$, $p < 0.001$) was between WFS and Cya-3-Glc. A relatively strong correlation was also noted between Cya-3,5-diGlc and Cya-3-Rut with WFS ($r = 0.27$ and $r = 0.26$, respectively, $p < 0.01$). Weaker correlations were noted between Cya-3-Sam, Cya-3-AcGlc-5-Glc, Cya-3-Xyl-Glc, Cya- *p*Cou-diGlc, and WFS ($r = 0.25$, 0.24, 0.23, and 0.23, respectively, $p < 0.05$). Other cyanidins (Cya-3-*p*Cou-Sam, Peo-3-Rut and Cya-3-Sam-5-Glc), delphinidin, and pelargonidin anthocyanin groups were not significantly ($p < 0.05$) associated with WFS (Table 4.9). LTT scores showed a similar correlation with Cya-3-Glc ($r = 0.38$, $p < 0.001$) and Cya-3-Rut and Cya-3,5-diGlc ($p < 0.01$; $r = 0.32$ and 0.31, respectively). Correlations of Cya-3-Sam, Cya-3-Xyl-Glc, and Cya-3-AcGlc-5-Glc with LTT ($r = 0.28$, $r = 0.29$, and $r = 0.30$, respectively; $p < 0.05$, Table 4.9) were less significant than Cya-3-Glc and Cya-3-Rut with LTT. However, no significant ($p > 0.05$) associations with LTT and other cyanidins (Cya-*p*Cou-diGlc, Cya-3-*p*Cou-Sam, Peo-3-Rut, and Cya-3-Sam-5-Glc) and the delphinidin and pelargonidin groups of anthocyanins were noted (Table 4.9). Delphinidins and pelargonidins overall did not seem to play a role in winter hardiness.

Table 4.9 Correlations between WFS, LTT, and anthocyanins.

Cyanidins	WFS	LTT	Delphinidins	WFS	LTT	Pelargonidins	WFS	LTT
Cya-3-Glc	0.35***	0.38***	Pet-3-*p*Cou-Glc	0.07	0.07	Pel-3-Sam	0.21	0.22
Cya-3,5-diGlc	0.27**	0.31**	Mal-3-*p*Cou-Glc	0.04	0.02	Pel-3-6-Mal-βGlc	0.19	0.18
Cya-3-Rut	0.26**	0.32**	Del-3-*p*Cou-Glc	0.01	-0.07	Pel-3-Glc	0.16	0.21
Cya-3-Sam	0.25*	0.28*	Del-3-Caf-Glc	-0.02	-0.03			
Cya-3-AcGlc-5-Glc	0.24*	0.30*	Del-3-*p*Cou-diGlc	-0.05	0.07			
Cya-3-Xyl-Glc	0.23*	0.29*						
Cya-*p*Cou-diGlc	0.23*	0.21						
Cya-3-*p*Cou-Sam	0.15	0.19						
Peo-3-Rut	0.07	0.17						
Cya-3-Sam-5-Glc	0.03	0.08						

Pearson correlation coefficient were determined at * $p<0.05$; ** $p<0.01$; *** $p < 0.001$

4.8 Structure analysis of GBS data generated for rye population

The GBS analysis generated a total of 357.1 million reads with an average read length of 108 nucleotides. Alignment of the processed sequences to scaffold sequences of rye inbred line Lo7 genome version 2 (Bauer *et al*., 2017) produced 252,158 SNP markers, of which 10,244 SNP markers remained upon filtering for read length, 5% minor allele frequency, and minimum read depth of six. All but 14 markers could be placed on a *de novo* assembled Lo7 genomic map of rye (Appendix 14; Rabanus-Wallace *et al*., 2021). The SNP data was subjected to a principal component analysis (PCA), which showed the first and second coordinates explained 3.5% and 2.7% of the total genetic variation, respectively (Fig. 4.9). Despite relatively low genetic diversity within the population, three clusters were distinguished from the PCA plot. Cluster II was largest and consisted of 63 genotypes and followed by cluster I with 28 genotypes (Fig. 4.9; Table 4.1). Only five genotypes were grouped in cluster III containing mainly perennial genotypes with relatively low winter hardiness. The large cluster II included 15 of the 19 (79%) genotypes with very high WFS, such as the Canadian cultivars Leth Coulee Rye, AC Remington, AC Rifle, Musketeer, and Prima. However, this cluster also contained relatively cold-sensitive genotypes such as Petkus and Carsten. Like cluster II, cluster I contained very winter-hardy Canadian genotypes intermingled with less cold-hardy genotypes (Fig. 4.9). The existence of three subpopulations was also supported by a STRUCTURE HARVESTER analysis, which deduced the maximum value for Delta K (ΔK) was three (Fig. 4.10). A neighbor-joining phylogenetic tree constructed according to Nei (Nei, 1972) repositioned the Canadian genotypes Puma, Cougar and Gazelle in cluster I of the PCA plot, to cluster II in the phylogenetic tree (Fig.4.11; Table 4.1). The phylogenetic tree also supported division of cluster II into two branches (IIa and IIb, respectively), where Petkus was placed in IIa and Carsten in IIb branch (Table 4.1; Fig. 4.11). A similar division of Petkus and Carsten into different gene pools has previously been reported and explained by the frequent use of these lines in different breeding programs (Fischer *et al*., 2010; Targońska *et al*., 2015). Overall the clustering of rye genotypes studied could not be related to their geographical origin, but a weak preference around the Carsten gene pool was noted for genotypes with high and very high WFS (Fig. 4.11).

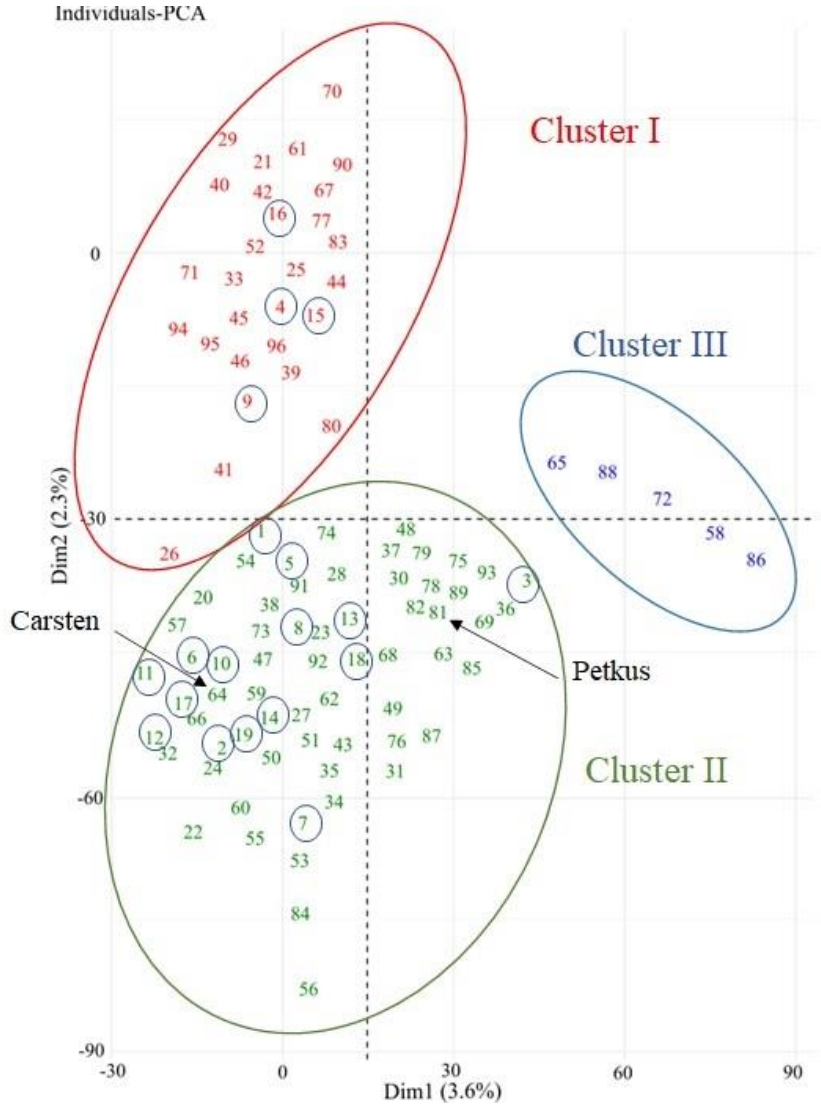

Fig. 4. 9. Principal component analysis (PCA) score plot. Plot generated from analysis of 10,244 SNP markers identified in rye population of 96 accessions. The x axis represents the eigenvalue for principal component 1 (PC1) and the y axis for PC2. Genotypes with highest WFS are indicated by arrowheads and long arrows refer to less cold hardy Petkus and Carsten, respectively. Data for the individual genotypes is listed in Table 4.1.

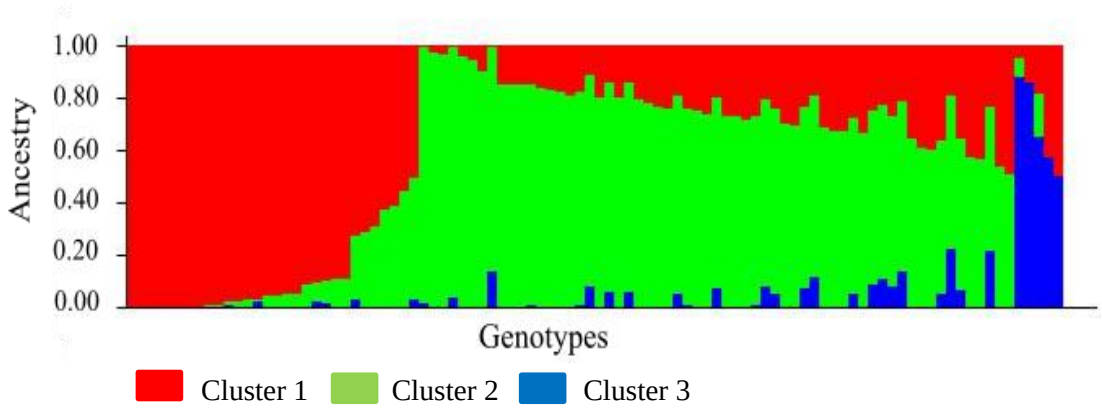

Fig. 4. 10. STRUCTURE plot for rye population. Plot was based on analysis of 10,244 SNP markers identified for 96 rye accessions. Each genotype is represented by a vertical line, for which colored segments indicate estimated fractions of three (ΔK=3) ancestral populations predicted for the population.

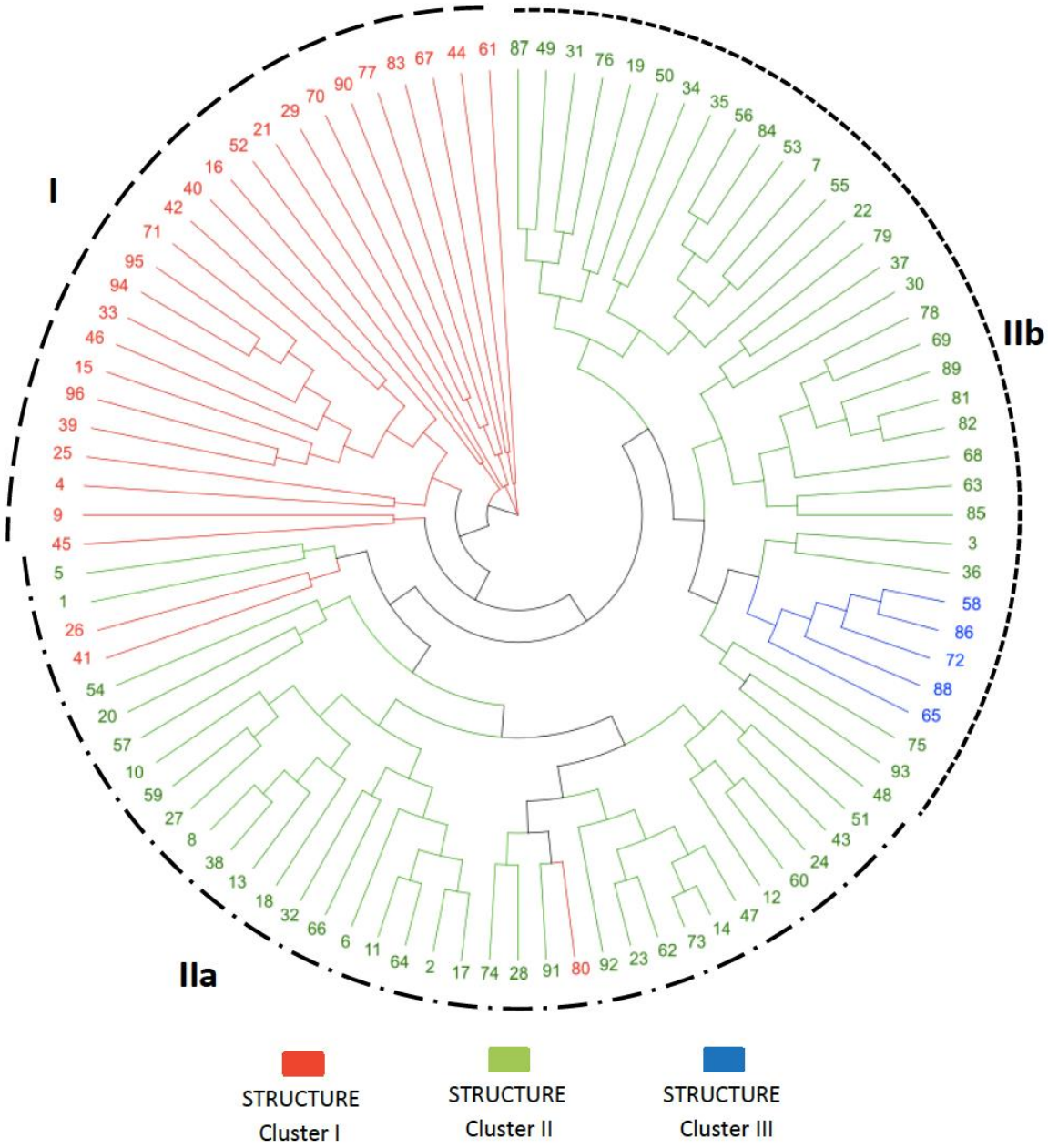

Fig. 4. 11. Neighbor-joining phylogenetic tree for rye population. The NJTree is based on standard genetic distance with 10,000 individual bootstraps and numbers refer to genotypes listed in Table 4.1.

4.9 Identification of SNP markers associated with developmental and cold tolerance traits

Analysis of phenotype and genotype data by the multi-linear model (MLM) revealed a total of 339 SNP markers and 504 marker-trait associations **(**MTAs) that were significantly (p <0.01) associated with developmental (FLN, PGH, DTA, PHT, TIL and FLA) or WFS and LTT for the rye population (Appendix 14). Among the 339 SNPs with p-value <0.01, 98 SNPs were associated with WFS, 75 with FLN, 71 with PGH, 61 with PHT, 61 with DTA, 59 with TIL, 51 with FLA, and 26 with LTT values (Appendix 14). Hundred and one of the SNPs associated with two up to six traits, but no marker was significant for all eight traits. WFS shared most markers with LTT (16 out of 26; 61.5%), followed by FLN (26 out of 75; 34.7 %), PGH (22 out of 71; 31.0%), TIL (10 out of 59; 16.9%), PHT (10 out of 61; 16.4%), DTA (9 out of 61; 14.7%), FLA (6 out of 51; 11.8%; Table 4.10) supporting the traits studies are genetically linked to WFS. Besides LTT shared most markers with PGH (10 out of 26; 38.5 %), followed by FLN (9 out of 26; 34.6 %), and FLN shared most markers with PGH (16 out of 75; 30.0 %), thus indicating the three traits may be genetically linked with each other. PHT shared most markers with TIL (32 out of 61; 52.5%), indicating PHT and TIL strongly associated with each other (Table 4.10).

The 339 SNP markers were divided into three groups based on their significance level. Group 1 markers of 10 SNPs were distinguished after a Bonferroni correction of mapping data, which generated a new significant p-value (p<1.49e-04; FDR <0.05) and identified a total of 27 MTAs and nine strong candidate genes discussed below (Table 4.11). The second group of 205 SNPs (p<0.001) identified 349 MTAs and matched with 82, Lo7 rye annotated genes (Appendix 14). A third group of 124 SNP markers (p-values <0.01 to 0.001) identified 128 MTAs and matched with 47, Lo7 rye annotated genes. 38.52% of the group 2 and 63.29% of the group 3 SNPs matches coincided with repetitive elements or non-transcribed regions, and thus, group 3 appeared to contain few MTAs, a higher frequency of false-positive SNPs and were given lower consideration in the study.

A match to coding region of genes was found for 99 of the 339 (29.20%) SNPs, and among these 44 SNP variations (14.1%) caused amino acid change in predicted gene product. Among the target genes for SNPs were genes encoding transcription factors (zinc finger and MYB proteins), glucosyltransferases, protein kinases and phosphatases, iron/ascorbate-dependant oxidoreductase family members, heat shock proteins, histone, DNA, and RNA modification proteins, ABC

Table 4.10 Total number and shared SNP markers between traits.

Trait	Total number of SNPs associated with trait	Number of markers shared							
		LTT	**FLN**	**PGH**	**DTA**	**PHT**	**TIL**	**FLA**	**TAC**
WFS	98	16	26	22	9	10	10	6	27
LTT	26		9	10	2	2	6	2	0
FLN	75			16	10	8	10	13	4
PGH	71				5	9	5	4	4
DTA	61					3	3	3	2
PHT	61						32	2	1
TIL	59							3	1
FLA	51								1
TAC	144								

Table 4.11 Most significant MTAs identified in the study.

Marker ID[1/]	SNP[2/]	SNP position (bp)[3/]	*p*-value[4/]	R^2	MTA	Corresponding gene; protein	Amino acid change
Xuos526258	T/G	Chr7:112,789,056	1.10E-05	20.7	Xuos526258_WFS	*SECCE7Rv1G0469720.1*;	V/G
			1.50E-05	18.5	Xuos526258_FLN	Benzothiadiazole-induced protein phosphatase 2C1	
			3.84E-05	16.4	Xuos526258_PGH	(BIPP2C1)	
			4.17E-05	17.9	Xuos526258_LTT		
Xuos530120	G/C	Chr7:23,476,103	5.66E-05	14.5	Xuos530120_WFS	*SECCE7Rv1G0458910.1*;	G/R
			6.62E-05	16.3	Xuos530120_PGH	Ice recrystallization inhibition protein 1 (IRIP1)	
			6.80E-05	16.2	Xuos530120_LTT		
Xuos615052	T/A	Chr3:937,715,415	7.94E-05	14.7	Xuos615052_WFS	*SECCE3Rv1G0209310.1*;	L/H
			8.06E-05	15.8	Xuos615052_FLN	Inducer of CBF expression 1 (ICE1)	
			8.12E-05	14.7	Xuos615052_PGH		
			1.04E-04	15.6	Xuos615052_LTT		
Xuos519455	T/A	Chr6:434,208,046	1.10E-04	13.1	Xuos519455_WFS	*SECCE6Rv1G0399250.1*;	F/I
						Phenylalanine ammonia lyase 8 (PAL8)	
Xuos613978	A/G	Chr5:727,383,260	1.11E-04	15.5	Xuos613978_WFS	*SECCE5Rv1G0354870.1*, *SECCE5Rv1G0354880.1*;	A/T
		Chr5:727,387,754	1.18E-04	15.3	Xuos613978_FLN	Cold-regulated plasma membrane 413 protein	
			1.19E-04	15.3	Xuos613978_PHT	(COR413-PM)	
			1.20E-04	13.8	Xuos613978_TIL		
Xuos75199	A/C	Chr1:716,317,947	1.20E-04	15.3	Xuos75199_WFS	*SECCE1Rv1G0061510.1*;	N/T
			1.33E-04	14.6	Xuos75199_FLN	Jasmonate-resistant 1 (JAR1)	
Xuos76228a	C/G	Chr2:933,364,126	1.39E-04	14.5	Xuos76228a_WFS	*SECCE2Rv1G0140890.1*;	Q/E
Xuos76228b	C/T	Chr2:933,364,202	1.44E-04	13.4	Xuos76228b_WFS	Chalcone synthase 2 (CHS2)	A/V
Xuos2264	T/G	Chr1:109,131,359	1.45E-04	12.5	Xuos2264_WFS	*SECCE1Rv1G0013960.1*;	None (G/G)
			1.45E-04	14.4	Xuos2264_PGH	Chloroplast unusual positioning protein 1 (CHUP1)	
			1.46E-04	14.8	Xuos2264_FLN		
Xuos372616	C/A	Chr5:755,939,404	1.47E-04	14.8	Xuos372616_WFS	FRIGIDA-like 4 (FRL4-like)	None (A/A)
			1.49E-04	14.8	Xuos372616_PHT	*SECCE5Rv1G0358510.1*	
			1.53E-04	13.6	Xuos372616_TIL		

[1/] Number refers to matching rye Lo7_v2_scaffold number (Bauer *et al*. 2017).
[2/] Reference/alternative allele.
[3/] Position on rye Lo7 pseudomolecules version 1 assembly (Rabanus-Wallace *et al*. 2021).
[4/] Calculated upon Bonferroni correction.

Transporters, and disease resistance proteins (Appendix 14). The 339 SNPs identified were distributed onto all seven rye chromosomes with the largest number mapping to chromosomes 2R (53), followed by chromosomes 7R (52) and 5R (46) (Fig. 4.12).

4.10 Ten most significant marker-trait associations (MTAs)

All 10 group 1 SNPs were associated with WFS and seven of them associated with other traits (Table 4.11). The SNPs were mapped to exons of nine different genes. For seven of the target genes, non-synonymous amino acid replacement was predicted for encoded protein. SNP markers Xuos530120, Xuos615052, Xuos519455, Xuos613978, Xuos76228a, and Xuos372616, showed allelic dominance for WFS, whereas overdominance allelic effects was shown for the four remaining markers Xuos526258, Xuos75199, Xuos76228b, and Xuos2264 (Figs 4.13-4.19).

4.10.1 BIPP2C1-like protein phosphatase

SNP marker Xuos526258 was the most significant marker identified in the study and correlated with WFS, LTT, FLN, and PGH trait values (Table 4.11). The marker sequence matched *SECCE7Rv1G0469720.*1, an exon sequence for a *PPM-type protein phosphatase 2C* (*PP2C*) gene mapped to chromosome 7R (112.788 Mb; Fig. 4.12). The encoded protein showed highest identity (84.1 %) to a benzothiadiazole-induced protein phosphatase 2 C1 (*BIPP2C1)* gene from *Triticum dicoccoides* (XP_037426067; Appendix 14). The T/G SNP variation for rye *BIPP2C1* was predicted to cause a V_{185} to G_{185} change in region located outside of the catalytic phosphatase domain. Like the Lo7 reference *BIPP2C1*, all genotypes with low or very low WFS encoded only the V_{185} variant for the phosphatase (38 out of 38 genotypes) and this allele variant was associated with low FLN, high LT_{50} values (i.e., low LTT), and erect growth habit (Fig. 4.13). However, both (V_{185}/G_{185}) or only G_{185} variant were frequent among BIPP2C1 produced by genotypes with high or very high WFS, (31 out of 39 genotypes, Appendix 15). Also, the BIPP2C1V_{185}/G_{185} variant was associated with high LTT, FLN values and PGH (Fig 4.13).

4.10.2 Ice Recrystallization Inhibition Protein 1 (IRIP1)

The high-significance marker Xuos530120 associated with WFS, LTT, and PGH (Table4.11) and matched *SECCE7Rv1G0458910.1* located on chromosome 7R (23.476 Mb; Fig

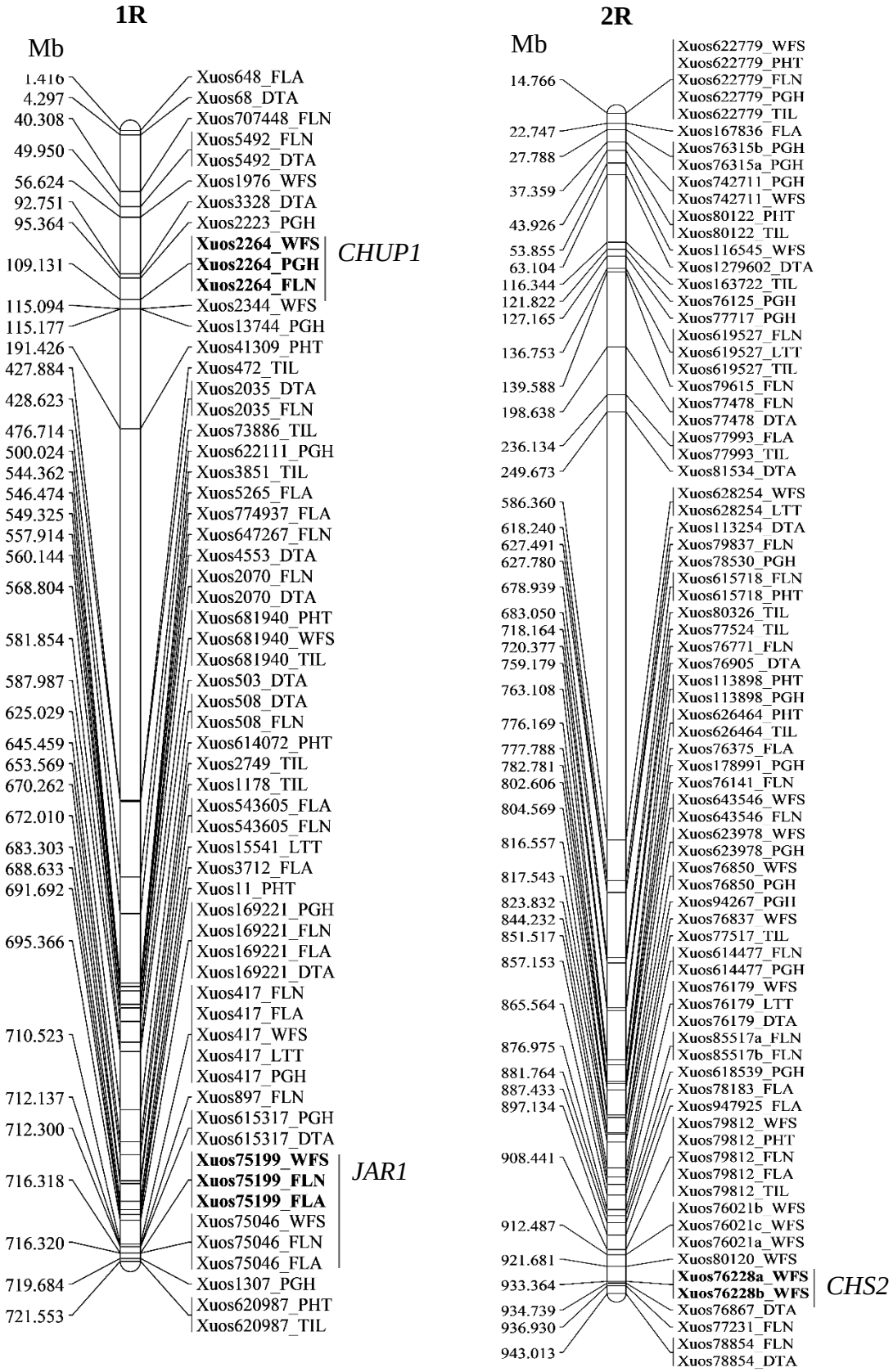
1R
Mb
1.416
4.297
40.308
49.950
56.624
92.751
95.364
109.131
115.094
115.177
191.426
427.884
428.623
476.714
500.024
544.362
546.474
549.325
557.914
560.144
568.804
581.854
587.987
625.029
645.459
653.569
670.262
672.010
683.303
688.633
691.692
695.366
710.523
712.137
712.300
716.318
716.320
719.684
721.553
Xuos648_FLA
Xuos68_DTA
Xuos707448_FLN
Xuos5492_FLN
Xuos5492_DTA
Xuos1976_WFS
Xuos3328_DTA
Xuos2223_PGH
Xuos2264_WFS
Xuos2264_PGH
Xuos2264_FLN
CHUP1
Xuos2344_WFS
Xuos13744_PGH
Xuos41309_PHT
Xuos472_TIL
Xuos2035_DTA
Xuos2035_FLN
Xuos73886_TIL
Xuos622111_PGH
Xuos3851_TIL
Xuos5265_FLA
Xuos774937_FLA
Xuos647267_FLN
Xuos4553_DTA
Xuos2070_FLN
Xuos2070_DTA
Xuos681940_PHT
Xuos681940_WFS
Xuos681940_TIL
Xuos503_DTA
Xuos508_DTA
Xuos508_FLN
Xuos614072_PHT
Xuos2749_TIL
Xuos1178_TIL
Xuos543605_FLA
Xuos543605_FLN
Xuos15541_LTT
Xuos3712_FLA
Xuos11_PHT
Xuos169221_PGH
Xuos169221_FLN
Xuos169221_FLA
Xuos169221_DTA
Xuos417_FLN
Xuos417_FLA
Xuos417_WFS
Xuos417_LTT
Xuos417_PGH
Xuos897_FLN
Xuos615317_PGH
Xuos615317_DTA
Xuos75199_WFS
Xuos75199_FLN
Xuos75199_FLA
JAR1
Xuos75046_WFS
Xuos75046_FLN
Xuos75046_FLA
Xuos1307_PGH
Xuos620987_PHT
Xuos620987_TIL
2R
Mb
14.766
22.747
27.788
37.359
43.926
53.855
63.104
116.344
121.822
127.165
136.753
139.588
198.638
236.134
249.673
586.360
618.240
627.491
627.780
678.939
683.050
718.164
720.377
759.179
763.108
776.169
777.788
782.781
802.606
804.569
816.557
817.543
823.832
844.232
851.517
857.153
865.564
876.975
881.764
887.433
897.134
908.441
912.487
921.681
933.364
934.739
936.930
943.013
Xuos622779_WFS
Xuos622779_PHT
Xuos622779_FLN
Xuos622779_PGH
Xuos622779_TIL
Xuos167836_FLA
Xuos76315b_PGH
Xuos76315a_PGH
Xuos742711_PGH
Xuos742711_WFS
Xuos80122_PHT
Xuos80122_TIL
Xuos116545_WFS
Xuos1279602_DTA
Xuos163722_TIL
Xuos76125_PGH
Xuos77717_PGH
Xuos619527_FLN
Xuos619527_LTT
Xuos619527_TIL
Xuos79615_FLN
Xuos77478_FLN
Xuos77478_DTA
Xuos77993_FLA
Xuos77993_TIL
Xuos81534_DTA
Xuos628254_WFS
Xuos628254_LTT
Xuos113254_DTA
Xuos79837_FLN
Xuos78530_PGH
Xuos615718_FLN
Xuos615718_PHT
Xuos80326_TIL
Xuos77524_TIL
Xuos76771_FLN
Xuos76905_DTA
Xuos113898_PHT
Xuos113898_PGH
Xuos626464_PHT
Xuos626464_TIL
Xuos76375_FLA
Xuos178991_PGH
Xuos76141_FLN
Xuos643546_WFS
Xuos643546_FLN
Xuos623978_WFS
Xuos623978_PGH
Xuos76850_WFS
Xuos76850_PGH
Xuos94267_PGH
Xuos76837_WFS
Xuos77517_TIL
Xuos614477_FLN
Xuos614477_PGH
Xuos76179_WFS
Xuos76179_LTT
Xuos76179_DTA
Xuos85517a_FLN
Xuos85517b_FLN
Xuos618539_PGH
Xuos78183_FLA
Xuos947925_FLA
Xuos79812_WFS
Xuos79812_PHT
Xuos79812_FLN
Xuos79812_FLA
Xuos79812_TIL
Xuos76021b_WFS
Xuos76021c_WFS
Xuos76021a_WFS
Xuos80120_WFS
Xuos76228a_WFS
Xuos76228b_WFS
CHS2
Xuos76867_DTA
Xuos77231_FLN
Xuos78854_FLN
Xuos78854_DTA

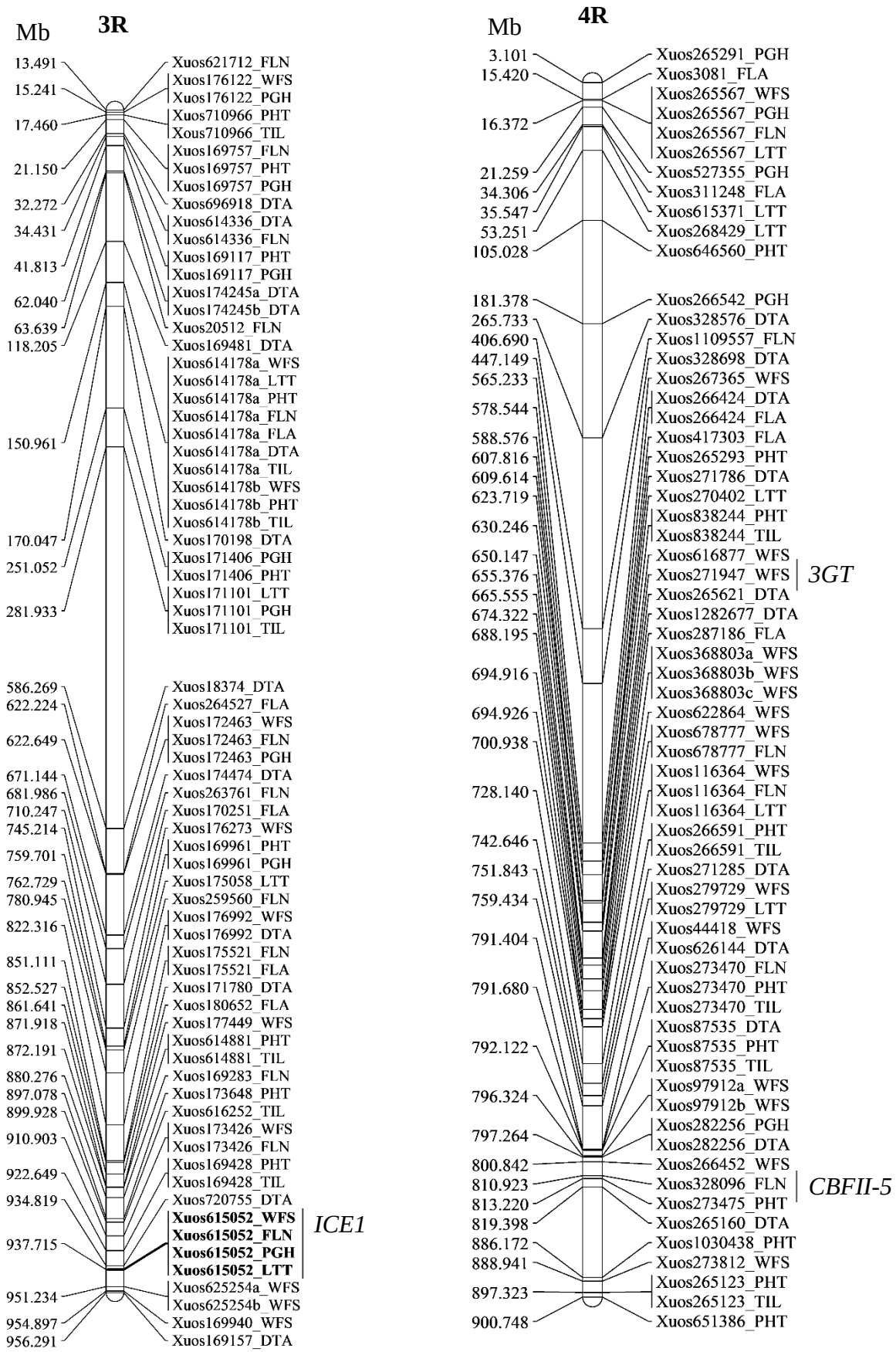
3R
Mb
13.491
15.241
17.460
21.150
32.272
34.431
41.813
62.040
63.639
118.205
150.961
170.047
251.052
281.933
586.269
622.224
622.649
671.144
681.986
710.247
745.214
759.701
762.729
780.945
822.316
851.111
852.527
861.641
871.918
872.191
880.276
897.078
899.928
910.903
922.649
934.819
937.715
951.234
954.897
956.291
Xuos621712_FLN
Xuos176122_WFS
Xuos176122_PGH
Xuos710966_PHT
Xous710966_TIL
Xuos169757_FLN
Xuos169757_PHT
Xuos169757_PGH
Xuos696918_DTA
Xuos614336_DTA
Xuos614336_FLN
Xuos169117_PHT
Xuos169117_PGH
Xuos174245a_DTA
Xuos174245b_DTA
Xuos20512_FLN
Xuos169481_DTA
Xuos614178a_WFS
Xuos614178a_LTT
Xuos614178a_PHT
Xuos614178a_FLN
Xuos614178a_FLA
Xuos614178a_DTA
Xuos614178a_TIL
Xuos614178b_WFS
Xuos614178b_PHT
Xuos614178b_TIL
Xuos170198_DTA
Xuos171406_PGH
Xuos171406_PHT
Xuos171101_LTT
Xuos171101_PGH
Xuos171101_TIL
Xuos18374_DTA
Xuos264527_FLA
Xuos172463_WFS
Xuos172463_FLN
Xuos172463_PGH
Xuos174474_DTA
Xuos263761_FLN
Xuos170251_FLA
Xuos176273_WFS
Xuos169961_PHT
Xuos169961_PGH
Xuos175058_LTT
Xuos259560_FLN
Xuos176992_WFS
Xuos176992_DTA
Xuos175521_FLN
Xuos175521_FLA
Xuos171780_DTA
Xuos180652_FLA
Xuos177449_WFS
Xuos614881_PHT
Xuos614881_TIL
Xuos169283_FLN
Xuos173648_PHT
Xuos616252_TIL
Xuos173426_WFS
Xuos173426_FLN
Xuos169428_PHT
Xuos169428_TIL
Xuos720755_DTA
Xuos615052_WFS
Xuos615052_FLN
Xuos615052_PGH
Xuos615052_LTT
Xuos625254a_WFS
Xuos625254b_WFS
Xuos169940_WFS
Xuos169157_DTA
ICE1
4R
Mb
3.101
15.420
16.372
21.259
34.306
35.547
53.251
105.028
181.378
265.733
406.690
447.149
565.233
578.544
588.576
607.816
609.614
623.719
630.246
650.147
655.376
665.555
674.322
688.195
694.916
694.926
700.938
728.140
742.646
751.843
759.434
791.404
791.680
792.122
796.324
797.264
800.842
810.923
813.220
819.398
886.172
888.941
897.323
900.748
Xuos265291_PGH
Xuos3081_FLA
Xuos265567_WFS
Xuos265567_PGH
Xuos265567_FLN
Xuos265567_LTT
Xuos527355_PGH
Xuos311248_FLA
Xuos615371_LTT
Xuos268429_LTT
Xuos646560_PHT
Xuos266542_PGH
Xuos328576_DTA
Xuos1109557_FLN
Xuos328698_DTA
Xuos267365_WFS
Xuos266424_DTA
Xuos266424_FLA
Xuos417303_FLA
Xuos265293_PHT
Xuos271786_DTA
Xuos270402_LTT
Xuos838244_PHT
Xuos838244_TIL
Xuos616877_WFS
Xuos271947_WFS
Xuos265621_DTA
Xuos1282677_DTA
Xuos287186_FLA
Xuos368803a_WFS
Xuos368803b_WFS
Xuos368803c_WFS
Xuos622864_WFS
Xuos678777_WFS
Xuos678777_FLN
Xuos116364_WFS
Xuos116364_FLN
Xuos116364_LTT
Xuos266591_PHT
Xuos266591_TIL
Xuos271285_DTA
Xuos279729_WFS
Xuos279729_LTT
Xuos44418_WFS
Xuos626144_DTA
Xuos273470_FLN
Xuos273470_PHT
Xuos273470_TIL
Xuos87535_DTA
Xuos87535_PHT
Xuos87535_TIL
Xuos97912a_WFS
Xuos97912b_WFS
Xuos282256_PGH
Xuos282256_DTA
Xuos266452_WFS
Xuos328096_FLN
Xuos273475_PHT
Xuos265160_DTA
Xuos1030438_PHT
Xuos273812_WFS
Xuos265123_PHT
Xuos265123_TIL
Xuos651386_PHT
3GT
CBFII-5

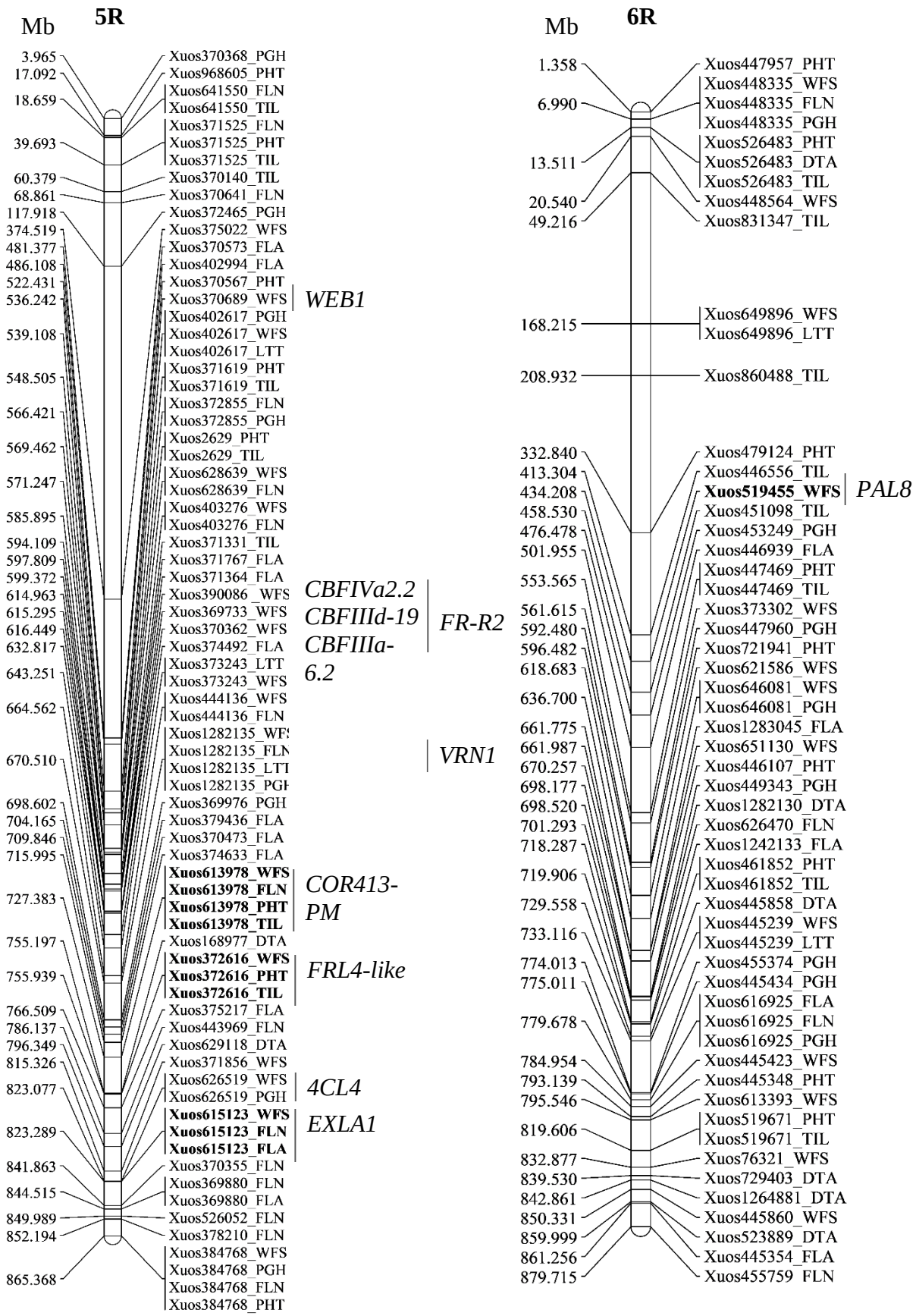
Mb
5R
3.965 Xuos370368_PGH
17.092 Xuos968605_PHT
18.659 Xuos641550_FLN
Xuos641550_TIL
Xuos371525_FLN
39.693 Xuos371525_PHT
Xuos371525_TIL
60.379 Xuos370140_TIL
68.861 Xuos370641_FLN
117.918 Xuos372465_PGH
374.519 Xuos375022_WFS
481.377 Xuos370573_FLA
486.108 Xuos402994_FLA
522.431 Xuos370567_PHT
536.242 Xuos370689_WFS
WEB1
539.108 Xuos402617_PGH
Xuos402617_WFS
Xuos402617_LTT
548.505 Xuos371619_PHT
Xuos371619_TIL
566.421 Xuos372855_FLN
Xuos372855_PGH
569.462 Xuos2629_PHT
Xuos2629_TIL
571.247 Xuos628639_WFS
Xuos628639_FLN
585.895 Xuos403276_WFS
Xuos403276_FLN
594.109 Xuos371331_TIL
597.809 Xuos371767_FLA
599.372 Xuos371364_FLA
614.963 Xuos390086_WFS
615.295 Xuos369733_WFS
616.449 Xuos370362_WFS
632.817 Xuos374492_FLA
643.251 Xuos373243_LTT
Xuos373243_WFS
664.562 Xuos444136_WFS
Xuos444136_FLN
Xuos1282135_WFS
670.510 Xuos1282135_FLN
Xuos1282135_LTT
Xuos1282135_PGH
CBFIVa2.2
CBFIIId-19
CBFIIIa-6.2
FR-R2
VRN1
698.602 Xuos369976_PGH
704.165 Xuos379436_FLA
709.846 Xuos370473_FLA
715.995 Xuos374633_FLA
Xuos613978_WFS
Xuos613978_FLN
727.383 Xuos613978_PHT
Xuos613978_TIL
COR413-PM
755.197 Xuos168977_DTA
Xuos372616_WFS
755.939 Xuos372616_PHT
Xuos372616_TIL
FRL4-like
766.509 Xuos375217_FLA
786.137 Xuos443969_FLN
796.349 Xuos629118_DTA
815.326 Xuos371856_WFS
Xuos626519_WFS
823.077 Xuos626519_PGH
4CL4
Xuos615123_WFS
823.289 Xuos615123_FLN
Xuos615123_FLA
EXLA1
841.863 Xuos370355_FLN
844.515 Xuos369880_FLN
Xuos369880_FLA
849.989 Xuos526052_FLN
852.194 Xuos378210_FLN
Xuos384768_WFS
Xuos384768_PGH
865.368 Xuos384768_FLN
Xuos384768_PHT
Mb
6R
1.358 Xuos447957_PHT
Xuos448335_WFS
6.990 Xuos448335_FLN
Xuos448335_PGH
Xuos526483_PHT
13.511 Xuos526483_DTA
Xuos526483_TIL
20.540 Xuos448564_WFS
49.216 Xuos831347_TIL
Xuos649896_WFS
168.215 Xuos649896_LTT
208.932 Xuos860488_TIL
332.840 Xuos479124_PHT
413.304 Xuos446556_TIL
434.208 Xuos519455_WFS
PAL8
458.530 Xuos451098_TIL
476.478 Xuos453249_PGH
501.955 Xuos446939_FLA
Xuos447469_PHT
553.565 Xuos447469_TIL
561.615 Xuos373302_WFS
592.480 Xuos447960_PGH
596.482 Xuos721941_PHT
618.683 Xuos621586_WFS
Xuos646081_WFS
636.700 Xuos646081_PGH
661.775 Xuos1283045_FLA
661.987 Xuos651130_WFS
670.257 Xuos446107_PHT
698.177 Xuos449343_PGH
698.520 Xuos1282130_DTA
701.293 Xuos626470_FLN
718.287 Xuos1242133_FLA
Xuos461852_PHT
719.906 Xuos461852_TIL
729.558 Xuos445858_DTA
Xuos445239_WFS
733.116 Xuos445239_LTT
774.013 Xuos455374_PGH
775.011 Xuos445434_PGH
Xuos616925_FLA
779.678 Xuos616925_FLN
Xuos616925_PGH
784.954 Xuos445423_WFS
793.139 Xuos445348_PHT
795.546 Xuos613393_WFS
Xuos519671_PHT
819.606 Xuos519671_TIL
832.877 Xuos76321_WFS
839.530 Xuos729403_DTA
842.861 Xuos1264881_DTA
850.331 Xuos445860_WFS
859.999 Xuos523889_DTA
861.256 Xuos445354_FLA
879.715 Xuos455759_FLN

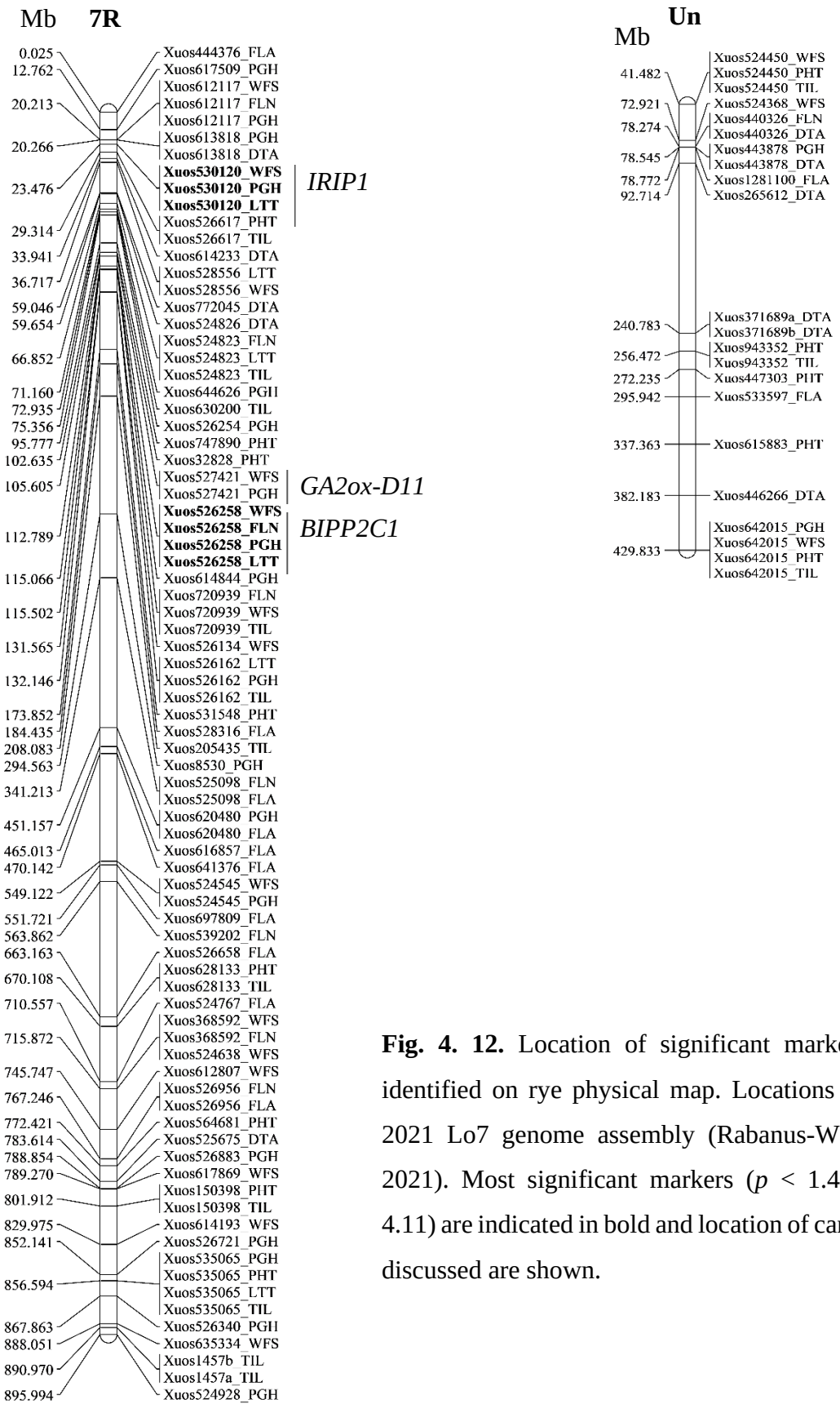

Fig. 4. 12. Location of significant markers for traits identified on rye physical map. Locations refers to the 2021 Lo7 genome assembly (Rabanus-Wallace *et al*., 2021). Most significant markers (p < 1.49e-04; Table 4.11) are indicated in bold and location of candidate genes discussed are shown.

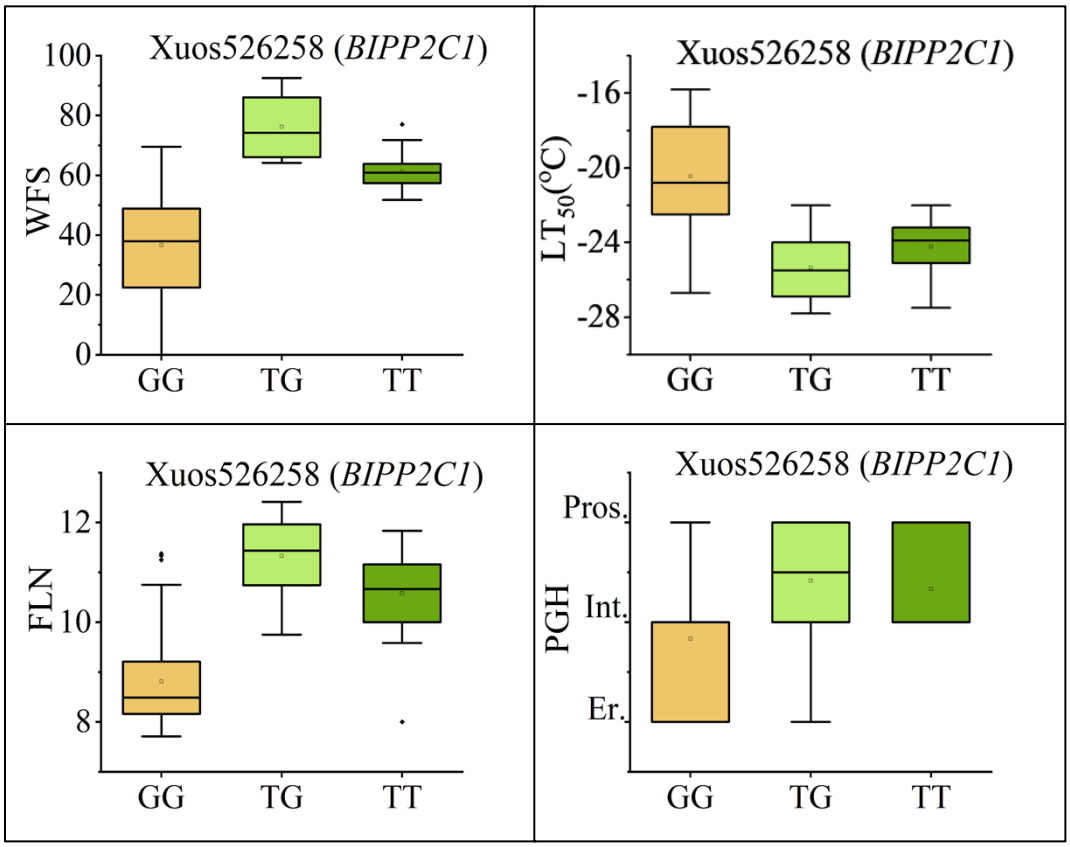

Fig. 4.13. Box-whisker plots showing the allele effects for the SNP marker (Xuos526258) ($p <$ 1.49e-04). The plots show median (horizontal bar), interquartile ranges (boxes), ranges (whiskers), and outliers (dots) for marker allele frequencies among the 96 rye genotypes.

4.12). The nucleotide sequence identity (>80%) was noted to 13 *ice recrystallization inhibition protein1* (*IRIP1*) and coding regions matched to *SECCE7Rv1G0458910.1* (Table 4.11). Only members of the Pooideae subfamily carry *IRIP* genes (Sandve *et al*., 2008). IRIPs carry a leucine-rich repeat (LRR) domain similar to those of phytosulfokine receptor tyrosine kinases and an ice-binding domain at the C-terminal end (Sandve *et al*., 2008). IRIPs are apoplastic proteins and play an important role in frost protection by binding to small ice crystals and inhibit further ice crystallization (Bredow and Walker, 2017; Gupta and Deswal, 2014). This inhibition is particularly important during freeze/thaw cycles as it prevents ice buildup from causing membrane damage leading to cell death. Other antifreeze proteins are also proposed to prevent bacteria from serving as ice-nucleators in the extra-cellular space (Tomalty and Walker, 2014). The Xuos530120 SNP targeting *IRIP* encoded a G_{36}/R_{36} variation within a preserved cysteine loops preceding the LRR-like region. In *Brachypodium distachyon* the LRR-like region is separated from the ice-binding region in the apoplastic space (Bredow *et al*., 2016*a*). Therefore, the amino acid substitution could affect the function of the N-terminal region including the LRR region without any influence on IRIP's interaction with ice crystals (Båga *et al*., 2022). Both SNP variants (G_{36}/R_{36}) were encoded by *IRIP* alleles carried by 27 out of the 39 genotypes with high and very high WFS (Appendix 15). The highest WFS and LTT, values were favored by the R_{36} IRIP1 variant (Fig. 4.14). The heterozygote alleles suggested presence of two near-identical *IRIP* genes. A very high frequency of C/C (G_{36}) alleles were carried by genotypes with low and very low WFS, which suggested that most of these genotypes carry only one of the two near-identical IRIP genes (36 out of 38; Appendix 15).

4.10.3 COR413-PM1-like

Marker Xuos613978 was associated with WFS, FLN, PHT, and TIL (Table 411) and showed highest sequence matches to *SECCE5Rv1G0354870.1* (89.1%), and *SECCE5Rv1G0354880.1* (89.2%), which coded for a COR413-PM protein and mapped close to (~11 Mb distal) the vernalization locus (*ScVRN-1*) on chromosome 5R (727.38 Mb; Table 4.11; Fig. 4.12). Sequence alignment to cold-regulated Arabidopsis and rice COR413-PM proteins suggested the rye COR413 proteins encoded from 5R locus predicted to be targeted to the plasma membrane. Studies in Arabidopsis show the *COR413-PM* gene is induced by cold, drought and ABA and proposed to have a role in protection of membrane structure (Su *et al*., 2018). The SNP

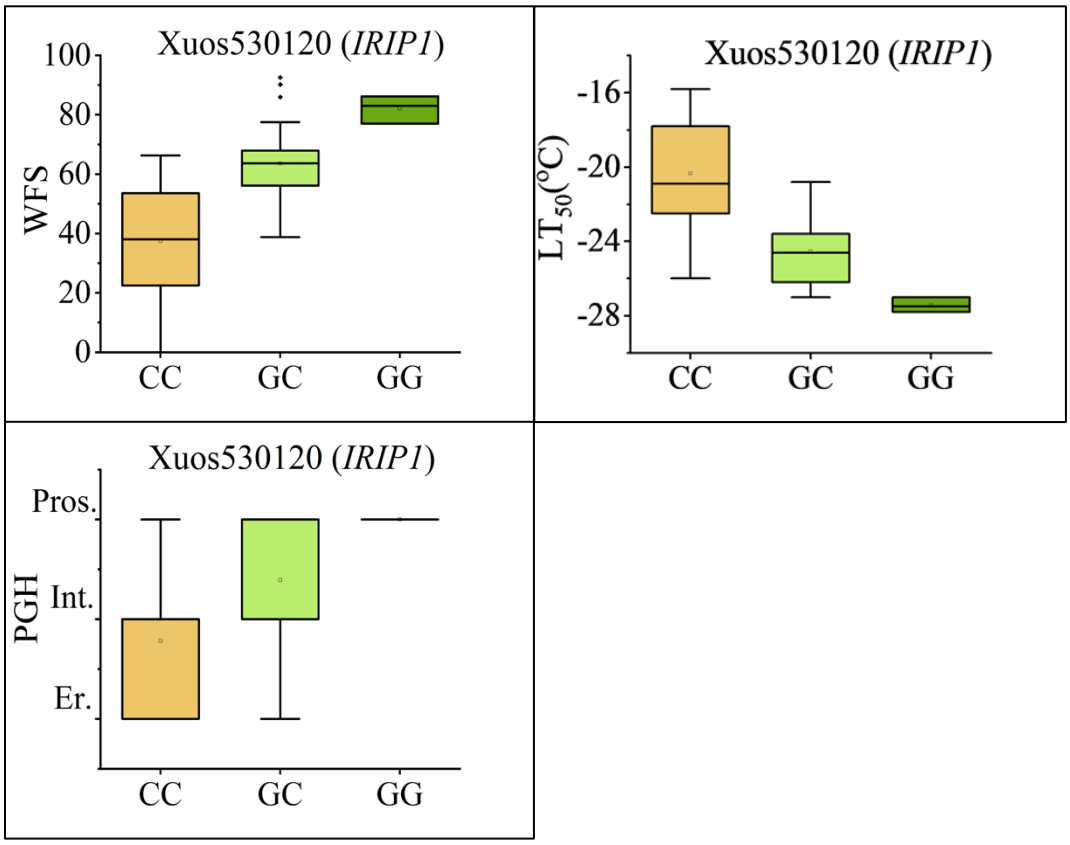

Fig. 4.14. Box-whisker plots showing the allele effects for the SNP marker (Xuos530120) ($p <$ 1.49e-04). The plots show median (horizontal bar), interquartile ranges (boxes), ranges (whiskers), and outliers (dots) for marker allele frequencies among the 96 rye genotypes.

for the rye *COR413-PM* encoded an A_{30} to T_{30} variation approximately 20 residues proximal of the first transmembrane region. All 38 genotypes with low or very low WFS encoded only the A_{30} variant for COR413-PM, which was also associated with low FLN (Fig. 4.15; Appendix 15). The T_{30} modification on COR413-PM, a possible phosphorylation site (Båga *et al*., 2022), or A_{30}/T_{30} variants were relatively common among COR413-PM encoded by genotypes with high or very high WFS (27 out of 39 genotypes: Appendix 15). High WFS was also associated with high FLN value, and medium and tall PHT and TIL (Fig. 4.15).

4.10.4 Inducer of CBF Expression 1 (ICE1)

Marker Xuos615052 associated with WFS, LTT, FLN and PGH (Table 4.11) coincided with an *Inducer of CBF Expression 1* (*ICE1*) gene (*SECCE3Rv1G0209310.1*) mapped to chromosome 3R (937.715 Mb; Fig. 4.12). ICE1, like the related ICE2 in Arabidopsis, are MYC-like basic helix-loop-helix (bHLH) transcriptional factors, which bind to MYC-recognition sequences present in *CBF* promoter regions and thereby stimulate cold-induced *CBF* expression (Chinnusamy *et al*., 2003; Fursova *et al*., 2009; Tang *et al*., 2020). Induced *CBF1* and *CBF3* then activate cold-dependent and ABA-independent expression of *COR* genes conferring cold tolerance in plants (Jaglo-Ottosen *et al*., 1998). *SECCE3Rv1G0209310.1* showed highest sequence identity to *ICE1* transcripts of several *Aegilops* and *Triticum* species (97-98%) including *TaICE41* (97%) encoded from group 3 chromosomes of hexaploid wheat. *TaICE41* has a role in cold tolerance as shown by conferring increased freezing tolerance when overexpressed in Arabidopsis (Badawi *et al*., 2008). The Xuos615052 SNP encoded a L_{283}/H_{283} variation at the end of the DNA-binding bHLH domain and start of the ZIP dimerization domain (Båga *et al*., 2022) as predicted for ICE proteins in *Vitis amurensi*ce (Xu *et al*., 2014). A basic residue, L_{283}, is present at corresponding site for ICE1-like isoforms XI and X2 produced by *Aegilops tauschii* subsp. *tauschii* (XP_020168495 and XP_020168503), and *AenICE2* and *AeuICE2* of *Aegilops neglecta* and *Aegilops umbellulata*, respectively (Jin *et al*., 2018). Among the 38 rye genotypes with low or very low WFS, 33 carried homozygous *ICE1* alleles encoding the basic residue H_{283}. H_{283} ICE1 variation was also associated with low LTT, and FLN values, and erect growth habit (Fig 4.16). Homozygous alleles encoding the L_{283} or heterozygous alleles encoding both variants (L_{283}/H_{283}) dominated among genotypes with very high and high WFS (24 out of 39 genotypes: Appendix 15). The ICE1 L_{283} variant was also associated with high LTT, and FLN values (Fig 4.16).

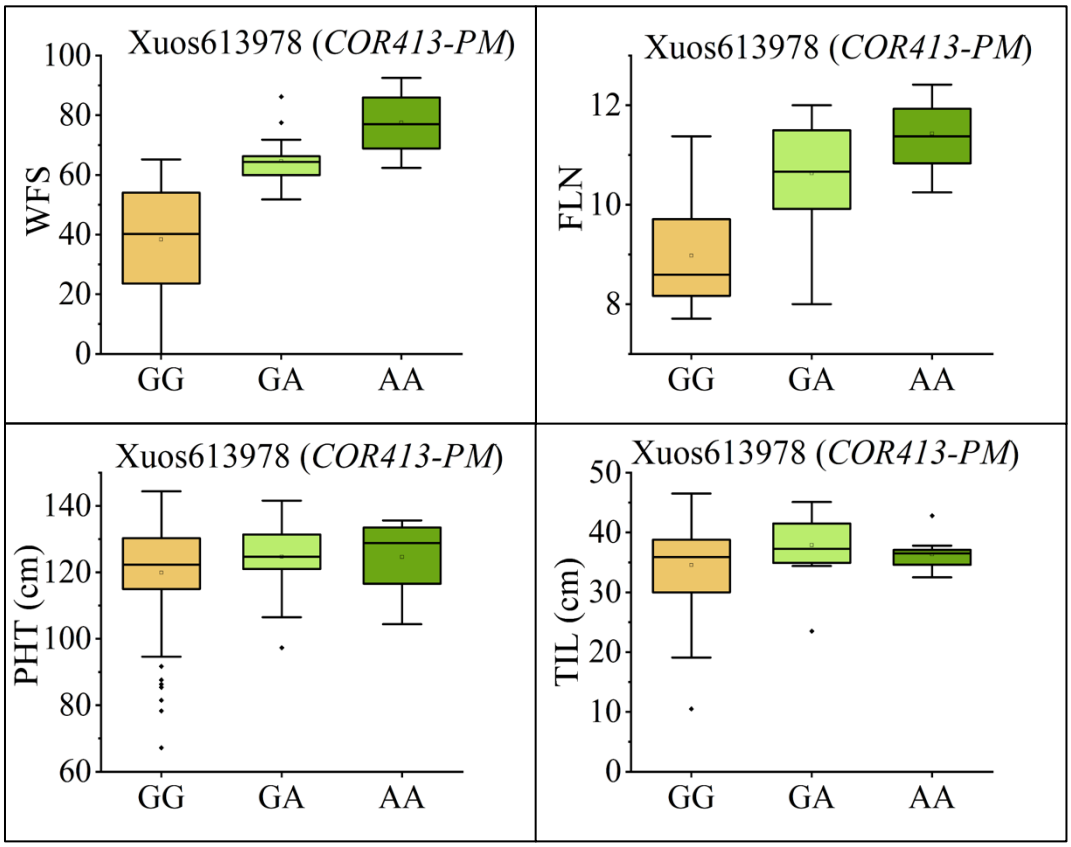

Fig. 4.15. Box-whisker plots showing the allele effects for the SNP marker (Xuos613978) ($p <$ 1.49e-04). The plots show median (horizontal bar), interquartile ranges (boxes), ranges (whiskers), and outliers (dots) for marker allele frequencies among the 96 rye genotypes.

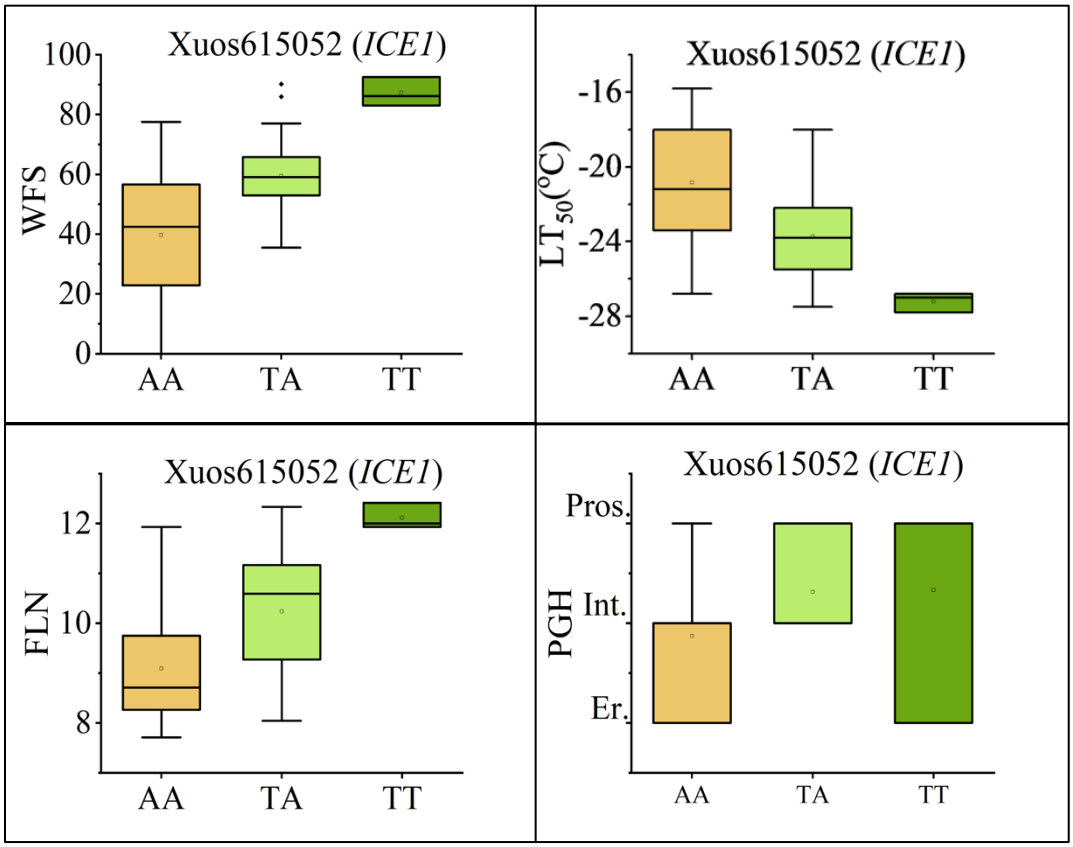

Fig. 4.16. Box-whisker plots showing the allele effects for the SNP marker (Xuos615052) ($p <$ 1.49e-04). The plots show median (horizontal bar), interquartile ranges (boxes), ranges (whiskers), and outliers (dots) for marker allele frequencies among the 96 rye genotypes.

4.10.5 Jasmonate-resistant 1 (JAR1)

Two markers (Xuos75199 and Xuos75046), both associated with WFS, FLN and FLA (Table 4.11; Appendix 14), targeted the same gene, (*SECCE1Rv1G0061510.1*) on chromosome 1R (~716.319 Mb; Fig 4.12). The *SECCE1Rv1G0061510.1* showed high identity (95%) to an *Aegilops tauschii* subsp. *tauschii* jasmonic acid-amido synthetase 1 (*JAR1*) transcript (Appendix 14) predicted to encode JAR1 isoform X3. The Xuos75199 SNP caused an N_{11}/T_{11} variation, whereas Xuos75046 SNP caused an N_{481}/I_{481} variation. Genotypes with low or very low WFS generally encoded JAR1 containing T_{11}/ N_{481} combination (29 out of 38), which was also associated with low FLN values, whereas genotypes with very high or high WFS carried the T_{11} alleles (27 out of 39 genotypes; Fig 4.17; Appendix 15). Highest WFS was also associated with high FLN values (Fig. 4.17). JAR1 is a cytosolic auxin-inducible enzyme catalyzing reversible conversion of jasmonic acid (JA) to JA-Ile (Staswick and Tiryaki, 2004), which is the true hormone in JA signaling (Fonseca *et al*., 2009). Both JA and methyl jasmonate (MeJA) can be converted to JA-Ile and participate in the activation of systemic defense (Wasternack and Song, 2017); thus, JA is involved in many plant processes including resistance to cold stress in Arabidopsis (Hu *et al*., 2017).

4.10.6 FRIGIDA4-like (FRL4-like)

Marker Xuos372616 showed high association with WFS, PHT, and TIL in the rye population (Table 4.11) and corresponded to *SECCE5Rv1G0358510.1* located on chromosome 5R (755.939 Mb; Fig. 4.12). The SNP was located within the first exon, but did not alter the encoded amino acid (A_{235}). Homozygous C/C alleles at SNP site dominated among 38 genotypes with low or very low WFS (36 out of 38), whereas heterozygous C/A alleles were most common among genotypes with very high and high WFS and medium and tall PHT and TIL (24 out of 39; Fig 4.18 Appendix 15). The partial FRIGIDA-like sequence showed identities to proteins annotated FRIGIDA-like carried by 5'-3' exoribonuclease 4 (XRN4) proteins encoded by *Brachypodium distachyon* (XP_024313537), and *Triticum urartu* (EMS54431.1). In Arabidopsis, FRIGIDA and FRIGIDA-like 1 and 2 (FRL1, FRL2) proteins cooperate to promote the winter annual habit (Michaels *et al*., 2003). FRIGIDA acts as a scaffolding protein for a FRL-C complex composed of both transcription and chromatin-modifying factors which regulate expression of the flowering repressor *FLC* gene through chromatin remodeling (Choi *et al*., 2011). Within the complex,

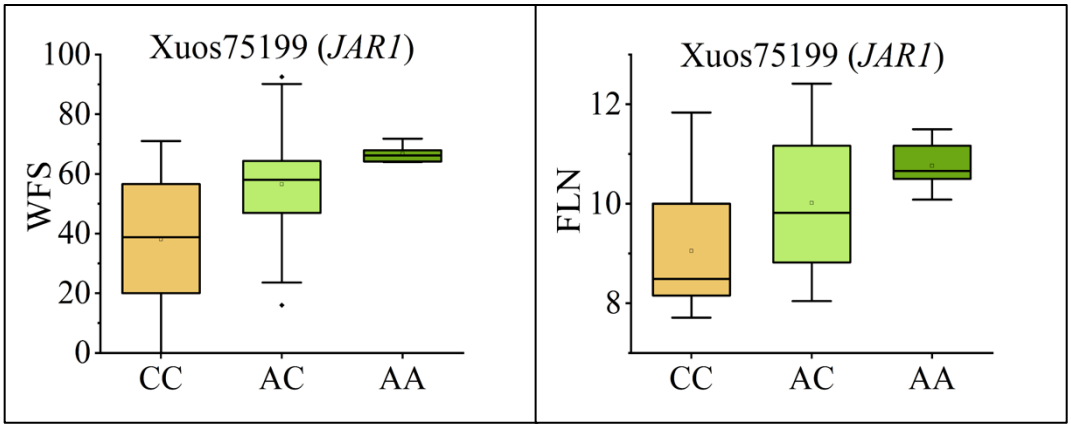

Fig. 4.17. Box-whisker plots showing the allele effects for the SNP marker (Xuos75199) (p < 1.49e-04). The plots show median (horizontal bar), interquartile ranges (boxes), ranges (whiskers), and outliers (dots) for marker allele frequencies among the 96 rye genotypes.

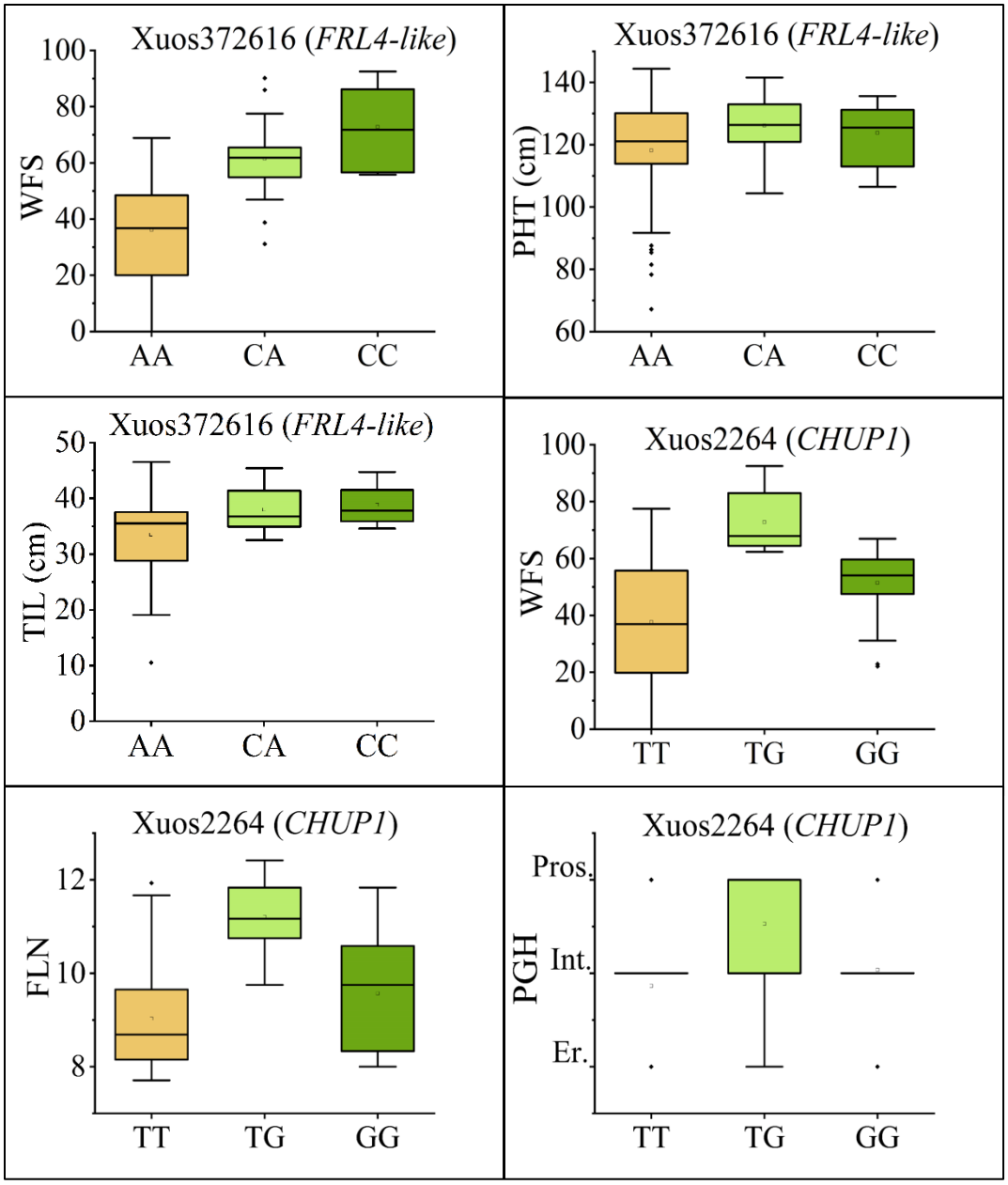

Fig. 4.18. Box-whisker plots showing the allele effects for the SNP markers (Xuos372616 and Xuos2264) (p < 1.49e-04). The plots show median (horizontal bar), interquartile ranges (boxes), ranges (whiskers), and outliers (dots) for marker allele frequencies among the 96 rye genotypes.

FRIGIDA interacts with the nuclear cap-binding complex bound to *FLC* mRNA and thereby regulates FLC transcription and splicing efficiency (Geraldo *et al*., 2009). However the *FLC* orthologues in cereals, *BdODDSOC2*/*TaAGL22*/*TaAGL33*, do not have a major role in vernalisation (Ruelens *et al*., 2013), which is regulated differently in dicot and monocot plants (Xu and Chong, 2018). Thus, the role of FRIGIDA-like proteins in monocot plants is unclear (Higgins *et al*., 2010).

4.10.7 Chloroplast Unusual Positioning Protein-1 (CHUP1)

Marker Xuos2264 on chromosome 1R (109.131 Mb; Fig 4.12) corresponded to *SECCE1Rv1G0013960.1* with a truncated gene encoding Chloroplast Unusual Positioning Protein-1 (CHUP1), which is localized to the chloroplast envelope (Oikawa *et al*., 2003). The SNP marker was associated with WFS, PGH and FLN (Table 4.11) but the SNP variation did not alter the rye CHUP1 protein sequence at G_2. Movement to the periclinal cell wall enhances photosynthesis under low light conditions, whereas movement to anticlinal cell wall is suggested to protect the photosynthetic apparatus from high light and photoinhibition (Wilson and Ruban, 2020). The Arabidopsis CHUP1 regulates polymerization and /or maintenance of chloroplast actin (cp-actin) and mediates light-regulated translocation of chloroplasts to specific sites on the plasma membrane depending on the intensity of incoming light (Wada and Kong, 2018). An additional marker (Xuos370689) identified for *SECCE5Rv1G0331080.1* associated with WFS and coincided with a *WEAK CHLOROPLAST MOVEMENT UNDER BLUE LIGHT 1* (*WEB1*) gene mapped to chromosome 5R (536.242 Mb; Appendix 14). WEB1 has a role in blue-light-induced reorganization of cp-actin filaments during the avoidance response of chloroplast movement and regulates the speed of chloroplast translocation (Kodama *et al*., 2010). The SNP variation maps to exon for *WEB1* gene, but the protein sequence is not altered by the SNP variation (R_{310}/R_{310}) (Appendix 14). The finding that two independent SNPs associated with WFS and targeting genes involved in chloroplast relocation suggest positioning of chloroplasts may be important factor for cold hardiness in rye.

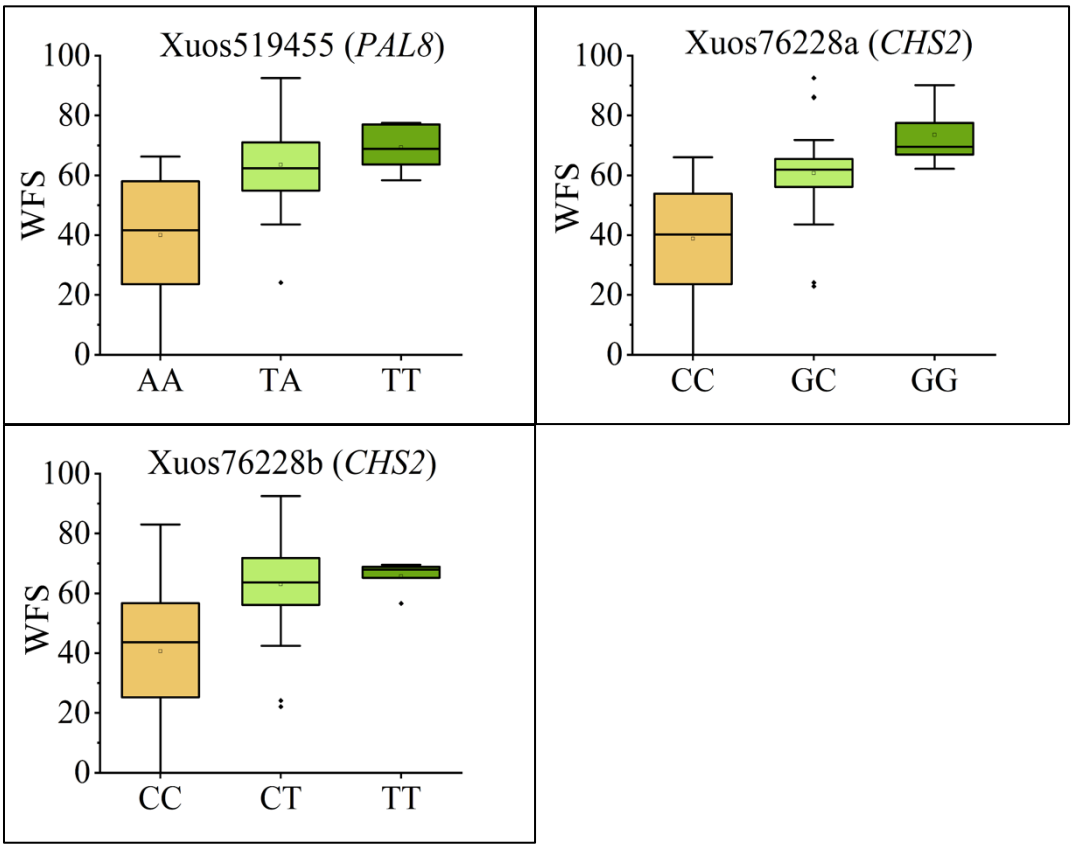

Fig. 4.19. Box-whisker plots showing the allele effects for the SNP markers (Xuos519455, Xuos76228a and Xuos76228b) (p < 1.49e-04). The plots show median (horizontal bar), interquartile ranges (boxes), ranges (whiskers), and outliers (dots) for marker allele frequencies among the 96 rye genotypes.

4.11 MTAs in group 2

Among the 205 SNPs of group 2, only 42 markers were associated with WFS and other traits (115 MTAs; Appendix 14), which matched 20 Lo7 rye annotated genes, and had lower significance than group 1 SNP markers. Of 20 genes matched with MTAs, 12 were matched to coding region of genes, and only four non-synonymous amino acid substitutions were predicted from the SNP variations (Table 4.12). SNP markers Xuos615123, Xuos527421, Xuos75046, Xuos79812, Xuos643546, Xuos448335, Xuos173426, Xuos176122, Xuos172463, and Xuos628254, showed allelic dominance for WFS, whereas overdominance allelic effects was shown for the two remaining markers Xuos614178a and Xuos76179 (Fig. 4.20-4.26).

4.11.1 Expansin-like 1 (EXLA)

Marker Xuos615123, associated with WFS, FLN, and FLA (Table 4.12), was found to correspond to *SECCE5Rv1G0367690.1* on chromosome 5R at 823.289 Mb (Fig. 4.12). The target gene codes for Expansin-like (EXLA) polypeptide and the SNP variation (T/C) was synonymous (Q/Q) (Table 4.12). Homozygous C/C alleles at SNP site dominated among 38 genotypes with low or very low WFS and low FLN values (33 out of 38), whereas heterozygous T/C alleles were most common among genotypes with very high and high WFS (23 out of 39; Fig. 4.20; Appendix 15). Expansins play a role in cell wall flexibility and plant growth programming under stress conditions (Cosgrove, 2000). Many of the genes involved in cell wall modifications in Arabidopsis are induced to higher levels during sub-zero acclimation than during cold acclimation (Le *et al*., 2015*a*). Expansin genes can positively regulate cold tolerance in Arabidopsis by causing cell wall loosening, which leads to preservation of cell turgor and increase in lignin and cellulose contents (Peng *et al*., 2019; Feng *et al*., 2019). Also, expansins can limit damage due to freezing by causing an increase in cell wall extensibility in the vascular transition zone (Willick *et al*., 2018). *AtEXLA* mutants in Arabidopsis showed reduced cold tolerance (Abuqamar *et al*., 2013). Furthermore, expansin expression analysis in wheat showed that *TaEXPs* might be involved in cold tolerance in winter-hardy cultivars (Zhang *et al*., 2018).

4.11.2 Gibberellin 2-beta-dioxygenase-A11 (GA2ox-D11)

Xuos527421 marker, associated both with WFS and PGH (Table 4.12), mapped to chromosome 7R at 105.605 Mb (Fig 4.12) and corresponded to *SECCE7Rv1G0469060.1* which

Table 4.12. Most significant MTAs identified among group 2 markers.

Marker ID[1/]	SNP[2/]	SNP position (bp)[3/]	*p*-value[4/]	R^2	MTA	Corresponding gene; protein	Amino acid change
Xuos615123	T/C	Chr5:823289392	1.68E-04	14.52	Xuos615123_WFS	*SECCE5Rv1G0367690.1;*	None (Q/Q)
			1.71E-04	14.05	Xuos615123_FLN	Expansin-like A (EXLA)	
			1.72E-04	13.04	Xuos615123_FLA		
Xuos527421	A/G	Chr7:105605404	1.90E-04	14.21	Xuos527421_WFS	*SECCE7Rv1G0469060.1;*	None (L/L)
			1.98E-04	11.90	Xuos527421_PGH	Gibberellin 2-beta-dioxygenase-A11 (GA2ox-D11)	
Xuos614178a	C/T	Chr3:150960806	2.05E-04	11.84	Xuos614178a_WFS	*SECCE3Rv1G0163720.1;*	None (Q/Q)
			2.11E-04	13.95	Xuos614178a_LTT	ABC transporter C-like family member 8 (ABCC8)	
			2.14E-04	13.93	Xuos614178a_PHT		
			2.15E-04	13.92	Xuos614178a_FLN		
			2.17E-04	13.89	Xuos614178a_FLA		
			2.22E-04	13.48	Xuos614178a_TIL		
			2.24E-04	13.42	Xuos614178a_DTA		
Xuos75046	T/A	Chr1:716320289	2.30E-04	11.60	Xuos75046_WFS	*SECCE1Rv1G0061510.1;*	I/N
			2.38E-04	12.33	Xuos75046_FLN	Jasmonic acid-amido synthetase (JAR1*)*	
			2.46E-04	11.46	Xuos75046_FLA		
Xuos79812	T/G	Chr2:908441047	2.56E-04	13.10	Xuos79812_WFS	*SECCE2Rv1G0135760.1;*	K/T
			2.56E-04	13.49	Xuos79812_PHT	Alpha-glucosidase	
			2.56E-04	13.11	Xuos79812_FLN		
			2.61E-04	13.08	Xuos79812_TIL		
			2.64E-04	13.04	Xuos79812_FLA		
Xuos76179	C/T	Chr2:865564352	2.83E-04	12.88	Xuos76179_WFS	*SECCE2Rv1G0128860.1;*	None (E/E)
			2.83E-04	13.24	Xuos76179_LTT	Zinc finger CCCH-30	
			2.83E-04	12.87	Xuos76179_DTA		
Xuos643546	C/G	Chr2:804568836	2.86E-04	11.15	Xuos643546_WFS	*SECCE2Rv1G0121100.1;*	None (T/T)
			2.98E-04	13.14	Xuos643546_FLN	Peroxisomal (S)-2-hydroxy-acid oxidase (GLO3)	
Xuos448335	T/G	Chr6:6989636	3.53E-04	12.71	Xuos448335_WFS	*SECCE6Rv1G0378210.1;*	None (S/S)
			3.56E-04	12.34	Xuos448335_FLN	Alpha-1,3-arabinosyltransferase (XAT3)	
			3.59E-04	12.33	Xuos448335_PGH		
Xuos173426	C/G	Chr3:910902745	3.97E-04	10.49	Xuos173426_WFS	*SECCE3Rv1G0206760.1;*	S/R
			4.01E-04	12.06	Xuos173426_FLN	Tyrosine kinase (HCK)	
Xuos176122	A/G	Chr3:15240693	4.44E-04	12.18	Xuos176122_WFS	*SECCE3Rv1G0147470.1;*	None (L/L)
			4.46E-04	12.15	Xuos176122_PGH	Lecithin-cholesterol acyltransferase1 (LCAT1)	
Xuos172463	C/T	Chr3:622648676	4.80E-04	10.11	Xuos172463_WFS	*SECCE3Rv1G0182130.1;*	None (N/N)
			4.83E-04	10.09	Xuos172463_FLN	Zinc finger protein (ZPR1-like)	
			4.84E-04	11.24	Xuos172463_PGH		
Xuos628254	G/A	Chr2:586360009	5.29E-04	10.61	Xuos628254_WFS	*SECCE2Rv1G0103040.1;*	W/Stop
			5.30E-04	11.41	Xuos628254_LTT	Chemocyanin	

[1/] Number refers to matching rye Lo7_v2_scaffold number (Bauer *et al*. 2017); [2/] Reference/alternative allele; [3/] Position on rye Lo7 pseudomolecules version 1 assembly (Rabanus-Wallace *et al.* 2021); [4/] Calculated upon Bonferroni correction.

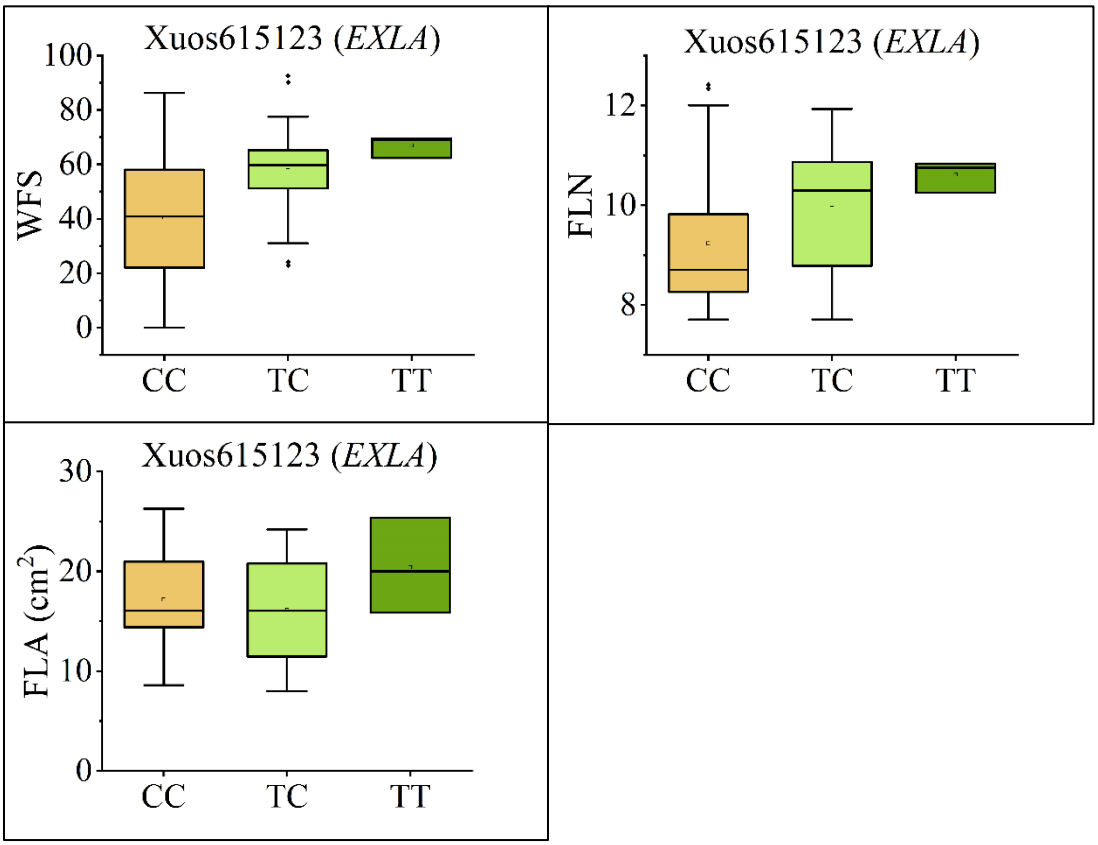

Fig. 4.20. Box-whisker plots showing the allele effects for the SNP marker (Xuos615123) ($p < 0.001$). The plots show median (horizontal bar), interquartile ranges (boxes), ranges (whiskers), and outliers (dots) for marker allele frequencies among the 96 rye genotypes.

showed sequence identity to the gibberellin 2-beta-dioxygenase-A11 (GA2ox-D11) gene. The SNP variation (A/G) did not alter (L/L) (Table 4.12), the rye GA2ox-D11 protein sequence. Genotypes with low or very low WFS generally containing G/G alleles (31 out of 38), whereas genotypes with very high or high WFS and PGH carried the A/G alleles (19 out of 39 genotypes; Fig.4.21; Appendix 15). Braun *et al*. (2019) mapped the GA-sensitive dwarfing gene *Ddw1* 0.4 cM distance with the C20-GA2ox gene (*ScGA2ox12*) on chromosome 5R, which has been observed in semi-dwarf rye genotypes. GAox genes are involved in GA biosynthetic pathway and have a significant effect on the ICE- CBF-COR regulatory network in Arabidopsis (Achard *et al*., 2008). In winter cereals, one of the results of ICE-CBF-COR regulatory network activation is an increase in *GA2ox* expression, which leads to a dwarf phenotype with enhanced freezing tolerance and an increase in photosynthetic apparatus (Kurepin *et al*., 2013).

4.11.3 ATP-binding cassette transporter C-like family member 8 (ABCC8)

Marker Xuos614178a, was associated with seven traits (WFS, PHT, TIL, LTT, FLN, DTA, and FLA), mapped to chromosome 3R (150.960 MB; Fig. 4.12), and located to *SECCE3Rv1G0163720.1* (Table 4.12) which showed sequence similarity to an ATP-binding cassette (ABC) transporter C-like family member 8 (ABCC8) gene. The Xuos614178a SNP did not cause any alterations in the encoded amino acid (Q) (Table 4.12). Among the 38 rye genotypes with low or very low WFS, 22 carried homozygous C/C alleles. C/C ABCC8 variation was also associated with low LTT, and FLN values (Fig. 4.21). Heterozygous alleles (C/T) dominated among genotypes with very high and high WFS, and high LTT (23 out of 39 genotypes; Appendix 15; Fig 4.21). ABC transporters hydrolyze ATP to drive transport in most membranes such as plasma membrane, tonoplast, chloroplasts, mitochondria and peroxisomes (Kang *et al*., 2011). ABC proteins are involved in detoxification processes, plant growth and development, and both abiotic and biotic stress responses (Martinoia *et al*., 1993; 2002; Wanke and Üner-Kolukisaoglu, 2010). Another marker, Xuos614178b that was associated with WFS and only PHT (Appendix 14) also corresponded to *SECCE3Rv1G0163720.1* located on chromosome 3R (150.960 Mb; Fig 4.12). The SNP variation (C/T) was also synonymous (Q/Q) as in Xuos614178a.

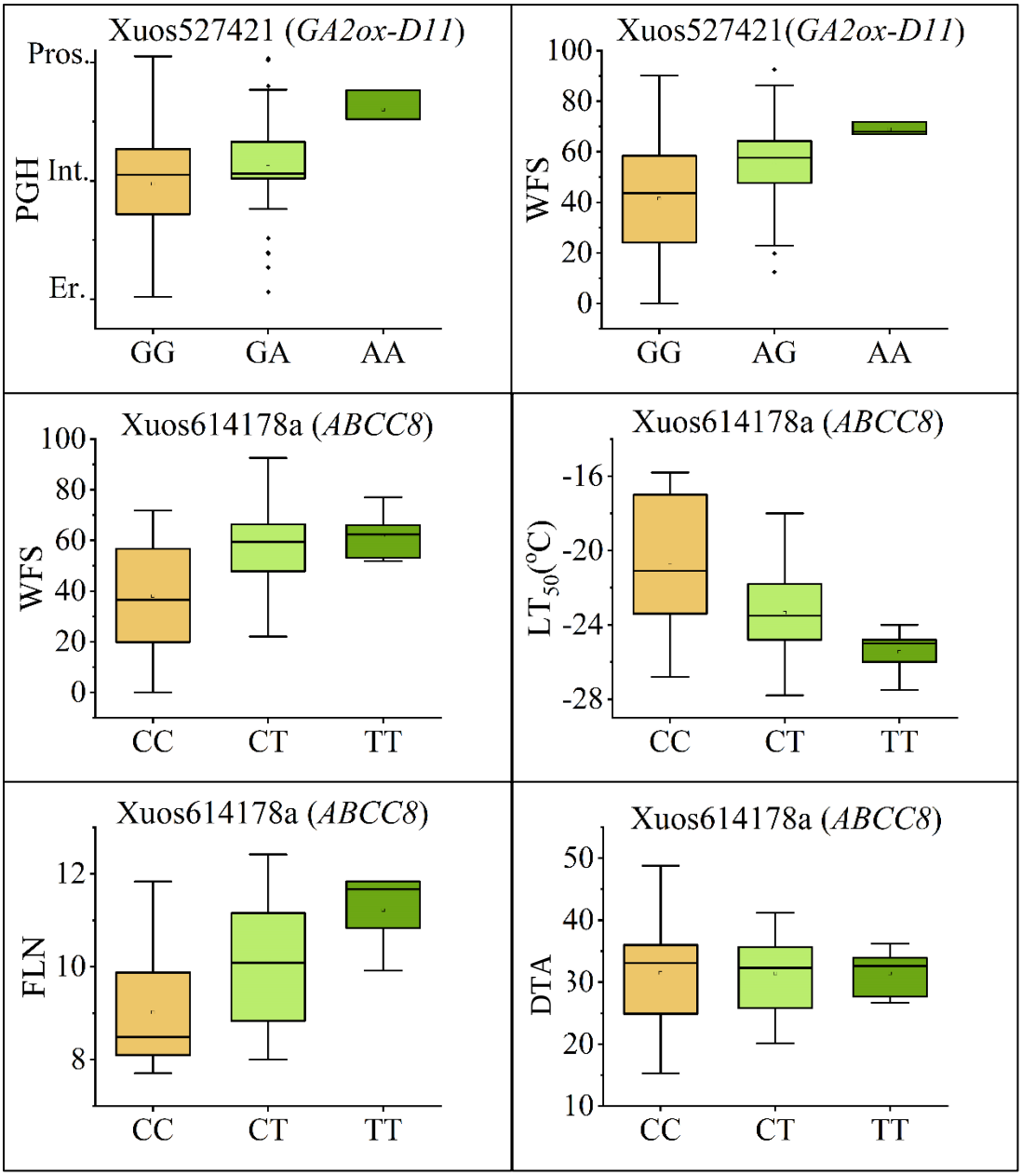
Xuos527421 (GA2ox-D11)
PGH
Pros.
Int.
Er.
GG
GA
AA
Xuos527421(GA2ox-D11)
WFS
100
80
60
40
20
0
GG
AG
AA
Xuos614178a (ABCC8)
WFS
100
80
60
40
20
0
CC
CT
TT
Xuos614178a (ABCC8)
LT50(°C)
-16
-20
-24
-28
CC
CT
TT
Xuos614178a (ABCC8)
FLN
12
10
8
CC
CT
TT
Xuos614178a (ABCC8)
DTA
50
40
30
20
10
CC
CT
TT

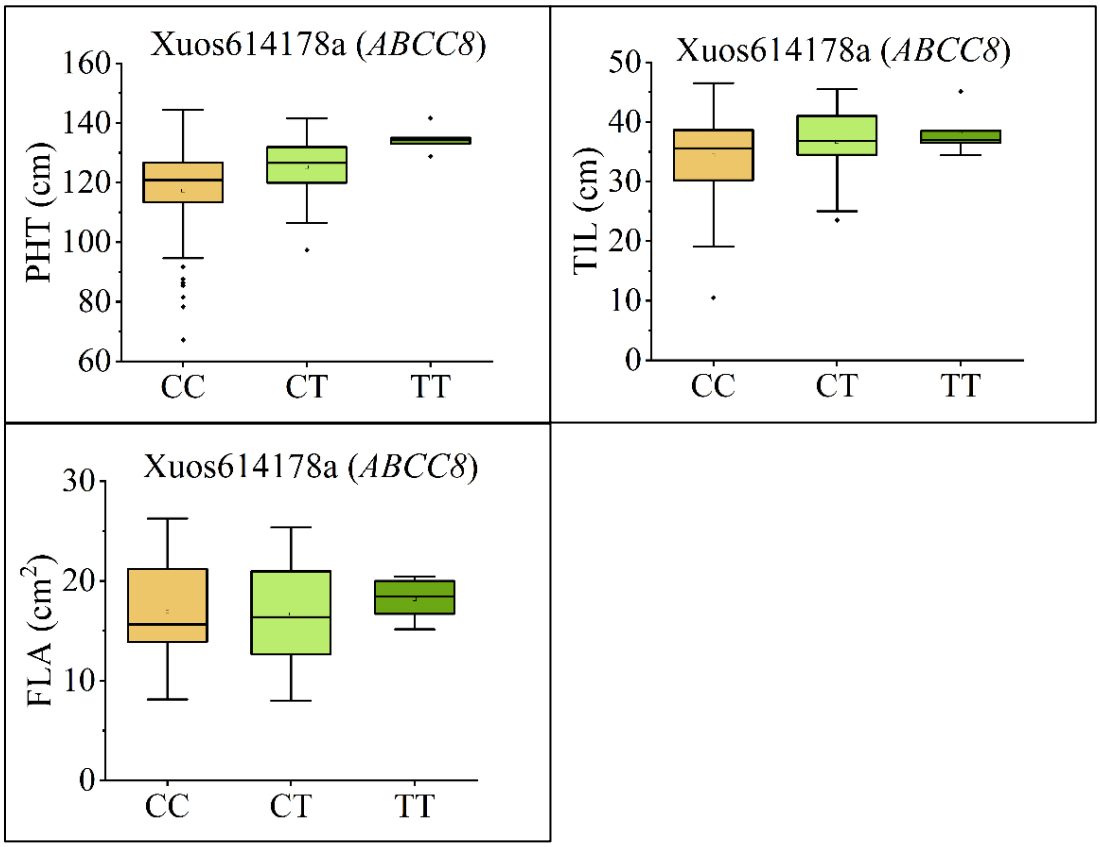

Fig. 4.21. Box-whisker plots showing the allele effects for the SNP markers (Xuos527421 and Xuos614178a) ($p < 0.001$). The plots show median (horizontal bar), interquartile ranges (boxes), ranges (whiskers), and outliers (dots) for marker allele frequencies among the 96 rye genotypes.

4.11.4 Alpha-glucosidase

Marker Xuos79812 was found to be associated with WFS, PHT, TIL, FLN, and FLA (Table 4.12) and targeted *SECCE2Rv1G0135760.1* gene on chromosome 2R (098.441 Mb; Fig. 4.12). The *SECCE2Rv1G0135760.1* transcript was similar in sequence to alpha-glucosidase (*Os06g0675700*) reported in *Oryza sativa*. The Xuos79812 SNP caused a K/T variation in the protein sequence (Table 4.12). 21 out of 38 genotypes with low or very low WFS encoded only the K variant for the alpha-glucosidase and this allele variant was also associated with low FLN values (Fig. 4.22). However, both (K/T) or only T variant were frequent among alpha-glucosidase produced by genotypes with high or very high WFS (25 out of 39 genotypes, Fig. 4.22; Appendix 15). Also, the alpha-glucosidase T variant were associated with high FLN values (Fig. 4.22).

4.11.5 Zinc finger CCCH-30

Marker Xuos76179 was associated with WFS, LTT, and DTA (Table 4.12) and matched *SECCE2Rv1G0128860.1* (chromosome 2R, 865.564 Mb; Fig. 4.12) coding for a zinc finger CCCH containing domain-30. The SNP was located within the exon but did not alter the encoded amino acid (E/E) (Table 4.12). Homozygous C/C alleles associated with low or very low WFS and low LTT (25 out of 38 genotypes), whereas heterozygous C/T alleles were most common among genotypes with very high and high WFS and high LTT (22 out of 39; Fig. 4.23; Appendix 15).

4.11.6 Peroxisomal (S)-2-hydroxy-acid oxidase 3 (GLO3)

A peroxisomal (S)-2-hydroxy-acid oxidase 3 (GLO3) gene (*SECCE2Rv1G0121100.1*) located on chromosome 2R (804.568 Mb; Fig. 4.12) was targeted by marker Xuos643546 that was associated with WFS and FLN. The SNP variation (C/G) for *GLO3* was synonymous (T/T) (Table 4.12). Genotypes with low or very low WFS generally containing C/C alleles (22 out of 38), which also associated with low FLN values, whereas genotypes with very high or high WFS carried the C/G alleles (17 out of 39 genotypes; Fig. 4.23; Appendix 15).

4.11.7 Alpha-1,3-arabinosyltransferase-like (XAT3)

Marker Xuos448335 associated with WFS, FLN, and PGH (Table 4.12) corresponded to *SECCE6Rv1G0378210.1* that was located on chromosome 6R (69.896 Mb; Fig. 4.12). This particular gene codes for an alpha-1,3-arabinosyltransferase-like (XAT3) enzyme. In rice, *OsXAT3*

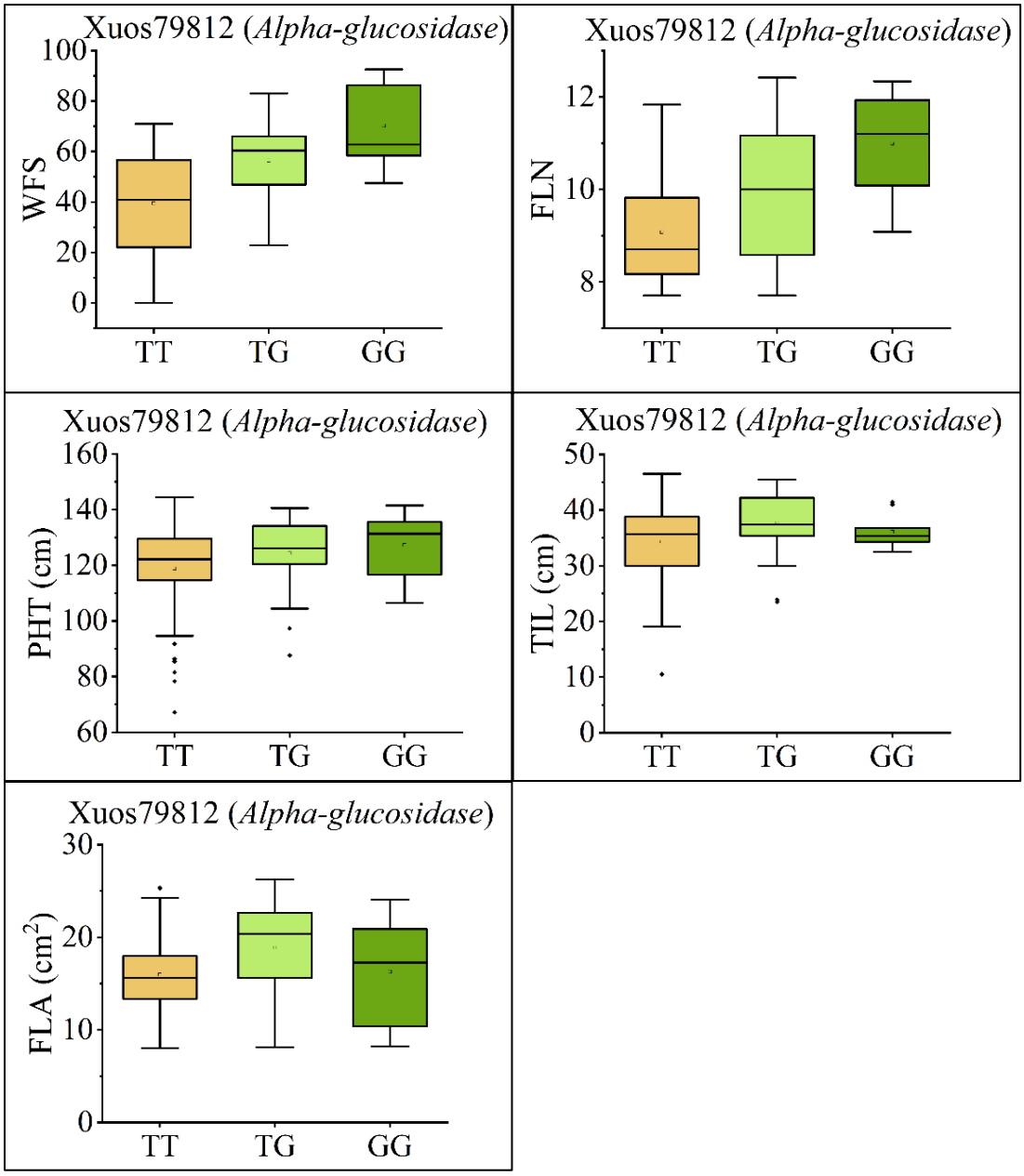

Fig. 4.22. Box-whisker plots showing the allele effects for the SNP marker (Xuos79812) ($p < 0.001$). The plots show median (horizontal bar), interquartile ranges (boxes), ranges (whiskers), and outliers (dots) for marker allele frequencies among the 96 rye genotypes.

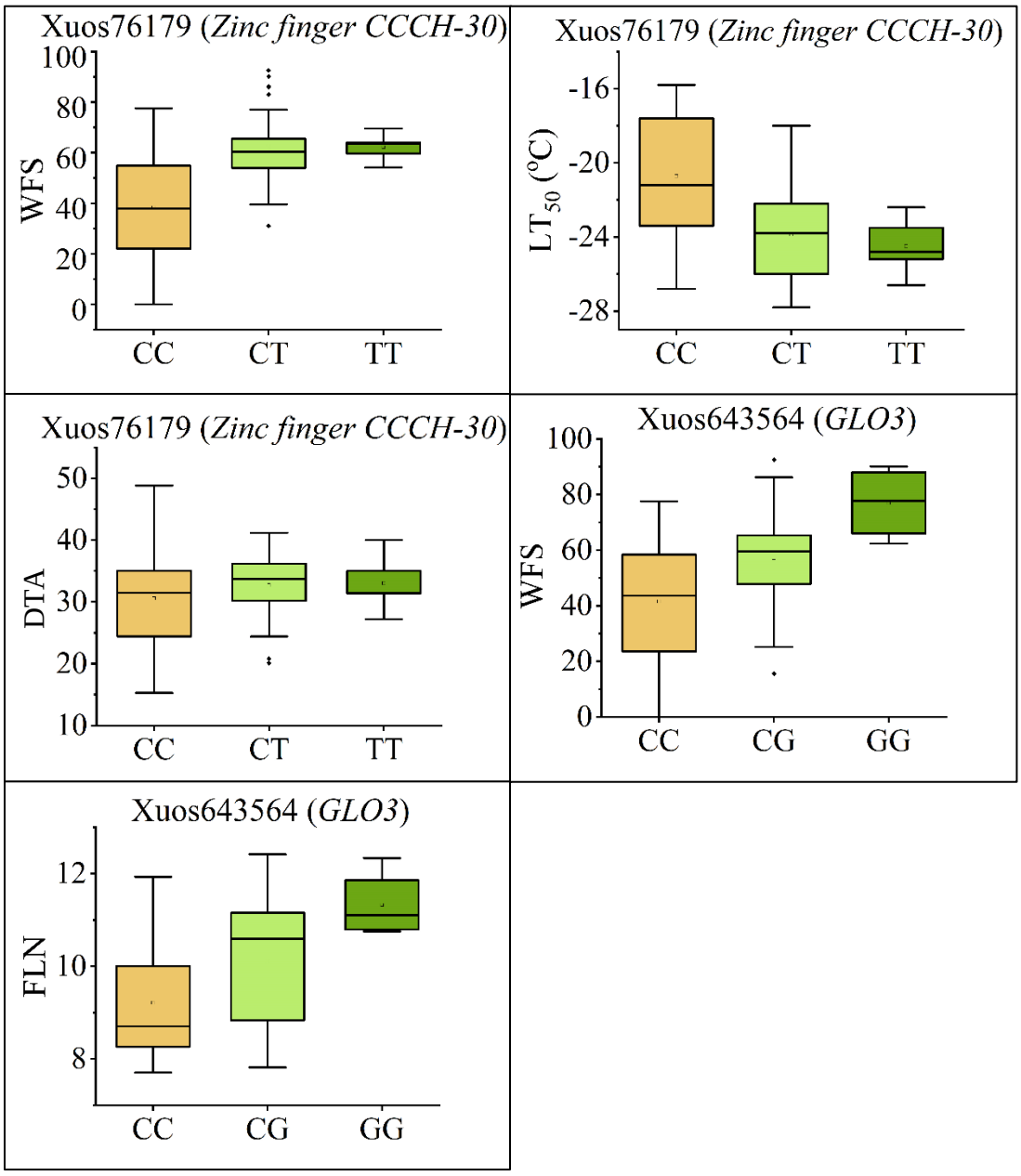

Fig. 4.23. Box-whisker plots showing the allele effects for the SNP markers (Xuos76179 and Xuos643564) ($p < 0.001$). The plots show median (horizontal bar), interquartile ranges (boxes), ranges (whiskers), and outliers (dots) for marker allele frequencies among the 96 rye genotypes.

is involved in xylan biosynthesis by transferring arabinosyl onto xylan located in the cell wall (Zhong *et al*., 2018). For the rye XAT3-like protein, the Xuos448335 SNP did not alter the encoded amino acid (S) (Table 4.12). Among the 38 rye genotypes with low or very low WFS, 27 carried homozygous G/G alleles. G/G variation was also associated with low FLN values (Fig. 4.24). Homozygous alleles (T/T) or heterozygous alleles (T/G) dominated among genotypes with very high and high WFS (22 out of 39 genotypes: Appendix 15). The T/T variant was also associated with high FLN values and PGH (Fig 4.24).

4.11.8 Tyrosine kinase (HCK)

Marker Xuos173426 associated with WFS and FLN (Table 4.12) was found to match *SECCE3Rv1G0206760.1* positioned on chromosome 3R (910.902 Mb; Fig. 4.12). The corresponding gene codes for a tyrosine kinase (HCK), involved in cellular defense responses to biotic and abiotic stresses (Miyamoto *et al*., 2019). Tyrosine phosphorylation plays a role in signal transduction, ABA and GA signaling (Ghelis *et al*., 2008; Fu *et al*., 2002), and cold stress-induced responses (Sangwan *et al*., 2001). The Xuos173426 SNP produced an S to R variation in the rye HCK protein (Table 4.12). Genotypes with low or very low WFS encoded only the S variant for HCK (26 out of 38), which was also associated with low FLN (Fig. 4.24). The R modification on HCK, or S/R variants were relatively common in genotypes with high or very high WFS (24 out of 39 genotypes: Appendix 15). R variant was also associated with high FLN values (Fig. 4.24).

4.11.9 Lecithin-cholesterol acyltransferase-like1 (LCAT1)

A SNP for WFS and PGH was carried by marker sequence Xuos176122 (Table 4.12), which mapped to chromosome 3R (152.406 Mb; Fig. 4.12), showed sequence identity to *SECCE3Rv1G0147470*.1, coding for a lecithin-cholesterol acyltransferase1 (LCAT1). The Xuos176122 SNP variation (A/G) did not cause an alteration in the encoded amino acid (L/L) (Table 4.12). Genotypes with low or very low WFS generally carried A/A alleles (23 out of 38), whereas heterozygous A/G alleles or homozygous G/G alleles were associated with high and very high WFS (33 out of 39 genotypes; Fig. 4.25; Appendix 15). Homozygous G/G alleles were also associated with PGH. High levels of the *AtLCAT-PLA* transcript were associated with root development and/or lipid metabolism in Arabidopsis (Chen *et al*. 2012).

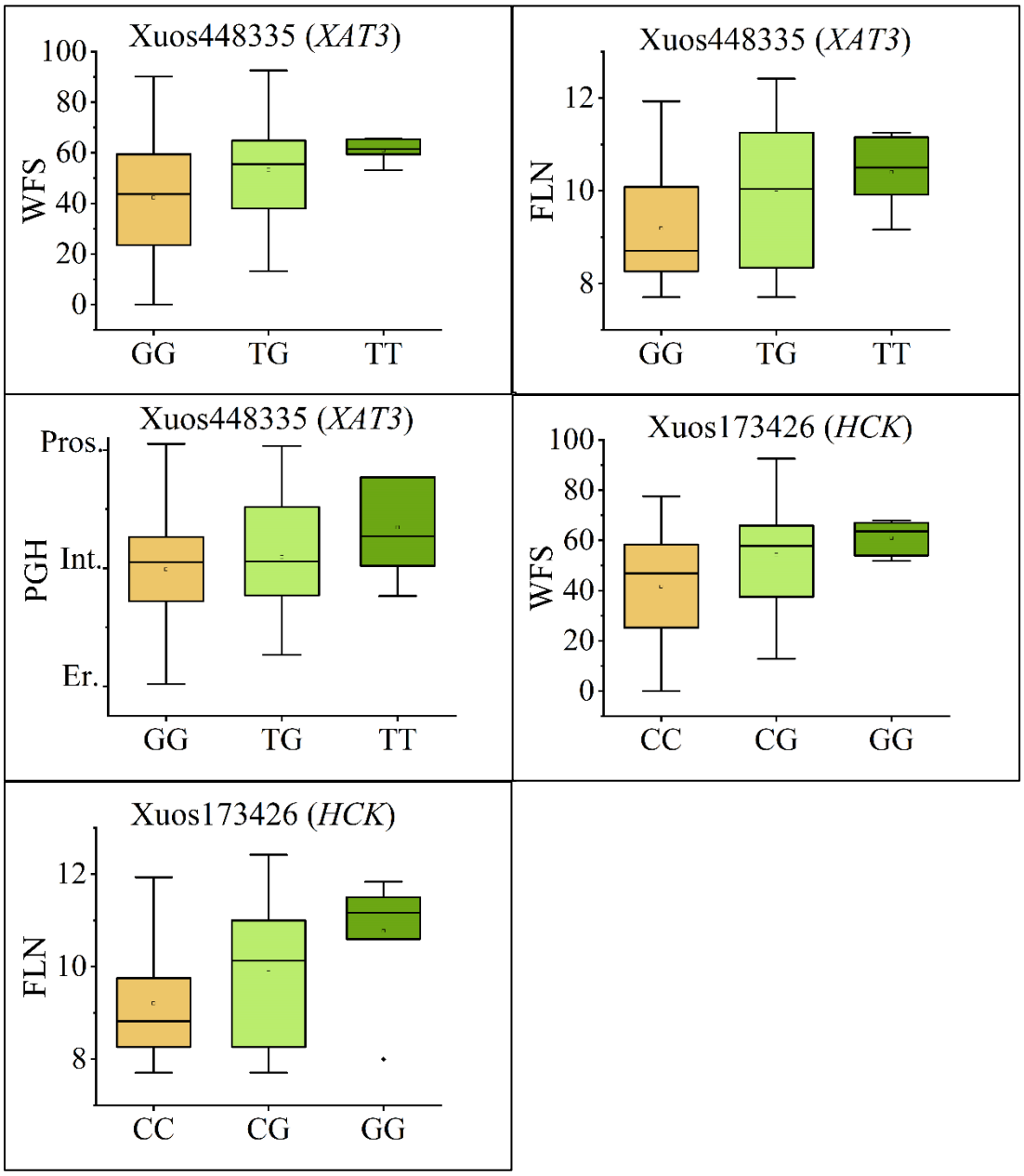

Fig. 4.24. Box-whisker plots showing the allele effects for the SNP markers (Xuos448335 and Xuos173426) ($p < 0.001$). The plots show median (horizontal bar), interquartile ranges (boxes), ranges (whiskers), and outliers (dots) for marker allele frequencies among the 96 rye genotypes.

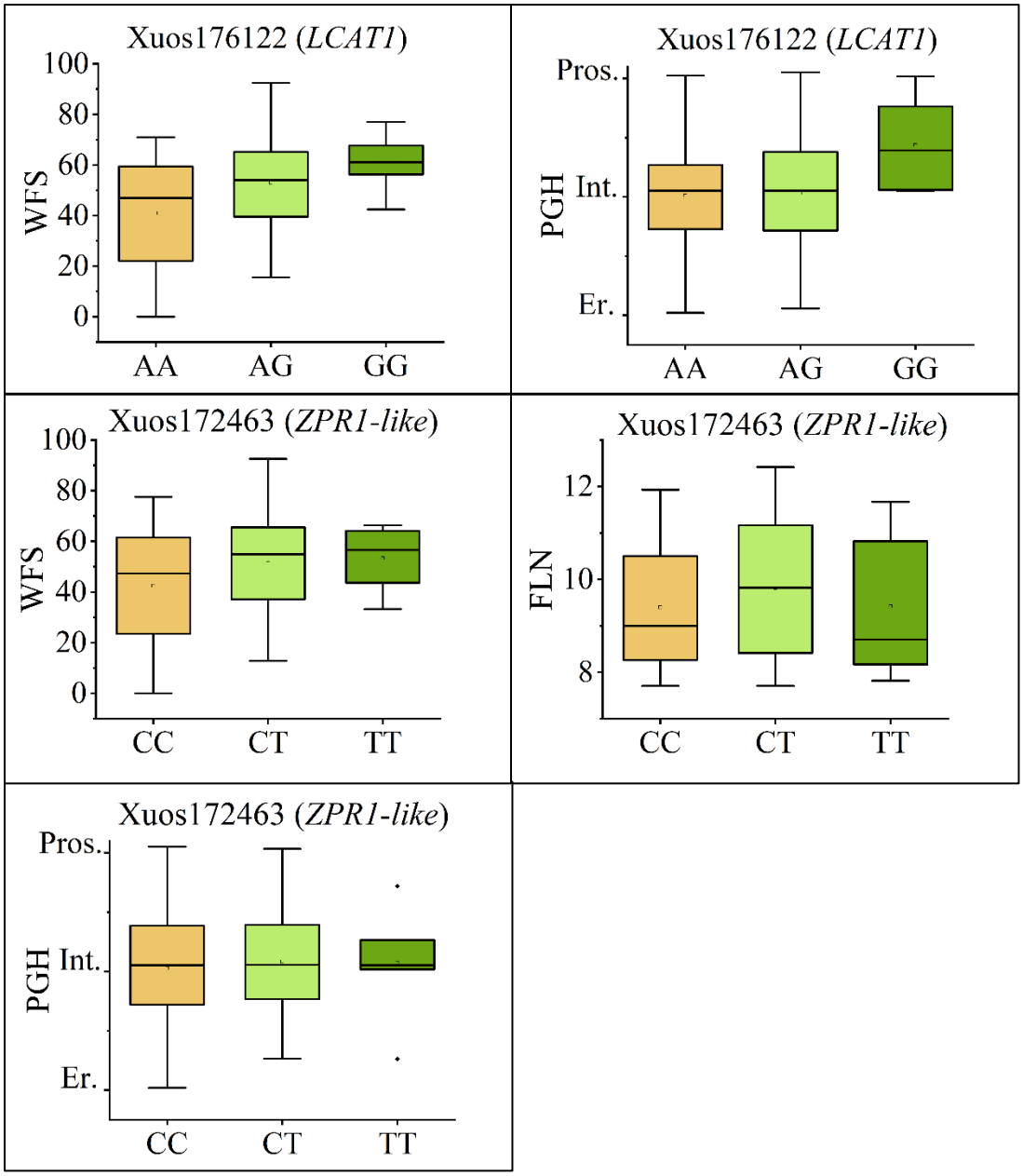

Fig. 4.25. Box-whisker plots showing the allele effects for the SNP markers (Xuos176122 and Xuos172463) ($p < 0.001$). The plots show median (horizontal bar), interquartile ranges (boxes), ranges (whiskers), and outliers (dots) for marker allele frequencies among the 96 rye genotypes.

4.11.10 Zinc finger protein1-like (ZPR1-like)

Marker Xuos172463 was found to be associated with WFS, FLN, and PGH (Table 4.12) and matched *SECCE3Rv1G0182130.1*, a zinc finger protein1-like (ZPR1-like) protein on chromosome 3R (622.648 Mb; Fig. 4.12). However, the SNP variation (C/T) did not cause and alterations in (N/N), the rye ZPR1-like protein sequence (Table 4.12). Homozygous C/C alleles were associated with low or very low WFS (22 out of 38 genotypes), whereas heterozygous C/T alleles or homozygous T/T were most common among genotypes with very high and high WFS (22 out of 39; Fig. 4.25; Appendix 15). C/T alleles also associated with high FLN values and intermediate growth habit (Fig 4.25).

4.11.12 Chemocyanin

Marker Xuos628254 associated with WFS and LTT (Table 4.12), matched to *SECCE2Rv1G0103040.*1, chemocyanin (named plantacyanin) that was positioned on chromosome 2R (586.360 Mb; Fig. 4.12). Plantacyanin is members of the blue copper protein family (phytocyanins). In Arabidopsis, plantacyanin affect anther development and pollination (Dong *et al*., 2005). The Xuos628254 SNP was the only SNP that caused the amino acid W to stop undergoing codon variation in the study (Table 4.12). Genotypes with low or very low WFS generally encoded plantacyanin containing W or W/stop combination (37 out of 38), which also associated with low LTT, whereas genotypes with very high or high WFS carried the heterozygous W/stop or homozygous stop alleles (23 out of 39 genotypes; Fig. 4.26; Appendix 15). Highest WFS also was associated with high LTT (Fig. 4.26).

4.11.13 MTAs located within intron or in untranslated regions

Marker Xuos417 was associated with five traits: WFS, LTT, FLN, PGH, and FLA (Appendix 14) and matched the *SECCE1Rv1G0060560.1*gene. The marker sequence (Xuos417) was located within an intron of an auxilin-like1 (AUXI1) protein located on chromosome 1R (710.523 Mb; Fig. 4.12). Auxin-like proteins, such as auxin like J-domain containing protein required for chloroplast accumulation response 1 (JAC1), regulate WEB1 (Kodama *et al*., 2010; Suetsugu *et al*., 2005). JAC1 was the first component characterized in the chloroplast movement pathway. Marker Xuos265567 associated with WFS, LTT, FLN, and PGH (Appendix 14). The

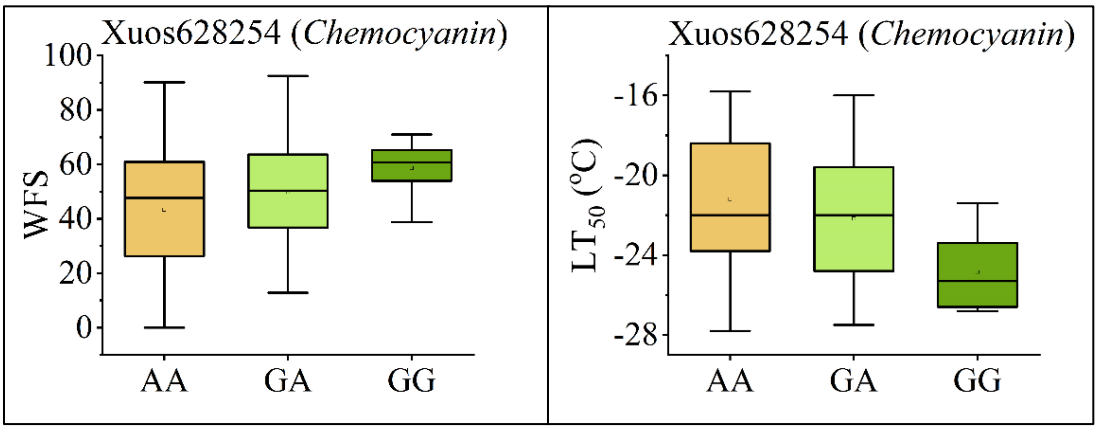

Fig. 4.26. Box-whisker plots showing the allele effects for the SNP marker (Xuos628254) ($p < 0.001$). The plots show median (horizontal bar), interquartile ranges (boxes), ranges (whiskers), and outliers (dots) for marker allele frequencies among the 96 rye genotypes.

Xuos265567 marker sequence was located within an intron of a chloroplast adenylosuccinate synthetase 2 gene (*SECCE4Rv1G0217460.1*; 4R: 16.372 Mb; Fig. 4.12), an enzyme that is responsible for conversion of inosine monophosphate to adenosine monophosphate.

The marker Xuos720939 was found to be associated with WFS, FLN, and TIL (Appendix 14) and targeted the gene, (*SECCE7Rv1G0470060.1*) on chromosome 7R (115.501 Mb; Fig. 4.12). The Xuos720939 sequence was located within an intron of *SECCE1Rv1G0061510.1* gene, code a hypothetical protein (from F-box family protein). Marker Xuos76850 was associated with both WFS and PGH (Appendix 14) and targeted *SECCE2Rv1G0122590.1*gene on chromosome 2R (817.543 Mb; Fig 4.12). However, the Xuos76850 marker sequence was located within an intron of a calcium-dependent protein kinase 13 gene, CPK13 (Appendix 14). Marker Xuos642015 was a significant marker for WFS, PHT, TIL, and PGH (Appendix 14) and matched with an unknown position in the *SECCEUnv1G0571650.1* gene (Fig. 4.12). The Xuos642015 sequence was located on 5'UTR of a cysteine protease, the ervatamin-B-like protease.

4.11.14 MTAs not matched with Lo7 rye annotated genes

Twenty-two markers did not coincide with the Lo7 rye annotated genes (Rabanus-Wallace *et al*., 2021); however, these markers were significantly (p <0.001) associated with WFS and developmental traits (Appendix 14). Among this group of markers, six SNP markers were associated with more than two traits: (1) marker Xuos116364 (4R 728.139 Mb; Fig. 4.12) associated with WFS, LTT, and FLN, (2) marker Xuos612117 (7R 20.212 Mb; Fig. 4.12) associated with WFS, FLN, and PGH, (3) marker Xuos622779 (2R 14.766 Mb; Fig. 4.12) associated with WFS, FLN, PGH, PHT, and TIL, (4) marker Xuos402617 (5R 539.107 Mb; Fig. 4.12) associated with WFS, LTT, and PGH, (5) marker Xuos384768 (5R 865.368 Mb; Fig. 4.12) associated with WFS, FLN, PGH, and PHT, and (6) marker Xuos1282135 (5R 670.509 Mb; Fig. 4.12) associated with WFS, LTT, FLN, and PGH. Five markers (Xuos279729, 4R 759.434 Mb; Xuos373243, 5R 643.250 Mb; Xuos445239, 6R 733.115 Mb; Xuos528556, 7R 36.717 Mb and Xuos649896, 6R 168.215 Mb; Fig. 4.12) were associated with WFS and LTT. Five other markers (Xuos403276, 5R 585.894 Mb; Xuos368592, 7R 715.871 Mb; Xuos444136, 5R 664.561 Mb; Xuos628639, 5R 571.246 Mb and Xuos678777, 4R 700.938 Mb; Fig. 4.12) were associated with WFS and FLN. Four markers (Xuos524545, 7R 549.121 Mb; Xuos623978, 2R 816.557 Mb; Xuos646081, 6R 636.699 and Xuos742711, 2R 37.358 Mb; Fig. 4.12) were associated with WFS

and PGH, and only two markers (Xuos681940, 1R 581.853 Mb and Xuos524450, position is unknown; Fig. 4.12) were associated with WFS, PHT, and TIL (Appendix 14).

4.12 Variation for CBF genes showed low significance for WFS in group 3

Variation for CBF genes encoded from *Fr-2* on group five chromosomes are generally associated with freezing tolerance in rye (Erath *et al*., 2017; Jung and Seo, 2019; Li *et al*., 2011*a*). In this study, five SNPs of relatively low significance levels ($p< 0.01$) targeted *CBF* genes (group 3 markers in Table 4.13 and Appendix 14). The three markers, associated with only WFS, were Xuos369733, Xuos390086, and Xuos370362, mapped to *SECCE5Rv1G0340540.1* (*CBFIIId-19*), *SECCE5Rv1G0340460.1* (*CBFIVa-2.2*), and *SECCE5Rv1G0340660.1* (*CBFIIIa-6.2*), respectively, (614.963-616.449 Mb chromosome 5R; Fig. 4.12 and Table 4.13). SNP in *TaCBFIa-CBFIIId-19* (Xuos369733) gene did not alter the encoded protein sequences (Table 4.13). Homozygous C/C alleles at SNP site were most common among genotypes with very low and low WFS (25 out of 38), whereas heterozygous C/T alleles were common among genotypes with high and moderate WFS (18 out of 39; Fig. 4.27; Appendix 15). SNP variation Xuos390086 altered a conserved H_{113} residue to P_{113} change (Tabl3 4.13) within AP2 DNA-binding region where variant residue was located immediately prior to signature motif on CBFIVa-2.2 (Båga *et al*., 2022). Genotypes with low or very low WFS generally containing C/C alleles (25 out of 38), whereas genotypes with very high or high WFS carried the A/C alleles (15 out of 39 genotypes; Fig.4.27; Appendix 15). SNP variation for *CBFIIIa-6* (Xuos370362*)* resulted in a L_{224} to H_{224} variation (Table 4.13) within the C-terminal region (Båga *et al*., 2022). Homozygous A/A alleles associated with low or very low WFS (25 out of 38 genotypes), whereas genotypes with very high or high WFS carried the T/A alleles (11 out of 39 genotypes; Fig. 4.27; Appendix 15). Two of the *CBF* genes were associated with DTA and FLN and mapped to chromosomes 2R (*TaCBFIa-11.2; SECCE2Rv1G0115950.1;* 759.179 Mb) and 4R (*CBFII-5; SECCE4Rv1G0278790.1*; 810.923 Mb; Fig. 4.12 and Table 4.13), respectively. SNP in *TaCBFIa-11.2* (Xuos76905) gene did not alter the encoded protein sequences (Table 4.13). Homozygous C/C alleles associated with early flowering (9 out of 96; Fig. 4.27; Appendix 15). The Xuos328096 SNP caused a R/P variation in the protein sequence (Table 4.13). Homozygous G/G alleles associated with low FLN (10 out of 96; Fig. 4.27; Appendix 15). Whether any of these non- synonymous amino acid substitutions affected the function encoded by, *CBFIVa-2.2*, *CBFIIIa-6* and *CBFII-5* remains to be demonstrated by

Table 4.13 Markers associated with CBF genes in group 3.

Marker ID[1/]	SNP[2/]	SNP position (bp)[3/]	*p*-value[4/]	R^2	MTA	Corresponding gene; protein	AA change
Xuos369733	C/T	Chr5:615295049	1.46E-03	1.50	Xuos369733_WFS	*SECCE5Rv1G0340540.1* C-repeat binding factor; (CBFIIId-19)	None (D/D)
Xuos390086	A/C	Chr5:614963367	2.84E-03	1.10	Xuos390086 _WFS	*SECCE5Rv1G0340460.1* C-repeat binding factor; (CBFIVa-2.2)	H/P
Xuos370362	T/A	Chr5:616448826	3.57E-03	0.87	Xuos370362_WFS	*SECCE5Rv1G0340660.1* C-repeat binding factor (CBFIIIa-6.2)	L/H
Xuos76905	C/T	Chr2:759179281	6.67E-03	0.74	Xuos76905 _DTA	*SECCE2Rv1G0115950.1* C-repeat factor; (CBFIa-11.2)	None (D/D)
Xuos328096	G/C	Chr4:810923109	7.24E-03	1.20	Xuos328096_FLN	*SECCE4Rv1G0278790.1* C-repeat factor; (CBFII-5)	R/P

1/ Number refers to matching rye Lo7_v2_scaffold number (Bauer *et al*. 2017).
2/ Reference/alternative allele.
3/ Position on rye Lo7 pseudomolecules version 1 assembly (Rabanus-Wallace *et al*. 2021).
4/ Calculated upon Bonferroni correction.

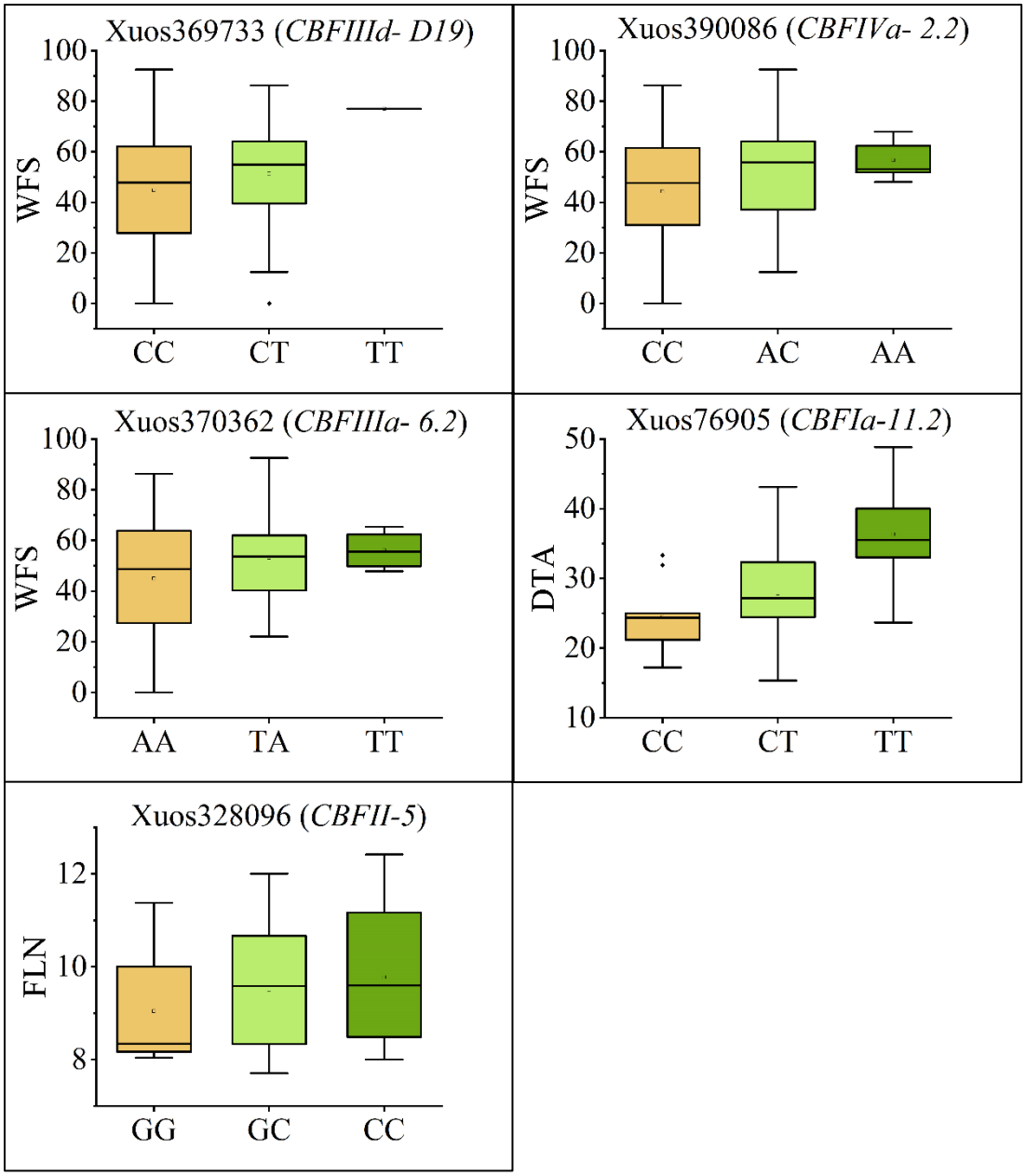

Fig. 4.27. Box-whisker plots showing the allele effects for the SNP markers (Xuos369733, Xuos390086, Xuos370362, Xuos76905 and Xuos328096) ($p < 0.01$). The plots show median (horizontal bar), interquartile ranges (boxes), ranges (whiskers), and outliers (dots) for marker allele frequencies among the 96 rye genotypes.

additional studies. A preference for the SNP alleles encoding the alternative alleles for *CBFIIId-19*, *CBFIVa-2.2*, and *CBFIIIa-6* was found for genotypes with low or very low WFS (Appendix 15).

4.13 Biplot analysis supports WFS and associated traits are controlled by several common genes.

A PCA bi-plot constructed for the six traits analyzed in the group 1 revealed that PC1 explained large trait variation (47.6 to 57.8%) followed by PC2 (9.7 to 11.9%) in the different plots (Figs. 4.28 – 4.33). Seven vectors representing SNP markers for candidate genes *IRIP1*, *COR413-PM*, *FRL4*-like, *JAR1*, *ICE1*, *BIPP2C1*, and *CHUP1* were visualized for each of the LTT, FLN, PGH, PHT and TIL plots. The first six vectors correlated relatively well with each other and contributed mainly to PC1, whereas *CHUP1* vector was mainly associated with PC2. *IRIP1*, *COR413-PM*, *FRL4-like*, *ICE1*, *BIPP2C1*, *CHUP1*, and *JAR1* were also represented as vectors for WFS, but *JAR1* and *CHUP1* vectors did not group with the other five vectors. WFS was also displayed by two additional vectors (markers Xuos527421, Xuos615123; Appendix 14) corresponding to GA2ox-D11 and EXLA genes, respectively (Fig. 4.28) grouped with the *IRIP1*, *COR413-PM*, *FRL4*-like, *ICE1*, and *BIPP2C1* vectors. Distinction for *JAR1* vector may reflect the very complex regulation of the gene by light quality (red/far-red ratio), other phytohormone-signaling pathways, and involvement in both abiotic and biotic stress responses (Chen *et al*., 2015; Wasternack and Song, 2017). Thus, *JAR1* is likely to have several roles during and after cold acclimation. *CHUP1* role in fine-tuning of light signals and/or regulating signaling pathways leading to photoinhibition protection (Wilson and Ruban, 2020) might be a reason for the distinction of this vector.

4.14 Identification of SNP markers associated with anthocyanins and WFS

From the 10,244 SNP markers, MLM revealed 144 SNP markers and 175 MTAs were significantly associated ($p < 0.001$) with anthocyanins. Ninety-seven markers (67.4%) were associated with leaf-extracted anthocyanidins, and 47 markers (32.6%) were associated with crown-extracted anthocyanidins (Appendix 16). All but seven markers could be placed on a *de novo* assembled Lo7 genomic map of rye (Rabanus-Wallace *et al*., 2021) as shown in Fig 4.34. In total, an FDR cut-off ($p < 0.05$) revealed that 39 SNPs (group 1) were strongly and significantly

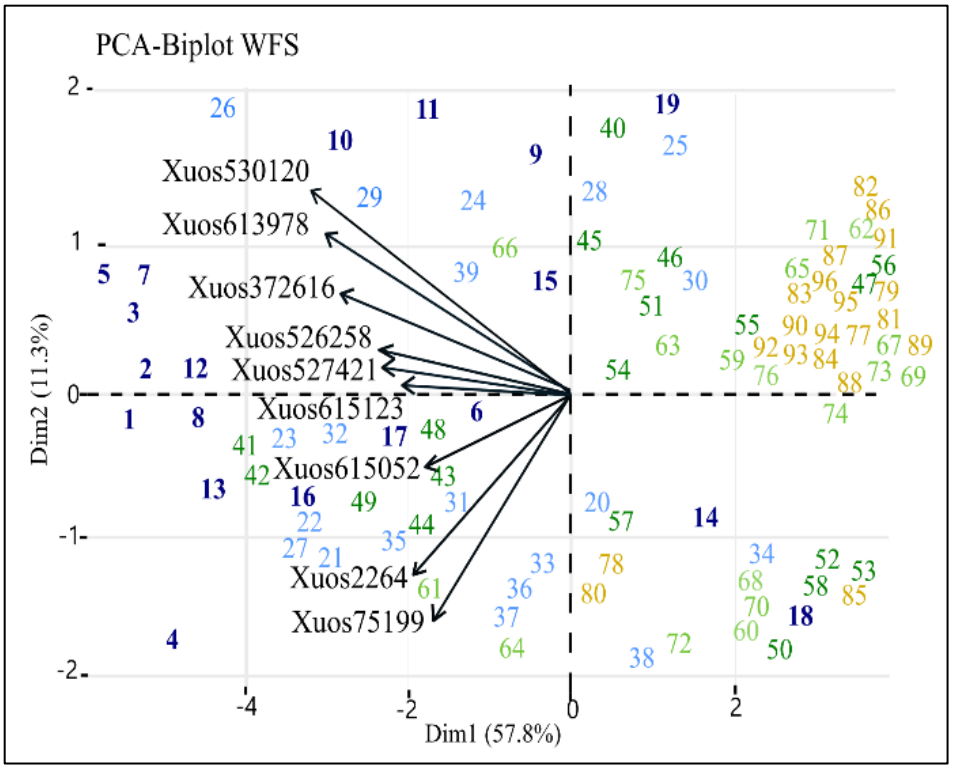

Fig. 4.28. PCA biplot visualizing the effect of SNPs WFS analyzed for rye population of 96 genotypes.

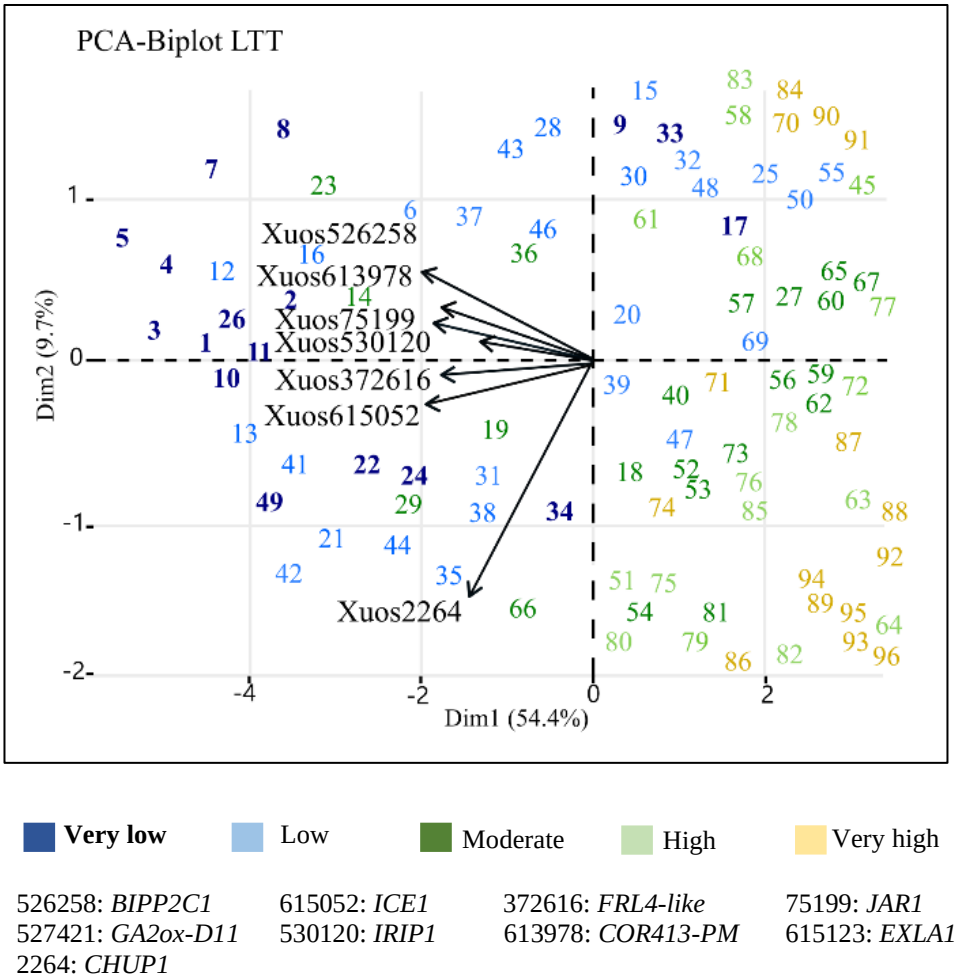

Fig. 4.29. PCA biplot visualizing the effect of SNPs on LTT analyzed for rye population of 96 genotypes.

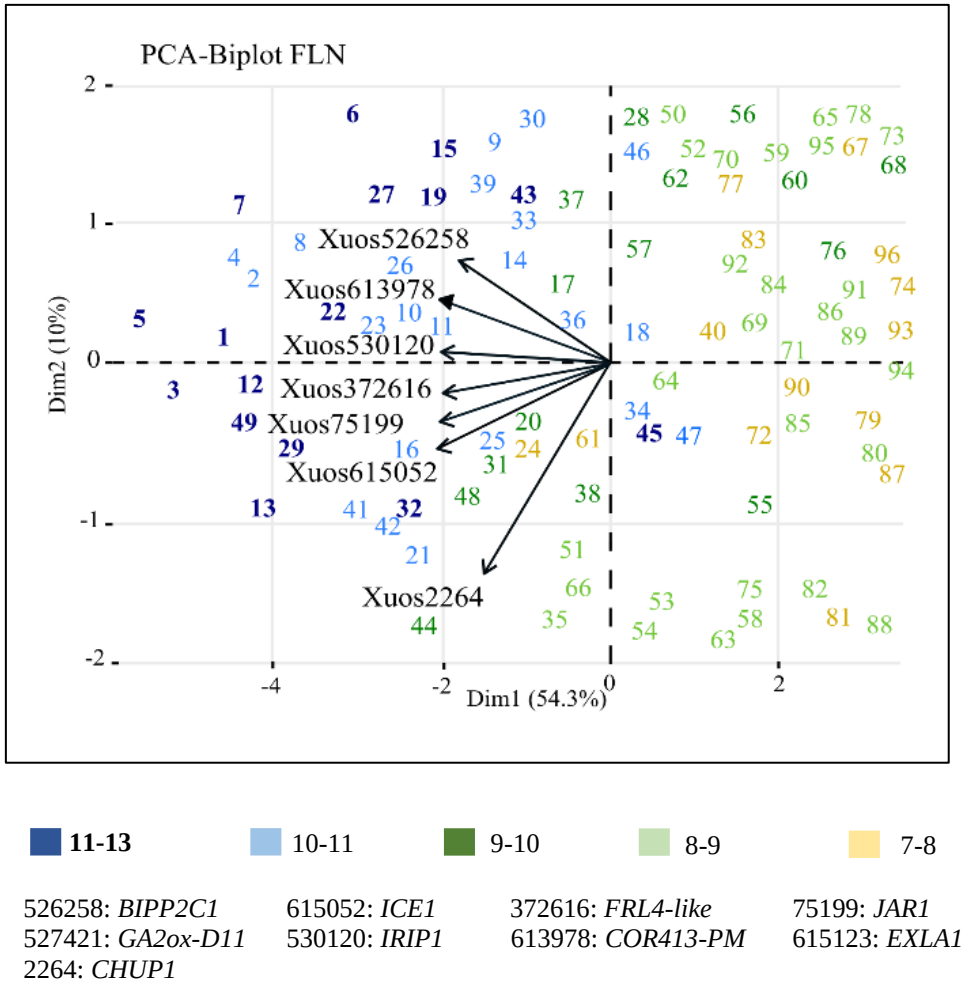

Fig. 4.30. PCA biplot visualizing the effect of SNPs on FLN analyzed for rye population of 96 genotypes.

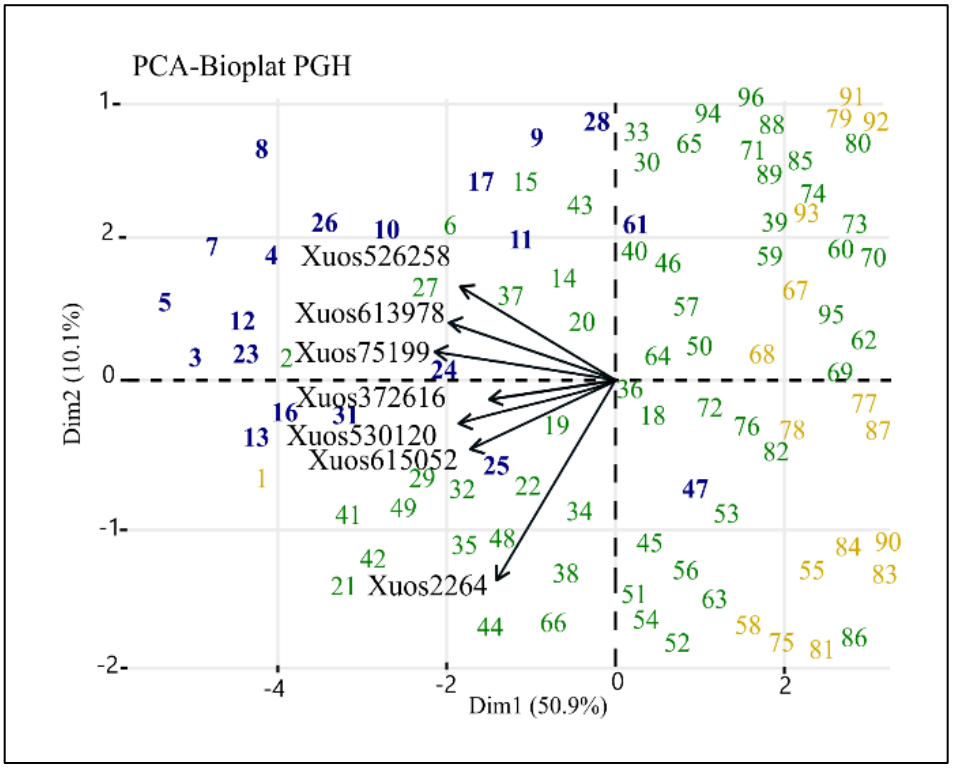

Fig. 4.31. PCA biplot visualizing the effect of SNPs on PGH analyzed for rye population of 96 genotypes.

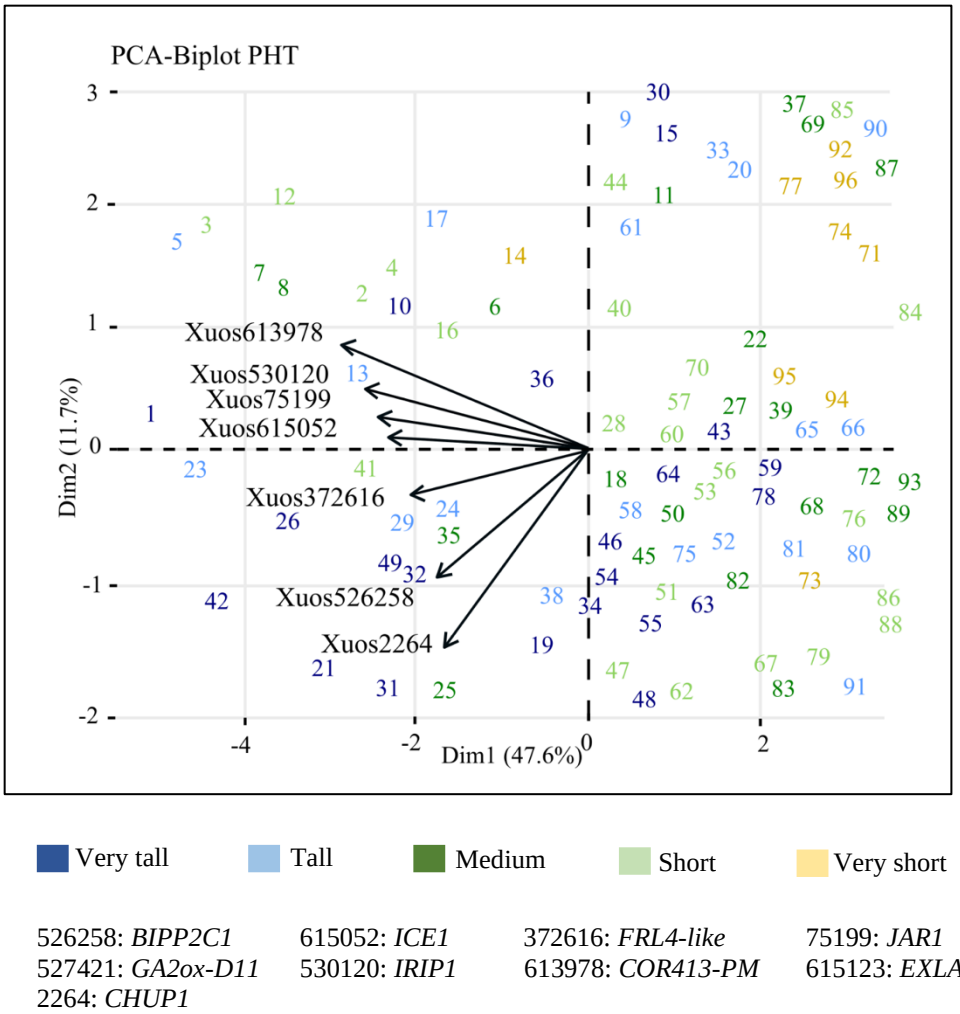

Fig. 4.32. PCA biplot visualizing the effect of SNPs on PHT analyzed for rye population of 96 genotypes.

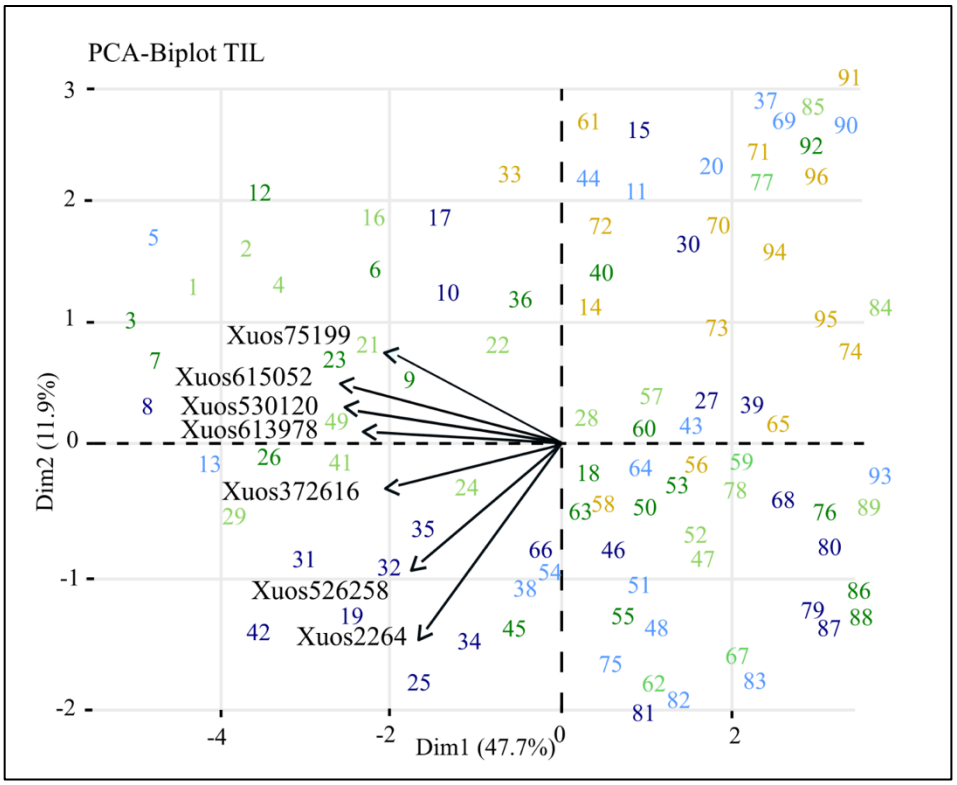

Fig. 4.33. PCA biplot visualizing the effect of SNPs on TIL analyzed for rye population of 96 genotypes.

($p < 2.76e-04$) associated with 66 MTAs and matched with 29 Lo7 rye annotated genes (Appendix 16). The second group of 105 SNPs ($p < 0.001$) were associated with 107 MTAs and matched with 17 Lo7 rye annotated genes. 56.10% of the group 1 and 84.11% of the group 2 SNPs matched to repetitive elements or non-transcribed regions, thus, group 2 contained a higher frequency of false-positive SNPs and were given lower consideration in the study. The 144 SNPs identified were distributed on all seven rye chromosomes, with the highest number mapping to chromosomes 7R (n = 28), 2R (n = 23), and 5R (n = 21), respectively (Fig 4.34 and Appendix 16). All seven rye chromosomes had SNP markers associated with the cyanidin, delphinidin, and pelargonidin groups of anthocyanins (Fig 4.34), except chromosome 6R, which showed no SNP associated with pelargonidins (Fig 4.34). The highest number of MTA involved cyanidins (109 out of 144, 75.7%; Appendix 16), and among these Pet-3-Rut, accounted for 31 (28.4%), Cya-3-Glc for 24 (22.0%), and Cya-3-Rut for 21 (19.3%). Two-thirds of the markers (Appendix 16) were associated with leaf extracted cyanidins (75 out of 109, 68.8%) and only one-third were associated with crown extracted cyanidins (34 out of 109, 32.2%). Chromosomes 7R, 2R, and 6R had the highest number of markers associated with cyanidins (20, 16, and 14, respectively), but all the seven rye chromosomes had SNP markers associated with anthocyanins and WFS. Twenty-six SNP markers were associated with both WFS and anthocyanins (Appendix 16). Chromosome 2R had the highest number of SNPs associated with WFS and anthocyanins (n=6) followed by chromosomes 7R (n=5) and 6R (n=4). Production of eleven different glycosylated anthocyanins associated with increased WFS (Table 4.14). Cyanidins shared most markers with WFS (23 out of 109, 21.1 %; Table 4.14 and Appendix 16), suggesting that the cyanidins may be genetically linked with WFS. Among the cyanidins, Cya-3-Glc (9 out of 23, 39.1%), followed by Cya-3-Rut (6 out of 23, 26.1%) shared most markers with WFS. Interestingly, none of the markers associated with anthocyanins and LTT.

A match to the coding region of genes was found for 31 of the 144 (21.52%) SNPs, and among these 10 SNP variations (6.94%) caused amino acid replacements in predicted gene products. Among the target genes for SNPs were genes encoding phenylpropanoid pathway enzymes, transcription factors (zinc finger and bHLH proteins), glucosyltransferases, protein kinases and phosphatases, DNA, and RNA modification enzymes (Appendix 16). In group 1, 22 of the SNP markers were mapped to exons of different genes (Appendix 16). For seven of the target genes, non-synonymous amino acid replacements were predicted for encoded proteins

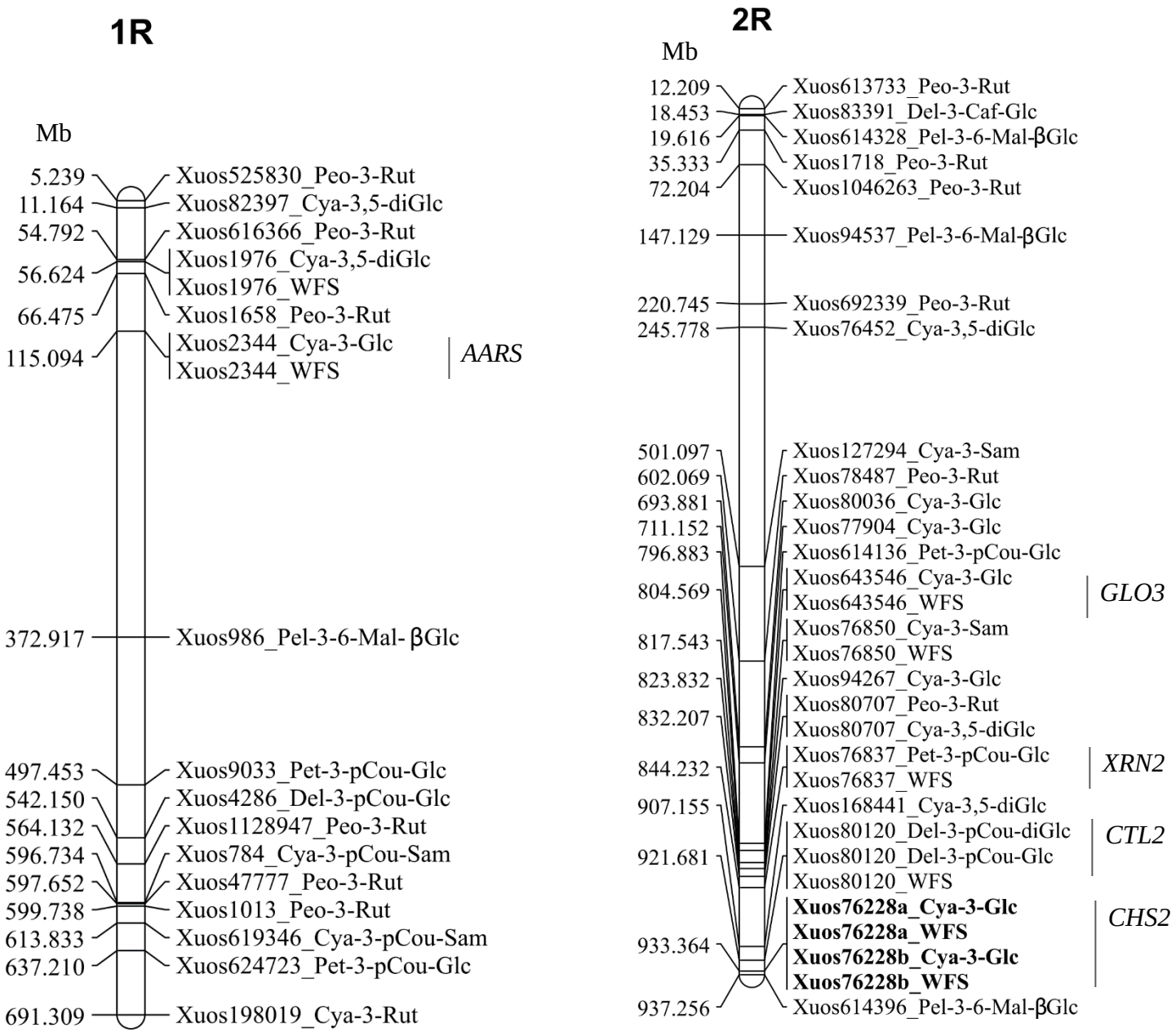
1R
Mb
5.239
11.164
54.792
56.624
66.475
115.094
372.917
497.453
542.150
564.132
596.734
597.652
599.738
613.833
637.210
691.309
Xuos525830_Peo-3-Rut
Xuos82397_Cya-3,5-diGlc
Xuos616366_Peo-3-Rut
Xuos1976_Cya-3,5-diGlc
Xuos1976_WFS
Xuos1658_Peo-3-Rut
Xuos2344_Cya-3-Glc
Xuos2344_WFS
AARS
Xuos986_Pel-3-6-Mal-βGlc
Xuos9033_Pet-3-pCou-Glc
Xuos4286_Del-3-pCou-Glc
Xuos1128947_Peo-3-Rut
Xuos784_Cya-3-pCou-Sam
Xuos47777_Peo-3-Rut
Xuos1013_Peo-3-Rut
Xuos619346_Cya-3-pCou-Sam
Xuos624723_Pet-3-pCou-Glc
Xuos198019_Cya-3-Rut
2R
Mb
12.209
18.453
19.616
35.333
72.204
147.129
220.745
245.778
501.097
602.069
693.881
711.152
796.883
804.569
817.543
823.832
832.207
844.232
907.155
921.681
933.364
937.256
Xuos613733_Peo-3-Rut
Xuos83391_Del-3-Caf-Glc
Xuos614328_Pel-3-6-Mal-βGlc
Xuos1718_Peo-3-Rut
Xuos1046263_Peo-3-Rut
Xuos94537_Pel-3-6-Mal-βGlc
Xuos692339_Peo-3-Rut
Xuos76452_Cya-3,5-diGlc
Xuos127294_Cya-3-Sam
Xuos78487_Peo-3-Rut
Xuos80036_Cya-3-Glc
Xuos77904_Cya-3-Glc
Xuos614136_Pet-3-pCou-Glc
Xuos643546_Cya-3-Glc
Xuos643546_WFS
GLO3
Xuos76850_Cya-3-Sam
Xuos76850_WFS
Xuos94267_Cya-3-Glc
Xuos80707_Peo-3-Rut
Xuos80707_Cya-3,5-diGlc
Xuos76837_Pet-3-pCou-Glc
Xuos76837_WFS
XRN2
Xuos168441_Cya-3,5-diGlc
Xuos80120_Del-3-pCou-diGlc
Xuos80120_Del-3-pCou-Glc
Xuos80120_WFS
CTL2
Xuos76228a_Cya-3-Glc
Xuos76228a_WFS
Xuos76228b_Cya-3-Glc
Xuos76228b_WFS
CHS2
Xuos614396_Pel-3-6-Mal-βGlc

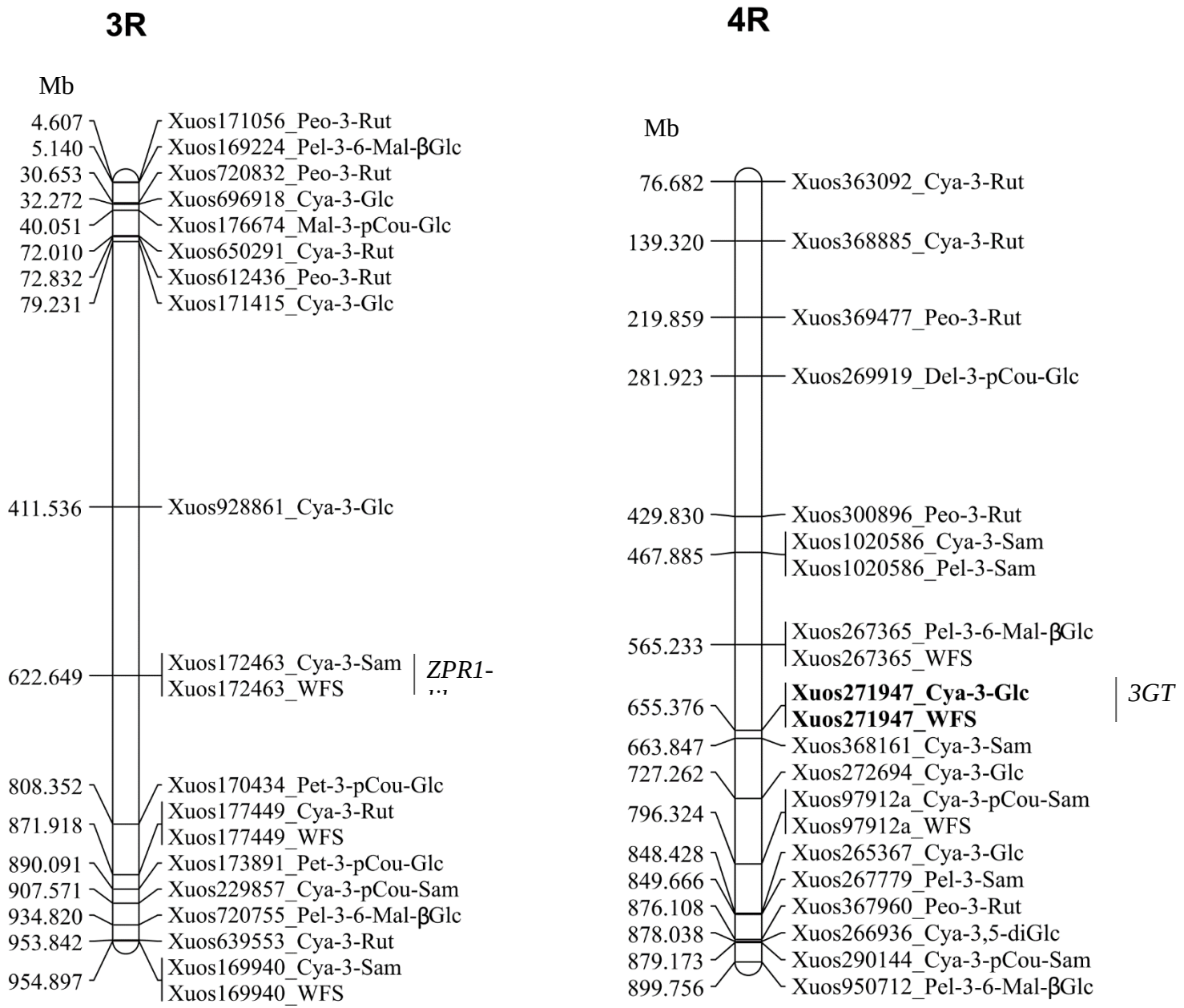
3R
Mb
4.607
5.140
30.653
32.272
40.051
72.010
72.832
79.231
Xuos171056_Peo-3-Rut
Xuos169224_Pel-3-6-Mal-βGlc
Xuos720832_Peo-3-Rut
Xuos696918_Cya-3-Glc
Xuos176674_Mal-3-pCou-Glc
Xuos650291_Cya-3-Rut
Xuos612436_Peo-3-Rut
Xuos171415_Cya-3-Glc
411.536
Xuos928861_Cya-3-Glc
622.649
Xuos172463_Cya-3-Sam
Xuos172463_WFS
ZPR1-
808.352
871.918
890.091
907.571
934.820
953.842
954.897
Xuos170434_Pet-3-pCou-Glc
Xuos177449_Cya-3-Rut
Xuos177449_WFS
Xuos173891_Pet-3-pCou-Glc
Xuos229857_Cya-3-pCou-Sam
Xuos720755_Pel-3-6-Mal-βGlc
Xuos639553_Cya-3-Rut
Xuos169940_Cya-3-Sam
Xuos169940_WFS
4R
Mb
76.682
139.320
219.859
281.923
429.830
467.885
565.233
655.376
663.847
727.262
796.324
848.428
849.666
876.108
878.038
879.173
899.756
Xuos363092_Cya-3-Rut
Xuos368885_Cya-3-Rut
Xuos369477_Peo-3-Rut
Xuos269919_Del-3-pCou-Glc
Xuos300896_Peo-3-Rut
Xuos1020586_Cya-3-Sam
Xuos1020586_Pel-3-Sam
Xuos267365_Pel-3-6-Mal-βGlc
Xuos267365_WFS
Xuos271947_Cya-3-Glc
Xuos271947_WFS
3GT
Xuos368161_Cya-3-Sam
Xuos272694_Cya-3-Glc
Xuos97912a_Cya-3-pCou-Sam
Xuos97912a_WFS
Xuos265367_Cya-3-Glc
Xuos267779_Pel-3-Sam
Xuos367960_Peo-3-Rut
Xuos266936_Cya-3,5-diGlc
Xuos290144_Cya-3-pCou-Sam
Xuos950712_Pel-3-6-Mal-βGlc

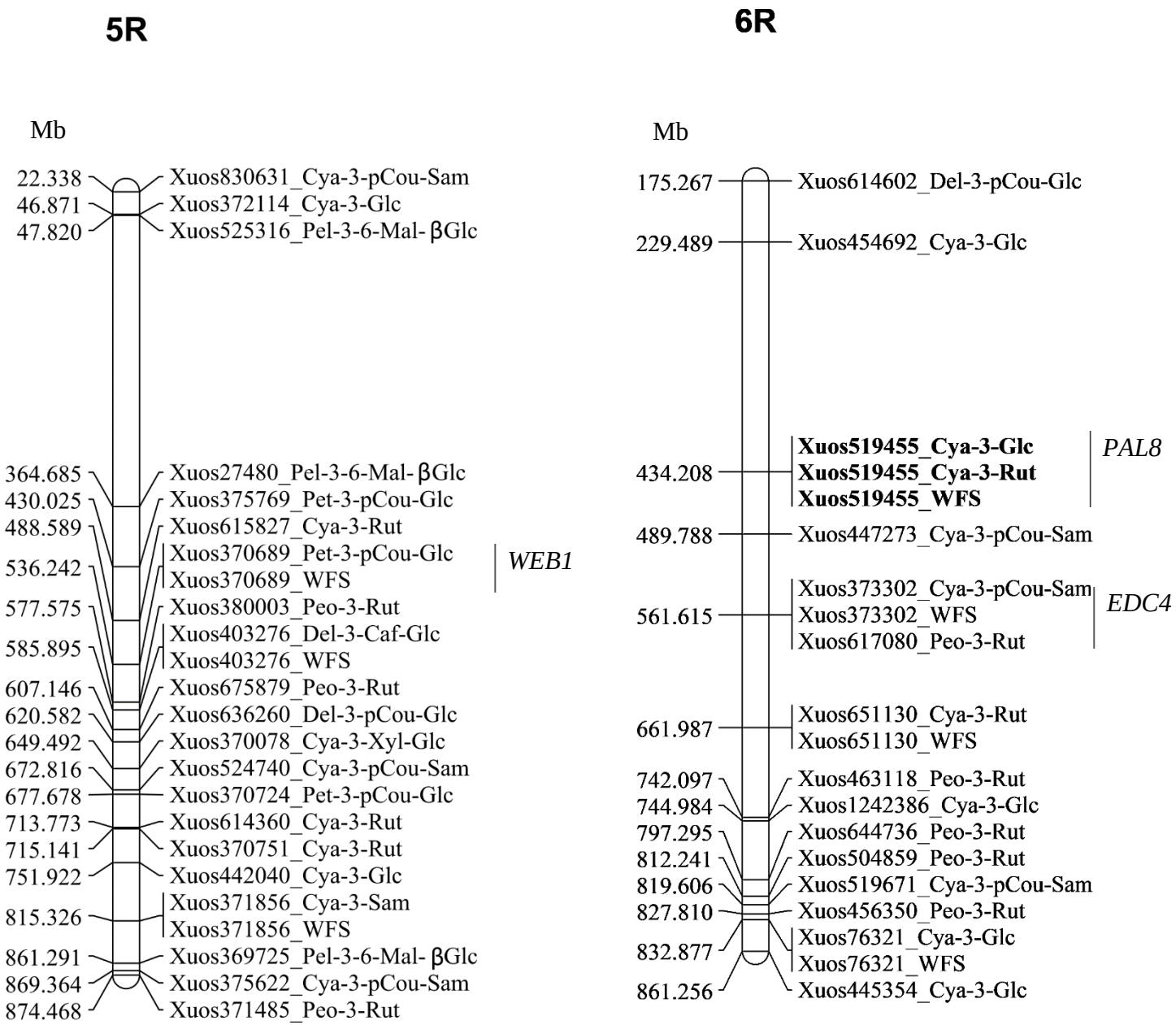
5R
Mb
22.338
46.871
47.820
Xuos830631_Cya-3-pCou-Sam
Xuos372114_Cya-3-Glc
Xuos525316_Pel-3-6-Mal-βGlc
364.685
430.025
488.589
536.242
577.575
585.895
607.146
620.582
649.492
672.816
677.678
713.773
715.141
751.922
815.326
861.291
869.364
874.468
Xuos27480_Pel-3-6-Mal-βGlc
Xuos375769_Pet-3-pCou-Glc
Xuos615827_Cya-3-Rut
Xuos370689_Pet-3-pCou-Glc
Xuos370689_WFS
Xuos380003_Peo-3-Rut
Xuos403276_Del-3-Caf-Glc
Xuos403276_WFS
Xuos675879_Peo-3-Rut
Xuos636260_Del-3-pCou-Glc
Xuos370078_Cya-3-Xyl-Glc
Xuos524740_Cya-3-pCou-Sam
Xuos370724_Pet-3-pCou-Glc
Xuos614360_Cya-3-Rut
Xuos370751_Cya-3-Rut
Xuos442040_Cya-3-Glc
Xuos371856_Cya-3-Sam
Xuos371856_WFS
Xuos369725_Pel-3-6-Mal-βGlc
Xuos375622_Cya-3-pCou-Sam
Xuos371485_Peo-3-Rut
WEB1
6R
Mb
175.267
229.489
434.208
489.788
561.615
661.987
742.097
744.984
797.295
812.241
819.606
827.810
832.877
861.256
Xuos614602_Del-3-pCou-Glc
Xuos454692_Cya-3-Glc
Xuos519455_Cya-3-Glc
Xuos519455_Cya-3-Rut
Xuos519455_WFS
Xuos447273_Cya-3-pCou-Sam
Xuos373302_Cya-3-pCou-Sam
Xuos373302_WFS
Xuos617080_Peo-3-Rut
Xuos651130_Cya-3-Rut
Xuos651130_WFS
Xuos463118_Peo-3-Rut
Xuos1242386_Cya-3-Glc
Xuos644736_Peo-3-Rut
Xuos504859_Peo-3-Rut
Xuos519671_Cya-3-pCou-Sam
Xuos456350_Peo-3-Rut
Xuos76321_Cya-3-Glc
Xuos76321_WFS
Xuos445354_Cya-3-Glc
PAL8
EDC4

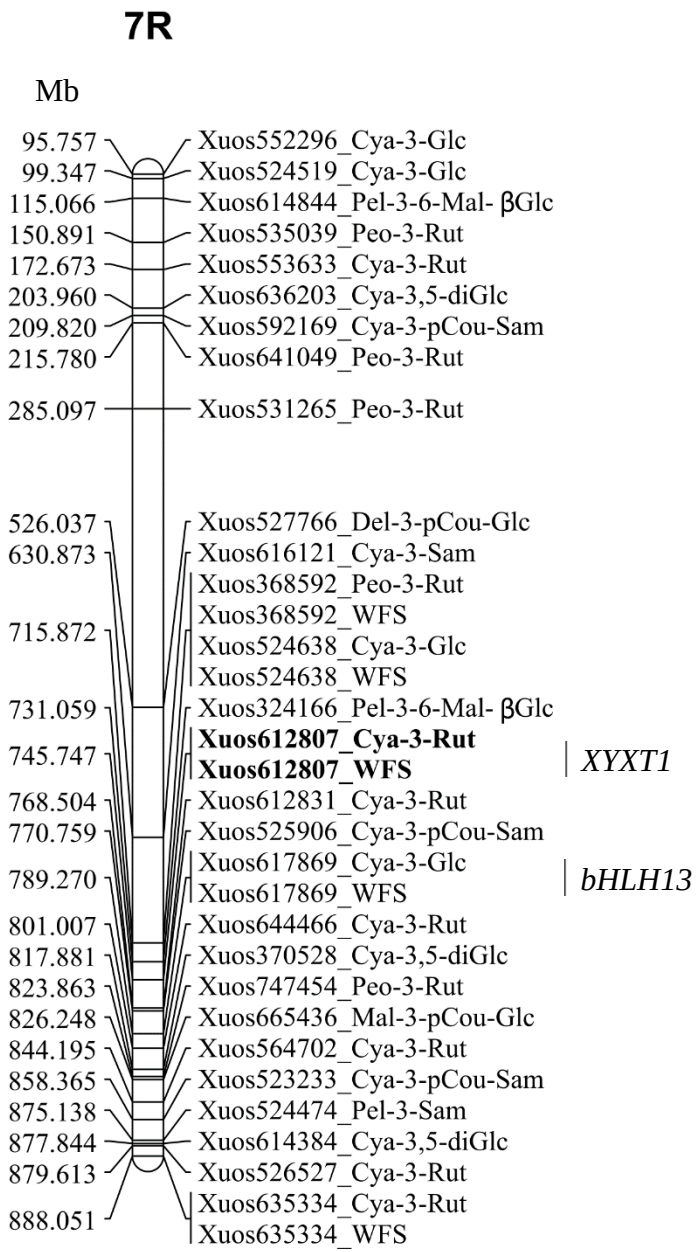

Fig. 4.34 Location of significant markers for anthocyanins identified on rye physical map. Locations refers to the 2021 Lo7 genome assembly (Rabanus-Wallace *et al*., 2021). Most significant markers (p < 2.76e-04; Tables 4.15; 4.16) are indicated in bold and location of candidate genes discussed are shown.

Table 4.14 Number of shared SNP markers between WFS and anthocyanins.

Cyanidins	Number of markers Shared with WFS	Delphinidins	Number of markers Shared with WFS	Pelargonidins	Number of markers Shared with WFS
Cya-3-Glc	9	Pet-3-*p*Cou-Glc	2	Pel-3-6-Mal-βGlc	1
Cya-3-Rut	6	Del-3-*p*Cou-Glc	1	Pel-3-Glc	0
Cya-3-Sam	4	Del-3-Caf-Glc	1	Pel-3-Sam	0
Cya-3-*p*Cou-Sam	2	Del-3-*p*Cou-diGlc	1		
Cya-3,5-diGlc	1	Mal-3-*p*Cou-Glc	0		
Peo-3-Rut	1				
Cya-3-Sam-5-Glc	0				
Cya-3-AcGlc-5-Glc	0				
Cya-3-Xyl-Glc	0				
Cya-*p*Cou-diGlc	0				
Total	23	Total	5	Total	1

(Appendix 16). Sixteen group 1 SNPs were associated with WFS and anthocyanins (Table 4.15) and corresponded to 15 Lo7 rye annotated genes (Rabanus-Wallace *et al*., 2021)

4.15 Most significant MTA related to anthocyanins, WFS and developmental traits

Sixteen of the group 1 SNPs associated with WFS and anthocyanins, matched with Lo7 rye genes (Tables 4.15 and 4.16). The SNPs were mapped to exons of 15 different genes. For seven of the target genes, non-synonymous amino acid replacements were predicted for encoded proteins. The SNP markers, Xuos519455, Xuos76228a, Xuos217947, Xuos370689, Xuos2344, Xuos643564, Xuos617869 Xuos76837, Xuos651130, Xuos373302, Xuos267565, Xuos80120 and Xuos172463 showed allelic dominance for WFS, whereas overdominance allelic effects were shown for the three remaining markers, Xuos76228b, Xuos612807, and Xuos524362. Eleven of these SNP markers showed allelic dominance for cyanidins; however, the remaining four SNP markers (Xuos267365, Xuos370689, Xuos524368, and Xuos617869) showed overdominance allelic effects (Fig. 4.35-4.38).

4.15.1 Enzymes of the phenylpropanoid pathway

Four SNP markers Xuos519455, Xuos76228a, Xuos76228b, and Xuos271947 in group 1 were associated with WFS and cyanidins group of anthocyanins and coincided with genes encoding phenylpropanoid pathway enzymes (Table 4.15). Sequence variations for genes encoding phenylalanine ammonia-lyase (PAL) and chalcone synthase (CHS) both enzymes in the phenylpropanoid pathway, were strongly associated with WFS in the rye population, but not with developmental traits (Table 4.15; Appendix 16). Marker Xuos519455 matched coding region of a PAL8 gene (SECCE6Rv1G0399250.1) located on chromosome 6R (434.208 Mb; Fig 4.34) and two markers (Xuos76228a and Xuos76228b) matched coding region of CHS2 gene (SECCE2Rv1G0140890.1) on chromosome 2R (933.364 Mb; Fig 4.34; Table 4.15). PAL is the first enzyme in the general phenylpropanoid pathway (Appendix 17) and catalyzes channeling of L-Phe from the primary metabolism to the synthesis of trans-cinnamic acid (Cochrane et al., 2004). This enzymatic step constitutes the starting point for several polyphenol compounds such as flavonols, stilbenes, lignin, and anthocyanins in plants (Zhang and Liu, 2015). The Xuos519455 SNP variation caused a F291/I291 variation in PAL8 polypeptide, where the I291 variant was common in genotypes with low and very low WFS (35 out of 38), but very rare in genotypes with

Table 4.15 Markers associated with phenylpropanoid pathway enzymes and WFS identified in the study.

Marker ID[1/]	SNP[2/]	SNP position (bp)[3/]	*p*-value[4/]	R^2	MTA	Corresponding gene; protein	AA change
Xuos519455	T/A	Chr6:434208137	2.29E-06	24.4	Xuos519455_Cya-3-Glc	*SECCE6Rv1G0399250.1*	F/I
			2.34E-06	24.3	Xuos519455_Cya-3-Rut	Phenylalanine ammonia-lyase 8;	
			1.10E-04	13.1	Xuos519455_WFS	(PAL8)	
Xuos76228a	C/G	Chr2:933364022	3.46E-06	23.7	Xuos76228a_Cya-3-Glc	*SECCE2Rv1G0140890.1*	Q/E
			1.39E-04	14.5	Xuos76228a_WFS	Chalcone synthase 2; (CHS2)	A/V
Xuos76228b	C/T	Chr2:933364022	3.79E-06	23.5	Xuos76228b_Cya-3-Glc		
			1.44E-04	13.4	Xuos76228b_WFS		
Xuos271947	G/C	Chr4:655375479	5.58E-06	22.9	Xuos271947_Cya-3-Glc	*SECCE4Rv1G0256300.1*	D/E
			1.99E-04	11.9	Xuos271947_WFS	Anthocyanidin 3-O-glucosyl-transferase; (3GT)	

[1/] Number refers to matching rye Lo7_v2_scaffold number (Bauer *et al*. 2017).
[2/] Reference/alternative allele.
[3/] Position on rye Lo7 pseudomolecules version 1 assembly (Rabanus-Wallace *et al.* 2021).
[4/] Calculated upon Bonferroni correction.

high and very high WFS (18 out of 39; Appendix 18). Genotypes encoding I_{291} for PAL8 had overall the least amount of cyanidin accumulation in leaves and crowns (Fig. 4.35). CHS2 acts downstream of PAL and diverts compounds away from the general phenylpropanoid pathway towards flavonoids (Appendix 17) by catalyzing condensation of three malonyl-CoA molecules with one 4-coumaroylCoA molecule to form naringenin chalcone (Heller and Hahlbrock, 1980). The Xuos76228a SNP caused a Q_{79}/E_{79} variation and Xuos76228b an A_{104}/V_{104} variation for the predicted rye CHS2 from translated *SECCE2Rv1G0140890.1* (Table 4.15). The two SNPs are not in phase with each other, suggesting the SNPs target two different *CHS2* genes. Genes encoding CHS2 with the Q_{79} and A_{104} variations were generally found for rye genotypes with low and very low WFS (34 out of 38 genotypes), which was also associated with low cyanidin accumulation (Fig. 4.35). In contrast, 16 out of 19 genotypes with very high WFS suggested presence of CHS2 (E_{79}/V_{104}) allele variants (Appendix 18). High cyanidin accumulation was associated with E_{79}/V_{104} modifications for CHS2 (Fig. 4.35). Both *PAL8* and *CHS2* genes in Arabidopsis are cold-inducible in a light-dependent manner (Leyva *et al*., 1995).

Two additional WFS SNP markers colocalized with genes encoding two additional enzymes of the phenylpropanoid pathway. SNP marker Xuos271947 was mapped to 655.375 Mb on chromosome 4R matched the *SECCE4Rv1G0256300.1* (Fig 4.34). Marker Xuos271947 coincides with the gene that encodes anthocyanidin 3-O-glucosyltransferase (3GT) and the G/C SNP caused D/E variation in rye 3GT protein sequence (Table 4.15). Among 38 rye genotypes with low or very low WFS, 33 carried *3GT* alleles encoding only the D *3GT* variation (Appendix18), and it was associated with low cyanidin accumulation (Fig. 4.35). Homozygous alleles encoding the E or alleles encoding both variants (D/E) dominated among genotypes with very high and high WFS (23 out of 39 genotypes; Fig. 4.35; Appendix 18). Besides high WFS, the 3GT variant was also associated with high cyanidin accumulation (Fig. 4.35). *3GT* gene is similar to Bronze-1 (*BZ1*) a UDP glucose-flavonoid 3-O-glucosyltransferase found in maize (Klein *et al*., 1989). UDP glucose-flavonoid 3-O-glucosyltransferase catalyzes the final step in the phenylpropanoid pathway that glycosylates anthocyanidin and produces anthocyanin pigments (Appendix 17; Yoshihara *et al*., 2005).

Marker Xuos626519 was located within an intron of a 4-coumarate-CoAligase-like 4 gene (4CL4; *SECCE5Rv1G0367660*; 5R 825.076 Mb; Appendix 14), whose product catalyzes conversion of *p*-coumarate to 4-coumaroyl-CoA. The marker Xuos626519 was associated with

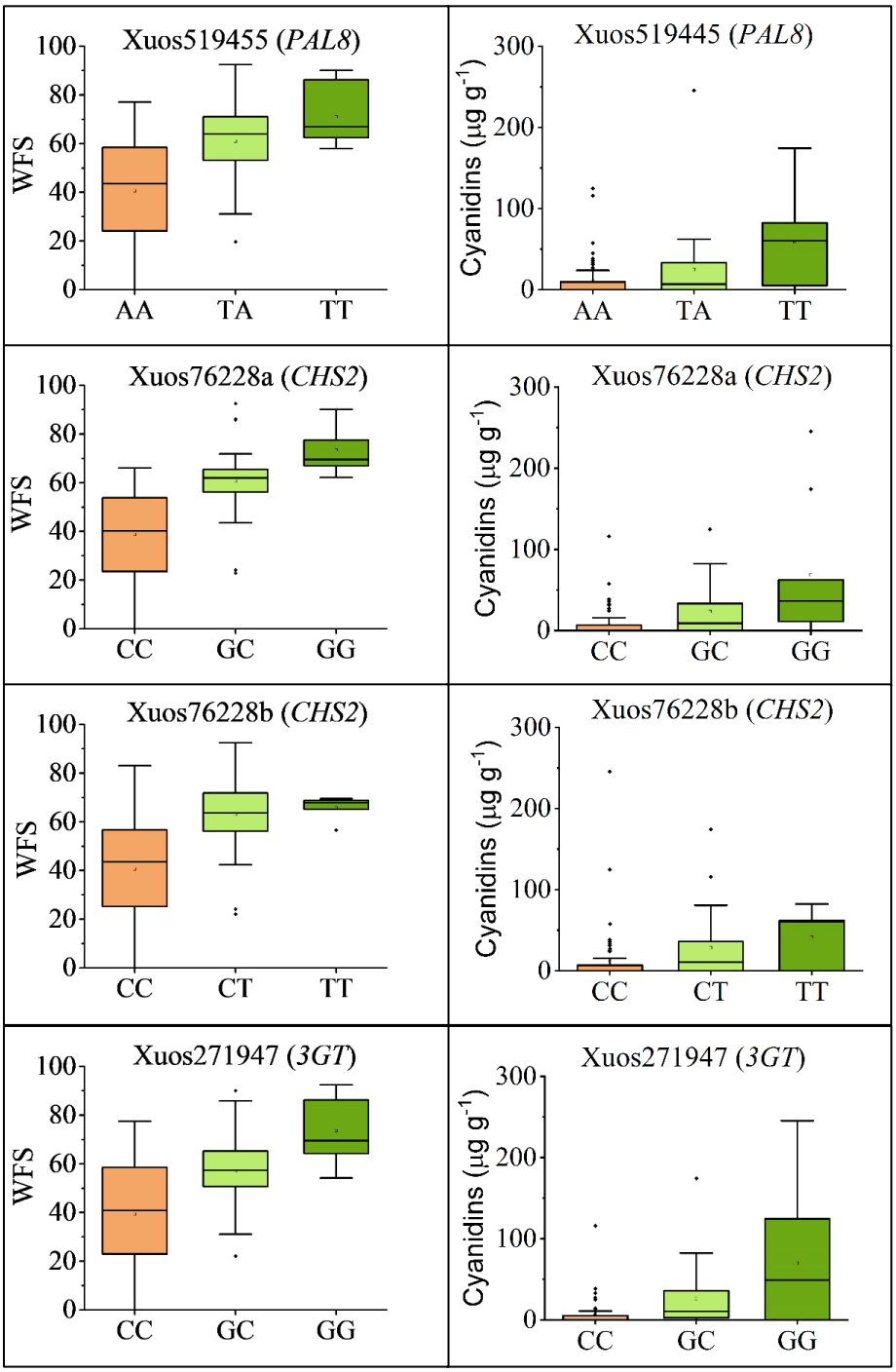

Fig. 4.35. Box-whisker plots showing the allele effects for the SNP markers (Xuos519455, Xuos76228a, Xuos76228b, and Xuos271947) (p < 2.76e-04). The plots show median (horizontal bar), interquartile ranges (boxes), ranges (whiskers), and outliers (dots) for marker allele frequencies among the 96 rye genotypes.

WFS and PGH but not with anthocyanins.

4.15.2 Markers associated with WFS and anthocyanins

Twelve SNPs in group 1 did not correspond to the genes involved in phenylpropanoid pathway; however, these eleven were associated with anthocyanins and WFS. Three SNP markers (Xuos612807, Xuos76837, and Xuos617869), were predicted to have non-synonymous amino acid replacements for the encoded proteins (Table 4.16). The SNP Xuos612807 associated with Cya-3-Rut and WFS and mapped on chromosome 7R (745.747 Mb; Fig. 4.34) corresponded to *SECCE7Rv1G0506080.1* (Table 4.16). The encoded protein showed identity to a β-1,2-xylosyltransferase1 (*XYXT1*). The G/A SNP variation for rye *XYXT1*was predicted to cause a P/L substitution (Table 4.16). Genotypes with low or very low WFS generally encoded XYXT1 containing the P/L combination (27 out of 38 genotypes; Appendix 18), which also was associated with low cyanidin accumulation (Fig. 4.36). XYXT1 associated with high and very high WFS showed the presence of both alleles (22 out of 39 genotypes; Appendix 18), but the L allele showed the highest association with high WFS and cyanidins accumulation. (Fig. 4.36). β1,2-Xylosyltransferase is responsible for the biosynthesis of N-glycoproteins and formation of heterogenous plant specific N-glycan structures (Jung *et al*., 2021). N-glycans are involved in protein folding and final structure determination. N-Glycosylation takes place in the endoplasmic reticulum (ER) and Golgi apparatus (Kajiura *et al*., 2012).

The SNP marker, Xuos76837, located on chromosome 2R (844.232 Mb *SECCE2Rv1G0125920.1*; Fig. 4.34) was associated with Pet-3-*p*Cou-Glc and WFS (Table 4.16). The Xuos76837 SNP variation (A/C) caused an L/R change in exoribonuclease-2-like (XRN2) polypeptide sequence (Table 4.16). XRN2 is involved in the processing of chloroplast rRNA and affects the photosynthetic apparatus in Arabidopsis (Mermigka *et al*., 2016). Among 38 rye genotypes with low or very low WFS, 26 carried *XRN2* alleles that encoded only the L variation (Appendix 18). The L *XRN2* variation was also associated with low cyanidin accumulation (Fig. 4.36). Homozygous alleles encoding the R or alleles encoding both variants (L/R) were dominant among genotypes with very high and high WFS (22 out of 39 genotypes: Appendix 18). Also, the *XRN2* R variant was associated with high cyanidins accumulation (Fig. 4. 36).

Marker Xuos617869 was associated with both WFS and Cya-3-Glc (Table 4.16) and corresponded to *SECCE7Rv1G0510370.1* located on chromosome 7R (789.269 Mb; Fig. 4.34).

Table 4.16 Most significant markers associated with anthocyanins and WFS identified in the study.

Marker ID[1/]	SNP[2/]	SNP position (bp)[3/]	*p*-value[4/]	R^2	MTA	Corresponding gene; protein	AA change
Xuos370689	A/G	Chr5:536242435	5.01E-06	23.1	Xuos370689_Pet-3-pCou-Glc	*SECCE5Rv1G0331080.1*	None (R/R)
			1.55E-04	13.3	Xuos370689_WFS	Weak chloroplast movement under blue light1; (WEB1)	
Xuos2344	A/G	Chr1:115094206	7.53E-06	22.4	Xuos2344_Cya-3-Glc	*SECCE1Rv1G0014530.1*	None (Y/Y)
			2.46E-04	13.6	Xuos2344_WFS	Histidine-tRNA ligase	
Xuos643546	C/G	Chr2:804568836	9.29E-06	22.1	Xuos643546_Cya-3-Glc	*SECCE2Rv1G0121100.1*	None (T/T)
			2.86E-04	11.2	Xuos643546_WFS	Peroxisomal (S)-2-hydroxy-acid oxidase-3; (GLO3)	
Xuos267365	T/A	Chr4:565232643	1.09E-05	21.8	Xuos267365_Pel-3-6-Mal-βGlc	*SECCE4Rv1G0247970.1*	None (A/A)
			3.21E-04	12.9	Xuos267365_WFS	Embryogenesis transmembrane protein-like	
Xuos617869	C/G	Chr7:789269736	1.32E-05	21.5	Xuos617869_Cya-3-Glc	*SECCE7Rv1G0510370.1*	Q/H
			3.30E-04	10.9	Xuos617869_WFS	Basic helix-loop-helix 133; (bHLH133)	
Xuos80120	G/A	Chr2:921680798	1.42E-05	21.3	Xuos80120_Del-3-pCou-diGlc	*SECCE2Rv1G0138460.1*	None (I/I)
			1.59E-05	21.2	Xuos80120_Del-3-pCou-Glc	Choline transporter-related protein 2 (CTL2)	
			3.35E-04	10.8	Xuos80120_WFS		
Xuos612807	G/A	Chr7:745747023	1.86E-05	20.9	Xuos612807_Cya-3-Rut	*SECCE7Rv1G0506080.1*	P/L
			3.38E-04	12.8	Xuos612807_WFS	Beta-1,2-xylosyltransferase1 -like (XYXT1-like)	
Xuos76837	A/C	Chr2:844232302	2.12E-05	20.7	Xuos76837_Pet-3-pCou-Glc	*SECCE2Rv1G0125920.1*	L/R
			3.42E-04	12.8	Xuos76837_WFS	Exoribonuclease-2; (XRN2)	
Xuos651130	T/C	Chr6:661987036	2.35E-05	20.5	Xuos651130_Cya-3-Rut	*SECCE6Rv1G0418290.1*	None (S/S)
			3.65E-04	12.6	Xuos651130_WFS	Serine-rich protein	
Xuos524368	A/G	ChrUn:72921231	2.80E-05	20.2	Xuos524368_Cya-3-Rut	*SECCEUnv1G0538500.1*	None (T/T)
			3.66E-04	11.4	Xuos524368_WFS	Methyltransferase	
Xuos373302	T/C	Chr6:561615373	3.34E-05	19.9	Xuos373302_Cya-3-pCou-Sam	*SECCE6Rv1G0407680.1*	None (D/D)
			3.89E-04	12.5	Xuos373302_WFS	Enhancer of mRNA-decapping protein 4; (EDC4)	
Xuos172463	C/T	Chr3: 622648676	8.53E-05	18.25	Xuos172463_Cya-3-Sam	*SECCE3Rv1G0182130.1*	None (N/N)
			4.80E-04	10.11	Xuos172463_WFS	Zinc finger protein; ZPR1-like (ZPR1-like)	

[1/] Number refers to matching rye Lo7_v2_scaffold number (Bauer *et al*. 2017); [2/] Reference/alternative allele; [3/] Position on rye Lo7 pseudomolecules version 1 assembly (Rabanus-Wallace *et al.* 2021); [4/] Calculated upon Bonferroni correction.

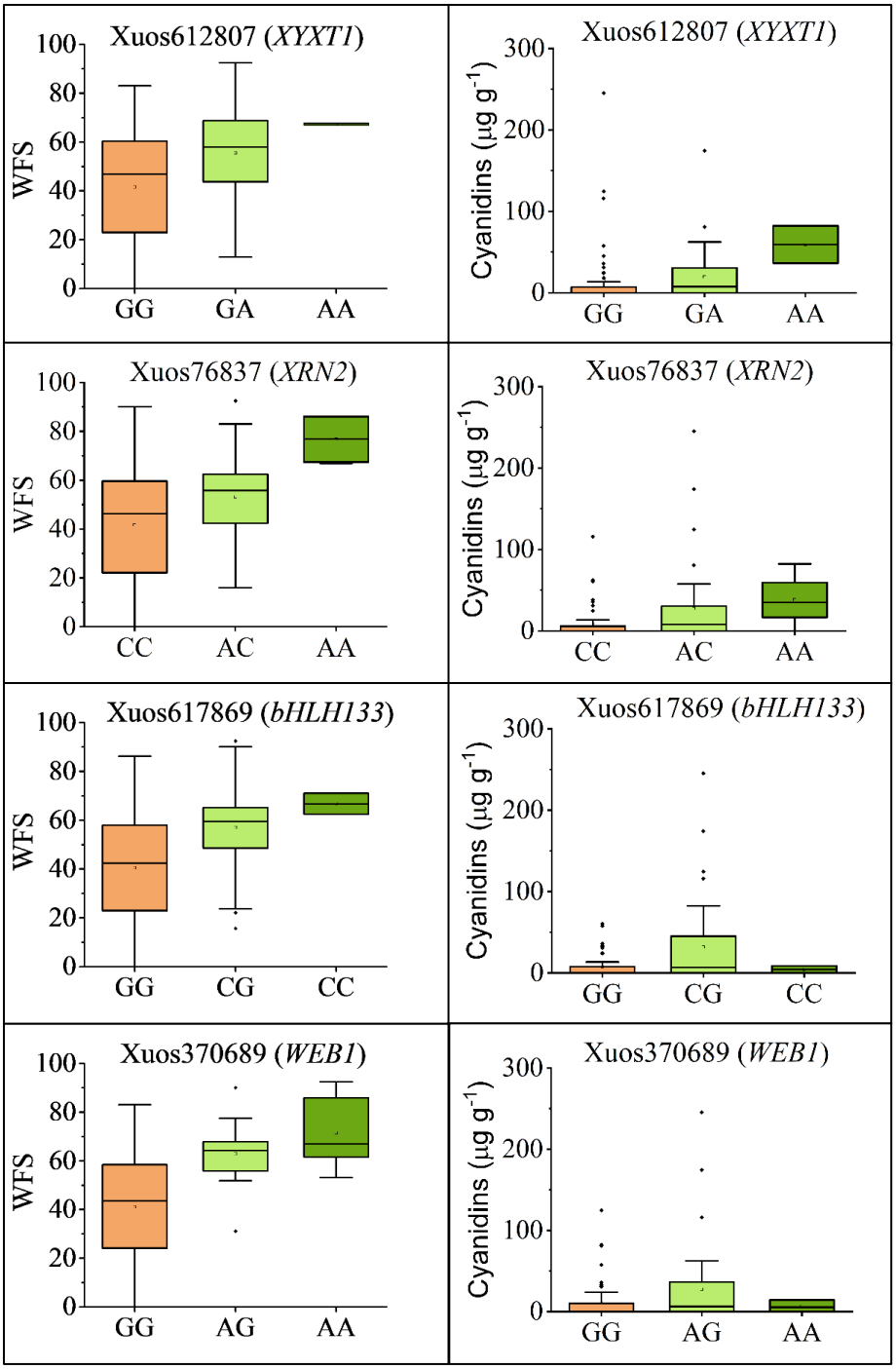

Fig. 4.36. Box-whisker plots showing the allele effects for the SNP markers (Xuos612807, Xuos76837, Xuos617869, and Xuos370689) (p < 2.76e-04). The plots show median (horizontal bar), interquartile ranges (boxes), ranges (whiskers), and outliers (dots) for marker allele frequencies among the 96 rye genotypes.

The targeted gene codes for a basic helix-loop-helix 133 (bHLH133). The Xuos617869 SNP produced a Q/H variation at the rye bHLH133 polypeptide. Among rye genotypes (30 out of 38) with low and very low WFS, and low cyanidins accumulation, only the Q bHLH133 variant was encoded, whereas both variants (Q/H) were common among genotypes with high and very high WFS (24 out of 39 genotypes, Appendix 18). The highest WFS and cyanidin accumulation was favored by the Q/H bHLH133 variants (Fig. 4.36).

The Pet-3-*p*Cou-Glc was associated with SNP marker Xuos370689 (Table 4.16) mapped on 536.243 Mb on chromosome 5R (Fig 4.34) corresponding to *SECCE5Rv1G0331080.1* encoding a polypeptide weak chloroplast movement under blue light 1 (WEB1). The SNP variation (A/G) did not alter the rye WEB1 polypeptide (R/R; Table 4.16). Genotypes with low or very low WFS, and low cyanidins accumulation generally containing G/G alleles (32 out of 38), whereas genotypes with very high or high WFS, and high cyanidins carried the A/G alleles (23 out of 39 genotypes; Fig.4.36; Appendix 18). WEB1 is a regulatory protein involved in blue light-induced chloroplast movements, controlling the velocity of chloroplast movement under strong light (Banaś *et al*., 2012). An auxin-like J-domain protein (JAC1) regulates WEB1 activity, and it modulates chloroplast photo-relocation (Kodama *et al*., 2010; Suetsugu *et al*., 2005). JAC1 was the first component characterized in the chloroplast movement pathway. Marker Xuos2344, associated with Cya-3-Glc, mapped to 115.094 Mb on chromosome 1R (Fig 4.34) and matched to *SECCE1Rv1G0014530.1* that encoded histidyl-tRNA synthetase (AARS; Table 4.16). The SNP (A/G) was located within the exon but did not cause an alteration in the encoded amino acid (Y/Y) sequence (Table 4.16). Among the 38 rye genotypes with low or very low WFS, 35 carried homozygous A/A alleles. A/A AARS variation was also associated with low cyanidins accumulation (Fig. 4.37). Heterozygous alleles (A/G) or homozygous alleles (G/G) associated with very high and high WFS, and high cyanidins accumulation (16 out of 39 genotypes; Fig 4.37; Appendix 18). Marker Xuos643546, associated with WFS and Cya-3-Glc (Table 4.16), was mapped to 804.568 Mb on chromosome 2R (Fig. 4.34) matched the *SECCE2Rv1G0121100.1* that codes for a peroxisomal (S)-2-hydroxy-acid oxidase (GLO3). The SNP variation (C/G) for *GLO3* did not alter the encoded protein sequence (T/T) (Table 4.16). Genotypes with low or very low WFS generally containing C/C alleles (32 out of 38), which also associated with low cyanidins accumulation, whereas genotypes with very high or high WFS carried the heterozygous alleles (C/G) or homozygous alleles (G/G) (21 out of 39 genotypes; Fig. 4.37; Appendix 18). Marker

Xuos267365 was found to be associated with WFS and Pel-3-6-Mal-βGlc (Table 4.16) and corresponded to *SECCE4Rv1G0247970.1* located on chromosome 4R (565.232 Mb; Fig. 4.34). The gene codes for an embryogenesis transmembrane-like protein. The Xuos267365 SNP variation (T/A) was synonymous (A/A) (Table 4.16). Among the 38 rye genotypes with low or very low WFS, 30 carried homozygous T/T alleles. T/T variation was also associated with low cyanidins accumulation (Fig. 4.37). Heterozygous alleles (T/A) dominated among genotypes with very high and high WFS (20 out of 39 genotypes: Appendix 18). T/A alleles were also associated with high cyanidins accumulation (Fig. 4.37). The SNP Xuos80120 associated with Del-3-*p*Cou-diGlc, Del-3-*p*Cou-Glc and WFS mapped on chromosome 2R (921.680 Mb; Fig.4.34) corresponded to *SECCE2Rv1G0138460.1* (Table 4.16). The encoded protein showed identity with a choline transporter-related protein 2 (CTL2). The SNP variation (G/A) for the protein sequence was synonymous (I/I). Genotypes with low or very low WFS generally carried G/G alleles (28 out of 38), whereas heterozygous (A/G) alleles or homozygous (A/A) alleles were associated with high and very high WFS (22 out of 39 genotypes; Fig. 4.37; Appendix 18). Homozygous A/A alleles were also associated with high cyanidins accumulation (Fig. 4.37). Marker Xuos651130 associated with WFS and Cya-3-Rut (Table 4.16), targeted the gene, *SECCE6Rv1G0418290.1* on chromosome 6R (661.986 Mb; Fig. 4.34). The *SECCE6Rv1G0418290.1* transcript showed sequence identity to a serine-rich protein, but the SNP variation (T/C) did not alter the encoded protein sequence (S/S). Among the 38 rye genotypes with low or very low WFS, 27 carried homozygous T/T alleles. T/T variation was also associated with low cyanidins accumulation (Fig. 4.38). Homozygous alleles (C/C) or heterozygous alleles (T/C) dominated among genotypes with very high and high WFS (21 out of 39 genotypes: Appendix 18). The C/C variant was also associated with high cyanidins accumulation (Fig 4.38). Marker Xuos524368 was found to be associated with WFS and Cya-3-Rut (Table 4.16) and coincided with a chloroplast methyltransferase gene (*SECCEUnv1G0538500.1*), but the location on the rye genome map could not be determined (Fig. 4.38). The SNP variation (A/G) was synonymous (T/T). Genotypes with low or very low WFS generally containing A/A alleles (27 out of 38), which also associated with low cyanidins accumulation, whereas genotypes with very high or high WFS and high cyanidins accumulation carried heterozygous alleles (A/G) or homozygous alleles (G/G) (32 out of 39 genotypes; Fig. 4.38; Appendix 18). Marker Xuos373302 associated with WFS Cya-3-pCou-Sam (Table 4.16) was found to match *SECCE6Rv1G0407680.1* located on chromosome 6R (561.615

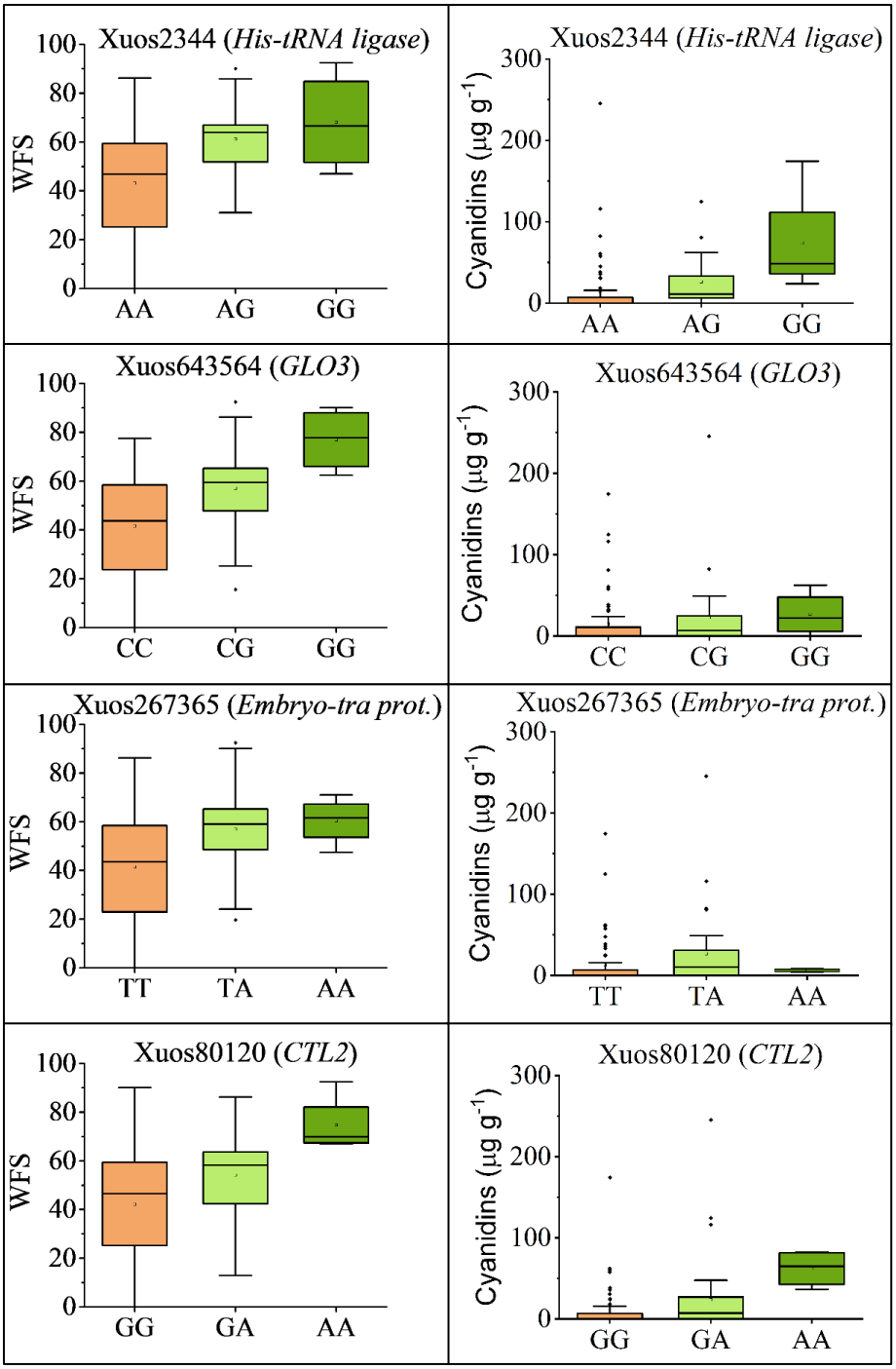

Fig. 4.37. Box-whisker plots showing the allele effects for the SNP markers (Xuos2344, Xuos643564, Xuos276365, and Xuos80120) (p < 2.76e-04). The plots show median (horizontal bar), interquartile ranges (boxes), ranges (whiskers), and outliers (dots) for marker allele frequencies among the 96 rye genotypes.

Mb; Fig. 4.34). The targeted gene codes for an enhancer of mRNA-decapping protein 4 (EDC4). The SNP variation (T/C) did not alter the rye EDC4 protein sequence (D/D). Homozygous T/T alleles at SNP site dominated among 38 genotypes with low or very low WFS and low cyanidins accumulation (37 out of 38), whereas heterozygous (T/C) alleles or homozygous (C/C) alleles were most common among genotypes with very high and high WFS (23 out of 39; Fig. 4.38; Appendix 18). C/C alleles were also associated with high cyanidins accumulation (Fig. 4.38). Marker Xuos172463 was associated with WFS and Cya-3-Sam (Table 4.16) and matched *SECCE3Rv1G0182130.1*, a zinc finger protein1-like (ZPR1-like) protein on chromosome 3R (622.648 Mb; Fig. 4.34). The SNP variation (C/T) for *ZPR1-like* was synonymous (N/N). Homozygous C/C alleles were associated with low or very low WFS (22 out of 38 genotypes), whereas heterozygous C/T alleles or homozygous T/T were most common among genotypes with very high and high WFS (22 out of 39; Fig. 4.38; Appendix 18). C/T alleles also associated with high cyanidins accumulation (Fig 4.38).

4.15.3 Markers associated with only anthocyanins

In group 1, eleven SNP markers were found to be significantly associated with anthocyanins, but not WFS, and nine of these were associated with glycosylated cyanidins (Table 4.17). Among these markers, markers Xuos171056 and Xuos1013 had the lowest *p*-values ($p < 0.001$ for both) and both were associated with Pet-3-Rut for which the encoded protein can affect cell wall (Table 4.17). The gene targeted by marker Xuos171056 (*SECCE3Rv1G0144530.1*) was mapped on chromosome 3R (4.607 Mb; Fig. 4.34) coincided with UDP-glycosyltransferase 72B3 (UGT72B3) and the G/A SNP located on 3'UTR (Table 4.17). UGT72 family has an important role in cell wall lignification in Arabidopsis (Lim *et al*., 2003; Lin *et al*., 2016). An aldehyde dehydrogenase (ALDH2C4) gene (*SECCE1Rv1G0044100.1*) was located on chromosome 1R at 599.738 Mb (Fig 4.34) and targeted by marker Xuos1013, but the SNP T/G did not alter the rye ALDH2C4 protein sequence (Y/Y; Table 4.17). Plant *aldehyde dehydrogenases from family 2* (*ALDH2*) have an essential role in cell wall formation and use aldehydes from the phenylpropanoid pathway (Končitíková *et al*., 2015).

Marker Xuos614384 was associated with Cya-3,5-diGlc and corresponded to an E3 ubiquitin-protein ligase, von Willebrand factor-type A (WAV3) gene (*SECCE7Rv1G0522500.1*), was found to be positioned on chromosome 7R (877.844 Mb; Fig. 4.34), and the SNP variation

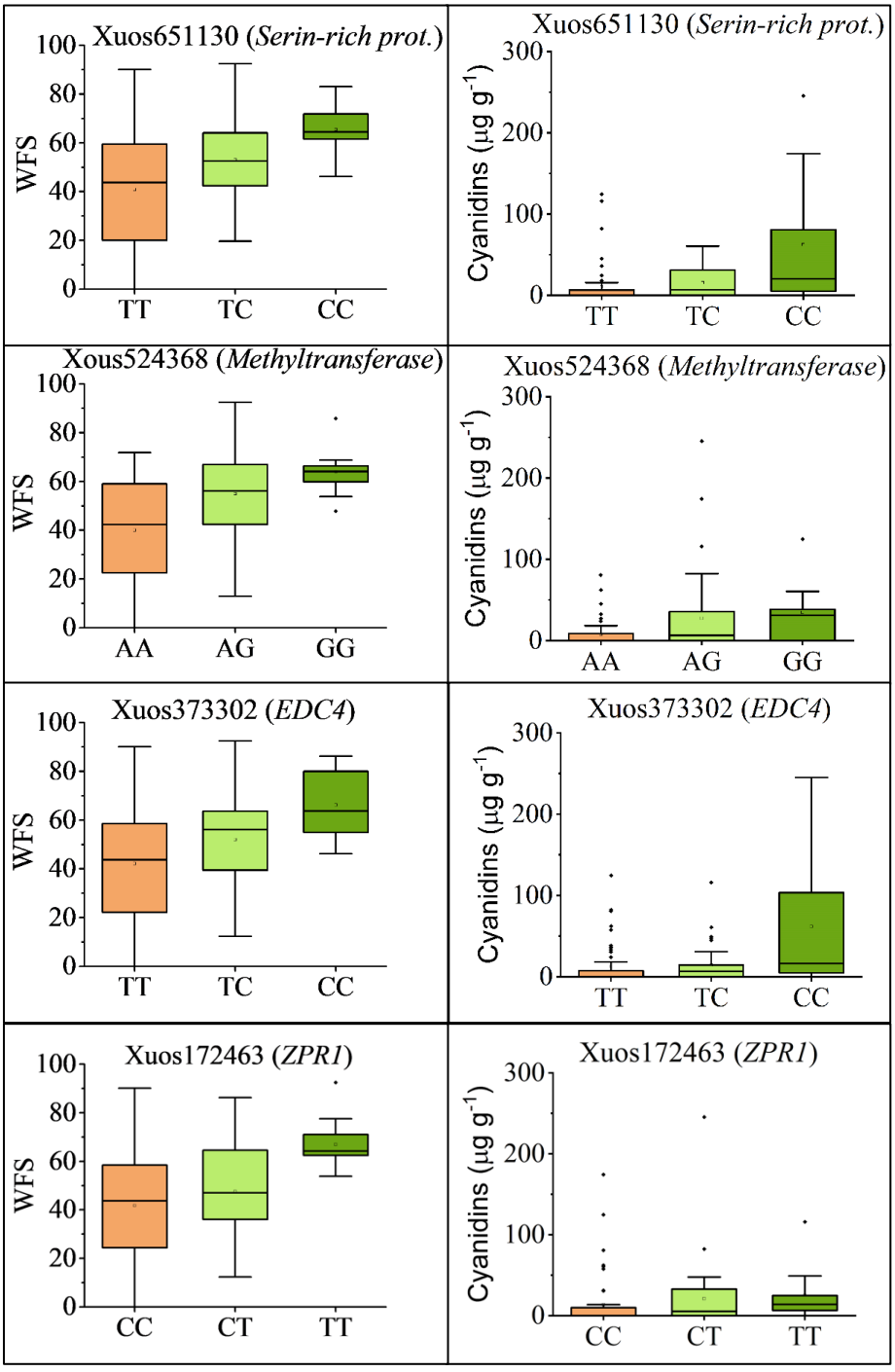

Fig. 4.38. Box-whisker plots showing the allele effects for the SNP markers (Xuos651130, Xuos524368, Xuos373302, and Xuos172463) (p < 2.76e-04). The plots show median (horizontal bar), interquartile ranges (boxes), ranges (whiskers), and outliers (dots) for marker allele frequencies among the 96 rye genotypes.

Table 4.17 Most significant markers associated with only anthocyanins identified in the study.

Marker ID[1/]	SNP[2/]	SNP position (bp)[3/]	*p*-value[4/]	R^2	MTA	Corresponding gene; protein	AA change
Xuos171056	G/A	Chr3: 4607065	4.81E-06	23.2	Xuos171056_Peo-3-Rut	*SECCE3Rv1G0144530.1* UDP-glucuronosyl/UDP-glucosyltransferase	3'UTR
Xuos1013	T/G	Chr1: 599737563	6.17E-06	22.7	Xuos1013_Peo-3-Rut	*SECCE1Rv1G0044100.1* Aldehyde dehydrogenase domain	Exon: None (Y/Y)
Xuos614384	G/C	Chr7: 877844366	1.71E-05	21.0	Xuos614384_Cya-3,5-diGlc	*SECCE7Rv1G0522500.1* von Willebrand factor, type A (WAV3)	5'UTR
Xuos94537	G/A	Chr2: 147129151	2.43E-05	20.4	Xuos94537_Pel-3-6-Mal-βGlc	*SECCE2Rv1G0081990.1* Glycoside hydrolase family 17	5'UTR
Xuos367960	T/C	Chr4: 876107547	5.01E-05	19.2	Xuos367960_Peo-3-Rut	*SECCE4Rv1G0291210.1* Transcription termination factor, mitochondrial/chloroplastic	Exon: None (P/P)
Xuos266936	G/A	Chr4: 878037756	7.69E-05	18.4	Xuos266936_Cya-3,5-diGlc	*SECCE4Rv1G0291710.1* Zinc finger, PHD-type	Exon: None (R/R)
Xuos78487	A/C	Chr2: 602068666	9.20E-05	18.1	Xuos78487_Peo-3-Rut	*SECCE2Rv1G0104190.1* Signal transduction response regulator, receiver domain	3'UTR
Xuos986	A/G	Chr1: 372917108	9.51E-05	18.1	Xuos986_Pel-3-6-Mal-βGlc	*SECCE1Rv1G0026650.1* Peptidase S10, serine carboxypeptidase	Exon: None (P/P)
Xuos524740	A/G	Chr5: 672815884	1.31E-04	17.5	Xuos524740_Cya-3-pCou-Sam	*SECCE5Rv1G0348170.1* Choline transporter-like	Exon: None (Y/Y)
Xuos368885	T/C	Chr4: 139319617	1.96E-04	16.8	Xuos368885_Cya-3-Rut	*SECCE4Rv1G0228780.1* Rx, N-terminal	Intron
Xuos552296	G/A	Chr7: 95756924	2.46E-04	16.4	Xuos552296_Cya-3-Glc	*SECCE7Rv1G0468270.1* Transcription elongation factor 1	Exon: None (Q/Q)

[1/] Number refers to matching rye Lo7_v2_scaffold number (Bauer *et al*. 2017).
[2/] Reference/alternative allele.
[3/] Position on rye Lo7 pseudomolecules version 1 assembly (Rabanus-Wallace *et al.* 2021).
[4/] Calculated upon Bonferroni correction.

(G/C) was found to be located on 5'UTR (Table 4.17). Marker Xuos94537, associated with Pel-3-6-Mal-βGlc (Table 4.17), targeted the gene, (*SECCE2Rv1G0081990.1*), and was located on chromosome 2R (147.129 Mb; Fig. 4.34). The *SECCE2Rv1G0081990.1* transcript showed identity with a glycoside hydrolase family 17 (glucan endo-1,3-beta-glucosidase GII-like), and the SNP variation (G/A) was located on 5'UTR (Table 4.17). Marker Xuos367960 was associated with Peo-3-Rut and coincided with a mitochondrial/chloroplastic transcription termination factor (MTERF15) gene (*SECCE4Rv1G0291210.1*) on chromosome 4R (876.107 Mb; Fig. 4.34), but the SNP Variation (T/C) did not alter the rye MTERF15 protein sequence (P/P). The marker Xuos266936 was associated with Cya-3,5-diGlc (Table 4.17) and was found to match *SECCE4Rv1G0291710.1* located on chromosome 4R (878.037 Mb; Fig. 4.34). The targeted gene codes for a zinc finger, PHD-type, but the SNP variation (G/A) was synonymous (R/R). Marker Xuos78487 associated with Peo-3-Rut (Table 4.17) corresponded to a signal transduction response regulator (ORR1) gene, (*SECCE2Rv1G0104190.1*) positioned on chromosome 2R (602.68 Mb; Fig. 4.34). The Xuos78487 SNP variation (A/C) was located on 3'UTR. Marker Xuos986 associated with Pel-3-6-Mal-βGlc (Table 4.17) corresponded to *SECCE1Rv1G0026650.1* located on chromosome 1R (372.917 Mb; Fig. 4.34). The corresponding gene codes for a serine carboxypeptidase (peptidase S10), but the Xuos986 SNP variation (A/G) did not alter the protein sequence (P/P). Marker Xuos524740 associated with Cya-3-pCou-Sam (Table 4.17) was found to match *SECCE5Rv1G0348170.1* that was located on chromosome 5R (672.815 Mb; Fig. 4.34). The targeted gene codes for a choline-like transporter, and the SNP variation (A/G) was synonymous (Y/Y). Marker Xuos368885 was found to be associated with Cya-3-Rut (Table 4.17). The Xuos368885 marker sequence was located within an intron of a disease resistance protein RGA2-like gene (*SECCE4Rv1G0228780.1*) mapped on chromosome 4R (139.319 Mb; Fig. 4.34). Marker Xuos552296 was associated with Cya-3-Glc (Table 4.17) and corresponded to *SECCE7Rv1G0468270.1* positioned on chromosome 7R (95.756 Mb; Fig. 4.34). The gene codes for a transcription elongation factor 1, but the SNP variation (G/A) was synonymous (Q/Q).

4.15.4 MTAs not matched with Lo7 rye annotated genes

Ten markers did not coincide with the Lo7 rye annotated genes (Rabanus-Wallace *et al*., 2021); however, these markers were significantly ($p < 2.76e-04$) associated with anthocyanins. Six markers [Xuos76321 (6R 832.876 Mb; Fig. 4.34), Xuos368592 (7R 715.871 Mb.; Fig. 4.34),

Xuos635334 (7R 888.050 Mb; Fig. 4.34), Xuos1976 (1R 56.623 Mb; Fig. 4.34), Xuos97912a (4R 796.323 Mb; Fig. 4.34), and Xuos177449 (3R 871.917 Mb; Fig. 4.34)] were associated with WFS and glycosylated cyanidins. Markers Xuos369477 (4R 219.858 Mb; Fig. 4.34), Xuos27480 (5R 364.685 Mb; Fig. 4.34), and Xuos950712 (4R 899.756 Mb; Fig. 4.34) were associated with a glycosylated cyanidin and pelargonidin. Marker Xuos403276 (5R 585.894 Mb; Fig. 4.34) was the only marker associated with WFS and glycosylated delphinidin (Appendix 16).

4.15.5 Markers associated with anthocyanins and developmental traits

Five SNP markers in group 1 (Xuos172463, Xuos643546, Xuos76850, Xuos368592, and Xuos403276) were identified in the study and were found to be significantly associated with anthocyanins, WFS and two developmental traits (Tables 4.12; 4.16; Appendices 14 and 16). Markers Xuos172463, Xuos643546, Xuos368592, and Xuos403276 were associated only with FLN, except Xuos172463, which also associated with PGH. The genes targeted by markers Xuos172463 (3R 622.648 Mb; Fig. 4.34) and Xuos643546 (2R 804.568 Mb; Fig. 4.34) were *ZPR1* (*SECCE3Rv1G0182130.1*) and *GLO3* (*SECCE2Rv1G0121100.1*), respectively, that were associated with Cya-3-Glc and Cya-3-Sam, respectively. Marker Xuos76850 was found to be associated with PGH and Cya-3-Sam (Appendices 14 and 16). The Xuos76850 marker sequence was located within an intron of a Calcium-dependent protein kinase 13 gene (CPK13) (*SECCE2Rv1G0122590.1*) mapped on chromosome 2R (817.643 Mb; Fig. 4.34). However, markers Xuos368592 (7R 815.871 Mb; Fig. 4.34) and Xuos403276 (5R 585.894 Mb; Fig. 4.34) did not correspond to Lo7 rye-annotated genes (Rabanus-Wallace *et al*., 2021) that were associated with Pet-3-Rut and Del-3-Caf-Glc, respectively (Appendices 14 and 16).

4.16 Markers associated with WFS and anthocyanins in group 2

Group 2 SNPs were significantly lower than those in group 1 (Appendix 16). Only two markers, Xuos371856 (5R 815.325 Mb; Fig. 4.34) and Xuos524638 (7R 715.871 Mb; Fig. 4.34) in group 2 were associated with WFS and anthocyanins, respectively, and both were associated with glycosylated cyanidins Cya-3-Sam and Cya-3-Glc, respectively. However, these two markers did not match with Lo7 rye-annotated genes (Rabanus-Wallace *et al*., 2021). An association with developmental traits was not observed in the MTAs of group 2 (Appendix 16).

4.17 Markers associated with anthocyanins and developmental traits in group 2

Six markers in group 2 (Xuos94267, Xuos445354, Xuos519671, Xuos614844, Xuos696918, and Xuos720755) were identified in the study associated with anthocyanins and developmental traits. Marker Xuos614844 associated with PGH and Pel-3-6-Mal-βGlc (Appendices 14 and 16) and matched *SECCE7Rv1G0469980.1* located on chromosome 7R (115.65 Mb; Fig 4.34). The nucleotide sequence identity (99%) was noted to Cytochrome b561. The SNP variation (C/G) maps to exon for *Cytochrome b561* gene, but the protein sequence is not altered by the SNP variation (V/V) (Appendix 16). Marker Xuos94267 associated with PGH and Cya-3-Glc located on chromosome 2R (823.831 Mb; Fig 4.34). Marker Xuos519671(6R; 819.606 Mb; Fig 4.34) associated with PHT, TIL and Cya-3-pCou-Sam. Markers Xuos696918 (3R; 32.271 Mb; Fig 4.34) and Xuos720755 (3R; 934.819 Mb; Fig 4.34) associated with DTA and also associated with Cya-3-Glc and Pel-3-6-Mal-βGlc, respectively (Appendices 14 and 16). Marker Xuos445354 located on chromosome 6R (861.256 Mb; Fig 4.34) associated with FLA and Cya-3-Glc (Appendices 14 and 16). Markers (Xuos94267, Xuos445354, Xuos519671, Xuos696918, and Xuos720755) did not coincide with the Lo7 rye annotated genes (Appendix 16; Rabanus-Wallace *et al*., 2021).

4.18 Biplot analysis supports WFS and associated cyanidins are controlled by several common genes.

A PCA bi-plot constructed for the two traits was analyzed in the study and showed a relatively high amount of trait variation explained by PC1 (46.8%–52.5%) and PC2 (12.3%–12.7%) in the different plots (Figs. 4.39 and 4.40). Six vectors representing SNP markers for candidate genes *PAL8*, two of *CHS2, 3GT, WEB1, and bHLH133* were visualized for the cyanidins plots. The first three vectors correlated relatively well with each other, contributed mainly to PC2, and were associated with winter-hardy Canadian rye genotypes, whereas *WEB1*, *3GT*, and *bHLH133* vectors were mainly associated with PC1 and correlated with rye genotypes with the highest cyanidin accumulation in the leaves and crown. *PAL8*, two of the *CHS2*, *3GT*, and *WEB1* were also represented as vectors for WFS. WFS was also displayed via an additional vector (marker Xuos612807) corresponding to *XYXT1* gene, but the *XYXT1* vector did not group with the other five vectors. The *XYXT1* vector was not involved in or related to the phenylpropanoid pathway, thus causing this separation.

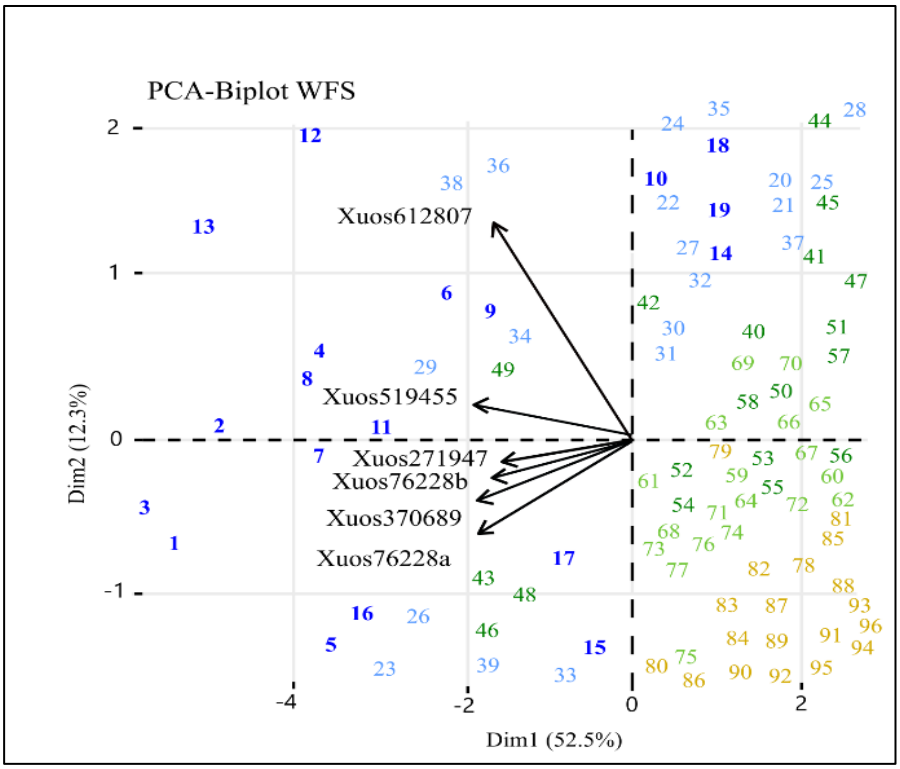

Fig. 4.39. PCA biplot visualizing SNP effects on WFS analyzed for rye population of 96 genotypes.

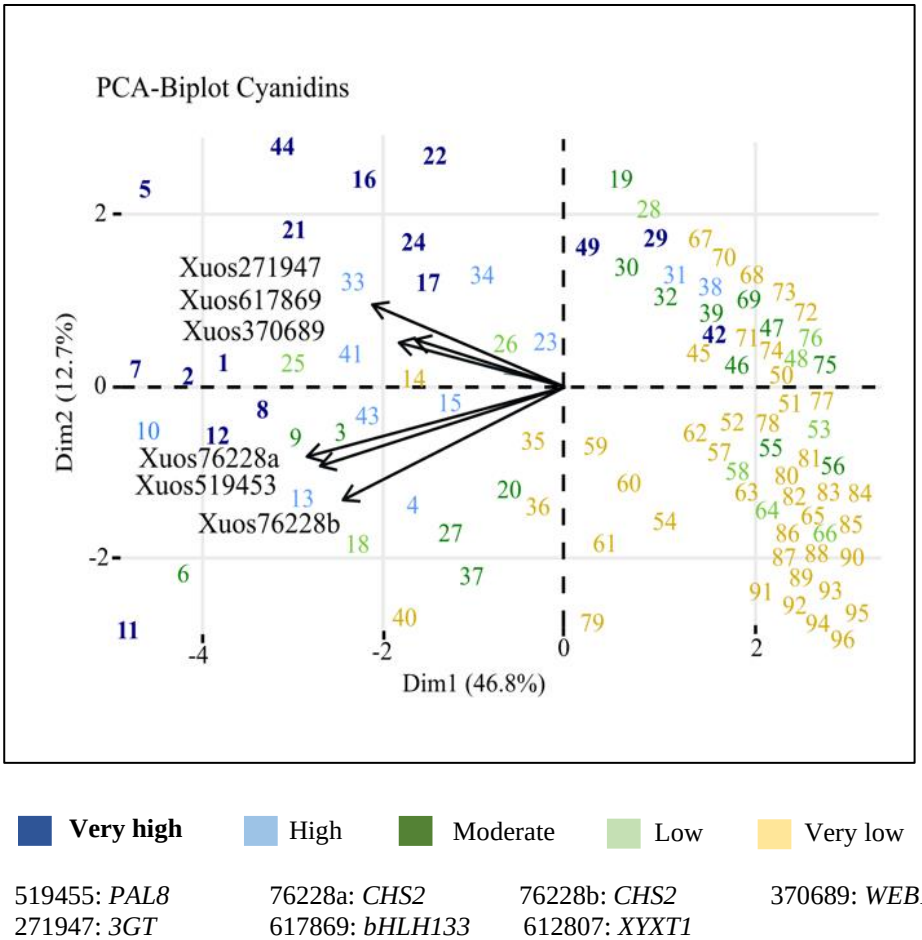

Fig. 4.40. PCA biplot visualizing SNP effects on cyanidins analyzed for rye population of 96 genotypes.

CHAPTER 5

DISCUSSION

5.1 Background

In the northern hemisphere temperate climates, autumn seeded winter crops present an ecologically friendly cropping system, providing soil cover in the late autumn and early spring. The early spring growth of winter crops make an efficient use of moisture provided by snow melt, out-compete weeds and usually result in higher yield than spring seeded crops. The major challenge for autumn seeded winter crops is the ability to survive harsh winter climates, when the temperature can dip as low as -30ºC. Among the autumn seeded winter cereals, rye (*Secale cereale* L.), is the most-cold hardy and it can survive extremely low temperatures (≤ -30ºC) during winter on the Canadian prairies (Fowler, 2008). Thus, rye can serve as a good model for winter hardiness studies in grasses.

The autumn seeded crops germinate and the young seedlings are exposed gradually to low temperatures, reduced day length (photoperiod) and changes in light quality (red/far-red ratio). These environmental cues trigger in plants, two major physiological processes, cold acclimation and vernalization. The cold acclimation process builds the freeze tolerance, whereas vernalization influences the developmental shift from vegetative to the reproductive phase (Thomashow, 1999). The work presented in this thesis was based on the hypothesis that WFS is complex, and it is an interaction between the LTT accumulated during cold acclimation and plant developmental traits influenced by the vernalization process. Rye being the most cold-hardy winter cereal, is cross pollinated thus presents with a high level of nucleotide diversity and a faster decay of linkage disequilibrium (LD), thus makes it amenable to association genetic studies (Li *et al*., 2011*b*; Auringer *et al*., 2016) to develop molecular markers for WFS and associated traits. The association genetic studies combined with the availability of rye genome sequences (Rabanus-Wallace *et al*., 2021) was used to identify molecular markers for WFS, LTT, and plant developmental traits including anthocyanins.

5.2 Rye population provided a wide variation of WFS

The rye population studied included a predominance of winter (72 genotypes), eight genotypes each of perennial, facultative and spring genotypes (Table 3.1), giving a range of WFS. Five years of field trials confirmed that winter types showed the highest WFS, whereas the spring types showed the least WFS. The year-to-year variation in WFS was high, but the genotype specific trends between the years were significantly correlated (Table 4.2). A significant ($p < 001$) effects of genotype, environment and genotype x environment was seen (Table 4.4) but the medium heritability (0.48) made it amenable for association genetic studies. The most winter-hardy rye genotypes in the study hold valuable information regarding WFS during very cold winters in the northern latitudes in Asia, Europe and North America, whereas the tender genotypes could identify traits not associated with WFS. Studies in barley, diploid and hexaploid wheat, show that frost tolerance variation in cereals depends on copy number and allele differences at the *VRN1* and *FR-2* loci, respectively, (Francia *et al*., 2016; Knox *et al*., 2008; Rizza *et al*., 2016; Zhu *et al*., 2014). In rye also, *Fr-R2* is confirmed as a major frost hardiness locus (Erath *et al*., 2017; Li *et al*., 2011*a*), but very little is known about other loci affecting WFS or LTT in rye. In wheat, interactions between *VRN1* and *Fr-A2* alleles modulate cold-induced *CBF* gene expression, that is critical for induction of COR genes and development of high LTT (Dhillon *et al*., 2010). Thus, the poor WFS displayed by spring rye types in this study is likely due to the lack of vernalization requirement combined with the inability to induce *COR* gene expression to high levels when exposed to low temperatures in the autumn (Fowler *et al*., 1996*b*; Ganeshan *et al*., 2008).

5.3 Efficiency of cold acclimation process was a major factor for WFS

One component of WFS is LTT determined as LT_{50} values and representing the level of cold hardiness built up in the plant during cold acclimation. However, the LT_{50} value is not expected to precisely mimic the outcome of cold acclimation in the field as freezing tests are done on plants grown under constant and controlled conditions. Short exposures of cold prior to a longer period of cold and/or a second hardening step at sub-zero temperature can trigger higher levels of freezing tolerance in plants (Leuendorf *et al*., 2020; Zuther *et al*., 2019). Also, the daily variation of light intensity and temperature that exists in the field can increase the total amount of LTT accumulated in field-grown plants (Mayer *et al*., 2020). Despite these differences between cold acclimation in-house and in the field, a very high correlation between LTT and WFS determined

from individual years (r = -0.54-0.82, $p < 0.001$) and BLUEs for WFS (r = -0.90, $p < 0.001$) was obtained in the study (Table 4.2). The identification of 16 SNPs in common for the two traits further showed WFS and LTT are strongly interlinked ($p < 0.001$; Appendix 14) and suggested that the efficiency of cold acclimation in the autumn was the main contributor to WFS in this study. Previous field tests of winter wheat genotypes performed in the Saskatoon region also demonstrate a very high correlation (r = 0.95) between LTT and WFS (Limin and Fowler, 2000). Saskatoon winters typically have low humidity levels, thin snow covers, and overall unfavorable conditions for snow mold infections, which can have a large negative impact on WFS (Gaudet *et al*., 1999; Ponomareva *et al*., 2021). In locations with long-lasting snow cover and humid conditions at ground level, the correlation between WFS and LTT are expected to be considerably lower than observed in this study.

5.4 A multi-trait approach to study WFS

5.4.1 WFS strongly correlated to LTT, FLN, PGH and PHT

WFS is a complex trait with many contributing factors such as rate and length of the cold acclimation process, developmental program of the plant, effects of biotic stress and deacclimation processes during winter, and plant vigor in the spring (Båga *et al*., 2009; Dhillon *et al*., 2010; Fowler and Limin, 2004; Körner, 2016). The results showed that FLN was strongly correlated ($p < 0.001$) with WFS (r = 0.80) and LTT (r = 0.71), respectively (Table 4.3). The high FLN in winter cereals relates to a delayed floral transition at the shoot apical meristem during cold acclimation, which contributes to development of high freezing tolerance (Fowler *et al*., 1996*a*; Fowler and Limin, 2004). This is consistent with genotypes Musketeer, AC Rifle, AC Remington with highest FLN values (≥12.0) were among the most winter-hardy genotypes (WFS ≥83%) and showed the highest LTT (LT_{50} <-27.0 °C) in the study (Table 4.1). The low FLN demonstrated by breeding lines Petkus and Carsten (8.0 and 8.6, respectively; Appendix 8) suggested a short cold acclimation process, resulting in the low LTT and WFS values for these two genotypes. The length of the vegetative phase in wheat is associated with allele differences at *VRN1* (Zhu *et al*., 2014). Among the many potential targets for *VRN1* are genes involved in metabolism of phytohormone levels such as jasmonic acid, abscisic acid and gibberellin (Deng *et al*., 2015), of which jasmonic acid is suggested to modulate vernalization response in wheat (Diallo *et al*., 2012).

In the rye population, PGH was also strongly associated ($p < 0.001$) with WFS (r = 0.61) and LTT (r = 0.59; Table 4.3). Plants displaying PGH have an altered negative gravitropism response, and this phenotype has likely evolved to avoid or mitigate cold stress (Körner, 2016; Tan *et al*., 2008). An asymmetric distribution of auxin is associated with the cold-induced gravitropic curvature as deduced from studies of *gravity persistent signal* (*gps*) mutants in Arabidopsis (Wyatt *et al*., 2002). Early studies in winter wheat suggest that vernalization locus chromosome 5A or closely linked *Fr-1* locus control cold-induced PGH (Roberts, 1990). Later wheat studies suggest sensitivity to vernalization and photoperiod are the two major factors associated with PGH during juvenile growth (Marone *et al*., 2020). In barley, recessive alleles at the chromosome 3H *sdw1*/*denso* locus were associated with gibberellin biosynthesis, controlled semi-dwarf growth, flowering time and induced early prostrate growth at normal temperature (Kuczyńska *et al*., 2014; Zhou *et al*., 2018), suggesting that phytohormone levels were associated the PGH phenotype.

A strong correlation was observed between PHT and WFS (r = 0.39, $p < 0.001$), and LTT (0.36, $p < 0.001$; Table 4.3). The strong association between LTT and PHT, suggested early events at SAM prior to floral transition influence PHT. The intercalary meristems, from which leaf initials, axillary buds, and internodes are formed, are laid down during the early stages of SAM development (McKim, 2019), but stem elongation is paused until vernalization, temperature, and photoperiod requirements are fulfilled (Chen *et al*., 2009). A signal transported from the shoot apex is suggested to control internode elongations starting with basal internodes elongating first and the peduncle last (McKim, 2019). Gibberellin concentrations have a role in stem elongation by promoting increased cell division and cell elongations at the intercalary meristems of the stem (McKim, 2019; Peng *et al*., 1999). The timing of stem elongation in the spring for winter type is important as early elongation can cause frost kill due to exhausted LTT at this stage. Like FLN and PGH, a major locus for stem elongation in hexaploid wheat is located close to *VRN-A1* locus on chromosome 5A (Chen *et al*., 2009).

A relatively weak but significant association was seen between WFS and DTA (r = 0.25, $p < 0.05$), but it was not significantly related with LTT (Table 4.3). The development of flowers in Triticeae species with fulfilled vernalization requirement starts when photoperiod and temperature requirements are met, which occur in the spring for winter cereals (Trevaskis *et al*., 2007). At this transition, the up-regulated *VRN1* and absence of *VRN2* expression in leaves leads to induced expression of *VRN3* (Deng *et al*., 2015). VRN3 is the cereal orthologue of Arabidopsis

FLOWERING LOCUS T (FT), a transmissible florigen signal promoting flower development (Corbesier *et al*., 2007). Besides variation for *VRN* alleles controlling vernalization requirement, allelic differences for *PHOTOPERIOD1* (*PPD1*), circadian clock related *earliness-per-se* (*Eps*), early maturity (*Eam*), and gibberellin-regulated genes are some of the factors modifying flowering time in cereals (Hill and Li, 2016). Like many developmental traits associated with WFS, gibberellin levels regulate development of inflorescence into flowers during long-days (Boden *et al*., 2014). Thus, the negative correlation between DTA and PHT (and TIL; Table 4.3) observed for the rye population could be due to gibberellins stimulating both early flowering (low DTA) and stem elongation (high PHT/TIL). The three developmental traits, DTA, TIL and FLA are expressed during the spring growth contribute to the agronomic performance grain yield but do not seem to influence WFS.

In conclusion, the results support the hypothesis that WFS is contributed by LTT accumulated during cold acclimation and by some developmental traits such as PGH, FLN and PHT induced during the vernalization process.

5.4.2 Rye – a good source of winter hardiness genes

The LD decay rate is the main factor limiting mapping resolution in GWAS and it is largely determined by the mating system (self or out-crosser), recombination rate, and distribution of recombination hot spots on the genome (Flint-Garcia *et al*., 2003). For the cross-pollinating rye, the estimated natural recombination frequency and genetic diversity are relatively high and contribute to a low average intra-genic LD of about 520 bp (Li *et al*., 2011*a*). Species with a low LD are especially well suited for association mapping as it provides a considerable higher mapping resolution than biparental mapping (Myles *et al*., 2009; Zhu *et al*., 2008). Further improvements of the resolution was obtained in the study by using a reduced-representation GBS library targeting low-copy hypo-methylated regions for SNP identification (Poland *et al*., 2012*b*). Successful accomplishment of this strategy was demonstrated by 140 out of 339 (41.3%) significant SNP markers mapped to genes (Appendix 14).

The rye population of 96 genotypes included three subpopulations as predicted by PCA and STRUCTURE analyses (Figs. 4.9, 4.10). The dominance of subpopulation II may be explained by Petkus and Carsten ancestry in many rye cultivars developed around the world (Fischer *et al*., 2010). Several of the winter-hardy Canadian rye cultivars clustered together with Carsten, which

showed relatively low winter hardiness, whereas other winter-hardy Canadian genotypes were grouped in subpopulation I that included genotypes of varying WFS (Table 4.1). In general, there was no strong relationship between subpopulation, winter hardiness or origin among the rye genotypes (Tables 4.1 and 3.1). Although breeding has narrowed the genetic pool of rye (Targońska *et al*., 2015), it has been still been possible to select/develop very cold hardy rye cultivars with winter hardiness far exceeding that of wheat and barley cultivars. For the self-pollinating wheat and barley, crop domestication and breeding primarily aimed at increasing yield has resulted in an extensive loss of genetic diversity (Voss-Fels and Snowdon, 2016), and particularly variability for genes involved in winter survival. Thus, the key genetic factors required to improve winter hardiness in tender cereals are present in certain rye genotypes.

The phenotypic relationships revealed in this study showed that LTT as determined by LT_{50} values, developmental traits like FLN and PGH with high heritability estimates (h^2 = 0.45 to 0.81) (Table 4.4), and cyanidins group of anthocyanins identified with HPLC-QTOF MS/MS in the rye population were useful to dissect the complex WFS trait. The abundance of markers provided by genotyping by sequencing (GBS), identification of common SNP markers between the traits by GWAS, combined with the Lo7 rye genome sequence aided identification in total 140 annotated candidate genes (p <0.01). The accuracy of the mapping is strengthened by finding seven of the nine strongest candidate genes have roles in plant adaptation during cold acclimation and contribute to enhanced winter hardiness in cereals and other plants.

5.5 Membrane integrity

The plasma membrane of plant cells is prone to freezing injury (Steponkus, 1984) and needs protection when exposed to freezing temperatures to withstand dehydration stress and fractures caused by ice crystals. The protection mechanisms applied during cold stress in cereals generally includes membrane rigidification (Örvar *et al*., 2000), prevention of ice crystal formation and growth (Bredow and Walker, 2017), and production of proteins with membrane stabilization properties (Uemura *et al*., 2006). One of the cold-induced plasma membrane proteins is the multi-spanning COR413-PM, for which sequence variations was associated with WFS, FLN, PHT and TIL (Table 4.11). In Arabidopsis, both *COR413-PM1* and related chloroplast *COR413-IM* belong to a set of 56 plant core environmental stress genes that are part of the systemic stress response (Hahn *et al*., 2013); however, the systemic signal inducing the core genes is not known. Induction

of *WCOR413* genes in cereals during cold stress correlates with the plant's capacity to develop freezing tolerance (Breton *et al*., 2003; Colton-Gagnon *et al*., 2014). Although the exact function of WCOR413 proteins has not been determined, they are suggested to maintain membrane fluidity at cold temperature (Su *et al*., 2018), act as a G protein-coupled receptors involved in signaling (Breton *et al*., 2003), or stabilize the membrane lipid structure (Zhou *et al*., 2018). Overexpression of *Phlox subulata PsCOR413-PM2* in transgenic Arabidopsis demonstrates COR413-PM proteins have a role in cold acclimation by producing higher Ca^{2+} flux in roots, increasing expression of *CBF1, CBF3*, and other cold-related *COR* genes to produce higher cold resistance (Zhou *et al*., 2018).

Like COR413 proteins, IRIPs are important for membrane protection. In this study, both WFS and LTT in the rye population were strongly associated with allele variation for one of many IRIP genes (Table 4.11). IRIPs ability to prevent ice recrystallization is shown by *in vitro* and *in vivo* studies (Gupta and Deswal, 2012; Bredow and Walker, 2017) and the proteins may also contribute to thermal hysteresis, although this effect seems to be low (0.3-1.2 °C) in rye (Griffith *et al*., 2005). *IRIP* are associated with frost-hardiness in cereals based on increased expression of *IRIP* genes during cold acclimation in wheat (Houde *et al*., 2006). In addition, improved freezing tolerance is observed in transgenic Arabidopsis expressing *LpIRI-a*, *LpIRI-b*, *LpIRI2*, or *LpIRI3* from *Lolium perenne* (Zhang *et al*., 2010), and lower freezing tolerance in *Brachypodium distachyon* when *IRIP* genes are down-regulated (Bredow *et al*., 2016*b*). Rye genotypes with the highest WFS and LTT showed in general heterozygosity for the *IRIP* alleles (Appendix 15). This may indicate additional copies of *IRIP* genes in cold-hardy genotypes as compared to the sequenced rye genome and genotypes with low cold-tolerance in this study. It is suggested that the *IRIP* gene clusters in cereals evolved in response to lower global temperatures early in the evolution of the Pooideae grass subfamily and led to a slightly different or novel function for the new *IRIP* alleles (Sandve *et al*., 2008).

The association between the rye variant IRIP isoform, WFS, and LTT observed in this study seems obvious (Table 4.11). However, the variant IRIP isoform was also associated with PGH, which suggests IRIPs influences plant development in addition to its role in frost protection. PGH, which likely results from a gravitropic responses (Dong *et al*., 2013), is only observed during cold acclimation in rye as plants revert to erect growth when returned to higher temperature. PGH is directed from the crown tissue, which is also one of first tissues that freezes, despite the lower

part of the plant is warmer than the upper part (Sandve *et al*., 2008). In monocots, freezing starts in the roots, followed by crown and leaf tissues. Survival of the crown tissue is vital for winter cereals, as it provides the start of new shoots and roots during spring regrowth. Thus, it can be suggested that very cold hardy cereals have evolved a more efficient frost protection in the meristematic tissues of the shoot apical meristem. However, there is little information regarding the tissue-specific expression of *IRIP* genes in cereals. In cold-hardy wheat cultivar Norstar, the *TaIRI-1* gene is upregulated in leaves, crowns, and roots during cold acclimation, whereas *TaIRI-2* is only activated in leaves (Tremblay *et al*., 2005). Thus, the tissue-specific expression of different *IRIP* alleles in rye during cold acclimation is needed to fully understand which IRIP isoforms make the largest contribution to frost hardiness.

5.6 Photosynthesis adjustment during cold acclimation

Allele differences for *CHUP1* and *WEB1* genes encoding two proteins involved in chloroplast movement (Oikawa *et al*., 2003; Wada, 2013; Wilson and Ruban, 2020) suggested optimal chloroplast position within cells was important for WFS in the rye population. From the PCA bi-plot analysis (Fig. 4.27), *CHUP1* allele variation was also a common contributing factor for PGH, FLN, and LTT, for which trait values are set during the cold acclimation process (Figs. 4.28- 4.30). This suggested chloroplast movements assist in fine-tuning incoming light signals to enhance the efficiency of cold acclimation in rye. A recent study of a *chup* mutant in Arabidopsis supports chloroplast positioning has an important role for proper regulation of photosynthesis and metabolism during cold acclimation (Kitashova *et al*., 2020). During warm days in the fall, increased light harvest and photosynthesis may be achieved by movement of chloroplasts to the periclinal cell walls. Under cold and bright days, movement of chloroplasts to the anticlinal cell walls may be needed to reduce light absorbance. The avoidance response was initially thought to reduce photoinhibition and photo damage (Wada and Kong, 2018) but later studies suggest fine-tuning of light signals is the primary reason for the chloroplast relocation (Wilson and Ruban, 2020). Thus, we speculate that efficiency of chloroplast repositioning may account for some of the high photosynthesis efficiency that exists for cold-hardy winter cereals during cold acclimation (Dahal *et al*., 2012). Although no amino acid difference could be associated with the SNPs for *CHUP1* or *WEB1*, it is possible these genes are differentially regulated by light and/or temperature signals in rye genotypes with different levels of WFS. Further analysis of CHUP1 and WEB1

genes and expression levels during cold acclimation are needed to confirm their role in cold acclimation in rye.

One of the orthologues to the rye *BIPP2C1* associated with WFS in this study is the Arabidopsis *AtPP2C26*, which is a PSII core phosphatase (PBCP) (Samol *et al*., 2012). PBCP has a role in adapting the photosynthetic apparatus to changes in light conditions (Puthiyaveetil *et al*., 2014; Singh *et al*., 2016). Thus, a similar role in optimizing photosynthesis and reducing photoinhibition during cold exposure may exist for the rye *BIPP2C1* associated with WFS, LTT, FLN, and PGH (Table 4.11) in this study.

5.7 ICE-CBF-COR regulon

The CBF regulon regulated from the *FR-2* locus in grasses has a central role during cold acclimation (Vágújfalvi *et al*., 2005). Like other Triticeae members, the rye *Fr-R2* carries a cluster of *CBF* genes (Campoli *et al*., 2009), for which haplotype variation is suggested to underlie differences in freezing tolerance among rye accessions (Jung and Seo, 2019; Li *et al*., 2011*a*; Rabanus-Wallace *et al*., 2021). However, we found only weak associations between WFS and three different *CBF* genes (*CBFIIId-D19*, *CBFIVa-2.2*, and *CBFIIIa-6*) at *FR-R2* (Appendix 14). Transcript analysis of rye *CBF* genes indicates existence of three *CBFIVa-2*.2 and two *CBFIIIa-6* genes in rye (Jung and Seo, 2019). This could possibly explain the low significance for individual *CBF* alleles as complementary functions may be exerted by an additional copy of near-identical *CBF* genes; thus, SNP variations for multi-copy *CBF* genes contribute little to phenotype differences within the population. Lack of association between SNP variations for individual *CBF* genes at *Fr-A2* and frost resistance is also seen in a panel of 1,739 European winter wheat genotypes studied by association mapping (Zhao *et al*., 2013). However, most mapping studies of bi-parental populations in wheat, barley, and rye show *Fr-2* has a major role for frost tolerance (Båga *et al*., 2007; Erath *et al*., 2017; Francia *et al*., 2004). Due to the limited number of recombination events within bi-parental populations, the QTL regions are large and defined by a composite effect from several *CBF* genes, their interactions, and copy number effects.

Although variation for *CBF* genes appeared to have a small role for WFS, several candidate *genes* belonging to the ICE-CBF-COR regulon were identified. One strong candidate gene was *ICE1*, for which amino acid variation at the end of the DNA binding bHLH region and/or start of zipper region (Båga *et al*., 2022) was associated with WFS, LTT, FLN and PGH (Table 4.11). In

a previous study, allele variation within an intron for *ScICE2*, probably allelic with *ICE1* identified in this study, was associated with variation for winter hardiness and freezing tolerance among 201 European rye genotypes (Li *et al*., 2011*b*). Thus, specific alleles for *ICE* genes may be important to incorporate winter hardiness in rye. Since genotypes with low or very low WFS generally encoded ICE1 containing the rare His_{283} modification, these ICE1 proteins may display a lower affinity for the MYC recognition elements (CANNTG) present in promoters of *CBFs* and several other cold-regulated genes (Chinnusamy *et al*., 2003; Tang *et al*., 2020). It is also possible that the His_{283} ICE1 variant affected heterodimer formation with other bHLH proteins (Xu *et al*., 2014). Further studies are needed to discern the specific effects of the Leu_{283}/His_{283} variation for rye ICE1.

ICE proteins are highly expressed in the shoot apex and leaf primordia of Arabidopsis plants, supporting ICE protect of these sensitive tissues from frost damage (Kurbidaeva *et al*., 2014). *ICE1* may also affect development at the shoot apical meristem as sequence variation for the protein was associated with FLN and PGH besides WFS and LTT (Table 4.11). A developmental role for ICE1 could possibly involve heterodimer formation with other bHLH factors. Both ICE1 and ICE2 are known to form dimers with various bHLH factors to control the establishment and differentiation of stomata in dicot plants (Kanaoka *et al*., 2008; Kurbidaeva *et al*., 2014) and stomata lineage formation in monocot plants (Raissig *et al*., 2016; Wu *et al*., 2019*b*). It is interesting to note that distribution of stomata is altered in a distinctive pattern on the adaxial and abaxial leaf surfaces during cold acclimation in rye cv Puma (Hüner *et al*., 1981). Whether this change in stomata distribution in cold-hardy rye is regulated by ICE1 and/or ICE2 protein activity during cold acclimation has not been demonstrated.

5.8 Jasmonic acid influence on cold acclimation

An association between SNP variation for *JAR1* gene and WFS and FLN (Table 4.11) suggested JA-Ile production or signaling could be an important factor during cold acclimation in rye. Methyl-JA, which can be converted to JA-Ile by jasmonate methyl transferase and JAR1 activities, confers increased cold tolerance with or without cold acclimation in Arabidopsis, whereas a block in JA biosynthesis and signaling makes plant hypersensitive to cold (Hu *et al*., 2013). JA-Ile produced by JAR1 activity during cold stress is perceived by a nuclear co-receptor complex (SCFCOI1-JAZ) composed of Skp1/Cullin/F-box (SCFCOI1) active as an E3 ubiquitin ligase with various JASMONATE ZIM (JAZ) domain proteins as targets for the

ubiquitination/26S-proteasome pathway (Hu *et al*., 2013). Upon JA-Ile activation of SCFCOI1-JAZ complex, JAZ is ubiquitinated and degraded. Examples of targeted proteins during cold stress are JAZ1 and JAZ4, which repress *ICE1/2* transcription when bound by DELLAs. Thereby, JA-Ile production induces the ICE-CBF-COR regulon, which could explain the association between *JAR1* and WFS in the study. In addition, JA can also affect cold acclimation independent of the CBF pathway via the COI1– JAZ–DELLA–PIF pathway, regulating growth (Yang *et al*., 2012).

JA also promotes the biosynthesis of cold-protective secondary metabolites, such as polyamines, glutathione, and anthocyanins during cold stress (Hu *et al*., 2017). The production of glycosylated cyanins in particular is associated with enhanced winter hardiness in rye population analyzed in this study (Bahrani *et al*., 2019). Thus, it was interesting to note that sequence variation for three early enzymes in the phenylpropanoid pathway (PAL8, CHS2, and 4CL4) (Table 4.11 and Appendix 14) and late enzyme 3GT were associated with WFS for the rye population (Appendix 16). Anthocyanins, which are one of final products in the phenylpropanoid pathway, are assumed to have antioxidative functions *in vivo* and protect plant tissues from damage caused by reactive oxygen species induced by stress (Nagata *et al*., 2003).

5.9 Alterations at shoot apical meristem (SAM) during cold acclimation process

It is hypothesized that genes controlling the duration of the vegetative stage are switches controlling the length of low-temperature induced gene expression (Fowler and Limin, 2004). According to the model, a long cold acclimation period would allow for higher accumulation of frost tolerance and more leaves initials to be produced at the shoot apical meristem, which would result in higher FLN on the mature plant. A very strong association was found between WFS and FLN ($r = 0.80$) for the rye population (Table 4.3), and therefore floral transition time was considered a major component of WFS. WFS and FLN also shared 26 significant ($p < 0.001$) SNPs (Appendix 14) emphasizing a strong genetic link between the two traits. One of the common and strong SNPs for both traits coincided with a *JAR1* gene (Table 4.11), which catalyzes JA-Ile biosynthesis. High *JAR1* activity can increase frost tolerance by both CBF-dependent and CBF-independent pathways based on studies in Arabidopsis (Hu *et al*., 2017, 2013), but delay the juvenile-to-adult transition at shoot apical meristem as shown in rice (Hibara *et al*., 2016) and maize (Osadchuk *et al*., 2019). In addition, the JA-Ile activated co-receptor complex, SCFCOI1-JAZ, represses expression of *FLOWERING LOCUS T* (*FT*) in Arabidopsis via degradation of

specific JAZ proteins targeting TARGET OF EAT1/2 repressors for *FT* (Zhai *et al*., 2015). Thus, it is possible the association between *JAR1*, WFS and FLN observed in this study involves *JAR1*-mediated regulation of the flowering integrator FT, which promotes the switch from vegetative to reproductive growth at the shoot apical meristem (Båga *et al*., 2022).

5.10 Accumulation of anthocyanin compounds upon LT exposure

Based on the visual grading of anthocyanin accumulation and the HPLC-QTOF MS analyses, all very high and high winter hardiness genotypes produced anthocyanins in leaves. The cold-hardy genotypes showed an overall higher amount and diversity of anthocyanins as compared to rye genotypes with low winter hardiness (Tables 4.7 and 4.8). Lack of anthocyanin production in certain genotypes could be due to the presence of one or several recessive *Vi1- 6* genes identified as anthocyanin inhibitor allele(s) in certain rye germplasm (Voylokov *et al*., 2015).

High photosynthate capture during the day combined with slow metabolism at night due to LT reduces photosynthate metabolism and a buildup of sugars in the leaves. The elevated sucrose concentrations combined with high light intensity promote anthocyanin production in plants by stimulation of the UV-5/HY5/COP1 pathway (Shin *et al*., 2013). In response to LT, HY5 levels regulated by CBF proteins and ABA-independent transcription factor pathways (Catalá *et al*., 2011). HY5 degradation resulted in a reduction in anthocyanin biosynthesis in *A. thaliana* (Perea-Resa *et al*., 2017). Thus, the light dependency of anthocyanin production likely underlies the consistent higher amounts of anthocyanins accumulated in the photosynthetic leaves versus the non-photosynthetic crown tissues (Table 4.7).

All of the cold-induced anthocyanins identified in this study contained one or two sugar groups or an acetylated sugar group added to the C3 and C5 positions (Table 4.6; Appendices 11-13) as frequently seen for anthocyanins accumulated in plants (Williams and Grayer, 2004). The glycosylation likely occurs simultaneously with the anthocyanidin biosynthesis at the cytoplasmic surface of the endoplasmic reticulum (Lepiniec *et al*., 2006; Zhao and Dixon, 2009). This modification is suggested to increase anthocyanin stability and solubility and/or direct transport to different sub-cellular compartments (Zhao, 2015). The anthocyanins in leaves are present within the epidermal or mesophyll cell layers (Chalker-Scott, 1999) and mostly found within vacuoles, although some anthocyanins are also present in the cytosol, nucleus, and plastids (Agati *et al*., 2012). Anthocyanins are the most oxidized flavonoids and have been shown by several studies to

neutralize ROS and/or reduce ROS production in plants (Catalá *et al*., 2011; Gould *et al*., 2002; Havaux and Kloppstech, 2001; Li *et al*., 2017*b*; McKown *et al*., 1996; Nakabayashi *et al*., 2014; Schulz *et al*., 2016). It is hypothesised that the spatial separation of high-energy photon absorption by anthocyanins located within vacuoles protects the chloroplasts from the photoinhibitory and photooxidative effects of excess light (Gould, 2004). Absorption of stress induced H_2O_2 imported into vacuoles is another function for anthocyanins in the vacuole (Gould *et al*., 2002). Although anthocyanin accumulation during cold acclimation enhances winter hardiness, it may not be a prerequisite for protection from oxidative stress in all plant species (Gould, 2004; Nagata *et al*., 2003). Thus, very low accumulation of anthocyanins during cold acclimation for some cold-hardy rye cultivars like Enzi, Esprit, and Rymin could have been due to effective alternative antioxidant defenses in these cultivars. The ascorbate-glutathione cycle, catalases, superoxide dismutase and peroxidases are relevant alternative ROS detoxification systems in stressed plants (Gill and Tuteja, 2010). Similarly, low molecular weight compounds like hydroxycinnamates, ascorbate, tocopherols, glutathione, and β-carotene can also provide antioxidant effects in plants.

5.11 Cyanidin group of anthocyanins are associated with enhanced winter hardiness

Among the groups of anthocyanins, only glycosylated cyanidins significantly correlated with WFS, and Cya-3-Glc had the strongest correlation ($r = 0.35$, $p < 0.001$) as shown in Table 4.9. Delphinidins and pelargonidins, the other anthocyanin groups, did not significantly correlate with WFS (Table 4.9). These results are consistent with studies in Arabidopsis showing that accumulation of Cya-3-Rut during cold acclimation causes an increase in antioxidant activity and LTT and also provides higher resistance to salt and drought stress (Li *et al*., 2017*b*). Thus, a similar role may exist for Cya-3-Rut and other glycosylated cyanidins that accumulate in rye tissues during cold acclimation.

The GWAS results for anthocyanins were consistent with HPLC-QTOF MS/MS results in the rye population. In this study, 16 of the group 1 SNPs associated with WFS and anthocyanins, 11 SNPs (Tables 4.15 and 4.16; Appendix 16) were associated with WFS and cyanidins. Ten out of 11 SNPs were associated with Cya-3-Glc and Cya-3-Rut. However, only five SNPs in group 1 associated with the delphinidin/pelargonidin group of anthocyanins and WFS. Six SNPs in group 1 were found to be associated with WFS, and the cyanidins present in crown tissue extracts, such as three MTAs, coincided with early enzymes in the phenylpropanoid pathway (PAL8 and CHS2;

Table 4.15; Appendix 16). Crown plays an important role in plant survival and regrowth of new shoots and roots in winter cereals, such as wheat and rye (Halford *et al*., 2011). Relatively high antioxidant activity has also been found in sugars, such as fructans (Peshev *et al*., 2013), which accumulate to a relatively large degree in rye crown tissues during cold acclimation. Due to the importance of protection against oxidative stress during LT stress, various mechanisms providing efficient photon and ROS scavenging activities are likely factors selected during development of rye genotypes for the Northern temperate climates. Some of the anthocyanins in crown tissues may have been produced via the anthocyanin biosynthesis pathways, which are light-independent (Yang *et al*., 2017) or alternatively imported from other tissues as transport of anthocyanins between plant tissues seems to occur (Buer *et al*., 2007). Irrespective of the mechanism by which anthocyanins and other antioxidants accumulate in crowns, protection against ROS is essential because WFS depends on complete survival of the crown tissue from which new shoots and roots develop during regrowth in the early spring.

5.12 MTAs with possible role in phenylpropanoid pathway

In this study, markers coincided with early enzymes in the phenylpropanoid pathway (PAL8, CHS2) and late enzyme (3GT) were associated with WFS and Cya-3-Glc in rye genotypes (Table 4.15). PAL and CHS are key enzymes in the phenylpropanoid pathway and control synthesis of these pigments in response to LT and light intensity fluctuations (Appendix 17; Dangl, 1992; Leyva *et al*., 1995, MacDonald and D'Cunha, 2007). Low temperature combined with light intensity change can reduce photosynthetic activity (Hüner *et al*., 1993). These phenomena increase anthocyanin accumulation in leaves and stems because anthocyanins act as light-screening pigments (Mancinelli, 1984). In potato tubers, anthocyanin synthesis was believed to be reduced by a decrease in transcription of the *PAL* gene (Dancs *et al*., 2008). During cold acclimation, the PAL protein significantly accumulated in *Brassica napus* (Parra *et al*., 1990). Cold-acclimated *A. thaliana* plants increased the level of PAL and CHS in their leaves in response to LT stress, but only in the presence of light (Leyva *et al*., 1995). Is has been suggested that the photoregulated synthesis of flavonoids is at least partially involved in the induction of *CHS* genes (Chappell and Hahlbrock, 1984). PAL activity also increased in wheat under other abiotic stresses, such as drought, lead to increase ROS scavenging activity (Sallam *et al*., 2019). PAL and CHS have a significant role in protecting rye against UV-B radiation (Reuber *et al*., 1996).

CHS is a cold-related gene in winter wheat (Tchagang *et al*., 2017). The CHS genes can be expressed in multiple organs of wheat, such as leaf, culm, coleoptile, and grain pericarp and root (Tereshchenko *et al*., 2013). Four different CHS genes were characterized in rye and the enzyme was mostly present in vacuoles, and highly active in the epidermal layers of primary leaves (Haussühl *et al*., 1996). However, other cereals (e.g., barley and maize) have only two CHS genes (Niesbach-Klosgen *et al*., 1987). The homology among the rye CHS gene family is very high (88–99%). These highly homologous CHS genes suggest gene duplication during the evolution of rye after it segregated from barley and teosinte (Koes *et al*., 1987).

Anthocyanidin 3-O-glucosyltransferase (3GT) is a UDP-glucose flavonoid-3-O-glucosyltransferase that stabilizes anthocyanidins by 3-O-glucosylation (Zhao, 2015). This modification occurs at the cytoplasmic surface of the endoplasmic reticulum and support transportation of anthocyanins to different sub-cellular compartments (Lepiniec *et al*., 2006; Zhao, 2015). UDP-glucose flavonoid-3-O-glucosyltransferase *UGT78D2* is responsible for encoding an enzyme that is comparable to Bronze-1 (*BZl*) in Arabidopsis (Lee *et al*., 2005). In Arabidopsis, control over the metabolic flux of anthocyanins essentially required reciprocal regulation of *UGT78D2* (Schulz *et al*., 2015). Therefore, the expression level of CHS and *UGT78D1* genes increased in response to LT stress in Arabidopsis. Li *et al*. (2017*b*) found that other UGT family genes (*UGT79B2/B3*) significantly increased anthocyanin accumulation in Arabidopsis and also increased ROS scavenging capacity. In response to LT stress, CBF1 regulated *UGT79B2/B3* expression. *UGT79B2/B3* expression resulted in the addition of UDP-rhamnose to cyanidin or Cya-3-Glc (Li *et al*., 2017*b*).

5.13 Higher heterozygosity of stress related alleles in winter-hardy rye

Rye genotypes with high and very high WFS showed an overall higher heterozygosity frequency for candidate genes than genotypes with low or very low cold hardiness (Figs. 4.13-4.19; Appendix 15). This tendency was particularly obvious for *IRIP1*, *COR413-PM*, *FRL4-like*, *BIPP2C*, *CHUP1*, *CHS2* and *PAL8*, for which only four or fewer genotypes with low or very low WFS indicated heterozygosity. The trend may suggest many cold-hardy genotypes carry an additional copy of the above-mentioned candidate genes as compared to the sequenced Lo7 rye genome and genotypes with low cold-tolerance. A near full-length assembly (98.47% of genome) of Chinese rye line Weining with low heterozygote rate (0.26%) supports extensive duplications

of many rye genes as compared to Lo7 rye genome and other cereals (Li *et al*., 2021). Duplicated cold-stress genes may become non-functional or alternatively undergo sub-functionalization or neo-functionalization to widen the species capacity to respond to varying stress conditions. Gene expansion is not unique to cereals but has occurred throughout the evolutionary history of plants and is predominantly found for stress-responsive genes (Hanada *et al*., 2008).

5.14 Conclusions

This study of WFS over five years combined with studies of LTT and six developmental traits showed LTT accumulated during the cold acclimation was an important factor contributing to WFS. The developmental traits PGH, and FLN were highly correlated both to WFS and LTT, suggesting that changes at SAM during vernalization also contributed to WFS. PHT and TIL, which showed lower correlation with WFS than FLN and PGH (Table 4.3), appeared to be related to WFS for a sub-group of the rye population (Figs. 4.5 and 4.6). Variation in WFS among the rye genotypes could to a large extent be explained by differences in the number of leaf initials produced during cold acclimation. A longer cold acclimation period allowed the meristematic processes at SAM to last for a longer time, affecting the frequency of leaf primordia formation and the gravitropic response in the apical shoots. Both these morphogenetic processes are influenced by plant growth regulator concentrations in the meristematic tissues. FLA and DTA are traits developed in the spring in winter types and showed no or low association with WFS and FLN, but variation for the traits are expected to impact agronomic performance and grain yield.

Anthocyanins are an interesting group of compounds that have been shown to be associated with cold hardiness and WFS. An interesting finding in this study was that anthocyanin content and diversity was associated with WFS, but not with LTT (Tables 4.15 and 4.16; Appendix 16). The anthocyanin concentrations and diversity were higher in leaves than in the crown tissue (Table 4.7), suggesting a protective role against free radicals produced due to cold stress conditions. Leaves being above ground are the first organs to perceive low temperature during the autumn.

The GWAS analyses revealed that WFS marker associations (group 1) and the predicted functions of the candidate genes (Table 5.1) are related to the biological processes contributing to the WFS. The plasma membranes are the first contact with LT, IRIP1 (Xuos530120) help membrane stability, followed by FRI4-like (Xuos 372616) that remodel chromatin to respond to

Table 5.1 Significant MTA affecting Winter Field Survival.

Marker ID[1/]	Corresponding gene	Traits								Suggested Role[2/]
		WFS	LTT	FLN	PGH	DTA	PHT	TIL	FLA	
Group 1:										
Xuos526258	BIPP2C1	+	+	+	+	-	-	-	-	V
Xuos530120	IRIP1	+	+	-	+	-	-	-	-	CA
Xuos615052	ICE1	+	+	+	+	-	-	-	-	CA
Xuos519455	PAL8	+	-	-	-	-	-	-	-	CA
Xuos613978	COR413-PM	+	-	+	-	-	+	+	-	CA
Xuos75199	JAR1	+	-	+	-	-	-	-	+	V
Xuos76228a	CHS2	+	-	-	-	-	-	-	-	CA
Xuos76228b	CHS2	+	-	-	-	-	-	-	-	CA
Xuos2264	CHUP1	+	-	-	-	-	-	-	-	CA
Xuos372616	FRI4-like	+	-	-	-	-	+	+	-	CA
Group 2:										
Xuos615123	EXLA	+	-	+	-	-	-	-	+	CA
Xuos527421	GA2ox-D11	+	-	-	+	-	-	-	-	V
Xuos614178a	ABCC8	+	+	+	-	+	+	+	+	CA
Xuos75046	JAR1	+	-	+	-	-	-	-	+	V
Xuos79812	Alpha-glucosidase	+	-	+	-	-	+	+	+	CA
Xuos76179	Zinc finger CCCH-30	+	+	-	-	+	-	-	-	CA
Xuos643546	GLO3	+	-	+	-	-	-	-	-	CA
Xuos448335	XAT3	+	-	+	+	-	-	-	-	CA
Xuos173426	HCK	+	-	+	-	-	-	-	-	CA
Xuos176122	LCAT1	+	-	-	+	-	-	-	-	CA
Xuos172463	ZPR1-like	+	-	+	+	-	-	-	-	CA
Xuos628254	Chemocyanin	+	+	-	-	-	-	-	-	CA
Group 3:										
Xuos369733	CBFIIId- D19	+	-	-	-	-	-	-	-	CA
Xuos390086	CBFIVa- 2.2	+	-	-	-	-	-	-	-	CA
Xuos370362	CBFIIIa- 6.2	+	-	-	-	-	-	-	-	CA
Xuos76905	CBFIa-11.2	-	-	-	-	+	-	-	-	CA
Xuos328096	CBFII-5	-	-	+	-	-	-	-	-	CA

[1/] Number refers to matching rye Lo7_v2_scaffold number (Bauer *et al*. 2017)

[2/] CA – Cold acclimation; V- Vernalization

LT. The ICE1 (Xuos615052) induces *cbf* expression that causes expression of COR gene (Xuos613978) producing COR413-PM. The CHUP1 (Xuos2264) participates in chloroplast actin binding to favorably position chloroplasts, a key factor during cold acclimation to maintain photosynthesis in an optimal state. The favorable positioning of chloroplast is also aided by the WEB1 (Xuos370689) which has a role in blue light induced reorganization of chloroplast actin filaments. The BIPP2C1 (Xuos526258) and JAR1 (Xuos75199) is associated with plant growth regulators that influence the SMA activities influencing the plant developmental traits such as FLN, PGH and PHT. The PAL8 (Xuos519455), and CHS2 (Xuos76288a and Xuos76228b) catalyze key steps in the phenylpropanoid metabolism that result in the anthocyanin accumulation in plant tissues to mitigate the effects of free radicals formed in response to LT.

The identification of candidate genes and associating their allelic variation to WFS, LTT and plant developmental traits provided molecular basis for genotypic differences for WFS supporting the first hypothesis. The second hypothesis that WFS is an interaction between LTT and plant developmental traits was supported by several candidate genes that were common between these three physiological processes. The increase in anthocyanin concentration during cold acclimation and two phenylpropanoid biosynthetic genes (*PAL and CHS*) were also associated with WFS support the hypothesis that anthocyanin accumulation during cold acclimation increased the WFS in rye.

Among the group 2, MTA, the correlations were weak with WFS, LTT and plant developmental traits. The markers corresponded to candidate genes that had generalized functions. The ABCC8 (Xuos614178a), Zinc finger CCCH-30 (Xuos76179) and Chemocyanin (Xuos628254) were associated with WFS and LTT. The ABCC8 and Zinc finger CCCH-30 have several functions in plants. Interestingly, ABCC8 (Xuos614178) was associated with all traits studied except PGH. The candidate genes EXLA (Xuos615123), Alpha-galactosidase (Xuos79812), XAT3 (Xuos448335) and LCAT1 (Xuos176122) have a role in cell wall / membrane modification in response to LT stress. The remaining MTA have an association with plant growth regulators thus were associated with plants developmental traits and WFS. The low significance of the group 2 MTA suggest that the candidate genes contribute to WFS, but the diversity of their functions and involvement in other phenological traits, may explain the reduced significance to WFS and developmental traits analyzed in this study. The group 3 comprised of CBF genes at *FR-R2* on chromosome 5R, corresponded to five markers significant for WFS but at lower

significance (p <0.01) level (Table 5.1). The genes were *CBFIIId-19 (*Xuos369733), *CBFIVa-2.2* (Xuos390086), *CBFIIIa-6.2* (Xuos370362), CBFIa-11.2 (Xuos76905) and CBFII-11.2 (Xuos328096) that have been part of the major QTL for LTT and WFS (Erath *et al*., 2017; Jung and Seo, 2019; Li *et al*., 2011*a*). Transcript analysis of rye *CBF* genes indicates existence of three *CBFIVa-2*.2 and two *CBFIIIa-6* genes (Jung and Seo, 2019). This could possibly explain the low significance for individual *CBF* alleles as complementary functions may be exerted by additional copies of near-identical *CBF*; thus, SNP variations for multi-copy *CBF* genes contribute little to phenotype differences within the population. In addition, most mapping studies of bi-parental populations in wheat, barley, and rye show *Fr-2* has a major role for frost tolerance (Francia *et al.,* 2004; Båga *et al.,* 2007; Erath *et al.,* 2017). However, narrow genetic variation in the parents combined with limited number of recombination the confidence intervals for QTL regions are large. The characterized *FR* loci on group five chromosomes were defined by a composite effect from several *CBF* genes, their expression levels, interactions, and copy number effects. The use of GWAS in an outcrossing species such as rye overcome some of the challenges associated with bi-parental mapping and allow the identification of candidate genes as demonstrated in this thesis. The candidate genes can be used to develop gene specific markers that can be used to identify new sources of cold hardiness to incorporate into other cereals such as winter wheat and barley to improve their WFS.

5.15 Future studies

The present work on genetic analysis of developmental traits and anthocyanins associated with enhanced winter field survival in autumn-seeded rye can be extended in the following directions:

- Developmental traits such as PHT and TIL associated with WFS. As most open-pollinated cold-hardy rye varieties are tall, future research should focus on new sources of height-reducing genes for winter rye.
- The two strong candidate genes, *BIPP2C* and *FRL4-like*, with no reported association to WFS in Triticeae species have been identified in this thesis. Similar genes in other monocot species are implicated in floral transition, studies of the rye *BIPP2C* and *FRL4-like* could provide new advancements of the LTT process in winter cereals.

- An alternative explanation for higher number of allele variants for some of the candidate genes in winter-hardy rye genotypes could be due to suppressed recombination that maintained heterozygous state for certain chromosomal regions. Further studies are needed to confirm the copy number and inheritance pattern for WFS candidate genes identified in the study.
- Further studies will be required to determine the role of the different glycosylated cyanidin produced during LT stress in cold hardy rye genotypes. More studies are also required to assess how candidate genes associated with glycosylated cyanidins, and WFS can improve WFS in autumn-seeded rye.
- More studies are needed to identify gene variants that enhance winter survival in rye and use this information to increase WFS in the very ecologically friendly temperate winter cereals of interest in the Northern hemisphere.

REFERENCES

Abdel-Aal El-SM, Hucl P. 2003. Composition and stability of anthocyanins in blue-grained wheat. Journal of Agricultural and Food Chemistry **51**, 2174–2180.

Abdrakhamanova A, Yan-Wang Q, Khokhlova L, Nick P. 2003 Is microtubule disassembly a trigger for cold acclimation? Plant and Cell Physiology **44**, 676-686.

Abe M, Kobayashi Y, Yamamoto S, Ichinoki H, Notaguchi M, Goto K, Araki T. 2005. FD , a bZIP protein mediating signals from the floral pathway integrator FT at the shoot apex. Science **309**, 1052–1057.

Abuqamar S, Ajeb S, Sham A, Enan MR, Iratni R, 2013. A mutation in the expansin like *A2* gene enhances resistance to necrotrophic fungi and hypersensitivity to abiotic stress in *Arabidopsis thaliana.* Molecular Plant Pathology **14**, 813-827.

Achard P, Gong F, Cheminant S, Alioua M, Hedden P, Genschik P. 2008. The cold-inducible CBF1 factor-dependent signaling pathway modulates the accumulation of the growth-repressing DELLA proteins via its effect on gibberellin metabolism. The Plant Cell **20**, 2117–2129

Acharya S N, Mir Z, Moyer J R. 2004. ACE-1 perennial cereal rye. Canadian Journal of Plant Science **84**, 819–821.

Agati G, Azzarello E, Pollastri S, Tattini M. 2012. Flavonoids as antioxidants in plants: location and functional significance. Plant Science **196**, 67–76.

Agati G, Tattini M. 2010. Multiple functional roles of flavonoids in photoprotection. New Phytologist **186**, 786–793.

Alexandre CM, Hennig L. 2008. FLC or not FLC: the other side of vernalization. Journal of Experimental Botany **59**, 1127–1135.

Alqudah AM, Sallam A, Baenziger PS, Börner A. 2020. GWAS: Fast-forwarding gene identification and characterization in temperate cereals: lessons from barley. Journal of Advanced Research **22**, 119–135.

Andrés F, Coupland G. 2012. The genetic basis of flowering responses to seasonal cues. Nature Reviews Genetics **13**, 627–39.

Auringer H J, Schönleben M, Lehermeier C, Schmidt M, Korzun V, Geiger H H, Piepho HP, Gordillo A, Wilde P, Bauer E, Schön C C. 2016. Model training across multiple breeding cycles significantly improves genomic prediction accuracy in rye *Secale cereale* L. Theoretical and Applied Genetics **129**, 2043–2053.

Ayele A G. 2011. Heritability and genetic advance in recombinant inbred lines for drought tolerance and other related traits in sorghum *Sorghum bicolor*. Continental Journal of Agricultural Science **5**, 1-9

Backes G, Graner A, Foroughi-Wehr B, Fischbeck G, Wenzel G, Jahoor A. 1995. Localization of quantitative trait loci QTL for agronomic important characters by the use of a RFLP map in barley *Hordeum vulgare* L. Theoretical and Applied Genetics **90**, 294–302.

Badawi M, Danyluk J, Boucho B, Houde M, Sarhan F. 2007. The CBF gene family in hexaploid wheat and its relationship to the phylogenetic complexity of cereal CBFs. Molecular Genetics and Genomics **277**, 533–554.

Badawi M, Reddy YV, Agharbaoui Z, Tominaga Y, Danyluk J, Sarhan F, Houde M. 2008. Structure and functional analysis of wheat *ICE* (Inducer of CBF Expression) genes. Plant and Cell Physiology **49**, 1237–1249.

Båga M, Bahrani H, Larsen J, Hackauf B, Graf R, Laroche A, Chibbar R N. 2022. Association mapping of autumn-seeded rye *Secale cereale* L reveals genetic linkages between genes controlling winter field survival freezing tolerance and plant development. Sceintific Reports **12**, 5793.

Båga M, Chodaparambil SV, Limin AE, Pecar M, Fowler DB, Chibbar RN. 2007. Identification of quantitative trait loci and associated candidate genes for low-temperature tolerance in cold-hardy winter wheat. Functional and Integrative Genomics **7**, 53–68.

Båga M, Fowler DB, Chibbar RN. 2009. Identification of genomic regions determining the phenological development leading to floral transition in wheat (*Triticum aestivum* L.). Journal of Experimental Botany **60**, 3575–3585.

Bahrani H, Båga M, Larsen J, Hackauf B, Graf R, Laroche A, Chibbar RN. 2021. The relationships between plant developmental traits and winter field survival in rye *Secale cereale* L. Plants **10**, 2455.

Bahrani H, Thoms K, Båga M, Larsen J, Graf R, Laroche A, Sammynaiken R, Chibbar R N. 2019. Preferential accumulation of glycosylated cyanidins in winter-hardy rye *Secale*

cereale L genotypes during cold acclimation. Environmental and Experimental Botany **164**, 203–212.

Banaś A K, Aggarwal C, Łabuz J, Sztatelman O, Gabryś H. 2012. Blue light signaling in chloroplast movements. Journal of Experimental Botany **63**, 1559–1574.

Barrero-Gil J, Salinas J. 2013. Post-translational regulation of cold acclimation response. Plant Science **205**–**206**, 48-54.

Barrero-Gil J, Salinas J. 2018. Gene regulatory networks mediating cold acclimation: the CBF pathway. In: Iwaya-Inoue M, Sakurai M, Uemura M, eds. Survival strategies in extreme cold and desiccation. Springer, 3-22.

Batley J, Barker G, O'Sullivan H, Edwards KJ, Edwards D. 2003. Mining for single nucleotide polymorphisms and insertions/deletions in maize expressed sequence tag data. Plant Physiology **132**, 84–91.

Bauer E, Schmutzer T, Barilar I, Mascher M, Gundlach H, Martis M M, Twardziok S O, Hackauf B, Gordilo A, Wilde P, Schmidt M, Korzun V, Mayer K F, Schmid K, Schön C C, Scholz U. 2017. Towards a whole-genome sequence for rye *Secale cereale* L. The Plant Journal **89**, 853–869.

Baulcombe DC, Dean C. 2014. Epigenetic regulation in plant responses to the environment. Cold Spring Harbor Perspectives in Biology **6,** a019471.

Baxter A, Mittler R, Suzuki N. 2014. ROS as key players in plant stress signalling. Journal of Experimental Botany **65**, 1229–1240.

Bazakos C, Hanemian M, Trontin C, Jimenez-Gomez JM, Loudet O. 2017. New strategies and tools in quantitative genetics: how to go from the phenotype to the genotype. Annual Review of Plant Biology **68**, 435–455.

Beales J, Turner A, Griffiths S, Snape JW, Laurie DA. 2007. A pseudo-response regulator is misexpressed in the photoperiod insensitive Ppd-D1a mutant of wheat (*Triticum aestivum* L.). Theoretical and Applied Genetics **115**, 721–733.

Benjamini Y, Hochberg Y. 1995. Controlling the false discovery rate: a practical and powerful approach to multiple testing. Journal of the Royal Statistical Society **57**, 289–300.

Beres B L, Harker K N, Clayton G W, Bremer E, Blackshaw R E, Graf R J. 2010. Weed-competitive ability of spring and winter cereals in the northern great plains. Weed Technology **24**, 108–116.

Beydler B, Osadchuk K, Cheng CL, Manak JR, Irish EE. 2016. The juvenile phase of maize sees upregulation of stress-response genes and is extended by exogenous jasmonic acid. Plant Physiology **171**, 2648–2658.

Boden SA, Weiss D, Ross JJ, Davies NW, Trevaskis B, Chandler PM, Swain SM. 2014. EARLY FLOWERING3 regulates flowering in spring barley by mediating gibberellin production and FLOWERING LOCUS T expression. The Plant Cell **26**, 1557–1569.

Bogeat-Triboulot M B, Brosché M, Renaut J, Jouve L, Le Thiec D, Fayyaz P, Vinocur B, Witters E, Laukens K, Teichmann T, Altman A, Hausman JF, Polle A, Kangasjärvi J, Dreyer E. 2007. Gradual soil water depletion results in reversible changes of gene expression protein profiles ecophysiology and growth performance in *Populus euphratica* a poplar growing in arid regions. Plant Physiology **143**, 876-892.

Bolger A M, Lohse M, Usadel B. 2014. Trimmomatic: a flexible trimmer for Illumina sequence data. Bioinformatics **30**, 2114-2120.

Bors W, Heller W, Michel C, Saran M. 1990. Flavonoids as antioxidants: Determination of radical-scavenging efficiencies. Methods in Enzymology **186**, 343–355.

Bradbury P J, Zhang Z, Kroon D E, Casstevens T M, Ramdoss Y, Buckler E S. 2007. TASSEL: software for association mapping of complex traits in diverse samples. Bioinformatics **23**, 2633–2635.

Bradley D, Ratcliffe O, Vincent C, Carpenter R, Coen E. 1997. Inflorescence commitment and architecture in Arabidopsis. Science **275**, 80–83.

Braun E M, Tsvetkova N, Rotter B, Siekmann D, Schwefel K, Krezdorn N, Plieske J, Winter P, Melz G, Voylokov A V, Hackauf B. 2019. Gene expression profiling and fine mapping identifies a gibberellin 2-oxidase gene co-segregating with the dominant dwarfing gene *Ddw1* in rye *Secale cereale* L. Frontiers in Plant Science **10**, 857.

Bredow M, Tomalty H, Smith L, Walker V K. 2016a. Ice and anti-nucleating activities of an ice-binding protein from the annual grass *Brachypodium distachyon.* Plant Cell and Environment **41**, 983-992

Bredow M, Vanderbeld B, Walker VK. 2016b. Knockdown of Ice-binding proteins in *brachypodium distachyon* demonstrates their role in freeze protection. PLoS ONE **11**, 1–23.

Bredow M, Vanderbeld B, Walker VK. 2017. Ice-binding proteins confer freezing tolerance in

transgenic *Arabidopsis thaliana*. Plant Biotechnology Journal **15**, 68–81.

Bredow M, Walker VK. 2017. Ice-binding proteins in plants. Frontiers in Plant Science **8**, 2153.

Breton G, Danyluk J, Frenette Charron JB, Sarhan F. 2003. Expression profiling and bioinformatic analyses of a novel stress-regulated multispanning transmembrane protein family from cereals and Arabidopsis. Plant Physiology **132**, 64–74.

Brown DE, Rashotte AM, Murphy AS, Normanly J, Tague BW, Peer WA, Taiz L, Muday GK. 2001. Flavonoids act as negative regulators of auxin transport in vivo in Arabidopsis. Plant Physiology **126**, 524–535.

Brule-Babel AL, Fowler DB. 1988. Genetic control of cold hardiness and vernalization requirement in winter wheat. Crop Science **28**, 879-884.

Brunetti C, Fini A, Sebastiani F, Gori A, Tattini M. 2018. Modulation of phytohormone signaling: A primary function of flavonoids in plant–environment interactions. Frontiers in Plant Science **9**, 1–8.

Buer CS, Imin N, Djordjevic MA. 2010. Flavonoids: New roles for old molecules. Journal of Integrative Plant Biology **52**, 98–111.

Buer CS, Muday GK, Djordjevic MA. 2007. Flavonoids are differentially taken up and transported long distances in Arabidopsis. Plant Physiology **145**, 478–490.

Buntjer J B, Sørensen A P, Peleman J D. 2005. Haplotype diversity: the link between statistical and biological association. Trends in Plant Science **10**, 466-471.

Campoli C, Matus-Cádiz MA, Pozniak CJ, Cattivelli L, Fowler DB. 2009. Comparative expression of *Cbf* genes in the Triticeae under different acclimation induction temperatures. Molecular Genetics and Genomics **282**, 141–152.

Canella D, Gilmour SJ, Kuhn LA, Thomashow MF. 2010. DNA binding by the Arabidopsis CBF1 transcription factor requires the PKKP/RAGRxKFxETRHP signature sequence. Biochimica et Biophysica Acta **1799**, 454–462.

Casal JJ, Qüesta JI. 2018. Light and temperature cues: multitasking receptors and transcriptional integrators. New Phytologist **217**, 1029–1034.

Catalá R, Medina J, Salinas J. 2011. Integration of low temperature and light signaling during cold acclimation response in *Arabidopsis.* Proceedings of the National Academy of Sciences of the United States of America **108**, 16475– 16480.

Cattivelli L, Baldi P, Crosatti C, Di Fonzo N, Faccioli P, Grossi M, Mastrangelo A M, Pecchioni N, Stanca A M. 2002. Chromosome regions and stress - related sequences involved in resistance to abiotic stress in Triticeae. Plant Molecular Biology **48**, 649 – 665.

Chailakhyan MKh. 1936. On the hormonal theory of plant development. Proceedings of the USSR Academy of Science, **3**, 443–447

Chalker-Scott L. 1999. Environmental significance of anthocyanins in plant stress responses Photochemistry and Photobiology **70**, 1–9.

Chao S, Dubcovsky J, Dvorak J, Luo M-C, Baenziger SP, Matnyazov R, Clark DR, Talbert LE, Anderson JA, Dreisigacker S, Glover K, Chen J, Campbell K, Bruckner PL, Rudd JC, Haley S, Carver BF, Perry S, Sorrells ME, Akhunov ED. 2010. Population- and genome-specific patterns of linkage disequilibrium and SNP variation in spring and winter wheat *Triticum aestivum* L. BMC Genomics **11**, 727.

Chappell J, Hahlbrock K. 1984. Transcription of plant defense genes in response to UV light or fungal elicitor. Nature **311**, 76–78.

Chavent M, Kuentz-Simonet V, Saracco J. 2012. Orthogonal rotation in PCAMIX. Advances in Data Analysis and Classification **6**, 131-146.

Chen G, Greer M S, Lager I, Yilmaz J L, Mietkiewska E, Carlsson A S, Stymne S, Weselake R J. 2012. Identification and characterization of an LCAT-like *Arabidopsis thaliana* gene encoding a novel phospholipase. FEBS Letters **586**, 373-377.

Chen H-J, Chen C-L, Hsieh H-L. 2015. Far-red light-mediated seedling development in *Arabidopsis* involves FAR-RED INSENSITIVE 219/JASMONATE RESISTANT 1-dependent and -independent pathways. PLoS ONE **10**, e013272.

Chen TH-H, Gusta L V, Fowler DB. 1983. Freezing injury and root development in winter cereals. Plant Physiology **73**, 773–777.

Chen Y, Carver BF, Wang S, Zhang F, Yan L. 2009. Genetic loci associated with stem elongation and winter dormancy release in wheat. Theoretical and Applied Genetics **118**, 881–889.

Chinnusamy V, Ohta M, Kanrar S, Lee BH, Hong X, Agarwal M, Zhu JK. 2003. ICE1: a regulator of cold-induced transcriptome and freezing tolerance in *Arabidopsis.* Genes and Development **17**, 1043–1054.

Chinnusamy V, Zhu J, Zhu JK. 2007. Cold stress regulation of gene expression in plants. Trends in Plant Science **12**, 444-452.

Choi K, Kim J, Hwang HJ, Kim S, Park C, Kim SY, Lee I. 2011. The FRIGIDA complex activates transcription of FLC a strong flowering repressor in Arabidopsis by recruiting chromatin modification factors. The Plant Cell **23**, 289–303.

Chouard P. 1960. Vemalization and its relations to dormancy. Annual Review of Plant Physiology **11**, 19l-238.

Christov NK, Imai R, Blume Y. 2008. Differential expression of two winter wheat alpha-tubulin genes during cold acclimation. Cell Biology International **32**, 574–578.

Christova PK, Christov NK, Imai R. 2006. A cold inducible multidomain cystatin from winter wheat inhibits growth of the snow mold fungus, *Microdochium nivale*. Planta **223**, 1207–18.

Clapham D E. 2007. Calcium signaling. Cell **131**, 1047 – 1058.

Clouse SD. 2011. Brassinosteroids. The Arabidopsis Book **9**, e0151.

Cochrane FC, Davin LB, Lewis NG. 2004. The Arabidopsis phenylalanine ammonia lyase gene family: Kinetic characterization of the four PAL isoforms. Phytochemistry **65**, 1557–1564.

Colton-Gagnon K, Ali-Benali MA, Mayer BF, Dionne R, Bertrand A, Do Carmo S, Charron JB. 2014. Comparative analysis of the cold acclimation and freezing tolerance capacities of seven diploid *Brachypodium distachyon* accessions. Annals of Botany **113**, 681–693.

Cook D, Fowler S, Fiehn O, Thomashow MF. 2004. A prominent role for the CBF cold response pathway in configuring the low-temperature metabolome of Arabidopsis. Proceedings of the National Academy of Sciences of the United States of America **101**, 15243–15248.

Corbesier L, Coupland G. 2006. The quest for florigen: a review of recent progress. Journal of Experimental Botany **57**, 3395–3403.

Corbesier L, Vincent C, Jang S, Fornara F, Fan Q, Searle I, Giakountis A, Farrona S, Gissot L, Turnbull C, Coupland G. 2007. FT protein movement contributes to long-distance signaling in floral induction of Arabidopsis. Science **316**, 1030–1033.

Cosgrove DJ. 2000. New genes and new biological roles for expansins. Current Opinion in Plant Biology **3**, 73-78.

Crosatti C, Polverino de Laureto P, Bassi R, Cattivelli L. 1999. The interaction between cold and light controls the expression of the cold-regulated barley gene *cor14b* and the

accumulation of the corresponding protein. Plant physiology **119**, 671–680.

Dahal K, Kane K, Gadapati W, Webb E, Savitch LV, Singh J, Sharma P, Sarhan F, Longstaffe FJ, Grodzinski B, Hüner NP. 2012. The effects of phenotypic plasticity on photosynthetic performance in winter rye, winter wheat and *Brassica napus*. Physiologia Plantarum **144**, 169–188.

Dancs G, Kondrák M, Bánfalvi Z. 2008. The effects of enhanced methionine synthesis on amino acid and anthocyanin content of potato tubers. BMC Plant Biology **8**, 65.

Danecek P, Auton A, Abecasis G, Albers C A, Banks E, DePristo M A, Handsaker R E, Lunter G, Marth G T, Sherry S T, McVean G, Durbin R, 1000 Genomes Project Analysis Group. 2011 the variant call format and VCFtools. Bioinformatics **27**, 2156–2158.

Dangl JL. 1992. Regulatory elements controlling developmental and stress induced expression of phenylpropanoid genes. In: Boller T, Meins F, eds. Plant gene research: genes involved in plant research. Springer-Verlag, 303-336

Danyluk J, Carpentier E, Sarhan F. 1996. Identification and characterization of a low temperature regulated gene encoding an actin-binding protein from wheat. FEBS Letters **389**, 324–327.

Danyluk J, Houde M, Rassart É, Sarhan F. 1994. Differential expression of a gene encoding an acidic dehydrin in chilling sensitive and freezing tolerant gramineae species. FEBS Letters **344**, 20–24.

Danyluk J, Kane NA, Breton G, Limin AE, Fowler DB, Sarhan F. 2003. TaVRT-1 , a putative transcription factor associated with vegetative to reproductive transition in cereals. Plant Physiology **132**, 1849–1860.

Danyluk J, Perron A, Houde M, Limin A, Fowler B, Benhamou N, Sarhan F. 1998. Accumulation of an acidic dehydrin in the vicinity of the plasma membrane during cold acclimation of wheat. The Plant cell **10**, 623–638.

Das PK, Shin DH, Choi SB, Park Y I. 2012. Sugar-hormone cross-talk in anthocyanin biosynthesis. Molecules and cells **34**, 501–507.

Davey JW, Hohenlohe PA, Etter PD, Boone JQ, Catchen JM, Blaxter ML. 2011. Genome-wide genetic marker discovery and genotyping using next-generation sequencing. Nature Reviews Genetics **12**, 499-510.

De Bruyne L, Höfte M, De Vleesschauwer D. 2014. Connecting growth and defense: The emerging roles of brassinosteroids and gibberellins in plant innate immunity. Molecular Plant **7**, 943–959.

DeFalco TA, Bender KW, Snedden WA. 2010. Breaking the code: Ca^{2+} sensors in plant signalling. Biochemical Journal **425**, 27 – 40.

Delgado JA, Sparks RT, Follett RF, Sharkoff JL, Riggenbach RR. 1999. Use of winter cover crops to conserve soil and water quality in the San Luis Valley of South Central Colorado. In: Lal R, ed. Soil quality and soil erosion. CRC Press, 125–142.

Delseny M, Han B, Hsing YI. 2010. High throughput DNA sequencing: The new sequencing revolution. Plant Science **179**, 407-422.

Deng W, Casao MC, Wang P, Sato K, Hayes PM, Finnegan EJ, Trevaskis B. 2015. Direct links between the vernalization response and other key traits of cereal crops. Nature Communications **6**, 6882.

Deng W, Ying H, Helliwell CA, Taylor JM, Peacock WJ, Dennis ES. 2011. FLOWERING LOCUS C (FLC) regulates development pathways throughout the life cycle of *Arabidopsis*. Proceedings of the National Academy of Sciences of the United States of America **108**, 6680–6685.

Devos KM, Atkinson MD, Chinoy CN, Francis HA, Harcourt RL, Koebner RMD, Liu C J, Masojć P, Xie D X, Gale M D. 1993. Chromosomal rearrangements in the rye genome relative to that of wheat. Theoretical and Applied Genetics **85**, 673–680.

Dhillon T, Pearce S P, Stockinger E J, Distelfeld A, Li C, Knox A K, Vashegyi I, Vágújfalvi A, Galiba G, Dubcovsky J. 2010. Regulation of freezing tolerance and flowering in temperate cereals: the *VRN-1* connection. Plant Physiology **153**, 1846–1858.

Diallo AO, Ali-Benali MA, Badawi M, Houde M, Sarhan F. 2012. Expression of vernalization responsive genes in wheat is associated with histone H3 trimethylation. Molecular Genetics and Genomics **287**, 575–590.

Díaz A, Zikhali M, Turner AS, Isaac P, Laurie DA. 2012. Copy number variation affecting the *photoperiod-B1* and *vernalization-A1* genes is associated with altered flowering time in wheat (*Triticum aestivum*). PLoS ONE **7**, e33234

Ding Y, Li H, Zhang X, Xie Q, Gong Z, Yang S. 2015. OST1 kinase modulates freezing tolerance by enhancing ICE1 stability in *Arabidopsis.* Developmental Cell **32**, 278–289.

Ding Y, Shi Y, Yang S. 2020. Molecular regulation of plant responses to environmental temperatures. Molecular Plant **13**, 544-564.

Divi UK, Krishna P. 2009. Brassinosteroid: a biotechnological target for enhancing crop yield and stress tolerance. New Biotechnology **26**, 131–136.

Dixon LE, Karsai I, Kiss T, Adamski NM, Liu Z, Ding Y, Allard V, Boden SA, Griffiths S. 2019. *VERNALIZATION1* controls developmental responses of winter wheat under high ambient temperatures. Development **146**, dev172684.

Doherty CJ, Van Buskirk H a, Myers SJ, Thomashow MF. 2009. Roles for Arabidopsis CAMTA transcription factors in cold-regulated gene expression and freezing tolerance. The Plant cell **21**, 972–84.

Doležel J, Čížková J, Šimková H, Bartoš J. 2018. One major challenge of sequencing large plant genomes is to know how big they really are. International Journal of Molecular Sciences **19**, 1–6.

Dong H, Yan S, Liu J, Liu P, Sun J. 2019. TaCOLD1 defines a new regulator of plant height in bread wheat. Plant Biotechnology Journal **3**, 687-699.

Dong J, Kim S T, Lord E M. 2005. Plantacyanin plays a role in reproduction in Arabidopsis. Plant Physiology **138**, 778–789.

Dong M a, Farré EM, Thomashow MF. 2011. Circadian clock-associated 1 and late elongated hypocotyl regulate expression of the C-repeat binding factor (CBF) pathway in Arabidopsis. Proceedings of the National Academy of Sciences of the United States of America **108**, 7241–6.

Dong S, Beckles DM. 2019. Dynamic changes in the starch-sugar interconversion within plant source and sink tissues promote a better abiotic stress response. Journal of Plant Physiology **234**–**235**, 80–93.

Dong Z, Jiang C, Chen X, Zhang T, Ding L, Song W, Luo H, Lai J, Chen H, Liu R, Zhang X, Jin W. 2013. Maize LAZY1 mediates shoot gravitropism and inflorescence development through regulating auxin transport auxin signaling and light response. Plant Physiology **163**, 1306–1322.

Dubcovsky J, Loukoianov A, Fu D, Valarik M, Sanchez A, Yan L. 2006. Effect of photoperiod on the regulation of wheat vernalization genes *VRN1* and *VRN2*. Plant Molecular Biology **60**, 469–480.

Duek PD, Fankhauser C. 2005. bHLH class transcription factors take centre stage in phytochrome signalling. Trends in Plant Science **10**, 51–4.

Eagles H a., Cane K, Trevaskis B. 2011. Veery wheats carry an allele of *Vrn-A1* that has implications for freezing tolerance in winter wheats. Plant Breeding **130**, 413–418.

Earl D A, Von Holdt B M. 2012. STRUCTURE HARVESTER: a website and program for visualizing STRUCTURE output and implementing the Evanno method. Conservation Genetics Resources **4**, 359-361.

Elshire RJ, Glaubitz JC, Sun Q, Poland JA, Kawamoto K, Buckler ES, Mitchell SE. 2011. A robust simple genotyping-by-sequencing GBS approach for high diversity species. PLoS ONE **6**, e19379.

Emiliani J, Grotewold E, Falcone Ferreyra ML, Casati P. 2013. Flavonols protect *Arabidopsis* plants against UV-B deleterious effects. Molecular Plant **6**, 1376–1379.

Ensminger I, Busch F, Huner NPA. 2006. Photostasis and cold acclimation : sensing low temperature through photosynthesis. Physiologia Plantarum **126**, 28–44.

Entz MH, Fowler DB. 1991. Agronomic performance of winter versus spring wheat. Agronomy Journal **83**, 527-532.

Erath W, Bauer E, Fowler DB, Gordillo A, Korzun V, Ponomareva M, Schmidt M, Schmiedchen B, Wilde P, Schön C-C. 2017. Exploring new alleles for frost tolerance in winter rye. Theoretical and Applied Genetics **130**, 2151–2164.

Eremina M, Rozhon W, Poppenberger B. 2016. Hormonal control of cold stress responses in plants. Cellular and Molecular Life Sciences **73**, 797–810.

Evanno G, Regnaut S, Goudet J. 2005. Detecting the number of clusters of individuals using the software STRUCTURE: a simulation study. Molecular Ecology **14**, 2611-2620.

Evans MMS, Poethig RS. 1995. Gibberellins promote vegetative phase change and reproductive maturity in maize. Plant Physiology **108**, 475–487.

Famoso A N, Zhao K, Clark R T, Tung C W, Wright M H, Bustamante C, Kochian L V, McCouch S R. 2011. Genetic architecture of aluminum tolerance in rice *Oryza sativa* determined through genome-wide association analysis and QTL mapping. PLoS Genetics **7**, e1002221.

FAO Organization. 2021. http://www.fao.org/docrep. Accessed December 2021.

FAOSTAT. 2019. FAO Statistics Division http://wwwfaoorg/faostat. Accessed June 2019.

Fedenko VS, Shemet SA, Landi M. 2017. UV–vis spectroscopy and colorimetric models for detecting anthocyanin-metal complexes in plants: an overview of *in vitro* and *in vivo* techniques. Journal of Plant Physiology **212**, 13–28.

Feng X, Xu Y, Peng L, Yu X, Zhao Q, Feng S, Zhao Z, Li F, Hu B. 2019. *TaEXPB7-B* a β-expansin gene involved in low-temperature stress and abscisic acid responses promotes growth and cold resistance in *Arabidopsis thaliana*. Journal of Plant Physiology **240**, 153004.

Fey V, Wagner R, Bräutigam K, Pfannschmidt T. 2005. Photosynthetic redox control of nuclear gene expression. Journal of Experimental Botany **56**, 1491–1498.

Fischer S, Melchinger AE, Korzun V, Wilde P, Schmiedchen B, Möhring J, Piepho HP, Dhillon BS, Würschum T, Reif JC. 2010. Molecular marker assisted broadening of the Central European heterotic groups in rye with Eastern European germplasm. Theoretical and Applied Genetics **120**, 291–299.

Flint-Garcia SA, Thornsberry JM, Buckler ES. 2003. Structure of linkage disequilibrium in plants. Annual Review of Plant Biology **l54**, 357–374.

Fonseca S, Chini A, Hamberg M, Adie B, Porzel A, Kramell R, Miersch O, Wasternack C, Solano R. 2009. +-7-iso-Jasmonoyl-L-isoleucine is the endogenous bioactive jasmonate. Nature Chemical Biology **5**, 344–350.

Fowler D B, Limin A E. 2004. Interactions among factors regulating phenological development and acclimation rate determine low - temperature tolerance in wheat. Annals of Botany **94**, 717 – 724.

Fowler DB, Byrns BM, Greer KJ. 2014. Overwinter low-temperature responses of cereals: Analyses and simulation. Crop Science **54**, 2395–2405.

Fowler DB, Carles RJ. 1979. Growth development and cold tolerance of fall-acclimated cereal-grains. Crop Science **19**, 915–922.

Fowler DB, Chauvin LP, Limin AE, Sarhan F. 1996a. The regulatory role of vernalization in the expression of low-temperature-induced genes in wheat and rye. Theoretical and Applied Genetics **93**, 554–559.

Fowler DB, Limin AE, Mahfoozi S, Sarhan F. 2001. Photoperiod and temperature interactions regulate low-temperature-induced gene expression in barley. Plant Physiology **127**, 1676–1681.

Fowler DB, Limin AE, Wang SY, Ward RW. 1996b. Relationship between low-temperature tolerance and vernalization response in wheat and rye. Canadian Journal of Plant Science **76**, 37–42.

Fowler DB. 2002. Winter wheat production manual. https://wwwusaskca/agriculture/plantsci/winter_cereals. Accessed June 2021.

Fowler DB. 2008. Cold acclimation threshold induction temperatures in cereals. Crop Science **48**, 1147 – 1154.

Fowler S, Thomashow MF. 2002. Arabidopsis transcriptome profiling indicates that multiple regulatory pathways are activated during cold acclimation in addition to the CBF cold response pathway. The Plant Cell **14**, 1675–1690.

Fowler SG, Cook D, Thomashow MF. 2005. Low temperature induction of Arabidopsis CBF1 , 2 , and 3 is gated by the circadian clock. Plant Physiology **137**, 961–968.

Francia E, Barabaschi D, Tondelli A, Laidò G, Rizza F, Stanca A M, Busconi M, Fogher C, Stockinger EJ, Pecchioni N. 2007. Fine mapping of a *HvCBF* gene cluster at the frost resistance locus *Fr-H2* in barley. Theoretical and Applied Genetics **115**, 1083–1091.

Francia E, Rizza F, Cattivelli L, Stanca AM, Galiba G, Tóth B, Hayes PM, Skinner JS, Pecchioni N. 2004. Two loci on chromosome 5H determine low-temperature tolerance in a 'Nure' (winter) x 'Tremois' (spring) barley map. Theoretical and Applied Genetics **108**, 670–680.

Francia E, Morcia C, Pasquariello M, Mazzamurro V, Milc JA, Rizza F, Terzi V, Pecchioni N. 2016. Copy number variation at the *HvCBF4–HvCBF2* genomic segment is a major component of frost resistance in barley. Plant Molecular Biology **92**, 161–175.

Franklin KA, Whitelam GC. 2007. Light-quality regulation of freezing tolerance in *Arabidopsis thaliana.* Nature Genetics **39**, 1410–1413.

Fu X, Richards D E, Ait-Ali T, Hynes L W, Ougham H, Peng J, Harberd N P. 2002. Gibberellin-mediated proteasome-dependent degradation of the barley DELLA protein SLN1 repressor. The Plant Cell **14**, 3191–3200.

Fujii Y, Ogasawara Y, Takahashi Y, Sakata M, Noguchi M, Tamura S, Kodama Y. 2020. The cold-induced switch in direction of chloroplast relocation occurs independently of changes in endogenous phototropin levels. PLoS ONE **15**, 1–15.

Fujii Y, Tanaka H, Konno N, Ogasawara Y, Hamashima N, Tamura S, Hasegawa S,

Hayasaki Y, Okajima K, Kodama Y. 2017. Phototropin perceives temperature based on the lifetime of its photoactivated state. Proceedings of the National Academy of Sciences of the United States of America **114**, 9206–9211.

Fursova O V, Pogorelko G V, Tarasov V A. 2009. Identification of *ICE2* a gene involved in cold acclimation which determines freezing tolerance in *Arabidopsis thaliana*. Gene **429**, 98–103.

Fürtauer L, Weiszmann J, Weckwerth W, Nägele T. 2019. Dynamics of plant metabolism during cold acclimation. International Journal of Molecular Sciences **20**, 5411.

Gaarslev N, Swinnen G, Soyk S. 2021. Meristem transitions and plant architecture—learning from domestication for crop breeding. Plant Physiology **187**, 1045–1056.

Gaikpa D S, Koch S, Fromme F J, Siekmann D, Würschum T, Miedaner T. 2020. Genome-wide association mapping and genomic prediction of Fusarium head blight resistance heading stage and plant height in winter rye *Secale cereale.* Plant Breeding **139**, 508-520.

Galán RJ, Bernal-Vasquez AM, Jebsen C, Piepho HP, Thorwarth P, Steffan P, Gordillo A, Miedaner T. 2020. Integration of genotypic, hyperspectral, and phenotypic data to improve biomass yield prediction in hybrid rye. Theoretical and Applied Genetics **133**, 3001–3015.

Galiba G, Vágújfalvi A, Li C, Soltész A, Dubcovsky J. 2009. Regulatory genes involved in the determination of frost tolerance in temperate cereals. Plant Science **176**, 12–19.

Gan P, Liu F, Li R, Wang S, Luo J. 2019. Chloroplasts- beyond energy capture and carbon fixation: Tuning of photosynthesis in response to chilling stress. International Journal of Molecular Sciences **20**, 5046.

Ganeshan S, Sharma P, Young L, Kumar A, Fowler DB, Chibbar RN. 2011. Contrasting cDNA-AFLP profiles between crown and leaf tissues of cold-acclimated wheat plants indicate differing regulatory circuitries for low temperature tolerance. Plant Molecular Biology **75**, 379–398.

Ganeshan S, Vitamvas P, Fowler DB, Chibbar RN. 2008. Quantitative expression analysis of selected *COR* genes reveals their differential expression in leaf and crown tissues of wheat (*Triticum aestivum* L.) during an extended low temperature acclimation regimen. Journal of Experimental Botany **59**, 2393–2402.

Garcia M, Eckermann P, Haefele S, Satija S, Sznajder B, Timmins A, Baumann U, Wolters P, Mather D E, Fleury D. 2019. Genome-wide association mapping of grain yield in a diverse collection of spring wheat *Triticum aestivum* L evaluated in southern Australia. PLoS ONE **14**, 1-19.

Garner WW, Allard HA. 1920. Effect of the relative length of day and night and other factors of the environment on growth and reproduction in plants. Journal of Agricultural Research **18**, 553–606.

Gaudet DA, Laroche A, Yoshida M. 1999. Low temperature-wheat-fungal interactions: A carbohydrate connection. Physiologia Plantarum **106**, 437–444.

Geiger HH, Miedaner T. 2009. Rye (*Secale cereale* L.). In: Carena MJ, ed. Cereals. Springer, 157–181.

Geraldo N, Bäurle I, Kidou SI, Hu X, Dean C. 2009. FRIGIDA delays flowering in Arabidopsis via a cotranscriptional mechanism involving direct interaction with the nuclear cap-binding complex. Plant Physiology **150**, 1611–1618.

Ghelis T, Bolbach G, Clodic G, Habricot Y, Miginiac E, Sotta B, Jeannette E. 2008. Protein tyrosine kinases and protein tyrosine phosphatases are involved in abscisic acid-dependent processes in Arabidopsis seeds and suspension cells. Plant Physiology **148**, 1668–1680.

Gill S S, Tuteja N. 2010. Reactive oxygen species and antioxidant machinery in abiotic stress tolerance in crop plants. Plant Physiology and Biochemistry **48**, 909–930.

Gilmour SJ, Fowler SG, Thomashow MF. 2004. Arabidopsis transcriptional activators CBF1 CBF2 and CBF3 have matching functional activities. Plant Molecular Biology **54**, 767–781.

Gilmour SJ, Sebolt A M, Salazar MP, Everard JD, Thomashow MF. 2000. Overexpression of the Arabidopsis *CBF3* transcriptional activator mimics multiple biochemical changes associated with cold acclimation. Plant Physiology **124**, 1854–1865.

Gilmour SJ, Thomashow MF. 1991. Cold acclimation and cold-regulated gene expression in ABA mutants of *Arabidopsis thaliana*. Plant Molecular Biology **17**, 1233–1240.

Gilmour SJ, Zarka DG, Stockinger EJ, Salazar MP, Houghton JM, Thomashow MF. 1998. Low temperature regulation of the *Arabidopsis* CBF family of AP2 transcriptional activators as an early step in cold-induced *COR* gene expression. The Plant Journal **16**, 433–442.

Gorsuch P a, Sargeant AW, Penfield SD, Quick WP, Atkin OK. 2010. Systemic low temperature signaling in Arabidopsis. Plant and Cell Physiology **51**, 1488–98.

Gould K S. 2004. Nature's Swiss army knife: The diverse protective roles of anthocyanins in leaves. Journal of Biomedicine and Biotechnology **5**, 314–320.

Gould KS, McKelvie J, Markham KR. 2002. Do anthocyanins function as antioxidants in leaves? Imaging of H_2O_2 in red and green leaves after mechanical injury. Plant Cell and Environment **25**, 1261–1269.

Graingenes, a database for Triticeae and Avena. 2021. https://wheat.pw.usda.gov/blast Accessed March 2021.

Gray GR, Chauvin LP, Sarhan F, Huner NPA. 1997. Cold acclimation and freezing tolerance. A complex interaction of light and temperature. Plant Physiology **114**, 467–474.

Greenup AG, Sasani S, Oliver SN, Talbot MJ, Dennis ES, Hemming MN, Trevaskis B. 2010. *ODDSOC2* is a MADS box floral repressor that is down-regulated by vernalization in temperate cereals. Plant Physiology **153**, 1062–73.

Griffith M, Lumb C, Wiseman S B, Wisniewski M, Johnson R W, Marangoni A G. 2005. Antifreeze proteins modify the freezing process in planta. Plant Physiology **138**, 330–340.

Griffith M, Yaish MWF. 2004. Antifreeze proteins in overwintering plants: a tale of two activities. Trends in Plant Science **9**, 399–405.

Guadagno CR, Ewers BE, Weinig C. 2018. Circadian rhythms and redox state in plants: Till stress do us part. Frontiers in Plant Science **9**, 1–9.

Guo X, Liu D, Chong K. 2018. Cold signaling in plants: Insights into mechanisms and regulation. Journal of Integrative Plant Biology **60**, 745–756.

Gupta R, Deswal R. 2012. Low temperature stress modulated secretome analysis and purification of antifreeze protein from *hippophae rhamnoides* a himalayan wonder plant. Journal of Proteome Research **11**, 2684–2696.

Gupta R, Deswal R. 2014. Antifreeze proteins enable plants to survive in freezing conditions. Journal of Biosciences **39**, 931–944.

Gusta L V, Wisniewski M. 2013. Understanding plant cold hardiness: an opinion. Physiologia Plantarum **147**, 4–14.

Gusta L V., Wisniewski M, Nesbitt NT, Gusta ML. 2004. The effect of water, sugars, and proteins on the pattern of ice nucleation and propagation in acclimated and nonacclimated

canola leaves. Plant Physiology **135**, 1642–1653.

Guy C, Kaplan F, Kopka J, Selbig J, Hincha DK. 2008. Metabolomics of temperature stress. Physiologia Plantarum **132**, 220–235.

Hahn A, Kilian J, Mohrholz A, Ladwig F, Peschke F, Dautel R, Harter K, Berendzen KW, Wanke D. 2013. Plant core environmental stress response genes are systemically coordinated during abiotic stresses. International Journal of Molecular Sciences **14**, 7617–7641.

Halford N G, Curtis T Y, Muttucumaru N, Postles J, Mottram D S. 2011. Sugars in crop plants. Annals of Applied Biology **158**, 1–25.

Hanada K, Zou C, Lehti-Shiu MD, Shinozaki K, Shiu SH. 2008. Importance of lineage-specific expansion of plant tandem duplicates in the adaptive response to environmental stimuli. Plant Physiology **148**, 993-1003.

Hanin M, Brini F, Ebel C, Toda Y, Takeda S, Masmoudi K. 2011. Plant dehydrins and stress tolerance: versatile proteins for complex mechanisms. Plant Signaling and Behavior **6**, 1503–1509.

Hannah M a, Wiese D, Freund S, Fiehn O, Heyer AG, Hincha DK. 2006. Natural genetic variation of freezing tolerance in Arabidopsis. Plant Physiology **142**, 98–112.

Hannah MA, Heyer AG, Hincha DK. 2005. A global survey of gene regulation during cold acclimation in *Arabidopsis thaliana.* PLoS Genetics **1**, 26.

Harmer SL. 2009. The circadian system in higher plants. Annual Review of Plant Biology **60**, 357–377.

Hasanuzzaman M, Bhuyan MHMB, Parvin K, Bhuiyan TF, Anee TI, Nahar K, Hossen MS, Zulfiqar F, Alam MM, Fujita M. 2020*a*. Regulation of ros metabolism in plants under environmental stress: A review of recent experimental evidence. International Journal of Molecular Sciences **21**, 1–44.

Hasanuzzaman M, Bhuyan MHMB, Zulfiqar F, Raza A, Mohsin SM, Al Mahmud J, Fujita M, Fotopoulos V. 2020*b*. Reactive oxygen species and antioxidant defense in plants under abiotic stress: Revisiting the crucial role of a universal defense regulator. Antioxidants **9**, 1–52.

Haussühl K, Rohde W, Weissenböck G. 1996. Expression of chalcone synthase genes in coleoptiles and primary leaves of *Secale cereale* L after induction by UV irradiation: evidence for UV-protective role of the coleoptile. Botanica Acta **109**, 229-238.

Havaux M, Kloppstech K. 2001. The protective functions of carotenoid and flavonoid pigments against excess visible radiation at chilling temperature investigated in *Arabidopsis npq* and *tt* mutants. Planta **213**, 953–966.

Hawkes EJ, Hennelly SP, Novikova IV, Irwin JA, Dean C, Sanbonmatsu KY. 2016. *COOLAIR* antisense RNAs form evolutionarily conserved elaborate secondary structures. Cell Reports. **16**, 3087-3096.

Hayes HK, Aamodt OS. 1927. Inheritance of winter hardiness and growth habit in crosses of 'Marquis' with 'Minhardi' and 'Miturki' wheats. Journal of Agricultural Research **35**, 223–236.

Hayes S. 2020. Interaction of light and temperature signalling in plants. In: ELS 1st ed. Wiley. https://doi.org/10.1002/9780470015902.a0027978.

Healey A, Furtado A, Cooper T, Henry RJ. 2014. Protocol: a simple method for extracting next-generation sequencing quality genomic DNA from recalcitrant plant species. Plant Methods **10**, 10-21.

Heide OM. 1994. Control of flowering and reproduction in temperate grasses. New Phytologist **128**, 347–362.

Heller W, Hahlbrock K. 1980. Highly purified "flavanone synthase" from parsley catalyzes the formation of naringenin chalcone. Archives of Biochemistry and Biophysics **200**, 617–619.

Herman EM, Rotter K, Premakumar R, Elwinger G, Bae R, Ehler-King L, Chen S, Livingston DP. 2006. Additional freeze hardiness in wheat acquired by exposure to -3 °C is associated with extensive physiological morphological and molecular changes. Journal of Experimental Botany **57**, 3601–3618.

Herrmann H A, Schwartz J M, Johnson G N. 2019. Metabolic acclimation—a key to enhancing photosynthesis in changing environments? Journal of Experimental Botany **70**, 3043–3056.

Heyno E, Mary V, Schopfer P, Krieger-Liszkay A. 2011. Oxygen activation at the plasma membrane: Relation between superoxide and hydroxyl radical production by isolated membranes. Planta **234**, 35–45.

Hibara KI, Isono M, Mimura M, Sentoku N, Kojima M, Sakakibara H, Kitomi Y, Yoshikawa T, Itoh JI, Nagato Y. 2016. Jasmonate regulates juvenile-to-adult phase transition in rice. Development **143**, 3407–3446.

Higgins JA, Bailey PC, Laurie DA. 2010. Comparative genomics of flowering time pathways using *brachypodium distachyon* as a model for the temperate grasses. PLoS ONE **5**, e10065.

Hill CB, Li C. 2016. Genetic architecture of flowering phenology in cereals and opportunities for crop improvement. Frontiers in Plant Science **7**, 1906.

Hincha DK, Hellwege EM, Heyer AG, Crowe JH. 2000. Plant fructans stabilize phosphatidylcholine liposomes during freeze- drying. European Journal of Biochemistry **267**, 535–540.

Houde M, Belcaid M, Ouellet F, Danyluk J, Monroy AF, Dryanova A, Gulick P, Bergeron A, Laroche A, Links MG, MacCarthy L, Crosby WL, Sarhan F. 2006. Wheat EST resources for functional genomics of abiotic stress. BMC Genomics **7**, 149.

Hsieh TH, Lee JT, Yang PT, Chiu LH, Charng YY, Wang YC, Chan MT. 2002. Heterology expression of the Arabidopsis *C-repeat/dehydration response element binding factor 1* gene confers elevated tolerance to chilling and oxidative stresses in transgenic tomato. Plant Physiology **129**, 1086–1094.

Hu Y, Jiang L, Wang F, Yu D. 2013. Jasmonate regulates the INDUCER OF CBF EXPRESSION–C-REPEAT BINDING FACTOR/DRE BINDING FACTOR1 cascade and freezing tolerance in *Arabidopsis*. The Plant Cell **25**, 2907–2924.

Hu Y, Jiang Y, Han X, Wang H, Pan J, Yu D. 2017. Jasmonate regulates leaf senescence and tolerance to cold stress: crosstalk with other phytohormones. Journal of Experimental Botany **68**, 1361–1369.

Huang X, Han B. 2014. Natural variations and genome-wide association studies in crop plants. Annual Review of Plant Biology **65**, 531–551.

Hundertmark M, Hincha DK. 2008. LEA (Late Embryogenesis Abundant) proteins and their encoding genes in *Arabidopsis thaliana*. BMC Genomics **9**, 1–22.

Hüner NPA, Bode R, Dahal K, Hollis L, Rosso D, Krol M, Ivanov AG. 2012. Chloroplast redox imbalance governs phenotypic plasticity: the "grand design of photosynthesis" revisited. Frontiers in Plant Science **3**, 255.

Hüner NPA, Öquist G, Hurry VM, Krol M, Falk S, Griffith M. 1993. Photosynthesis photoinhibition and low temperature acclimation in cold tolerant plants. Photosynthesis Research **37**, 19–39.

Hüner NPA, Palta JP, Li PH, Carter J V. 1981. Anatomical changes in leaves of Puma rye in response to growth at cold-hardening temperatures. Botanical Gazette **142**, 55–62.

Ibrahim AK, Zhang L, Niyitanga S, Afzal M Z, Xu Y, Zhang L, Zhang L, Qi J. 2020. Principles and approaches of association mapping in plant breeding. Tropical Plant Biology **13**, 212–224.

Ingram J, Bartels D. 1996. The molecular basis of dehydration tolerance in plants. Annual Review of Plant Biology **47**, 377–403.

Jaglo KR, Kleff S, Amundsen KL, Zhang X, Haake V, Zhang JZ, Deits T, Thomashow MF. 2001. Components of the Arabidopsis C-repeat/dehydration- responsive element binding factor cold-response pathway are conserved in *Brassica napus* and other plant species. Plant Physiology **127**, 910–917.

Jaglo-Ottosen KR, Gilmour SJ, Zarka DG, Schabenberger O, Thomashow MF. 1998. *Arabidopsis CBF1* overexpression induces *COR* genes and enhances freezing tolerance. Science **280**, 104–106.

Jia Y, Ding Y, Shi Y, Zhang X, Gong Z, Yang S. 2016. The *cbfs* triple mutants reveal the essential functions of *CBFs* in cold acclimation and allow the definition of CBF regulons in *Arabidopsis*. The New Phytologist **212**, 345–353.

Jiang B, Shi Y, Peng Y, Jia Y, Yan Y, Dong X, Li H. 2020. Cold-induced CBF-PIF3 interaction enhances freezing tolerance by stabilizing the phyB thermosensor in *Arabidopsis*. Molecular Plant. **13**, 894-906.

Jin Y, Zhai S, Wang W, Ding X, Guo Z, Bai L, Wang S. 2018. Identification of genes from the ICE-CBF-COR pathway under cold stress in *Aegilops-Triticum* composite group and the evolution analysis with those from Triticeae. Physiology and Molecular Biology of Plants **24**, 211–229.

Jones JD, Flavell RB. 1982. The structure amount and chromosomal localization of defined repeated DNA sequences in species of the genus *Secale.* Chromosoma **86**, 613–64.

Jung HS, Chory J. 2010. Signaling between chloroplasts and the nucleus: Can a systems biology approach bring clarity to a complex and highly regulated pathway? Plant Physiology **152**,

453–459.

Jung JH, Domijan M, Klose C, Biswas S, Ezer D, Gao M, Khattak AK, Box MS, Charoensawan V, Cortijo S, Kumar M, Grant A, Locke JC, Schäfer E, Jaeger KE, Wigge PA. 2016. Phytochromes function as thermosensors in Arabidopsis. Science **354**, 886–889.

Jung JW, Shin JH, Lee WK, Begum H, Min C-H, Jang M-H, Oh H-B, Yang M-S, Kim S-R. 2021. Inactivation of the β 1 2-xylosyltransferase and the α 1 3-fucosyltransferase gene in rice *Oryza sativa* by multiplex CRISPR/Cas9 strategy. Plant Cell Reports **40**, 1025–1035.

Jung W J, Seo Y W. 2019. Identification of novel *C-repeat binding factor CBF* genes in rye (*Secale cereale* L) and expression studies. Gene **684**, 82-94.

Kagale S, Divi UK, Krochko JE, Keller WA, Krishna P. 2007. Brassinosteroid confers tolerance in *Arabidopsis thaliana* and *Brassica napus* to a range of abiotic stresses. Planta **225**, 353–364.

Kahle N, Sheerin DJ, Fischbach P, Koch LA, Schwenk P, Lambert D, Rodriguez R, Kerner K, Hoecker U, Zurbriggen MD, Hiltbrunner A. 2020. COLD REGULATED 27 and 28 are targets of CONSTITUTIVELY PHOTOMORPHOGENIC 1 and negatively affect phytochrome B signalling. Plant Journal **104**, 1038–1053.

Kajiura H, Okamoto T, Misaki R, Matsuura Y, Fujiyama K. 2012. Arabidopsis β12-xylosyltransferase: substrate specificity and participation in the plant-specific N-glycosylation pathway. Journal of Bioscience and Bioengineering **113**, 48-54.

Kanaoka MM, Pillitteri LJ, Fujii H, Yoshida Y, Bogenschutz NL, Takabayashi J, Zhu JK, Torii KU. 2008. *SCREAM/ICE1* and *SCREAM2* specify three cell-state transitional steps leading to Arabidopsis stomatal differentiation. The Plant Cell **20**, 1775–1785.

Kang J, Park J, Choi H, Burla B, Kretzschmar T, Lee Y, Martinoia E. 2011. Plant ABC transporters. The Arabidopsis Book **9**, e0153.

Kaplan F, Kopka J, Sung DY, Zhao W, Popp M, Porat R, Guy CL. 2007. Transcript and metabolite profiling during cold acclimation of Arabidopsis reveals an intricate relationship of cold-regulated gene expression with modifications in metabolite content. The Plant Journal **50**, 967–981.

Kasuga J, Hashidoko Y, Nishioka A, Yoshiba M, Arakawa K, Fujikawa S. 2008. Deep supercooling xylem parenchyma cells of katsura tree *Cercidiphyllum japonicum* contain flavonol glycosides exhibiting high anti-ice nucleation activity. Plant Cell and Environment **31**, 1335– 1348.

Kellogg EA. 1998. Relationships of cereals crops and other grasses. Proceedings of the National Academy of Sciences of the United States of America **95**, 2005-2010.

Kennedy A, Geuten K. 2020. The role of FLOWERING LOCUS C relatives in cereals. Frontiers in Plant Science **11**, 617340.

Kerr GP, Carter J V. 1990*a*. Tubulin isotypes in rye roots are altered during cold acclimation. Plant Physiology **93**, 83–88.

Kerr GP, Carter J V. 1990*b*. Relationship between freezing tolerance of poot-tip cells and cold stability of microtubules in rye (*Secale cereale* L. cv Puma). Plant Physiology **93**, 77–82.

Kim H-J, Kim Y-K, Park J-Y, Kim J. 2002. Light signalling mediated by phytochrome plays an important role in cold-induced gene expression through the C-repeat/dehydration responsive element (C/DRE) in *Arabidopsis thaliana*. The Plant journal **29**, 693–704.

Kim YS, Lee M, Lee J-H, Lee H-J, Park C-M. 2015. The unified ICE–CBF pathway provides a transcriptional feedback control of freezing tolerance during cold acclimation in *Arabidopsis.* Plant Molecular Biology **89**, 187–201.

Kippes N, Debernardi JM, Vasquez-Gross HA, Akpinar BA, Budak H, Kato K, Chao S, Akhunov E, Dubcovsky J. 2015. Identification of the VERNALIZATION 4 gene reveals the origin of spring growth habit in ancient wheats from South Asia. Proceedings of the National Academy of Sciences of the United States of America **112**, E5401–E5410.

Kircher S, Gil P, Kozma-Bognár L, Fejes E, Speth V, Husselstein-Muller T, Bauer D, Ádám É, Schäfer E, Nagy F. 2002. Nucleocytoplasmic partitioning of the plant photoreceptors phytochrome A, B, C, D, and E is regulated differentially by light and exhibits a diurnal rhythm. Plant Cell **14**, 1541–1555.

Kitashova A, Schneider K, Fürtauer L, Schröder L, Scheibenbogen T, Fürtauer S, Nägele T. 2020. Impaired chloroplast positioning affects photosynthetic capacity and regulation of the central carbohydrate metabolism during cold acclimation. Photosynthesis Research **147**, 49–60.

Klein T M, Roth B A, Fromm M E. 1989. Regulation of anthocyanin biosynthetic genes introduced into intact maize tissues by microprojectiles. Proceedings of the National Academy of Sciences of the United States of America **86**, 6681–6685.

Kleine T, Leister D, Lmu LM. 2013. Retrograde signals galore. Frontiers in Plant Science **4**, 45.

Knaupp M, Mishra K B, Nedbal L, Heyer AG. 2011. Evidence for a role of raffinose in stabilizing photosystem II during freeze-thaw cycles. Planta **234**, 477–486.

Knight H, Trewavas A J, Knight MR. 1996. Cold calcium signaling in Arabidopsis involves two cellular pools and a change in calcium signature after acclimation. The Plant Cell **8**, 489-503.

Knight H, Zarka DG, Okamoto H, Thomashow MF, Knight MR. 2004. Abscisic acid induces *CBF* gene transcription and subsequent induction of cold-regulated genes via the CRT promoter element. Plant Physiology **135**, 1710–1717.

Knox AK, Dhillon T, Cheng H, Tondelli A, Pecchioni N, Stockinger EJ. 2010. *CBF* gene copy number variation at *Frost Resistance-2* is associated with levels of freezing tolerance in temperate-climate cereals. Theoretical and Applied Genetics **121**, 21–35.

Kobayashi Y, Kaya H, Goto K, Iwabuchi M, Araki T. 1999. A pair of related genes with antagonistic roles in mediating flowering signals. Science **286**, 1960–1962.

Kodama Y, Suetsugu N, Kong S G, Wada M. 2010. Two interacting coiled-coil proteins WEB1 and PMI2 maintain the chloroplast photorelocation movement velocity in *Arabidopsis.* Proceedings of the National Academy of Sciences of the United States of America **107**, 19591–19596.

Koes R E, Spelt C E, Mol J N M, Gerats A G M. 1987. The chalcone synthase multigene family of *Petunia hybrida* V30: Sequence homology chromosomal localization and evolutionary aspects. Plant Molecular Biology **10**, 159-169.

Kollist H, Zandalinas SI, Sengupta S, Nuhkat M, Kangasjärvi J, Mittler R. 2019. Rapid responses to abiotic stress: Priming the landscape for the signal transduction network. Trends in Plant Science **24**, 25–37.

Končitíková R, Vigouroux A, Kopečná M, Andree T, Bartoš J, Šebela M, Moréra S, Kopečný D. 2015. Role and structural characterization of plant aldehyde dehydrogenases from family 2 and family 7. Biochemical Journal **468**, 109–123.

Kong Y, Zhang T, Guan Y, Gu X, Yang S. 2020. Comparative transcriptome analysis reveals the responses of winter rye to cold stress. Acta Physiologiae Plantarum **42**, 77.

Korn M, Peterek S, Mock H-P, Heyer AG, Hincha DK. 2008. Heterosis in the freezing tolerance and sugar and flavonoid contents of crosses between *Arabidopsis thaliana* accessions of widely varying freezing tolerance. Plant Cell and Environment **31**, 813–827.

Körner C. 2016. Plant adaptation to cold climates. F1000Research **5**, Faculty Rev 2769.

Kosová K, Prášil I T, Vitámvás P, Dobrev P, Motyka V, Floková K, Novák O, Turečková V, Rolčik J, Pešek B, Trávničková A, Gaudinová A, Galiba G, Janda T, Vlasáková E, Prášilová P, Vanková R. 2012. Complex phytohormone responses during the cold acclimation of two wheat cultivars differing in cold tolerance winter Samanta and spring Sandra. Journal of Plant Physiology **169**, 567 – 576.

Kosová K, Prášil IT, Vítámvás P. 2008. The relationship between vernalization- and photoperiodically-regulated genes and the development of frost tolerance in wheat and barley. Biologia Plantarum **52**, 601–615.

Kosová K, Vítámvás P, Planchon S, Renaut J, Vanková R, Prášil IT. 2013. Proteome analysis of cold response in spring and winter wheat (*Triticum aestivum*) crowns reveals similarities in stress adaptation and differences in regulatory processes between the growth habits. Journal of Proteome Research **12**, 4830–4845.

Koster KL, Lynch D V. 1992. Solute accumulation and compartmentation during the cold acclimation of puma rye. Plant Physiology **98**, 108–113.

Kovacs D, Kalmar E, Torok Z, Tompa P. 2008. Chaperone activity of ERD10 and ERD14, two disordered stress-related plant proteins. Plant Physiology **147**, 381–390.

Kreps JA, Wu Y, Chang HS, Zhu T, Wang X, Harper JF. 2002. Transcriptome changes for Arabidopsis in response to salt osmotic and cold stress. Plant Physiology **130**, 2129–2141.

Krzeszowiec W, Novokreshchenova M, Gabryś H. 2020. Chloroplasts in C3 grasses move in response to blue-light. Plant Cell Reports **39**, 1331–1343.

Kuczyńska A, Mikołajczak K, Ćwiek H. 2014. Pleiotropic effects of the *sdw1* locus in barley populations representing different rounds of recombination. Electronic Journal of Biotechnology **17**, 217–223.

Kumar J, Pratap A, Solanki RK, Gupta DS, Goyal A, Chaturvedi SK, Nadarajan N, Kumar S. 2012. Genomic resources for improving food legume crops. Journal of Agricultural Science 150, 289–318.

Kume S, Kobayashi F, Ishibashi M, Ohno R, Nakamura C, Takumi S. 2005. Differential and coordinated expression of *Cbf* and *Cor/Lea* genes during long-term cold acclimation in two wheat cultivars showing distinct levels of freezing tolerance. Genes and Genetic Systems **80**, 185–97.

Kurbidaeva A, Ezhova T, Novokreshchenova M. 2014. *Arabidopsis thaliana ICE2* gene: phylogeny structural evolution and functional diversification from *ICE1*. Plant Science **229**, 10–22.

Kurepin LV, Dahal KP, Savitch LV, Singh J, Bode R, Ivanov AG, Hurry V, Hüner NPA. 2013. Role of CBFs as integrators of chloroplast redox phytochrome and plant hormone signaling during cold acclimation. International Journal of Molecular Sciences **14**, 12729–12763.

Kutchan TM, Gershenzon J, Moller BL, Gang R. 2015. Natural products. In: Buchanan BB, Gruissem W, Jones RL, eds. Biochemistry and molecular biology of plants. John Wiley and Sons, West Sussex, 1132-1206.

Lång V, Mäntylä E, Welin B, Sundberg B, Palva ET. 1994. Alterations in water status, endogenous abscisic acid content, and expression of *rab18* gene during the development of freezing tolerance in *Arabidopsis thaliana*. Plant Physiology **104**, 1341–1349.

Langmead B, Salzberg S L. 2012. Fast gapped-read alignment with Bowtie 2. Nature Methods **9**, 357–359.

Larcher W. 200.3 Plant under stress. In: Larcher W. ed. Physiological plant ecology. Springer Verlag, 345 – 348.

Larsen RJ, Beres BL, Blackshaw RE, Graf RJ. 2018. Extending the growing season: winter cereals in western Canada. Canadian Journal of Plant Science **98**, 267-277.

Law CN, Jenkins G. 1970. A genetic study of cold resistance in wheat. Genetics Research **15**, 197–208.

Law CN, Worland AJ. 1997. Genetic analysis of some flowering time and adaptive traits in wheat. New Phytologist **137**, 19–28.

Le GH, Philippe F, Domon JM, Gillet F, Pelloux J, Rayon C. 2015a. Cell wall metabolism in

response to abiotic stress. Plants **4**, 112–166.

Le MQ, Pagter M, Hincha DK. 2015b. Global changes in gene expression assayed by microarray hybridization and quantitative RT-PCR during acclimation of three *Arabidopsis thaliana* accessions to sub-zero temperatures after cold acclimation. Plant Molecular Biology **87**, 1–15.

Lee CM, Thomashow MF. 2012. Photoperiodic regulation of the C-repeat binding factor CBF cold acclimation pathway and freezing tolerance in *Arabidopsis thaliana.* Proceedings of the National Academy of Sciences of the United States of America **109**, 15054–15059.

Lee HG, Seo PJ. 2015. The MYB96-HHP module integrates cold and abscisic acid signaling to activate the CBF-COR pathway in Arabidopsis. The Plant Journal **82**, 962–977.

Lee Y, Yoon HR, Paik YS, Liu JR, Chung W, Cho G. 2005. Reciprocal regulation of *Arabidopsis* UGT78D2 and BANYULS is critical for regulation of the metabolic flux of anthocyanidins to condensed tannins in developing seed coats. Journal of Plant Biology **48**, 356–370.

Legris M, Klose C, Burgie ES, Rojas CC, Neme M, Hiltbrunner A, Wigge PA, Schäfer E, Vierstra RD, Casal JJ. 2016. Phytochrome B integrates light and temperature signals in Arabidopsis. Science **354**, 897–900.

Legris M, Nieto C, Sellaro R, Prat S, Casal JJ. 2017. Perception and signalling of light and temperature cues in plants. Plant Journal **90**, 683–697.

Legris M, Szarzynska-Erden BM, Trevisan M, Petrolati LA, Fankhauser C. 2021. Phototropin-mediated perception of light direction in leaves regulates blade flattening. Plant Physiology **187**, 1235–1249.

Leibniz Institute of Plant Genetics and Crop Plant Research IPK. 2021. https://galaxy-webipk-gaterslebende. Accessed March 2021.

Lenné T, Bryant G, Holcomb R, Koster KL. 2007. How much solute is needed to inhibit the fluid to gel membrane phase transition at low hydration? Biochimica et Biophysica Acta - Biomembranes **1768**, 1019–1022.

Lepiniec L, Debeaujon I, Routaboul JM, Baudry A, Pourcel L, Nesi N, Caboche M. 2006. Genetics and biochemistry of seed flavonoids. Annual Review of Plant Biology **57**, 405–430.

Leuendorf JE, Frank M, Schmülling T. 2020. Acclimation, priming and memory in the response

of *Arabidopsis thaliana* seedlings to cold stress. Scientific Reports **10**, 689.

Leyva A, Jarillo J A, Salinas J, Martinez-Zapater J M. 1995. Low temperature induces the accumulation of phenylalanine ammonia-lyase and chalcone synthase mRNAs of *Arabidopsis thaliana* in a light-dependent manner. Plant Physiology **108**, 39–46.

Li C, Dubcovsky J. 2008. Wheat FT protein regulates VRN1 transcription through interactions with FDL2. The Plant journal **55**, 543–54.

Li G, Wang L, Yang J, He H, Jin H, Li X, Ren T, Ren Z, Li F, Han X, Zhao X, Dong L, Li Y, Song Z, Yan Z, Zheng N, Shi C, Wang Z, Yang S, Xiong Z, Zhang M, Sun G, Zheng X, Gou M, Ji C, Du J, Zheng H, Doležel J, Deng XW, Stein N, Yang Q, Zhang K, Wang D. 2021. A high-quality genome assembly highlights rye genomic characteristics and agronomically important genes. Nature Genetics **53**, 574–584.

Li G, Yu M, Fang T, Cao S, Carver BF, Yan L. 2013. Vernalization requirement duration in winter wheat is controlled by TaVRN-A1 at the protein level. Plant Journal **76**, 742–753.

Li H, Ye K, Shi Y, Cheng J, Zhang X, Yang S. 2017a. BZR1 positively regulates freezing tolerance via CBF-dependent and CBF-independent pathways in *Arabidopsis.* Molecular Plant **10**, 545–559.

Li H. 2011. A statistical framework for SNP calling mutation discovery association mapping and population genetical parameter estimation from sequencing data. Bioinformatics **27**, 2987–2993.

Li L, Sheen J. 2016. Dynamic and diverse sugar signaling. Current Opinion in Plant Biology **33**, 116–125.

Li P, Li Y J, Zhang F J, Zhang G Z, Jiang X Y, Yu H M, Hou B K. 2017b. The Arabidopsis UDP-glycosyltransferases UGT79B2 and UGT79B3 contribute to cold salt and drought stress tolerance via modulating anthocyanin accumulation. The Plant Journal **89**, 85–103.

Li Q, Zheng Q, Shen W, Cram D, Fowler DB, Wei Y, Zou J. 2015. Understanding the biochemical basis of temperature-induced lipid pathway adjustments in plants. The Plant cell **27**, 86–103.

Li W, Li M, Zhang W, Welti R, Wang X. 2004. The plasma membrane-bound phospholipase Dδ enhances freezing tolerance in *Arabidopsis thaliana*. Nature Biotechnology **22**, 427–433.

Li Y, Böck A, Haseneyer G, Korzun V, Wilde P, Schön C-C, Ankerst DP, Bauer E. 2011a. Association analysis of frost tolerance in rye using candidate genes and phenotypic data from controlled semi-controlled and field phenotyping platforms. BMC Plant Biology **11**, 146.

Li Y, Haseneyer G, Schön C-C, Ankerst D, Korzun V, Wilde P, Bauer E. 2011b. High levels of nucleotide diversity and fast decline of linkage disequilibrium in rye (*Secale cereale* L) genes involved in frost response. BMC Plant Biology **11**, 6.

Lim E K, Baldauf S, Li Y, Elias L, Worrall D, Spencer S P, Jackson R G, Taguchi G, Ross J, Bowles D J. 2003. Evolution of substrate recognition across a multigene family of glycosyltransferases in *Arabidopsis.* Glycobiology **3**, 139-145.

Limin A E, Houde M, Chauvin L P, Fowler D B, Sarhan F. 1995. Expression of the cold - induced wheat gene *wcs120* and its homologs in related species and interspecific combinations. Genome **38**, 1023 – 1031.

Limin AE, Fowler DB. 2000. Morphological and cytological characters associated with low-temperature tolerance in wheat (*Triticum aestivum* L. em Thell.). Canadian Journal of Plant Science **80**, 687–692.

Lin J S, Huang X X, Li Q, Cao Y, Bao Y, Meng X F, Li Y J, Fu C, Hou B K. 2016. UDP-glycosyltransferase 72B1 catalyzes the glucose conjugation of monolignols and is essential for the normal cell wall lignification in *Arabidopsis thaliana.* The Plant Journal **88**, 26–42.

Lissarre M, Ohta M, Sato A, Miura K. 2010. Cold-responsive gene regulation during cold acclimation in plants. Plant Signaling and Behavior **5**, 948–52.

Liu F, Marquardt S, Lister C, Swiezewski S, Science S, Series N, Jan N. 2021. Silencing linked references are available on JSTOR for this article : Targeted 3 ' processing of antisense transcripts triggers Arabidopsis FLC chromatin silencing. Science **327**, 94–97.

Liu Q, Kasuga M, Sakuma Y, Abe H, Miura S, Yamaguchi-Shinozaki K, Shinozaki K. 1998. Two transcription factors DREB1 and DREB2 with an EREBP/ AP2 DNA binding domain separate two cellular signal transduction pathways in drought- and low-temperature responsive gene expression respectively in Arabidopsis. The Plant Cell **10**, 1391–1406.

Liu Z, Jia Y, Ding Y, Shi Y, Li Z, Guo Y, Gong Z, Yang S. 2017. Plasma membrane CRPK1-mediated phosphorylation of 14-3-3 proteins induces their nuclear import to fine-tune CBF signaling during cold response. Molecular Cell **66**, 117-128.

Livingston DP, Hincha DK, Heyer AG. 2009. Fructan and its relationship to abiotic stress tolerance in plants. Cellular and Molecular Life Sciences **66**, 2007–2023.

Livingston DP, Tuong TD, Murphy JP, Gusta L V., Willick I, Wisniewski ME. 2018. High-definition infrared thermography of ice nucleation and propagation in wheat under natural frost conditions and controlled freezing. Planta **247**, 791–806.

Livingston DP. 1996. The second phase of cold hardening: freezing tolerance and fructan isomer changes in winter cereal crowns. Crop Science **36**, 1568–1573.

Los DA, Murata N. 2004. Membrane fluidity and its roles in the perception of environmental signals. Biochimica et Biophysica Acta - Biomembranes **1666**, 142–157.

Lundqvist A. 1956. Self-incompatibility in rye. I. Genetic control in the diploid. Hereditas **42**, 293–395.

Ma Y, Dai X, Xu Y, Luo W, Zheng X, Zeng D, Pan Y, Lin X, Liu H, Zhang D, Xiao J, Guo X, Xu S, Niu Y, Jin J, Zhang H, Xu X, Li L, Wang W, Qian Q, Ge S, Chong K. 2015. COLD1 confers chilling tolerance in rice. Cell **160**, 1209-1221.

MacDonald MJ, D'Cunha GB. 2007. A modern view of phenylalanine ammonia lyase. Biochemistry and Cell Biology **85**, 273-282.

Mahfoozi S, Limin AE, Fowler DB. 2001. Developmental regulation of low-temperature tolerance in winter wheat. Annals of Botany **87**, 751–757.

Mahfoozi S, Limin AE, Hayes PM, Hucl P, Fowler DB. 2000. Influence of photoperiod response on the expression of cold hardiness in wheat and barley. Canadian Journal of Plant Science **80**, 721–724.

Mancinelli AL. 1984. Photoregulation of anthocyanin synthesis VIII Effect of light pretreatments. Plant Physiology **75**, 447-453.

Mardis ER. 2008. Next-generation DNA sequencing methods. Annual Review of Genomics and Human Genetics **9**, 387-402.

Marone D, Rodriguez M, Saia S, Papa R, Rau D, Pecorella I, Laidò G, Pecchioni N, Lafferty J, Rapp M, Longin FH, De Vita P. 2020. Genome-wide association mapping of prostrate/erect growth habit in winter durum wheat. International Journal of Molecular Sciences **21**, 394.

Martinoia E, Grill E, Tommasini R, Kreuz K, Amrhein N. 1993. ATP-dependent glutathione S-conjugate export pump in the vacuolar membrane of plants. Nature **364**, 247–249.

Martinoia E, Klein M, Bovet L, Forestier C, Kolukisaoglu Ü, Műller-Rover B, Schulz B. 2002. Multifunctionality of plant ABC transporters-more than just detoxifiers. Planta **214**, 345–355.

Martis M M, Zhou R, Haseneyer G, Schmutzer T, Vrána J, Kubaláková M, König S, Kugler K G, Scholz U, Hackauf B, Korzun V, Schön C C, Dolezel J, Bauer E, Mayer K F, Stein N. 2013. Reticulate evolution of the rye genome. The Plant Cell **25**, 3685–3698.

Mascher M, Schuenemann VJ, Davidovich U, Marom N, Himmelbach A, Hübner S, Korol A, David M, Reiter E, Riehl S, Schreiber M, Vohr SH, Green RE, Dawson IK, Russell J, Kilian B, Muehlbauer GJ, Waugh R, Fahima T, Krause J, Weiss E, Stein N. 2016. Genomic analysis of 6000-year-old cultivated grain illuminates the domestication history of barley. Nature Genetics **48**, 1089-1093.

Mascher M, Wu S, Amand P S, Stein N, Poland J. 2013. Application of genotyping-by-sequencing on semiconductor sequencing platforms: a comparison of genetic and reference-based marker ordering in barley. PloS ONE **8**, e76925.

Matsoukas IG, Massiah AJ, Thomas B. 2012. Florigenic and antflorigenic signaling in plants. Plant and Cell Physiology **53**, 1827–42.

Mayer BF, Bertrand A, Charron JB. 2020. Treatment analogous to seasonal change demonstrates the integration of cold responses in *Brachypodium distachyon.* Plant Physiology **182**, 1022–1038.

McAinsh MR, Pittman JK. 2009. Shaping the calcium signature. New Phytologist **181**, 275–294.

McKim SM. 2019 How plants grow up. Journal of Integrative Plant Biology **61**, 257–277.

McKown R, Kuroki G, Warren G. 1996. Cold responses of *Arabidopsis* mutants impaired in freezing tolerance. Journal of Experimental Botany **47**, 1919–1925.

McLeod J G, McBean D S, Buzinski S R. 1981. Musketeer winter rye. Canadian Journal of Plant Science **61**, 993–994.

McLeod J G, McBean D S, Payne J F, Buzinski S R. 1985. Prima winter rye. Canadian Journal of Plant Science **65**, 447–448.

Meguro-Maoka A, Yoshida M. 2016. Analysis of seasonal expression levels of wheat fructan exohydrolase (FEH) genes regulating fructan metabolism involved in wintering ability. Journal of Plant Physiology **191**, 54–62.

Meng LS, Bao QX, Mu XR, Tong C, Cao XY, Huang JJ, Xue LN, Liu CY, Fei Y, Loake GJ.

2021. Glucose- and sucrose-signaling modules regulate the Arabidopsis juvenile-to-adult phase transition. Cell Reports **36**, 109348.

Mermigka G, Helm JM, Vlatakis I, Schumacher HT, Vamvaka E, Kalantidis K. 2016. ERIL1 the plant homologue of ERI-1 is involved in the processing of chloroplastic rRNAs. The Plant Journal **88**, 839-853.

Meyer RS, Choi JY, Sanches M, Plessis A, Flowers JM, Amas J, Dorph K, Barretto A, Gross B, Fuller DQ, Bimpong IK, Ndjiondjop MN, Hazzouri KM, Gregorio GB, Purugganan MD. 2016. Domestication history and geographical adaptation inferred from a SNP map of African rice. Nature Genetics **48**, 1083-1088.

Michaels SD, Amasino RM. 1999. FLOWERING LOCUS C encodes a novel MADS domain protein that acts as a repressor of flowering. Plant Cell **11**, 949–956.

Michaels SD, He Y, Scortecci KC, Amasino RM. 2003. Attenuation of FLOWERING LOCUS C activity as a mechanism for the evolution of summer-annual flowering behavior in Arabidopsis. Proceedings of the National Academy of Sciences of the United States of America **100**, 10102–10107.

Mignolet-Spruyt L, Xu E, Idänheimo N, Hoeberichts FA, Mühlenbock P, Brosche M, Van Breusegem F, Kangasjärvi J. 2016. Spreading the news: Subcellular and organellar reactive oxygen species production and signalling. Journal of Experimental Botany **67**, 3831–3844.

Miller A K, Galiba G, Dubcovsky J. 2006. A cluster of 11 CBF transcription factors is located at the frost tolerance locus *Fr - A m 2* in *Triticum monococcum.* Molecular Genetics and Genomics **275**, 193 – 203.

Mittler R, Vanderauwera S, Gollery M, Van Breusegem F. 2004. Reactive oxygen gene network of plants. Trends in Plant Science **9**, 490–498.

Miyamoto T, Uemura T, Nemoto K, Daito M, Nozawa A, Sawasaki T, Arimura G. 2019. Tyrosine kinase-dependent defense responses against herbivory in Arabidopsis. Frontiers in Plant Science **10**, 776.

Monroy AF, Dhindsa RS. 1995. Low-temperature signal transduction: Induction of cold acclimation-specific genes of alfalfa by calcium at 25°C. Plant Cell **7**, 321–331.

Monte E, Al-Sady B, Leivar P, Quail PH. 2007. Out of the dark: How the PIFs are unmasking a dual temporal mechanism of phytochrome signalling. Journal of Experimental Botany **58**,

3125–3133.

Moon J, Suh S-S, Lee H, Choi K-R, Hong CB, Paek N-C, Kim S-G, Lee I. 2003. The SOC1 MADS-box gene integrates vernalization and gibberellin signals for flowering in Arabidopsis. The Plant Journal **35**, 613–623.

Moore G, Devos KM, Wang Z, Gale MD. 1995. Grasses line up and form a circle. Current Biology **5**, 737–739.

Mori K, Renhu N, Naito M, Nakamura A, Shiba H, Yamamoto T, Suzaki T, Iida H, Miura K. 2018. Ca^{2+} permeable mechanosensitive channels MCA1 and MCA2 mediate cold-induced cytosolic Ca^{2+} increase and cold tolerance in Arabidopsis. Scientific Reports **8**, 550.

Murata N, Los D A. 1997. Membrane fluidity and temperature perception. Plant Physiology **115**, 875–879.

Murphy A, Peer WA, Taiz L. 2000. Regulation of auxin transport by aminopeptidases and endogenous flavonoids. Planta **211**, 315–324.

Muterko A, Salina E. 2018. Origin and distribution of the VRN-A1 exon 4 and exon 7 haplotypes in domesticated wheat species. Agronomy **8**, 1–14.

Myles S, Peiffer J, Brown PJ, Ersoz ES, Zhang Z, Costich DE, Buckler E S. 2009. Association mapping: critical considerations shift from genotyping to experimental design. The Plant Cell **21**, 2194–2202.

Nagata T, Todoriki S, Masumizu T, Suda I, Furuta S, Du Z, Kikuchi S. 2003. Levels of active oxygen species are controlled by ascorbic acid and anthocyanin in *Arabidopsis*. Journal of Agricultural and Food Chemistry **51**, 2992–2999.

Nägele T, Heyer AG. 2013. Approximating subcellular organisation of carbohydrate metabolism during cold acclimation in different natural accessions of *Arabidopsis thaliana*. New Phytologist **198**, 777–787.

Nägele T, Stutz S, Hörmiller II, Heyer AG. 2012. Identification of a metabolic bottleneck for cold acclimation in *Arabidopsis thaliana*. Plant Journal **72**, 102–114.

Nakabayashi R, Yonekura-Sakakibara K, Urano K, Suzuki M, Yamada Y, Nishizawa T, Matsuda F, Kojima M, Sakakibara H, Shinozaki K, Michael AJ, Tohge T, Yamazaki M, Saito K. 2014. Enhancement of oxidative and drought tolerance in Arabidopsis by overaccumulation of antioxidant flavonoids. The Plant Journal **77**, 367-379.

Nakamichi N, Kita M, Niinuma K, Ito S, Yamashino T, Mizoguchi T, Mizuno T. 2007. Arabidopsis clock-associated pseudo-response regulators PRR9, PRR7 and PRR5 coordinately and positively regulate flowering time through the canonical CONSTANS-dependent photoperiodic pathway. Plant and Cell Physiology **48**, 822–832.

National Center for Biotechnology Information US National Library of Medicine Rockville Pike. 2019. https://blastncbinlmnihgov/Blastcgi. Accessed May 2019.

Nei M. 1972. Genetic distance between populations. The American Naturalist **106**, 283–292.

Neill S, Gould KS. 1999. Optical properties of leaves in relation to anthocyanin concentration and distribution. Canadian journal of Botany **77**, 1777–1782.

Newell MA, Butler TJ. 2013. Forage rye improvement in the southern United States: A review. Crop Science **53**, 38–47.

Nguyen KL, Grondin A, Courtois B, Gantet P. 2019. Next-generation sequencing accelerates crop gene discovery. Trends in Plant Science **24**, 263–274.

Niesbach-Klosgen U, Barzen E, Bernhardt J, Rohde W, SchwarzSommer Z, Reif H J, Wienand U, Saedler H. 1987. Chalcone synthase genes in plants: a tool to study evolutionary relationships. Journal of Molecular Evolution **26**, 213 -225.

Nishizawa A, Yabuta Y, Shigeoka S. 2008 Galactinol and raffinose constitute a novel function to protect plants from oxidative damage. Plant Physiology **147**, 1251 – 1263.

Noctor G, Foyer CH. 2016. Intracellular redox compartmentation and ROS-related communication in regulation and signaling. Plant Physiology **171**, 1581–1592.

Nordin K, Vahala T, Palva ET. 1993. Differential expression of two related low-temperature-induced genes in *Arabidopsis thaliana* L. Heynh. Plant Molecular Biology **21**, 641–653.

Oikawa K, Kasahara M, Kiyosue T, Kagawa T, Suetsugu N, Takahashi F, Kanegae T, Niwa Y, Kadota A, Wada M. 2003. CHLOROPLAST UNUSUAL POSITIONING1 is essential for proper chloroplast positioning. The Plant Cell **15**, 2805–2815.

Olien C R. 1984. An adaptive response of rye to freezing. Crop Science **24**, 51 – 54.

Oliver SN, Finnegan EJ, Dennis ES, Peacock WJ, Trevaskis B. 2009. Vernalization-induced flowering in cereals is associated with changes in histone methylation at the *VERNALIZATION1* gene. Proceedings of the National Academy of Sciences USA **106**, 8386–8391.

Örvar BL, Sangwan V, Omann F, Dhindsa R S. 2000. Early steps in cold sensing by The Plant Cells: the role of actin cytoskeleton and membrane fluidity. The Plant Journal **23**, 785-794.

Osadchuk K, Cheng CL, Irish EE. 2019. Jasmonic acid levels decline in advance of the transition to the adult phase in maize. Plant Direct **3**, 1–13.

Ouellet F, Carpentier E, Cope MJ, Monroy AF, Sarhan F. 2001. Regulation of a wheat actin-depolymerizing factor during cold acclimation. Plant Physiology **125**, 360–368.

Pagter M, Arora R. 2013. Winter survival and deacclimation of perennials under warming climate: Physiological perspectives. Physiologia Plantarum **147**, 75–87.

Paik I, Huq E. 2019. Plant photoreceptors: Multi-functional sensory proteins and their signaling networks. Seminars in Cell and Developmental Biology **92**, 114–121.

Pankin A, Altmüller J, Becker C, von Korff M. 2018. Targeted resequencing reveals genomic signatures of barley domestication. New Phytologist **218**, 1247–1259.

Park J, Lim CJ, Shen M, Park HJ, Cha JY, Iniesto E, Rubio V, Mengiste T, Zhu JK, Bressan RA, Lee SY, Lee B h, Jin JB, Pardo JM, Kim WY, Yun DJ. 2018. Epigenetic switch from repressive to permissive chromatin in response to cold stress. Proceedings of the National Academy of Sciences of the United States of America **115**, 400-409.

Park S, Lee CM, Doherty CJ, Gilmour SJ, Kim Y, Thomashow MF. 2015. Regulation of the Arabidopsis CBF regulon by a complex low-temperature regulatory network. The Plant Journal **82**, 193–207.

Parra C, Sdez J, Pérez H, Alberdi M, Delseny M, Hubert E, Meza-Basso L. 1990. Cold resistance in rapeseed *Brassicu nupus* seedlings searching biochemical markers of cold-tolerance. Archivos de Biología y Medicina Experimentales **23**, 187-194.

Patzke K, Prananingrum P, Klemens PAW, Trentmann O, Rodrigues CM, Keller I, Fernie AR, Geigenberger P, Bölter B, Lehmann M, Schmitz-Esser S, Pommerrenig B, Haferkamp I, Neuhaus HE. 2019. The plastidic sugar transporter pSuT influences flowering and affects cold responses 1. Plant Physiology **179**, 569–587.

Pavangadkar K, Thomashow MF, Triezenberg SJ. 2010. Histone dynamics and roles of histone acetyltransferases during cold-induced gene regulation in Arabidopsis. Plant Molecular Biology **74**, 183–200.

Pearce R S. 2001. Plant freezing and damage. Annals of Botany **87**, 417–424.

Pearce S, Zhu J, Boldizsár A, Vágújfalvi A, Burke A, Garland-Campbell K, Galiba G, Dubcovsky J. 2013. Large deletions in the *CBF* gene cluster at the *Fr-B2* locus are associated with reduced frost tolerance in wheat. Theoretical and Applied Genetics **126**, 2683–2697.

Peng J, Richards DE, Hartley NM, Murphy GP, Devos KM, Flintham JE, Beales J, Fish LJ, Worland AJ, Pelica F, Sudhakar D, Christou P, Snape JW, Gale MD, Harberd NP. 1999. "Green revolution" genes encode mutant gibberellin response modulators. Nature **400**, 256–261.

Peng LN, Xu Y, Wang X, Feng X, Zhao Q, Feng S, Zhao Z, Hu B, Li F. 2019. Overexpression of paralogues of the wheat expansin gene *TaEXPA8* improves low-temperature tolerance in Arabidopsis. Plant Biology **21**, 1119–1131.

Perea-Resa C, Rodríguez-Milla MA, Iniesto E, Rubio V, Salinas J. 2017. Prefoldins negatively regulate cold acclimation in *Arabidopsis thaliana* by promoting nuclear proteasome-mediated HY5 degradation. Molecular Plant **10**, 791–804.

Peshev D, Vergauwen R, Moglia A, Hideg É, Van Den Ende W. 2013. Towards understanding vacuolar antioxidant mechanisms: a role for fructans? Journal of Experimental Botany **64**, 1025–1038.

Peterson BK, Weber JN, Kay EH, Fisher HS, Hoekstra HE. 2012. Double digest RADseq: an inexpensive method for *de novo* SNP discovery and genotyping in model and non-model species. PloS ONE **7**, e37135.

Petridis A, Döll S, Nichelmann L, Bilger W, Mock HP. 2016. *Arabidopsis thaliana* G2-LIKE FLAVONOID REGULATOR and BRASSINOSTEROID ENHANCED EXPRESSION1 are low-temperature regulators of flavonoid accumulation. New Phytologist **211**, 912–925.

Piepho H P, Richter C, Williams E. 2008. Nearest neighbour adjustment and linear variance models in plant breeding trials. Biomedical Journal **50**, 164-189.

Pietta PG. 2000. Flavonoids as antioxidants. Journal of Natural Products **63**, 1035–1042.

Pigolev A V, Miroshnichenko D N, Pushin A S, Terentyev V V, Boutanayev A M, Dolgov S V, Savchenko T V. 2018. Overexpression of Arabidopsis *OPR3* in hexaploid wheat *Triticum aestivum* L alters plant development and freezing tolerance. International Journal of Molecular Sciences **19**, 3989.

Pociecha E, Płazek A, Janowiak F, Dubert F, Kolasińska I, Irla M. 2013. Factors contributing

to enhanced pink snow mould resistance of winter rye (*Secale cereale* L.) - Pivotal role of crowns. Physiological and Molecular Plant Pathology **81**, 54–63.

Poland J, Endelman J, Dawson J, Rutkoski J, Wu S, Manes Y, Dreisigacker S, Crossa J, Sánchez-Villeda H, Sorrells M, Jannink J L. 2012a. Genomic selection in wheat breeding using genotyping-by-sequencing. Plant Genome **5**, 103-113.

Poland JA, Brown PJ, Sorrells ME, Jannink JL. 2012b. Development of high-density genetic maps for barley and wheat using a novel two-enzyme genotyping-by-sequencing approach. PLoS ONE **7**, e32253.

Ponomareva ML, Gorshkov VY, Ponomarev SN, Korzun V, Miedaner T. 2021. Snow mold of winter cereals: a complex disease and a challenge for resistance breeding. Theoretical and Applied Genetics **134**, 419–433.

Pourcel L, Irani NG, Koo AJK, Bohorquez-Restrepo A, Howe GA, Grotewold E. 2013. A chemical complementation approach reveals genes and interactions of flavonoids with other pathways. The Plant Journal **74**, 383–397.

Price A L, Patterson N J, Plenge R M, Weinblatt M E, Shadick N A, Reich D. 2006. Principal components analysis corrects for stratification in genome-wide association studies. Nature Genetics **38**, 904–909.

Pritchard J K, Stephens M, Donnelly P. 2000. Inference of population structure using multilocus genotype data. Genetics **155**, 945–959.

Puhakainen T, Hess MW, Mäkelä P, Svensson J, Heino P, Palva ET. 2004. Overexpression of multiple dehydrin genes enhances tolerance to freezing stress in Arabidopsis. Plant Molecular Biology **54**, 743–753.

Puniran-Hartley N, Hartley J, Shabala L, Shabala S. 2014. Salinity-induced accumulation of organic osmolytes in barley and wheat leaves correlates with increased oxidative stress tolerance: In planta evidence for cross-tolerance. Plant Physiology and Biochemistry **83**, 32–39.

Purvis ON, Gregory FG. 1937. A comparative study of vernalisation of winter rye by low temperature and by short days. Annals of Botany **1**, 1–26.

Puthiyaveetil S, Woodiwiss T, Knoerdel R, Zia A, Wood M, Hoehner R, Kirchhoff H. 2014. Significance of the photosystem II core phosphatase PBCP for plant viability and protein repair in thylakoid membranes. Plant and Cell Physiology **55**, 1245–1254.

Putterill J, Robson F, Lee K, Simon R, Coupland G. 1995. The CONSTANS gene of arabidopsis promotes flowering and encodes a protein showing similarities to zinc finger transcription factors. Cell **80**, 847–857.

Rabanus-Wallace M T, Hackauf B, Mascher M, Lux T, Wicker T, Gundlach H, Báez M, Houben A, Mayer K F X, Guo L, Poland J, Pozniak C J, Walkowiak S, Melonek J, Praz C, Schreiber M, Budak H, Heuberger M, Steuernagel B, Wulff B, Borner A, Byrns B, Cizkova J, Fowler DB, Fritz A, Himmelbach A, Kaithakotti G, Keilwagen J, Keller B, Konkin D, Larson J, Li Q, Myskow B, Padmarasu S, Rawat N, Sesiz U, Sezgi B, Sharpe A, Simkova H, Small I, Swarbreck D, Toegelova H, Tsvtkova N, Voylokov VA, Vrana J, Bauer E, Bolibok-Bragoszewska H, Dolezel J, Hall A, Jia J, Korzun V, Laroche A, Ma XF, Ordon F, Ozkan H, Rakoczy-Trojanowska M, Scholz U, Schulman AH, Siekmann D, Stojatowski S, Tiwari V, Spannagl M, Stein N. 2021. Chromosome-scale genome assembly provides insights into rye biology evolution and agronomic potential. Nature Genetics **53**, 564–573.

Rafalski A. 2002. Applications of single nucleotide polymorphisms in crop genetics. Current Opinion in Plant Biology **5**, 94-100.

Rafalski JA. 2010 Association genetics in crop improvement. Current Opinion in Plant Biology **13**, 174–180.

Raissig MT, Abrash E, Bettadapur A, Vogel JP, Bergmann DC. 2016. Grasses use an alternatively wired bHLH transcription factor network to establish stomatal identity. Proceedings of the National Academy of Sciences of the United States of America **113**, 8326–8331.

Rajashekar CB, Lafta A. 1996. Cell-wall changes and cell tension in response to cold acclimation and exogenous abscisic acid in leaves and cell cultures. Plant Physiology **111**, 605–612.

Ramos-Madrigal J, Smith BD, Moreno-Mayar JV, Gopalakrishnan S, Ross-Ibarra J, Gilbert MTP, Wales N. 2016. Genome sequence of a 5310-year-old maize cob provides insights into the early stages of maize domestication. Current Biology **26**, 3195-3201.

Ramsay NA, Glover BJ. 2005. MYB-bHLH-WD40 protein complex and the evolution of cellular diversity. Trends in Plant Science **10**, 63–70.

Rapacz M, Jurczyk B, Sasal M. 2017. Deacclimation may be crucial for winter survival of cereals under warming climate. Plant Science **256**, 5–15.

Reinert S, Kortz A, Léon J, Naz A A. 2016. Genome-wide association mapping in the global diversity set reveals new QTL controlling root rystem and related shoot variation in barley. Frontiers in Plant Science **7**, 1061.

Reuber S, Bornman JF, Weissenböck G. 1996. Phenylpropanoid compounds in primary leaf tissues of rye *Secale cereale* Light response of their metabolism and the possible role in UV-B protection. Physiologia Plantarum **97**, 160-168.

Richter R, Bastakis E, Schwechheimer C. 2013. Cross-repressive interactions between SOC1 and the GATAs GNC and GNL/CGA1 in the control of greening cold tolerance and flowering time in Arabidopsis. Plant Physiology **162**, 1992–2004.

Rizza F, Karsai I, Morcia C, Badeck F-W, Terzi V, Pagani D, Kiss T, Stanca AM. 2016. Association between the allele compositions of major plant developmental genes and frost tolerance in barley *Hordeum vulgare* L germplasm of different origin. Molecular Breeding **36**, 156.

Roberts DWA. 1990. Identification of loci on chromosome 5A of wheat involved in control of cold hardiness vernalization leaf length rosette growth habit and height of hardened plants. Genome **33**, 247-259.

Robertson D S, Wildenhain J, Javanmard A, Karp NA. 2019. Online FDR: An R package to control the false discovery rate for growing data repositories. Bioinformatics **35**, 4196–4199.

Rockwell NC, Su YS, Lagarias JC. 2006. Phytochrome structure and signaling mechanisms. Annual Review of Plant Biology **57**, 837–858.

Romero C C T, Vels A, Niks RE. 2018. Identification of a large-effect QTL associated with kernel discoloration in barley. Journal of Cereal Science **84**, 62–70.

Rothberg JM, Hinz W, Rearick TM, Schultz J, Mileski W, Davey M, Leamon J H, Johnson K, Milgrew M J, Edwards M, Hoon J, Simons J F, Marran D, Myers J W, Davidson J F, Branting A, Nobile J R, Puc B P, Light D, Clark T A, Huber M, Branciforte J T, Stoner I B, Cawley S E, Lyons M, Fu Y, Homer N, Sedova M, Miao X, Reed B, Sabina J, Feierstein E, Schorn M, Alanjary M, Dimalanta E, Dressman D, Kasinskas R, Sokolsky T, Fidanza J A, Namsaraev E, McKernan K J, Williams A G, Roth T, J Bustillo. 2011. An integrated semiconductor device enabling non-optical genome sequencing. Nature **475**, 348-352.

Ruelens P, De Maagd RA, Proost S, Theißen G, Geuten K, Kaufmann K. 2013. FLOWERING LOCUS C in monocots and the tandem origin of angiosperm-specific MADS-box genes. Nature Communications **4**, 2280.

Ruelland E, Vaultier MN, Zachowski A, Hurry V. 2009. Cold signalling and cold acclimation in plants. Advances in Botanical Research **49**, 35-150.

Sakuma Y, Liu Q, Dubouzet JG, Abe H, Shinozaki K, Yamaguchi-Shinozaki K. 2002. DNA-binding specificity of the ERF/AP2 domain of *Arabidopsis* DREBs, transcription factors involved in dehydration- and cold-inducible gene expression. Biochemical and Biophysical Research Communications **290**, 998–1009.

Sallam A, Alqudah A M, Dawood M, Baenziger P S, Börner A. 2019. Drought stress tolerance in wheat and barley: advances in physiology breeding and genetics research. International Journal of Molecular Sciences **20**, 3137.

Samach A, Onouchi H, Gold SE, Ditta GS, Schwarz-sommer Z, Yanofsky MF, Coupland G. 2000. Distinct roles of CONSTANS target genes in reproductive development of Arabidopsis. Science **288**, 1613–1617.

Samol I, Shapiguzov A, Ingelsson B, Fucile G, Crèvecoeur M, Vener A V, Rochaix JD, Goldschmidt-Clermont M. 2012. Identification of a photosystem II phosphatase involved in light acclimation in Arabidopsis. The Plant Cell **24**, 2596–2609.

Sandve SR, Rudi H, Asp T, Rognli OA. 2008. Tracking the evolution of a cold stress associated gene family in cold tolerant grasses. BMC Evolutionary Biology **8**, 245.

Sangwan V, Foulds I, Singh J, Dhindsa R S. 2001. Cold-activation of *Brassica napus* BN115 promoter is mediated by structural changes in membranes and cytoskeleton and requires Ca^{2+} influx. The Plant Journal **27**, 1–12.

Sasaki K, Imai R. 2012. Pleiotropic roles of cold shock domain proteins in plants. Frontiers in Plant Science **2,** 116.

Saskatchewan Ministry of Agriculture. 2019. http://www.agriculture.gov.sk.ca. Accessed June 2019.

Savitch L V, Leonardos E D, Krol M, Jansson S, Grodzinski B, Hüner N P A, Öquist G. 2002. Two different strategies for light utilization in photosynthesis in relation to growth and cold acclimation. Plant Cell and Environment **25**, 761 – 771.

Schlegel RHJ. 2014. Rye: Genetics breeding and cultivation. CRC Press.

Schneider T, Keller F. 2009. Raffinose in chloroplasts is synthesized in the cytosol and transported across the chloroplast envelope. Plant and Cell Physiology **50**, 2174–2182.

Schulz E, Tohge T, Zuther E, Fernie A R, Hincha D K. 2015. Natural variation in flavonol and anthocyanin metabolism during cold acclimation in *Arabidopsis thaliana* accessions. Plant Cell and Environment **38**, 1658–1672.

Schulz E, Tohge T, Zuther E, Fernie A R, Hincha D K. 2016. Flavonoids are determinants of freezing tolerance and cold acclimation in *Arabidopsis thaliana*. Scientific Reports **6**, 34027.

Schuster S C. 2008. Next-generation sequencing transforms today's biology. Nature Methods **5**, 16-18.

Scott IM, Clarke SM, Wood JE, Mur LAJ. 2004. Salicylate accumulation inhibits growth at chilling temperature in Arabidopsis. Plant Physiology **135**, 1040–1049.

Seifert GJ, Blaukopf C. 2010. Irritable walls: The plant extracellular matrix and signaling. Plant Physiology **153**, 467–478.

Seki M, Narusaka M, Abe H, Kasuga M, Yamaguchi-Shinozaki K, Carninci P, Hayashizaki Y, Shinozaki K. 2001. Monitoring the expression pattern of 1300 Arabidopsis genes under drought and cold stresses by using a full-length cDNA microarray. The Plant Cell **13**, 61–72.

Sharma N, Ruelens P, D'Hauw M, Maggen T, Dochy N, Torfs S, Kaufmann K, Rohde A, Geuten K. 2017. A flowering locus C homolog is a vernalization-regulated repressor in *Brachypodium* and is cold regulated in wheat. Plant Physiology **173**, 1301–1315.

Shaw LM, Turner AS, Laurie D. 2012. The impact of photoperiod insensitive *Ppd-1*a mutations on the photoperiod pathway across the three genomes of hexaploid wheat (*Triticum aestivum*). The Plant journal : for cell and molecular biology **71**, 71–84.

Sheard LB, Tan X, Mao H, Withers J, Ben-Nissan G, Hinds TR, Kobayashi Y, Hsu FF, Sharon M, Browse J, He SY, Rizo J, Howe GA, Zheng N. 2011. Jasmonate perception by inositol phosphate-potentiated COI1- JAZ co-receptor. Nature **468**, 400–405.

Shendure J, Balasubramanian S, Church G, Gilbert W, Rogers J, Schloss J A, Waterston R H. 2017. DNA sequencing at 40: past present and future. Nature **550**, 345–353.

Shi Y, Ding Y, Yang S. 2015. Cold signal transduction and its interplay with phytohormones during cold acclimation. Plant and Cell Physiology **56**, 7–15.

Shi Y, Tian S, Hou L, Huang X, Zhang X, Guo H, Yang S. 2012. Ethylene signaling negatively regulates freezing tolerance by repressing expression of CBF and type-A ARR genes in Arabidopsis. The Plant Cell **24**, 2578–95.

Shim JS, Kubota A, Imaizumi T. 2017. Circadian clock and photoperiodic flowering in arabidopsis: CONSTANS is a hub for signal integration. Plant Physiology **173**, 5–15.

Shin DH, Choi M, Kim K, Bang G, Cho M, Choi S-B, Choi G, Park YI. 2013. HY5 regulates anthocyanin biosynthesis by inducing the transcriptional activation of the MYB75/PAP1 transcription factor in *Arabidopsis.* FEBS Letters **587**, 1543–1547.

Shinozaki K, Yamaguchi-Shinozaki K. 1996. Molecular responses to drought and cold stress. Current Opinion in Biotechnology **7**, 161–167.

Sicher R. 2011. Carbon partitioning and the impact of starch deficiency on the initial response of Arabidopsis to chilling temperatures. Plant Science **181**, 167–176.

Sieber A-N, Longin CFH, Leiser WL, Würschum T. 2016. Copy number variation of *CBF-A14* at the *Fr-A2* locus determines frost tolerance in winter durum wheat. Theoretical and Applied Genetics **129**, 1087–1097.

Singh A, Pandey A, Srivastava AK, Tran LSP, Pandey GK. 2016. Plant protein phosphatases 2C: from genomic diversity to functional multiplicity and importance in stress management. Critical Reviews in Biotechnology **36**, 1023–1035.

Singh M, Ceccarelli S, Hamblin J. 1993. Estimation of heritability from varietal trials data. Theoretical and Applied Genetics **86**, 473-441.

Skinner DZ, Bellinger BS. 2011. Differential response of wheat cultivars to components of the freezing process in saturated soil. Crop Science **51**, 69.

Skinner J S, von Zitzewitz J, Szucs P, Marquez - Cedillo L, Filichkin T, Amundsen K, Stockinger E J, Thomashow M F, Chen T H, Hayes P M. 2005. Structural functional and phylogenetic characterization of a large *CBF* gene family in barley. Plant Molecular Biology **59**, 533 – 551.

Smékalová V, Doskočilová A, Komis G, Samaj J. 2013. Crosstalk between secondary messengers hormones and MAPK modules during abiotic stress signaling in plants. Biotechnology Advances **32**, 2-11.

Solanke AU, Sharma AK. 2008. Signal transduction during cold stress in plants. Physiology and Molecular Biology of Plants **14**, 69–79.

Soto-Cerda BJ, Cloutier S. 2012. Association mapping in plant genomes. In: Caliskan M. ed Genetic diversity in plants. Intechopen, 30-54.

Staswick PE, Tiryaki I. 2004. The oxylipin signal jasmonic acid is activated by an enzyme that conjugate it to isoleucine in Arabidopsis. The Plant Cell **16**, 2117–2127.

Steffen A, Elgner M, Staiger D. 2019. Regulation of flowering time by the RNA-binding proteins *AtGRP7* and *AtGRP8*. Plant and Cell Physiology **60**, 2040–2050.

Steponkus PL. 1984. Role of the plasma membrane in freezing injury and cold acclimation. Annual Review of Plant Physiology **35**, 543–584.

Steponkus PL, Lynch D V. 1989. Freeze/thaw-induced destabilization of the plasma membrane and the effects of cold acclimation. Journal of Bioenergetics and Biomembranes **21**, 21–41.

Steyn WJ, Wand SJE, Holcroft DM, Jacobs G. 2002. Anthocyanins in vegetative tissues: a proposed unified function in photoprotection. New Phytologist **155**, 349–361.

Stitt M, Hurry V. 2002. A plant for all seasons: alterations in photosynthetic carbon metabolism during cold acclimation in *Arabidopsis.* Current Opinion in Plant Biology **5**, 199–206.

Stockinger EJ, Gilmour SJ, Thomashow MF. 1997. *Arabidopsis thaliana CBF1* encodes an AP2 domain-containing transcriptional activator that binds to the C-repeat/DRE a cis-acting DNA regulatory element that stimulates transcription in response to low temperature and water deficit. Proceedings of the National Academy of Sciences of the United States of America **94**, 1035–1040.

Stockinger EJ, Skinner JS, Gardner KG, Francia E, Pecchioni N. 2007. Expression levels of barley *Cbf* genes at the *Frost resistance-H2* locus are dependent upon alleles at *Fr-H1* and *Fr-H2*. The Plant Journal **51**, 308–321.

Strauss G, Schurtenberger P, Hauser H. 1986. The interaction of saccharides with lipid bilayer vesicles: stabilization during freeze-thawing and freeze-drying. Biochimica et Biophysica Acta - Biomembranes **858**, 169–180.

Su C, Chen K, Ding Q, Mou Y, Yang R, Zhao M, Ma B, Xu Z, Ma Y, Pan Y, Chen M, Xi Y. 2018. Proteomic analysis of the function of a novel cold-regulated multispanning transmembrane protein COR413-PM1 in Arabidopsis. International Journal of Molecular Sciences **19**, 1–22.

Suetsugu N, Kagawa T, Wada M. 2005. An auxilin-like J-domain protein JAC1 regulates phototropin-mediated chloroplast movement in Arabidopsis. Plant Physiology **139**, 151–162.

Sutka J, Snape JW. 1989. Location of a gene for frost resistance on chromosome 5A of wheat Euphytica **42**, 41–44.

Suzuki N, Mittler R. 2006. Reactive oxygen species and temperature stresses: A delicate balance between signaling and destruction. Physiologia Plantarum **126**, 45–51.

Svensson JT, Crosatti C, Campoli C, Bassi R, Stanca AM, Close TJ, Cattivelli L. 2006. Transcriptome analysis of cold acclimation in barley albina and xantha mutants. Plant Physiology **141**, 257–270.

Syvanen AC. 2001. Accessing genetic variation: genotyping single nucleotide polymorphisms. Nature Reviews Genetics **2**, 930–942.

Takahashi D, Gorka M, Erban A, Graf A, Kopka J, Zuther E, Hincha DK. 2019. Both cold and sub-zero acclimation induce cell wall modification and changes in the extracellular proteome in *Arabidopsis thaliana*. Scientific Reports **9,** 2289.

Tamura K, Sanada Y, Tase K, Yoshida M. 2014. Fructan metabolism and expression of genes coding fructan metabolic enzymes during cold acclimation and overwintering in timothy (*Phleum pratense*). Journal of Plant Physiology **171**, 951–958.

Tan L, Li X, Liu F, Sun X, Li C, Zhu Z, Fu Y, Cai H, Wang X, Xie D, Sun C. 2008. Control of a key transition from prostrate to erect growth in rice domestication. Nature Genetics **40**, 1360–1364.

Tanaka N, Itoh H, Sentoku N, Kojima M, Sakakibara H, Izawa T, Itoh JI, Nagato Y. 2011. The COP1 ortholog PPS regulates the juvenile-adult and vegetative-reproductive phase changes in rice. Plant Cell **23**, 2143–2154.

Tang K, Zhao L, Ren Y, Yang S, Zhu J-K, Zhao C. 2020. The transcription factor ICE1 functions in cold stress response by binding to the promoters of *CBF* and *COR* genes. Journal of Integrative Plant Biology **62**, 258–263.

Tanino KK, McKersie BD. 1985. Injury within the crown of winter wheat seedlings after freezing and icing stress. Canadian Journal of Botany **63**, 432–436.

Targońska M, Bolibok-Brągoszewska H, Rakoczy-Trojanowska M. 2015. Assessment of genetic diversity in *Secale cereale* based on SSR markers. Plant Molecular Biology **34**, 37-51.

Tarkowski ŁP, Van den Ende W. 2015. Cold tolerance triggered by soluble sugars: a multifaceted countermeasure. Frontiers in Plant Science **6**, 203.

Taylor LP, Grotewold E. 2005. Flavonoids as developmental regulators. Current Opinion in Plant Biology **8**, 317–323.

Tchagang A B, Fauteux F, Tulpan D, Pan Y. 2017. Bioinformatics identification of new targets for improving low temperature stress tolerance in spring and winter wheat. BMC Bioinformatics **18**, 174.

Teige M, Scheikl E, Eulgem T, Dóczi R, Ichimura K, Shinozaki K, Dangl JL, Hirt H. 2004. The MKK2 pathway mediates cold and salt stress signaling in Arabidopsis. Molecular Cell **15**, 141–152.

Teng S, Keurentjes J, Bentsink L, Koornneef M, Smeekens S. 2005. Sucrose-specific induction of anthocyanin biosynthesis in Arabidopsis requires the *MYB75/PAP1* gene. Plant Physiology **139**, 1840–1852.

Tereshchenko OY, Arbuzova VS, Khlestkina EK. 2013. Allelic state of the genes conferring purple pigmentation in different wheat organs predetermines transcriptional activity of the anthocyanin biosynthesis structural genes. Journal of Cereal Science **57**, 10-13.

Thalmann M, Santelia D. 2017. Starch as a determinant of plant fitness under abiotic stress. New Phytologist **214**, 943–951.

Thomas B. 2006. Light signals and flowering. Journal of Experimental Botany **57**, 3387–3393.

Thomashow MF, Gilmour SJ, Stockinger EJ, Jaglo-ottosen KR, Zarka DG. 2001. Role of the Arabidopsis CBF transcriptional activators in cold acclimation. Physiologia Plantarum **112**, 171–175.

Thomashow MF. 1999. Plant cold acclimation: Freezing tolerance genes and regulatory mechanisms. Annual Review of Plant Physiology and Plant Molecular Biology **50**, 571–599.

Tohge T, Perez de Souza L, Fernie AR. 2018. On the natural diversity of phenylacylated-flavonoid and their in planta function under conditions of stress. Phytochemistry Reviews **17**, 279–290.

Tomalty H E, Walker V K. 2014. Perturbation of bacterial ice nucleation activity by a grass antifreeze protein. Biochemical and Biophysical Research Communications **452**, 636–641.

Tremblay K, Ouellet F, Fournier J, Danyluk J, Sarhan F. 2005. Molecular characterization and origin of novel bipartite cold-regulated ice recrystallization inhibition proteins from cereals. Plant and Cell Physiology **46**, 884–891.

Trevaskis B, Bagnall DJ, Ellis MH, Peacock WJ, Dennis ES. 2003. MADS box genes control vernalization-induced flowering in cereals. Proceedings of the National Academy of Sciences of the United States of America **100**, 13099–13104.

Trevaskis B, Hemming MN, Dennis ES, Peacock WJ. 2007. The molecular basis of vernalization-induced flowering in cereals. Trends in Plant Science **12**, 352–357.

Tripathi RK, Bregitzer P, Singh J. 2018. Genome-wide analysis of the SPL/miR156 module and its interaction with the AP2/miR172 unit in barley. Scientific Reports **8**, 1–13.

Uemura M, Joseph RA, Steponkus PL. 1995. Cold - acclimation of *Arabidopsis thaliana* - effect on plasma - membrane lipid - composition and freeze - induced lesions. Plant Physiology **109**, 15 – 30.

Uemura M, Tominaga Y, Nakagawara C, Shigematsu S, Minami A, Kawamura Y. 2006. Responses of the plasma membrane to low temperatures. Physiologia Plantarum **126**, 81–89.

Vágújfalvi A, Aprile A, Miller A, Dubcovsky J, Delugu G, Galiba G, Cattivelli L. 2005. The expression of several *Cbf* genes at the *Fr-A2* locus is linked to frost resistance in wheat. Molecular Genetics and Genomics **274**, 506–514.

Van Den Ende W, De Coninck B, Van Laere A. 2004. Plant fructan exohydrolases: A role in signaling and defense? Trends in Plant Science **9**, 523–528.

Vaultier MN, Cantrel C, Vergnolle C, Justin AM, Demandre C, Benhassaine-Kesri G, Çiçek D, Zachowski A, Ruelland E. 2006. Desaturase mutants reveal that membrane rigidification acts as a cold perception mechanism upstream of the diacylglycerol kinase pathway in Arabidopsis cells. FEBS Letters **580**, 4218–4223.

Verdeprado H, Kretzschmar T, Begum H, Raghavan C, Joyce P, Lakshmanan P, Cobb JN, Collard B C Y. 2018. Association mapping in rice: basic concepts and perspectives for molecular breeding. Plant Production Science **21**, 159–176.

Vereyken IJ, Chupin V, Demel RA, Smeekens SCM, De Kruijff B. 2001. Fructans insert

between the headgroups of phospholipids. Biochimica et Biophysica Acta - Biomembranes **1510**, 307–320.

Vergnolle C, Vaultier M-N, Taconnat L, Renou J, Kader J, Zachowski A, Ruelland E. 2005. The cold-induced early activation of phospholipase C and D pathways determines the response of two distinct clusters of genes in Arabidopsis cell suspensions. Plant Physiology **139**, 1217–1233.

Versluys M, Tarkowski ŁP, Van Den Ende W. 2017. Fructans as DAMPs or MAMPs: Evolutionary prospects, cross-tolerance, and multistress resistance potential. Frontiers in Plant Science **7**, 1–7.

Vítámvás P, Kosová K, Musilová J, Holková L, Mařík P, Smutná P, Klíma M, Prášil IT. 2019. Relationship between dehydrin accumulation and winter survival in winter wheat and barley grown in the field. Frontiers in Plant Science **10**, 7.

Vlachonasios KE, Thomashow MF, Triezenberg SJ. 2003. Disruption mutations of *ADA2b* and *GCN5* transcriptional adaptor genes dramatically affect Arabidopsis growth, development, and gene expression. The Plant cell **15**, 626–638.

Vogel JT, Zarka DG, Van Buskirk H A, Fowler SG, Thomashow MF. 2005. Roles of the CBF2 and ZAT12 transcription factors in configuring the low temperature transcriptome of Arabidopsis. The Plant Journal **41**, 195–211.

Vogel KP, Sarath G, Mitchell RB. 2014 Micromesh fabric pollination bags for switchgrass. Crop Science **54**, 1621–1623.

von Zitzewitz J, Szűcs P, Dubcovsky J, Yan L, Francia E, Pecchioni N, Casas A, Chen THH, Hayes PM, Skinner JS. 2005. Molecular and structural characterization of barley vernalization genes. Plant Molecular Biology **59**, 449–467.

Voorrips R E. 2002. MapChart: Software for the graphical presentation of linkage maps and QTLs. Journal of Heredity **93**, 77-78.

Voss-Fels K, Snowdon RJ. 2016. Understanding and utilizing crop genome diversity via high-resolution genotyping. Plant Biotechnology Journal **14**, 1086–1094.

Voylokov A V, Lykholay A N, Smirnov V G. 2015. Genetic control of anthocyanin coloration in rye. Russian Journal of Genetics Applied Research 5, 262–267.

Wada M, Kong S-G. 2018. Actin-mediated movement of chloroplasts. Journal of Cell Science **131**, 210310.

Wada M. 2013. Chloroplast movement. Plant Science **210**, 177–182.

Waddington SR, Cartwright PM, Wall PC. 1983. A quantitative scale of spike initial and pistil development in barley and wheat. Annals of Botany **51**, 119–130.

Wang G, Schmalenbach I, von Korff M, Léon J, Kilian B, Rode J, Pillen K. 2010. Association of barley photoperiod and vernalization genes with QTLs for flowering time and agronomic traits in a BC2DH population and a set of wild barley introgression lines. Theoretical and Applied Genetics **120**, 1559-1574.

Wang H, Zaman Q U, Huang W, Mei D, Liu J, Wang W, Ding B, Hao M, Fu L, Cheng H, Hu Q. 2019. QTL and candidate gene identification for silique length based on high-dense genetic map in *Brassica napus* L. Frontiers in Plant Science **10**, 1579.

Wanke D, Üner Kolukisaoglu H. 2010. An update on the ABCC transporter family in plants: many genes many proteins but how many functions? Plant Biology **12**, 15-25.

Wasternack C, Song S. 2017. Jasmonates: biosynthesis metabolism and signaling by proteins activating and repressing transcription. Journal of Experimental Botany **68**, 1303–1321.

Weatherlink. 2020. https://wwwweatherlinkcom. Accessed March 2020.

Wei X, Liu S, Sun C, Xie G, Wang L. 2021. Convergence and divergence: signal perception and transduction mechanisms of cold stress in Arabidopsis and rice. Plants **10**, 1864.

Williams CA, Grayer RJ. 2004. Anthocyanins and other flavonoids. Natural Product Reports **21**, 539–573.

Willick I R, Takahashi D, Fowler D B, Uemura M, Tanino K K. 2018. Tissue-specific changes in apoplastic proteins and cell wall structure during cold acclimation of winter wheat crowns. Journal of Experimental Botany **69**, 1221–1234.

Wilson S, Ruban A V. 2020. Rethinking the influence of chloroplast movements on non-photochemical quenching and photoprotection. Plant Physiology **183**, 1213–1223.

Winfield MO, Lu C, Wilson ID, Coghill JA, Edwards KJ. 2009. Cold- and light-induced changes in the transcriptome of wheat leading to phase transition from vegetative to reproductive growth. BMC Plant Biology **9**, 55.

Winfield MO, Lu C, Wilson ID, Coghill JA, Edwards KJ. 2010. Plant responses to cold: transcriptome analysis of wheat. Plant Biotechnology Journal **8**, 749–771.

Winkel-Shirley B. 2001. Flavonoid biosynthesis A colorful model for genetics biochemistry cell biology and biotechnology. Plant Physiology **126**, 485–493.

Wu G, Poethig RS. 2006. Temporal regulation of shoot development in *Arabidopsis thaliana* by *miRr156* and its target *SPL3*. Development **133**, 3539–3547.

Wu G, Yeon PM, R CS, Jia-Wei W, Weigel D, Poethig RS. 2009. The sequential action of *miR156* and *miR172* regulates developmental timing in Arabidopsis. Cell **6**, 1249–1254.

Wu J, Wang W, Xu P, Pan J, Zhang T, Li Y, Li G, Yang H, Lian H. 2019a. PhyB interacts with BES1 to regulate brassinosteroid signaling in Arabidopsis. Plant and Cell Physiology **60**, 353–366.

Wu Z, Chen L, Yu Q, Zhou W, Gou X, Li J, Hou S. 2019b. Multiple transcriptional factors control stomata development in rice. New Phytologist **223**, 220–232.

Würschum T, Longin CFH, Hahn V, Tucker MR, Leiser WL. 2017. Copy number variations of *CBF* genes at the *Fr-A2* locus are essential components of winter hardiness in wheat. The Plant Journal **89**, 764–773.

Wyatt SE, Rashotte AM, Shipp MJ, Robertson D, Muday GK. 2002. Mutations in the gravity persistence signal loci in Arabidopsis disrupt the perception and/or signal transduction of gravitropic stimuli. Plant Physiology **130**, 1426–1435.

Xiao J, Xu S, Li C, Xu Y, Xing L, Niu Y, Huan Q, Tang Y, Zhao C, Wagner D, Gao C, Chong K. 2014. O-GlcNAc-mediated interaction between VER2 and TaGRP2 elicits *TaVRN1* mRNA accumulation during vernalization in winter wheat. Nature Communications **5**, 1–13.

Xie C, Zhang R, Qu Y, Miao Z, Zhang Y, Shen X, Wang T, Dong J. 2012. Overexpression of *MtCAS31* enhances drought tolerance in transgenic Arabidopsis by reducing stomatal density. New Phytologist **195**, 124–135.

Xin Z, Browse J. 1998. *eskimo1* mutants of *Arabidopsis* are constitutively freezing-tolerant. Proceedings of the National Academy of Sciences of the United States of America **95**, 7799–7804.

Xiong L, Ishitani M, Lee H, Zhu JK. 2001. The *Arabidopsis LOS5/ABA3* locus encodes a molybdenum cofactor sulfurase and modulates cold stress- and osmotic stress-responsive gene expression. The Plant Cell **13**, 2063–2068.

Xu D, Deng XW. 2020. CBF-phyB-PIF module links light and low temperature signaling. Trends in Plant Science **25**, 952–954.

Xu J, Li Y, Sun J, Du L, Zhang Y, Yu Q, Liu X. 2013. Comparative physiological and proteomic response to abrupt low temperature stress between two winter wheat cultivars differing in low temperature tolerance. Plant Biology **15**, 292–303.

Xu M, Hu T, Scott Poethig R. 2021. Low light intensity delays vegetative phase change. Plant Physiology **187**, 1177–1188.

Xu S, Chong K. 2018. Remembering winter through vernalization. Nature Plants **4**, 997–1009.

Xu S, Xiao J, Yin F, Guo X, Xing L, Xu Y, Chong K. 2019. The protein modifications of O-GlcNAcylation and phosphorylation mediate vernalization response for flowering in winter wheat. Plant Physiology **180**, 1436–1449.

Xu W, Jiao Y, Li R, Zhang N, Xiao D, Ding X, Wang Z. 2014. Chinese wild-growing *Vitis amurensis ICE1* and *ICE2* encode *MYC*-type bHLH transcription activators that regulate cold tolerance in Arabidopsis. PLoS ONE **9**, 1–12.

Yamazaki T, Kawamura Y, Minami A, Uemura M. 2008. Calcium-dependent freezing tolerance in Arabidopsis involves membrane resealing via synaptotagmin SYT1. The Plant Cell **20**, 3389–404.

Yan L, Fu D, Li C, Blechl A, Tranquilli G, Bonafede M, Sanchez A, Valarik M, Yasuda S, Dubcovsky J. 2006. The wheat and barley vernalization gene *VRN3* is an orthologue of *FT*. Proceedings of the National Academy of Sciences of the United States of America **103**, 19581–19586.

Yan L, Loukoianov A, Blechl A, Tranquilli G, Ramakrishna W, SanMiguel P, Bennetzen JL, Echenique V, Dubcovsky J. 2004. The wheat *VRN2* gene is a flowering repressor down-regulated by vernalization. Science **303**, 1640–1644.

Yan L, Loukoianov A, Tranquilli G, Helguera M, Fahima T, Dubcovsky J. 2003. Positional cloning of the wheat vernalization gene *VRN1*. Proceedings of the National Academy of Sciences of the United States of America **100**, 6263–6268.

Yang D-L, Yao J, Mei C-S, Tong X-H, Zeng L-J, Li Q, Xiao L-T, Sun T, Li J, Deng X-W, Lee CM, Thomashow MF, Yang Y, He Z, He SY. 2012. Plant hormone jasmonate prioritizes defense over growth by interfering with gibberellin signaling cascade. Proceedings of the National Academy of Sciences of the United States of America **109**, 1192-1200.

Yang JF, Chen YZ, Kawabata S, Li YH, Wang Y. 2017. Identification of light independent anthocyanin biosynthesis mutants induced by ethyl methane sulfonate in turnip "Tsuda" *Brassica rapa.* International Journal of Molecular Sciences **18**, 1288.

Yang L, Xu M, Koo Y, He J, Scott Poethig R. 2013. Sugar promotes vegetative phase change in *Arabidopsis thaliana* by repressing the expression of *MIR156A* and *MIR156C*. Elife **2013**, 1–15.

Yonemaru Ji, Mizobuchi R, Kato H, Yamamoto T, Yamamoto E, Matsubara K, Hirabayashi H, Takeuchi Y, Tsunematsu H, Ishii T, Ohta H, Maeda H, Ebana K, Yano M. 2014. Genomic regions involved in yield potential detected by genome-wide association analysis in Japanese high-yielding rice cultivars. BMC Genomics **15**, 346.

Yoshida M, Abe J, Moriyama M, Kuwabara T. 1998. Carbohydrate levels among winter wheat cultivars varying in freezing tolerance and snow mold resistance during autumn and winter. Physiologia Plantarum **103**, 8–16.

Yoshihara N, Imayama T, Fukuchi-Mizutani M, Okuhara H, Tanaka Y, Ino I, Yabuya T. 2005. cDNA cloning and characterization of UDP-glucose: anthocyanidin 3-O-glucosyltransferase in *Iris hollandica.* Plant Science **169**, 496–501.

Younis A, Ramzan F, Ramzan Y, Zulfiqar F, Ahsan M, Lim K B. 2020. Molecular markers improve abiotic stress tolerance in crops: A review. Plants Basel Switzerland **9**, 1374.

Yu XM, Griffith M. 2001. Winter rye antifreeze activity increases in response to cold and drought, but not abscisic acid. Physiologia Plantarum **112**, 78–86.

Zhai Q, Zhang X, Wu F, Feng H, Deng L, Xu L, Zhang M, Wang Q, Li C. 2015. Transcriptional mechanism of jasmonate receptor COI1-mediated delay of flowering time in Arabidopsis. The Plant Cell **27**, 2814–2828.

Zhang C, Fei Z, Arora R, Hannapel DJ. 2010. Ice recrystallization inhibition proteins of perennial ryegrass enhance freezing tolerance. Planta **232**, 155–164.

Zhang D, Guo X, Xu Y, Li H, Ma L, Yao X, Weng Y, Guo Y, Liu CM, Chong K. 2019. OsCIPK7 point-mutation leads to conformation and kinase-activity change for sensing cold response. Journal of Integrative Plant Biology **61**, 1194–1200.

Zhang J F, Xu Y Q, Dong J M, Peng L N, Feng X, Wang X, Li F, Miao Y, Yao S K, Zhao Q Q, Feng S S, Hu B Z, Li F L. 2018. Genome-wide identification of wheat *Triticum*

*aestivu*m expansins and expansin expression analysis in cold-tolerant and cold-sensitive wheat cultivars. PloS ONE **13**, e0195138.

Zhang X, Liu CJ. 2015. Multifaceted regulations of gateway enzyme phenylalanine ammonia-lyase in the biosynthesis of phenylpropanoids. Molecular Plant **8**, 17–27.

Zhang Y, Zheng S, Liu Z, Wang L, Bi Y. 2011. Both HY5 and HYH are necessary regulators for low temperature-induced anthocyanin accumulation in *Arabidopsis* seedlings. Journal of Plant Physiology **168**, 367–374.

Zhang Z, Li J, Li F, Liu H, Yang W, Chong K, Xu Y. 2017. OsMAPK3 Phosphorylates OsbHLH002/OsICE1 and inhibits Its ubiquitination to activate *OsTPP1* and enhances rice chilling tolerance. Developmental Cell **43**, 731-743.e5.

Zhao C, Wang P, Si T, Hsu CC, Wang L, Zayed O, Yu Z, Zhu Y, Dong J, Tao WA, Zhu JK. 2009. MAP kinase cascades regulate the cold response by modulating ICE1 protein stability. Nature **15**, 682–689.

Zhao C, Zhang Z, Xie S, Si T, Li Y, Zhu J-K. 2016. Mutational evidence for the critical role of CBF transcription factors in cold acclimation in Arabidopsis. Plant Physiology **171**, 2744–2759.

Zhao J, Dixon RA. 2009. MATE transporters facilitate vacuolar uptake of epicatechin 3′-O-glucoside for proanthocyanidin biosynthesis in *Medicago truncatula* and *Arabidopsis.* The Plant Cell **21**, 2323–2340.

Zhao J. 2015. Flavonoid transport mechanisms: how to go and with whom. Trends in Plant Science **20**, 576–585.

Zhao Y, Gowda M, Wurschum T, Longin CFH, Korzun V, Kollers S, Schachschneider R, Zeng J, Fernando R, Dubcovsky J, Reif JC. 2013. Dissecting the genetic architecture of frost tolerance in Central European winter wheat. Journal of Experimental Botany **1**, 1–8.

Zhou A, Liu E, Li H, Li Y, Feng S, Gong S, Wang J. 2018. PsCor413pm2 a plasma membrane-localized cold-regulated protein from *phlox subulata* confers low temperature tolerance in Arabidopsis. International Journal of Molecular Sciences **19**, 4–6.

Zhou H, Muehlbauer G, Steffenson B. 2012. Population structure and linkage disequilibrium in elite barley breeding germplasm from the United States. Journal of Zhejiang University Science B **13**, 438–451.

Zhu C, Gore M, Buckler ES, Yu J. 2008. Status and prospects of association mapping in plants. Plant Genome **1**, 5–20.

Zhu J, Pearce S, Burke A, See DR, Skinner DZ, Dubcovsky J, Garland-Campbell K. 2014. Copy number and haplotype variation at the *VRN-A1* and central *FR-A2* loci are associated with frost tolerance in hexaploid wheat. Theoretical and Applied Genetics **127**, 1183–1197.

Zuther E, Juszczak I, Lee YP, Baier M, Hincha DK. 2015. Time-dependent deacclimation after cold acclimation in *Arabidopsis thaliana* accessions. Scientific Reports **5**, 12199.

Zuther E, Schaarschmidt S, Fischer A, Erban A, Pagter M, Mubeen U, Giavalisco P, Kopka J, Sprenger H, Hincha DK. 2019. Molecular signatures associated with increased freezing tolerance due to low temperature memory in Arabidopsis. Plant Cell and Environment **42**, 854–873.